

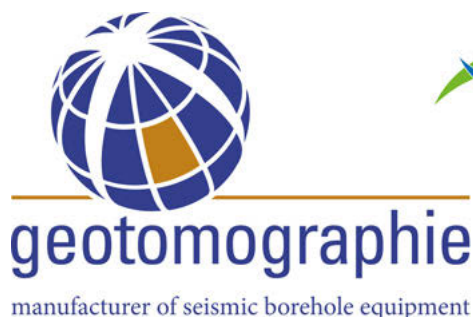


**85. Jahrestagung**  
**Deutsche Geophysikalische**  
**Gesellschaft**

**24.–27. Februar 2025 in Bochum**

**TAGUNGSBAND**

Wir danken unseren Sponsoren und Aussteller\*innen.



*Engineering & Consulting*

# **Herzlich Willkommen zur 85. Jahrestagung der Deutschen Geophysikalischen Gesellschaft in Bochum!**

Wir freuen uns, Sie nach 15 Jahren wieder in Bochum zur DGG-Jahrestagung begrüßen zu dürfen.

Wie gewohnt, bieten wir ein Forum für Diskussionen zu allen Themen der Geophysik. Berichte von Studierenden über ihre Abschlussarbeiten sind ebenso erwünscht wie herausragende Ergebnisse großer Forschungsprojekte.

Neben den etablierten Themenbereichen setzen wir mit unseren Schwerpunktthemen Akzente, die auch einen besonderen Bezug zur geophysikalischen Forschung in Bochum haben.

In vier Plenarvorträgen stellen namhafte WissenschaftlerInnen Arbeiten zu tektonischer Geodäsie, Erkundung des tiefen Erdinneren, induzierter Polarisation und induzierter Seismizität vor.

Neben dem wissenschaftlichen Programm präsentieren sich zahlreiche Firmen. Für die Beteiligung bedanken wir uns bereits jetzt; ohne das Sponsoring wäre vieles hier Angebotene nicht möglich.

Veranstaltungen speziell für Studierende und NachwuchswissenschaftlerInnen und natürlich der traditionelle Gesellschaftsabend runden das Programm ab.

Die Stadt Bochum liegt im Zentrum einer Region im Wandel. Die hier ansässigen Forschungseinrichtungen widmen sich insbesondere Fragen der Wärme-wende, ein Thema das im Abendvortrag und im sich an die Tagung anschließenden SEG-DGG Workshop „*Geophysical Exploration in Urban Environments*“ im Fokus stehen wird.

Wir freuen uns darauf, Sie in Bochum begrüßen zu dürfen.

***Jörg Renner und das Tagungsteam***



## Centaur Gen5 Series of Data Loggers



## The Future of Data Acquisition

The new Centaur Gen5 series of data loggers, featuring Strata OS, builds upon the Nanometrics legacy of quality and ease-of-use for digitizing, processing, recording and streaming the data that you rely upon. Centaur Gen5 combines exceptional performance, adaptability and reliability, allowing you to seamlessly integrate various sensor types into one energy-efficient station. By consolidating your data acquisition, you'll benefit from streamlined workflows, reduced power costs, and enhanced data security. Unlock new possibilities for seismology, volcanology, glaciology and beyond.

**Centaur  
GEN5**

To learn more, visit IGM and Nanometrics' DGG booth.



Ingenieurgesellschaft für  
Geophysikalische Messtechnik mbH  
[www.igm-geophysik.de](http://www.igm-geophysik.de) | [info@igm-geophysik.de](mailto:info@igm-geophysik.de)

**Beratung  
Service  
Vertrieb**

# INHALTSVERZEICHNIS

## Tagungsorganisation

Tagungsort / Veranstalter / Ausrichter / Eventmanagement / Lokales Organisationsteam ... **6**

## Einladung zur DGG-Mitgliederversammlung

## Session – Themenübersicht

## Schwerpunktthemen S1 bis S4

## Allgemeine Hinweise

## Eröffnungsveranstaltung – Programm

## Veranstaltungen

Begrüßungsabend / Firmenausstellung / Studentischer Abend / Gesellschaftsabend .... **19**

Öffentlicher Abendvortrag / Meet & Greet / Lunchseminar / Lunch'n Learn .... **20**

## DGG-Kolloquium

## Sitzungstermine

## Organisatorische Informationen

Internetzugang, Essen/Ausgehen, öffentlicher Nahverkehr .... **23**

Campusplan/Stadtplan .... **24/25**

## Übersicht Tagungsprogramm

### Programm

24. Februar 2025 – <b>Montag</b>	<b>31–34</b>
25. Februar 2025 – <b>Dienstag</b>	<b>35–42</b>
26. Februar 2025 – <b>Mittwoch</b>	<b>43–49</b>
27. Februar 2025 – <b>Donnerstag</b>	<b>50–54</b>

### Abstracts

Plenarvorträge S1–S4	<b>56</b>
S1 – Rekonstruktion der Dynamik des tiefen Erdinnern ...	<b>59</b>
S2 – Induzierte Seismizität	<b>67</b>
S3 – Tektonische Geodäsie	<b>77</b>
S4 – Induzierte Polarisation: Ein Paradigmenwechsel.	<b>84</b>
AG – Airborne Geophysics / Fernerkundung	<b>95</b>
BL – Wissenschaftliches Bohren / Logging / Gesteins- und Mineralphysik ( <i>nur Poster</i> )	<b>98</b>
GD – Geodynamik/Tectonophysik ( <i>nur Vorträge</i> )	<b>104</b>
GO/OS – Geophysik in der Öffentlichkeit und im Wandel der Zeit/ Open Source in Forschung und Lehre	<b>106</b>
GT – Geothermie / Radiometrie ( <i>nur Poster</i> )	<b>111</b>
KD – Kampfmitteldetektion	<b>113</b>
KI – KI-Verfahren in der Geophysik	<b>117</b>
MG – Marine Geophysik ( <i>nur Poster</i> )	<b>121</b>
MI – Modellierung / Imaging	<b>125</b>
OG – Oberflächennahe Geophysik	<b>136</b>
PV – Potentialverfahren ( <i>nur Poster</i> )	<b>163</b>
SM – Seismik	<b>165</b>
SO – Seismologie	<b>172</b>
VU – Vulkanologie	<b>198</b>

## Autorenindex



## 85. JAHRESTAGUNG DER DEUTSCHEN GEOPHYSIKALISCHEN GESELLSCHAFT

### **TAGUNGSSORT**

#### **Ruhr-Universität Bochum**

#### **Veranstaltungszentrum**

Webseite: [dgg2025.dgg-tagung.de](http://dgg2025.dgg-tagung.de)  
E-Mail: [dgg2025@rub.de](mailto:dgg2025@rub.de)  
Adresse: Universitätsstraße 150, 44801 Bochum

Anreiseinformation und Lagepläne:  
[www.ruhr-uni-bochum.de/de/anreise-zur-ruhr-universitaet](http://www.ruhr-uni-bochum.de/de/anreise-zur-ruhr-universitaet)

### **VERANSTALTER**

#### **Deutsche Geophysikalische Gesellschaft e.V.**

Geschäftsstelle: Bundesanstalt für Geowissenschaften und Rohstoffe  
Stilleweg 2, 30655 Hannover  
E-Mail: [geschaeftsfuehrung@dgg-online.de](mailto:geschaeftsfuehrung@dgg-online.de)  
Internet: [www.dgg-online.de](http://www.dgg-online.de)

### **AUSRICHTER**

#### **Institut für Geologie, Mineralogie und Geophysik**

#### **Ruhr-Universität Bochum**

Universitätsstraße 150, 44801 Bochum

### **EVENTMANAGEMENT**

#### **WITAGO – Agentur für Kongress- und Eventmanagement**

Adresse: Quintschlag 37, 28207 Bremen  
Zuständig: Kerstin Biegemann  
Telefon: +49 (0)421 48 543 526 (Büro), +49 (0)176 20736349 (vor Ort)  
E-Mail: [dgg2025@witago.com](mailto:dgg2025@witago.com)  
Internet: [www.witago.com](http://www.witago.com)

### **LOKALES ORGANISATIONSTEAM/KONTAKTE**

**Tagungsleitung** Jörg Renner, Kasper Fischer, Bodo Lehmann

**Firmenausstellung** Claudia Finger

**& Sponsoring**

**Tagungsbüro** Kerstin Biegemann



Du bist begeistert von innovativer Technologie und willst die Zukunft der Geophysik mitgestalten?  
Bei ASDRO kombinieren wir modernste Dronentechnologie mit fortschrittlicher Sensorik, um neue Maßstäbe in der Datenerfassung und Analyse zu setzen.

24.02 bis 27.02  
Vereinbare während der DGG-Tagung  
einen Termin mit uns!

QR Code scannen!



Katernberger Str. 107,  
45327 Essen



[asdro.de](http://asdro.de)

Telefon: +49 20172028417

E-Mail: [info@asdro.de](mailto:info@asdro.de)



Acoustic • Seismic • Vibration



#### WIR BIETEN

Produkte für Seismik, Geoelektrik, Magnetik, Elektromagnetik, Magnetotellurik, Georadar, NMR, Cosmic Ray, NDT, uvm

BERATUNG

VERKAUF

VERMIETUNG

REPARATUREN

TRAINING

ENTWICKLUNG

Next generation  
Distributed Acoustic  
Sensing - DAS

Transform a standard  
fiber optic cable into  
thousands of sensors

terra 15



Ingenieurunternehmen für integrierte  
Planungs- und Bauleistungen  
+ Beratung + Planung + Projektrealisierung

Vertriebspartner der Guideline Geo | ABEM

## ABEM

Resistivity and IP Seismic Surveying  
Surveying



Terrameter LS2



Terraloc Pro 2

TDEM Surveying



GroundTEM



WalkTEM 2

## MALA

GPR for Utility  
Locating



Easy Locator  
Core

Flexible GPR  
Solution



Ground Explorer

Large Scale 3D  
GPR Mapping



Mira Compact



Easy Locator  
Widerange



Mira HDR

CDM Smith SE  
Ingersheimer Str. 10 | D-70499 Stuttgart  
+49 711 83076-0 | geophysik@cdmsmith.com

GUIDELINE GEO AB (PUBL)  
Hemvärvngatan 9 | SE-171 54 Stockholm, Sweden  
+46 8 557 613 00 | sales@guidelinegeo.com



Umwelt- und Geoservices  
**Wir gehen den Dingen auf  
den Grund**

Neben der Erfassung georeferenzierter Bestandsdaten, beraten wir Sie in allen Umweltfragen. Unsere Fachteams für Umweltplanung, Geodäsie, Geotechnik, Georadar, Abfall- und Entsorgungstechnik sowie Umweltservice unterstützen Sie bei der Umsetzung und Abwicklung Ihrer Projekte und setzen dabei auf innovativ erhobene Daten.

**DB Engineering & Consulting**

## FEREX 4.034

Präzises Erfassen  
von geomagnetischen  
Anomalien



[foerster-detection.com](http://foerster-detection.com)



# EINLADUNG ZUR DGG-MITGLIEDERVERSAMMLUNG

## 26. FEBRUAR 2025 IN BOCHUM



Im Namen des Vorstands der Deutschen Geophysikalischen Gesellschaft (DGG) e.V. laden wir alle Mitglieder der DGG im Rahmen unserer 85. Jahrestagung zur Mitgliederversammlung am **Mittwoch, 26. Februar 2025, von 17:00 Uhr bis ca. 19:00 Uhr ein**. Ort der Veranstaltung ist der Saal 2a des Veranstaltungszentrums. Die Veranstaltung findet nur in Präsenz statt.

Änderungen werden rechtzeitig auf der Tagungswebseite <https://dgg2025.dgg-tagung.de> bekannt gegeben.

### TAGESORDNUNG FÜR DIE DGG-MITGLIEDERVERSAMMLUNG 2025

- TOP 1: Begrüßung, Feststellung der fristgerechten Einberufung und der Beschlussfähigkeit
- TOP 2: Genehmigung der Tagesordnung
- TOP 3: Genehmigung des Protokolls der Mitgliederversammlung vom 10. März 2024 in Jena
- TOP 4: Bericht des Präsidenten
- TOP 5: Bericht der Geschäftsführung
- TOP 6: Bericht des Schatzmeisters
- TOP 7: Bericht der Kassenprüferinnen und Entlastung des Schatzmeisters
- TOP 8: Bericht zum Geophysical Journal International
- TOP 9: Berichte der „Rote Blätter“- und der GMIT-Redaktionen
- TOP 10: Kurzberichte der Leiterinnen und Leiter der DGG-Komitees:  
Publikationen, PRO-Public Relations & Out-reach, Ehrungen, Firmen, Mitglieder, Studierende, Studienfragen, Kooperationen, Chancengleichheit, Zukunft
- TOP 11: Kurzberichte der Sprecherinnen und Sprecher der DGG-Arbeitskreise:  
Angewandte Geophysik, Endlager Geophysik, Elektro-magnetische Tiefenforschung, Induzierte Polarisation, Seismik, Hydro- und Ingenieur-Geophysik, Dynamik des Erdinneren, Geodäsie/Geophysik, Vulkanologie, Geschichte der Geophysik, DGG-Archiv, Geothermie, Seismologie, Marine Geophysik, Kampfmitteldetektion, Geomagnetik
- TOP 12: Neues vom Dachverband Geowissenschaften (DVGeo) und aus den geowissenschaftlichen Gesellschaften
- TOP 13: Aussprache
- TOP 14: Entlastung des Vorstands
- TOP 15: Wahlen zum Vorstand (Präsidium und Beirat)
- TOP 16: Protokollarische Feststellung des Vorstands
- TOP 17: Wahl der Kassenprüferinnen und Kassenprüfer
- TOP 18: Anträge und Beschlüsse
- TOP 19: Verschiedenes

# Anregung, Aufzeichnung und Übertragung seismischer Daten.

DiGOS ist Ihr Ansprechpartner für zuverlässige und feld-erprobte Datenerhebung und Telemetrie. Unsere Lösungen stehen für einfache und sichere Handhabung, Präzision, geringen Strombedarf und hohe Produktqualität. Mehr als 3800 DATA-CUBE<sup>3</sup> oder CCUBE werden weltweit in über 45 Ländern erfolgreich für seismische und artverwandte Messungen eingesetzt.



## Entdecken Sie unsere neueste Entwicklung!

Wir freuen uns, Ihnen einen ortsaufgelöst dynamisch messenden faseroptischen Dehnungssensor, mit einer Auflösung im nm/m Bereich vorstellen zu können.

DiGOS

# ERKUNDUNGEN

mit dem Electrodynmaic Vibrator System EIViS VII

PLANUNG UND DURCHFÜHRUNG SEISMISCHER MESSUNGEN

BEARBEITUNG UND INTERPRETATION DER SEISMISCHEN DATEN

OBERFLÄCHENNAH UND HOCHAUFLÖSEND

**Gesamtgewicht:** ca. 130 kg

**Gewicht:** ca 32 kg (Quelle)

**Nutzfrequenzbereich:** 20-240 Hz

**Spitzenkraft:** ca. 1.100 N

**Energieversorgung:** 12 V DC

**Eindringungstiefe:**

S-Wellen bis zu 150 m

P-Wellen bis zu 500 m

**GEOSYM**

## SESSION – THEMENÜBERSICHT

**S1** – Rekonstruktion der Dynamik des tiefen Erdinnern über geologische Zeiträume

**S2** – Induzierte Seismizität

**S3** – Tektonische Geodäsie

**S4** – Induzierte Polarisation: Ein Paradigmenwechsel

**AG** – Airborne Geophysics / Fernerkundung

**BL** – Wissenschaftliches Bohren / Logging / Gesteins- und Mineralphysik  
*(nur Poster)*

**GD** – Geodynamik/Tectonophysik *(nur Vorträge)*

**GO** – Geophysik in der Öffentlichkeit und im Wandel der Zeit

**GT** – Geothermie/Radiometrie *(nur Poster)*

**KD** – Kampfmitteldetektion

**KI** – KI-Verfahren in der Geophysik

**MG** – Marine Geophysik  
*(nur Poster)*

**MI** – Modellierung/Imaging

**OG** – Oberflächennahe Geophysik

**OS** – Open Source in Forschung und Lehre

**PV** – Potentialverfahren  
*(nur Poster)*

**SM** – Seismik

**SO** – Seismologie

**VU** – Vulkanologie

**SENSYS®**  
Magnetometers & Survey Solutions

# Magnetic Survey

Aerial and ground based exploration

SENSYS magnetometer and TDEM solutions allow for precise measurement of magnetic fields and anomalies hidden underground.

[WWW.SSENSYS.DE](http://WWW.SSENSYS.DE)

Join our team!

## SCHWERPUNKTTHEMA S1

### **S1 – Rekonstruktion der Dynamik des tiefen Erdinnern über geologische Zeiträume**

*Stuart Gilder (Ludwig-Maximilians-Universität München)*

Mehrere hundert Male hat sich das Erdmagnetfeld im Lauf der Erdgeschichte umgepolt. Aus der Frequenz dieser Umpolungen schließen Forschende, dass es einen Zusammenhang des Geodynamos mit der Dynamik des Erdmantels gibt - diese Mechanismen sind jedoch noch nicht gut verstanden. Hier setzt das 2023 gestartete DFG Schwerpunktprogramm DeepDyn an, dessen Ziel es ist, mithilfe paläomagnetischer Daten und mathematischer Simulationen die Dynamik im Kern-Mantel-System über geologische Zeiträume hinweg zu rekonstruieren, um die Umpolungen des Erdmagnetfelds zu verstehen. In diesem interdisziplinären Projekt untersuchen PaläomagnetikerInnen, Experten für die Modellierung von Geodynamo und Erdmantel, SeismologInnen, MaterialwissenschaftlerInnen und BiologInnen gemeinsam, wie sich Temperaturänderungen an der Grenze zwischen Erdkern und Mantel während der letzten 100 Millionen Jahre auswirkten. Damit wird erstmals die Expertise aus allen relevanten Bereiche zusammengeführt: von der Biologie, die untersucht, ob fossile Überreste magnetotaktischer Bakterien helfen können, das magnetische Feld zu rekonstruieren, über die numerische Modellierung der Kopplung von Geodynamo- und Erdmantel bis hin zur Seismologie, die für die ModelliererInnen Strukturen an der Kern-Mantel-Grenze möglichst genau auflöst.

**PLENARVORTRAG:**

(Montag, 24.02.2025, Saal 2a)

**Andreas Fichtner**

*(Departement Erd- und Planetenwissenschaften, ETH Zürich, Schweiz):*

**REVEAL: Data-adaptive global full-waveform inversion**

## SCHWERPUNKTTHEMA S2

### S2 – Induzierte Seismizität

Rebecca Harrington (*Ruhr-Universität Bochum*)

Claudia Finger (*Fraunhofer IEG*)

Bei vielen Anwendungen, die auf eine Untergrundnutzung für die grüne Energiewende abzielen, wurde eine Aktivierung von vorhandenen Störungen beobachtet. Neben kleinen (mikroseismischen) Ereignissen, die mit industriellen Aktivitäten korreliert sein können, die den Spannungszustand im Untergrund verändern, gibt es eine wachsende Zahl von Beobachtungen und Modellierungen, die zeigen, dass auch aseismischer Bewegung induziert werden kann. Dennoch sind wir noch weit davon entfernt, die Kombination geologischer Bedingungen und Spannungs- und Betriebsparameter zu identifizieren, für die Seismizität auftritt, oder die Wechselwirkungen und Beobachtungen zwischen seismischen und aseismischen Bewegungen zu verstehen. Aktuelle Ansätze, die eine Vielzahl von georäumlichen Daten, neuartige Analysetechniken und Modellierungsansätze integrieren, bieten eine Perspektive für die Identifizierung der aktiven Prozesse, die zu einer unbeabsichtigten Störungsaktivierung durch eine Untergrundnutzung führen. Die Sitzungen werden sich auf Forschungsarbeiten konzentrieren, die darauf abzielen, hochauflösende Beobachtungen von induzierten seismischen und aseismischen Verschiebungen und deren Wechselwirkungen in Zeit und Raum zu integrieren, wobei ein besonderer Schwerpunkt auf kombinierten Daten und integrierten Multiphysik-Modellierungen aus dem breiten Spektrum von Geo-Energie-Anwendungen liegt, einschließlich der Nutzung geothermischer Energie, der unterirdischen Speicherung, der Kohlenstoffabscheidung und -speicherung (CCS), des Bergbaus, der Aufstauung von Reservoirn für die Wasserkraft und ähnlicher Aktivitäten.

#### PLENARVORTRAG:

(Dienstag, 25.02.2025, Saal 2a)

**Bettina Goertz-Allmann** (*NORSA, Norwegen*):

**Lessons learned from microseismic monitoring of induced seismicity at megaton-scale CCS sites**

## SCHWERPUNKTTHEMA S3

### S3 – Tektonische Geodäsie

Jonathan Bedford (*Ruhr-Universität Bochum*)

Peter LaFemina (*AWI Bremen*),

Sabrina Metzger (*GFZ Potsdam*)

Tektonische Geodäsie nutzt vor allem InSAR- und GNSS-Messungen für Untersuchungen von Plattengrenzen. In Deutschland gibt es mehrere Forschungsgruppen, die diese Messungen für tektonische Untersuchung auf verschiedenen räumlichen und zeitlichen Skalen einsetzen. Das Schwerpunktthema ist besonders aktuell, da die Menge an InSAR-Daten (insbesondere von den europäisch finanzierten Copernicus-Sentinel-Satellitenmissionen) in den letzten Jahren explodiert ist. Außerdem profitieren wir jetzt von der besseren Positionierungsgenauigkeit der europäischen Galileo-GNSS-Konstellation, während die Kosten für tektonisch hochwertige GNSS-Empfängertechnologie in den letzten Jahren drastisch gesunken sind, was viele spannende Möglichkeiten zur Verbesserung der Datenqualität und -menge eröffnet. Wir freuen uns auf Beiträge, die die Merkmale der Deformation der Erdoberfläche von lokalen Verwerfungen bis hin zur Plattenebene untersuchen. Wir erwarten auch Beiträge aus dem Kreis von WissenschaftlerInnen, die Methoden zur Datenverarbeitung entwickeln und mit tektonischer Geodäsie verbundenen Themen, wie geophysikalische Flüssigkeitsbelastungszyklen und langfristige isostatische Bewegungen, erforschen.

#### PLENARVORTRAG:

(Mittwoch, 26.02.2025, Saal 2a)

#### Enrico Serpelloni

(*Universität Bologna und Nationales Institut für Geophysik und Vulkanologie, Italien*):

**Continental scale strain mapping with GNSS: hydrological signals and seismotectonic phenomena**

## SCHWERPUNKTTHEMA S4

### S4 – Induzierte Polarisation: Ein Paradigmenwechsel

Katrin Breede (*Universität Clausthal-Zellerfeld*)

Matthias Bücker (*Universität Kiel*)

Matthias Halisch (*Leibniz-Institut für Angewandte Geophysik, Hannover*)

Tina Martin (*Lund University*)

Die induzierte Polarisation (IP) wurde nach ihrer kommerziellen Einführung in den 1950er Jahren vor allem für die mineralische Rohstoffexploration eingesetzt. Die frühen Anwendungen machten die Methode vor allem in der Bergbauindustrie unverzichtbar und ebneten den Weg für zahlreiche weitere geophysikalische Untersuchungen im Explorationsbereich. In der jüngeren Vergangenheit hat sich die IP von einer rein explorativen Methode hin zu einer vielseitigen Technologie entwickelt, die sowohl in der Grundlagenforschung als auch in der prozess- und anwendungs-bezogenen Forschung eine wichtige Rolle spielt. Diese Transformation wurde durch technologische Fortschritte und durch ein tieferes Verständnis der physikalischen Prozesse ermöglicht, die der IP zugrunde liegen. Insbesondere die Entwicklung von Spektraler IP (SIP) und die Integration von IP-Daten mit anderen geophysikalischen Methoden haben neue Perspektiven eröffnet. So findet IP heute Anwendung bei der Erforschung des geologischen Untergrunds und der Erfassung von Kontaminationen im Umweltbereich bis hin zur Überwachung von Prozessen in der Hydrologie und der Geotechnik, besonders für die Charakterisierung grundwasserführender Schichten und im Bereich des Klimaschutzes und der Klimaanpassung, so zum Beispiel zur Überwachung von Permafrostböden und zur Erkennung von Kohlenstoffspeicherungspotentialen. Sie schlägt dabei eine Brücke zwischen den physikalischen Eigenschaften des Untergrunds und der Modellierung geophysikalischer Prozesse. Mit der Integration neuer Technologien und Methoden, wie der 3D-Inversion und der Kombination von IP-Daten mit maschinellem Lernen, befindet sich die IP an der Schwelle zu einer neuen Ära.

**PLENARVORTRAG:**

(Donnerstag, 27.02.2025, Saal 2a)

**Jana H. Börner (TU BA Freiberg):**

**Beyond Boundaries: Advancing Induced Polarization in Challenging Geophysical Contexts**

# ALLGEMEINE HINWEISE

## POSTER

Täglich finden bis zu zwei Postersessions à 60 Minuten statt. Während dieser Zeit finden keine Vorträge statt. Während der Posterpräsentation der jeweiligen Session muss einer der AutorInnen anwesend sein.

Das Format ist A0 Hochformat. Alle Poster können während der gesamten Tagung besichtigt werden. Die Poster sollten vor Beginn der ersten Postersession am **Montagvormittag** aufgehängt werden.

## VORTRÄGE

Die Vortragszeit beträgt 15 Minuten zzgl. 5 Minuten für die Diskussion. Bitte laden Sie die Vorträge spätestens in der Pause vor der Session auf die Computer im Vortragssaum. Alternativ können Sie eigene Laptops benutzen. Diese können Sie in den Pausen testen.

## AUSZEICHNUNGEN

Die drei besten Poster und Vorträge des wissenschaftlichen Nachwuchses (Studierende und Promovierende mit noch nicht abgeschlossener Promotion) werden mit jeweils 150 € prämiert.

**Die Ausgezeichneten erhalten ihre Urkunde bei der Abschlussveranstaltung am Donnerstag.**

## FIRMENAUSSTELLUNG / JOBBÖRSE

Die Firmenausstellung findet im Zentrum des Konferenzgeschehens statt. Im Foyer des Veranstaltungszentrums und im Saal 1 sind die Stände zahlreicher Firmen zu finden.

Nutzen Sie als Konferenzteilnehmer/in die Möglichkeit, Kontakt zu Firmen aufzunehmen und sich über ihre neuesten Produkte und Entwicklungen sowie Jobangebote zu informieren. Ein schwarzes Brett für Stellenangebote und Stellengesuche wird bereitstehen.

## UMFRAGE



[www.empirio.de](http://www.empirio.de)

Liebe Tagungsteilnehmende,  
erneut bitten wir Sie/euch, an der Umfrage zur Tagungsstatistik teilzunehmen. Es sind insgesamt 10 Fragen, deren Beantwortung 3-4 Minuten beansprucht. Die Umfrage ist anonym und DSGVO konform. Vielen Dank!

*Für das Komitee Chancengleichheit Katrin Hannemann & Stefanie Donner bekannt gegeben.*

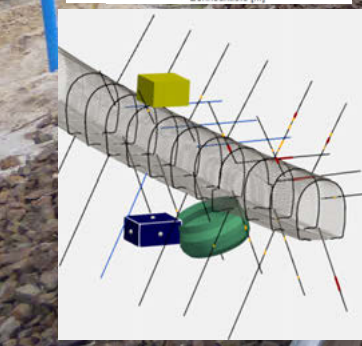
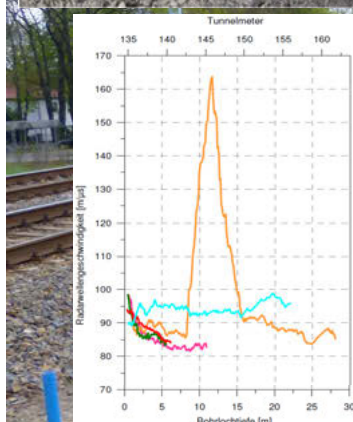
# Wir suchen einen Endlagerstandort für Deutschland



BUNDESGESELLSCHAFT  
FÜR ENDLAGERUNG



[www.bge.de](http://www.bge.de) | [www.einblicke.de](http://www.einblicke.de)



Kompetenz in  
geophysikalischer Erkundung

- + Kampfmittel
- + Leitungen/Einbauten
- + Baugrund
- + Hohlräume
- + Verkarstung
- + Subrosion
- + Störungen/Klüfte
- + Altbergbau

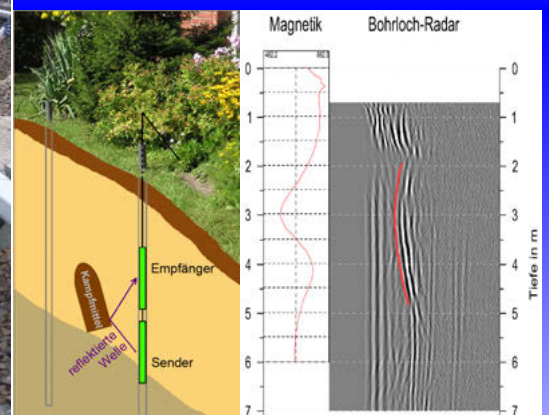


*Wir machen das  
Unsichtbare sichtbar*

 **Bo-Ra-tec**

Hegelstraße 5  
99423 Weimar  
Tel: +49 (0) 3643 / 7736920

Mail: [info@boratec.net](mailto:info@boratec.net)  
Net: [www.boratec.net](http://www.boratec.net)



# ERÖFFNUNGSVERANSTALTUNG – PROGRAMM

Montag, den 24.02.2025 von 16:00 bis ca. 17:30 Uhr im Saal 2a

---

Begrüßung durch die Tagungsleitung

**Prof. Dr. Jörg Renner**

---

*Musikalische Umrahmung*

---

Grußwort des Prorektors für Forschung  
und Transfer der RUB

**Prof. Dr. Günther Meschke**

---

Grußwort des Dekans der Fakultät für  
Geowissenschaftlichen

**Prof. Dr. Adrian Immenhauser**

---

Grußwort des Bürgermeister  
der Stadt Bochum

**Dr. Sascha Dewender**

---

Grußwort des Präsidenten der DGG

**Prof. Dr. Bodo Lehmann**

---

Verleihung der Ehrungen und Preise 2025

**Prof. Dr. Bodo Lehmann**

Walter-Kertz-Medaille

Dr. Ulrike Mattig, Wiesbaden

Rebeur-Paschwitz-Medaille

Prof. Dr. Vera Schlindwein, Bremerhaven

Karl-Zoeppritz-Preis

Dr. Lukas Römhild, Halle

Günter-Bock-Preis

Dr. Cora Strobel, Tübingen

Preis für herausragende Lehre

Dr. Jana Börner, Freiberg

---

*Musikalische Umrahmung*

---

im Anschluss (17:00 – 17:30 Uhr)

**COMPANY SLAM –> Dr. Claudia Finger**

Motto: „**1 Folie in 1 Minute**“ und anschließender **Eröffnung  
der Firmenausstellung** (ab 17:30 Uhr) mit Getränken und Brezeln  
im Foyer des Veranstaltungszentrums der RUB.

# VERANSTALTUNGEN

## Begrüßungsabend

Der Begrüßungsabend wird am **Sonntag**, den 23.02.2025 ab 18 Uhr in der Gaststätte „Kumpels“ (im Deutschen Bergbaumuseum: [www.kumpels.de](http://www.kumpels.de)) stattfinden. Registrierte Teilnehmer, die sich für den Begrüßungsabend angemeldet haben, erhalten dort ihre Tagungsunterlagen.

## Eröffnungsveranstaltung ↗

Die feierliche Eröffnungsveranstaltung findet am **Montag**, den 24.02.2025 von 16.00 Uhr bis 17.30 Uhr in Saal 2a des Veranstaltungszentrums statt.

## Eröffnung der Firmenausstellung ↗

Die Firmenausstellung beginnt am **Montag**, den 24. Februar im Anschluss an die Eröffnungsveranstaltung. In unserem 30-minütigen „Company Slam“ haben die ausstellenden Firmen die Möglichkeit, sich auf einer Folie kurz vorzustellen. Im Anschluss an die Vorstellung wird die Ausstellung bei Snacks und Getränken eröffnet.

## Studentischer Abend

Der studentische Abend findet am **Montag**, den 24. Februar 2025, ab 19:00 im Gebäude IC Ebene 03 Raum 149 (IC 03/149) statt und wird durch Studierende im Studiengang Geowissenschaften an der RUB organisiert.

## Gesellschaftsabend

Der traditionelle Gesellschaftsabend der DGG findet am **Dienstag**, den 25.02.2025 ab 19:00 Uhr (Einlass ab 18.30 Uhr) im Kolpinghaus Höntrop, Wattenscheider Hellweg 76, 44869 Bochum, statt.

Für Getränke findet eine Einzelabrechnung mittels persönlicher Verzehrkarten inkl. Rück erstattung nicht ausgeschöpfter Beträge statt. Eine Verzehrkarte im Wert von € 12 ist im Anmeldungspreis enthalten; weitere Karten können am Abend erstanden werden.

Zur Teilnahme am Gesellschaftsabend ist eine gesonderte Anmeldung bei der Registrierung erforderlich. Die Anreise ist mit den Straßenbahnenlinien 305 und 310 vom Hauptbahnhof Bochum möglich. Das Kolpinghaus Höntrop liegt kurz vor der Endhaltestelle Höntrop-Kirche. Die Fahrzeit von der Ruhr-Universität beträgt ca. 30 Minuten (inkl. Umstieg am HBF). Park möglichkeiten bestehen auf dem Parkplatz der Sparkasse Bochum in der Westenfelder Str. 199.

## DGG-Kolloquium Angewandte Geophysik ↗

Das DGG-Kolloquium findet am **Mittwoch**, den 26. Februar 2025 parallel zu den anderen wissenschaftlichen Sitzungen statt. Das Kolloquium wird vom Arbeitskreis „Angewandte Geophysik“ organisiert.

# VERANSTALTUNGEN

## Öffentlicher Abendvortrag

Der öffentliche Abendvortrag der DGG findet am **Mittwoch**, den 26. Februar 2025, 20:00–21:00 Uhr im Deutschen Bergbaumuseum statt.

Der Vortrag „Geothermische Wärme- und Kälteversorgung auf dem Areal Mark 51° in Bochum“ wird gehalten von Jochen Raube (*Stadtwerke Bochum*) und Dimitra Teza (*Fraunhofer IEG*).

Das Deutsche Bergbaumuseum ist über die Linie U35 direkt von der Ruhr-Universität Bochum erreichbar. Die Fahrzeit beträgt ca. 12 Minuten.

## Meet & Greet Frühstück für Wissenschaftlerinnen

Zum neunten Mal wird das **Meet & Greet Frühstück für Wissenschaftlerinnen** in diesem Jahr stattfinden. Das Frühstück findet am **Mittwoch**, den 26. Februar 2025 von 8:00 bis 9:30 Uhr im Tagungsraum 2 auf der Ebene des Haupteingang der Mensa oberhalb des Veranstaltungszentrums statt.

*Für die Teilnahme ist eine gesonderte Anmeldung bei der Registrierung erforderlich.*

## Lunchseminar Karriereperspektiven

Am **Mittwoch**, den 26.02.2025 von 13:00–14:00 Uhr im Saal 4 findet das „**Lunch-Seminar Karriereperspektiven**“ statt.

Geophysikerinnen und Geophysiker stellen exemplarisch ihre Werdegänge im Bereich der Geophysik vor und stehen für Fragen zur Verfügung.

*Es ist eine Anmeldung bei der Registrierung erforderlich.*

## Lunch'n Learn

Am **Donnerstag**, den 27. Februar von 13:00–14:00 Uhr im Saal 4 findet ein **Lunch'n Learn** statt. Ziel dieser Veranstaltung mit einem Impuls vortrag und Mittagsimbiss ist die Vernetzung junger Geowissenschaftler/innen, um den Austausch sowohl auf der professionellen als der persönlichen Ebene zu fördern.  
*Es ist eine Anmeldung bei der Registrierung erforderlich.*

# DGG-KOLLOQUIUM

## **DGG-Kolloquium Angewandte Geophysik**

Das DGG-Kolloquium legt dieses Jahr den Fokus auf das Thema „Seismisches Monitoring“. Es findet am **Mittwoch, 26.2.2025, im Saal 3** statt. Das Kolloquium wird vom Arbeitskreis Angewandte Geophysik organisiert. Die Kurzfassungen werden in einem Sonderband der DGG-Mitteilungen veröffentlicht.

- 
- 09.20 - 09.50    **Fibre optic sensing of fast and slow volcanic processes.**

Philippe Jousset (GFZ), Gilda Currenti (INGV), Egill Á. Gudnason (ISOR),  
Lise Holstein (GFZ), Christopher Wollin (GFZ), Sergio Diaz-Meza (GFZ),  
Michele Prestifilippo (INGV), Gylfi P. Hersir (ISOR) and C. Krawczyk (GFZ)

---

- 9.50 - 10.20    **Advances in monitoring of induced seismicity at the Balmatt Deep Geothermal Energy plant in Mol, Belgium.**

Luc Moutote, Simon Kremers, Lorenz Marten,  
Ralf Fritschen (DMT GmbH & Co KG), Matsen Broothaers,  
Ben Laenen (VITO)

---

- 10.20 - 11.20    Kaffepause
- 

- 11.20 - 11.50    **Monitoring of a CO<sub>2</sub> Injection at the Selvik test-site in Norway using cross-hole seismic methods**

Thomas Fechner, Uta Koedel, (Geotomographie GmbH)  
und Anna Stork (Silixa Ltd.)

---

- 11.50 - 12.20    **Geotechnisches Monitoring zur Erfassung von Deformationen im Baugrund und Baugrubenverbau - Praxisbeispiele zu Anwendungen der Beobachtungsmethode.**

Sebastian Brenne und Markus Stolz (Solexperts AG)

---

- 12.20 - 12.50    **Sensoren und Datenlogger für die seismische Bergbauüberwachung.**

Thomas Schicht (K-UTEC AG)

# SITZUNGSTERMINE

## Sitzungen der Arbeitskreise und Komitees

Die Arbeitskreise und Komitees der DGG haben die Möglichkeit, sich während der Jahrestagung zu treffen. Hierfür werden Seminarräume zur Verfügung gestellt.

---

**Komitee Studienfragen**, 24.02.2025, 19:00–21:00, Raum IA 01/113

---

**AG Induzierte Seismizität**, 24.02.2025, 19:00–21:00, Raum IA 01/480-481

---

**FKPE AK Observatorien**, 25.02.2025, 11:30–13:00, Raum IA 02/4880-481

---

**Berufsverband Deutscher Geowissenschaftler (BDG)**, 25.02.2025, 14:00–17:00, Tagungsraum 2

---

**Komitee Firmen**, 25.02.2025, 17:00 - 18:00, Tagungsraum 2 (*im Anschluss an das BDG Treffen*)

---

**AK Elektromagnetische Tiefenforschung**, 25.02.2025, 17:00–19:00, Raum IA 02/480-481

---

**AK Hydro- und Ingenieurgeophysik und AK Seismik**, 25.02.2025, 18:00–18:30, Saal 2a

---

**AK Induzierte Polarisation**, 26.02.2025, 09:00–09:40, Saal 4

---

## Weitere Sitzungstermine

### **FKPE-Sitzung (auf Einladung)**

Sonntag, 23. Februar 2025, 11:00–18:00 Uhr, Raum IA 1/117

### **DGG-Vorstandssitzungen (auf Einladung)**

Dienstag, 25.02.2025, 9:00–13:00 Uhr, Tagungsraum 2

Donnerstag, 27.02.2025, ca. 16:00–16:30 Uhr

(im Anschluss an die Abschlussveranstaltung im selben Saal)

## EXKUSIONEN

Aus dem reichhaltigen Kulturprogramm hat das Organisationsteam für die Tagungsteilnehmer eine Reihe von Anregungen für Unternehmungen in Bochum und Umgebung zusammengestellt. Details dazu finden Sie auf der Homepage der Tagung ↗. Sprechen Sie uns gerne an, wenn Sie dazu Fragen haben.

## WEITERE ORGANISATORISCHE INFORMATIONEN

### Internetzugang

Während der DGG-Tagung wird permanent kostenloser WLAN-Zugang möglich sein. Es werden zwei Verbindungsmöglichkeiten bereitgestellt:

- 1) Die Ruhr-Universität Bochum ist Mitglied im weltweiten universitären eduroam Netz. Alle, die in ihrer Heimatinstitution einen eduroam-Zugang haben, können sich bei uns mit ihren normalen Benutzerdaten mit dem Internet verbinden. Dies Variante ist die einfachste und bevorzugte.
- 2) Für alle anderen (oder falls es Login-Probleme geben sollte) stellt die Ruhr-Universität Bochum individuelle Gast-Zugänge bereit. Hierzu wird bei der Registrierung vor Ort ein personalisierter Anmeldezettel verteilt, dem die Zugangsinformationen zu entnehmen sind.

### Essen/Ausgehen

Direkt oberhalb des Tagungszentrums befindet sich die Hauptmensa der Ruhr-Universität Bochum sowie das vegane Selbstbedienungsrestaurant „Rote Bete“ und eine Kaffeebar.

Auf dem Campus befinden sich noch das Q-West, das auch abends geöffnet ist, und mehrere Cafeterien (z. B. im Gebäude IB). Diese Einrichtungen sind auch für Gäste geöffnet.

**Es ist nur Kartenzahlung möglich.** Nördlich der Ruhr-Universität befindet sich das Einkaufszentrum „UniCenter“ mit zahlreichen Geschäften und Restaurants.

Abends bietet sich das Bermuda3Eck an. Es ist Bochums Ausgehviertel schlechthin und ist über die Stadtgrenzen hinaus bekannt. Fast 90 Bars, Restaurants und Kneipen sorgen für Vielfalt und gute Stimmung und laden sowohl zum Versacken als auch zum Weiterziehen ein. Egal ob entspanntes Feierabendbier, ein leckerer Cocktail oder Party bis in die Nacht – hier wird dein Abend zum Erlebnis, denn es gibt viel zu entdecken. Und wer weiß, vielleicht verlierst auch du dich im Bermuda3Eck Bochum und lernst die diversen Locations in der kultigen Partymeile Bochums kennen.

### Öffentlicher Nahverkehr in Bochum

Am nördlichen Rand befinden sich die Haltestellen mehrere Buslinien und eine Haltestelle der U-Bahn Linie U35. Diese verbindet die Universität mit der Innenstadt.

Die Fahrzeit zum **Hauptbahnhof** beträgt ca. 10 Minuten.

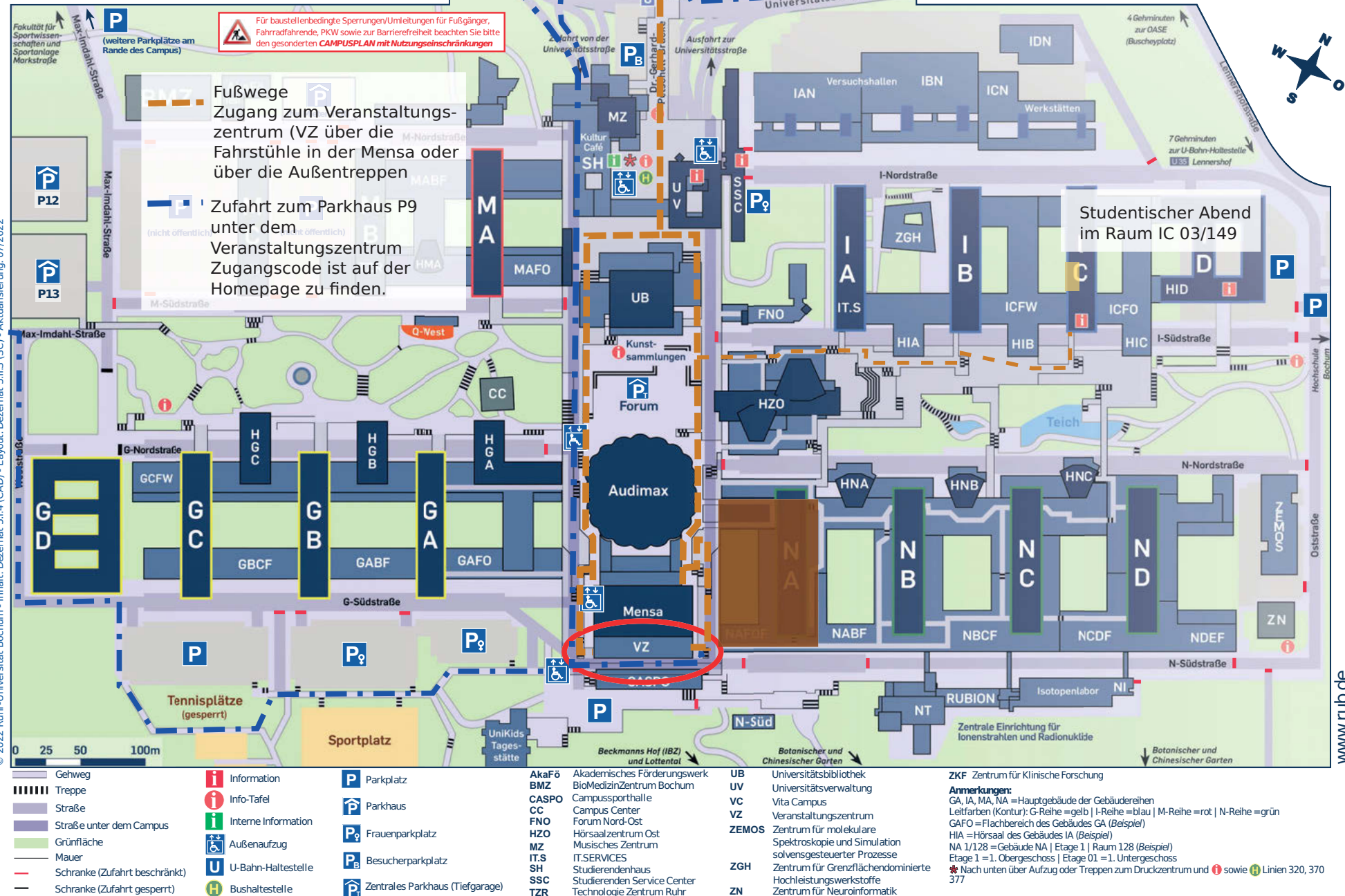
Für Fahrten innerhalb der Stadtgrenze Bochums ist eine Fahrkarte der Preisstufe A nötig. Fahrkarten können am Automaten erworben werden. In den Bussen können Fahrkarten auch beim Fahrer (nur Einzelfahrkarten) erworben werden. Selbstverständlich ist auch das DeutschlandTicket gültig. Ansonsten empfehlen wir Mehrfachfahrkarten:

*4-er- oder 10-er-Karten – nur über die App des Verkehrsbetriebs Bogestra oder des Verkehrsverbundes VRR.*

# CAMPUSPLAN

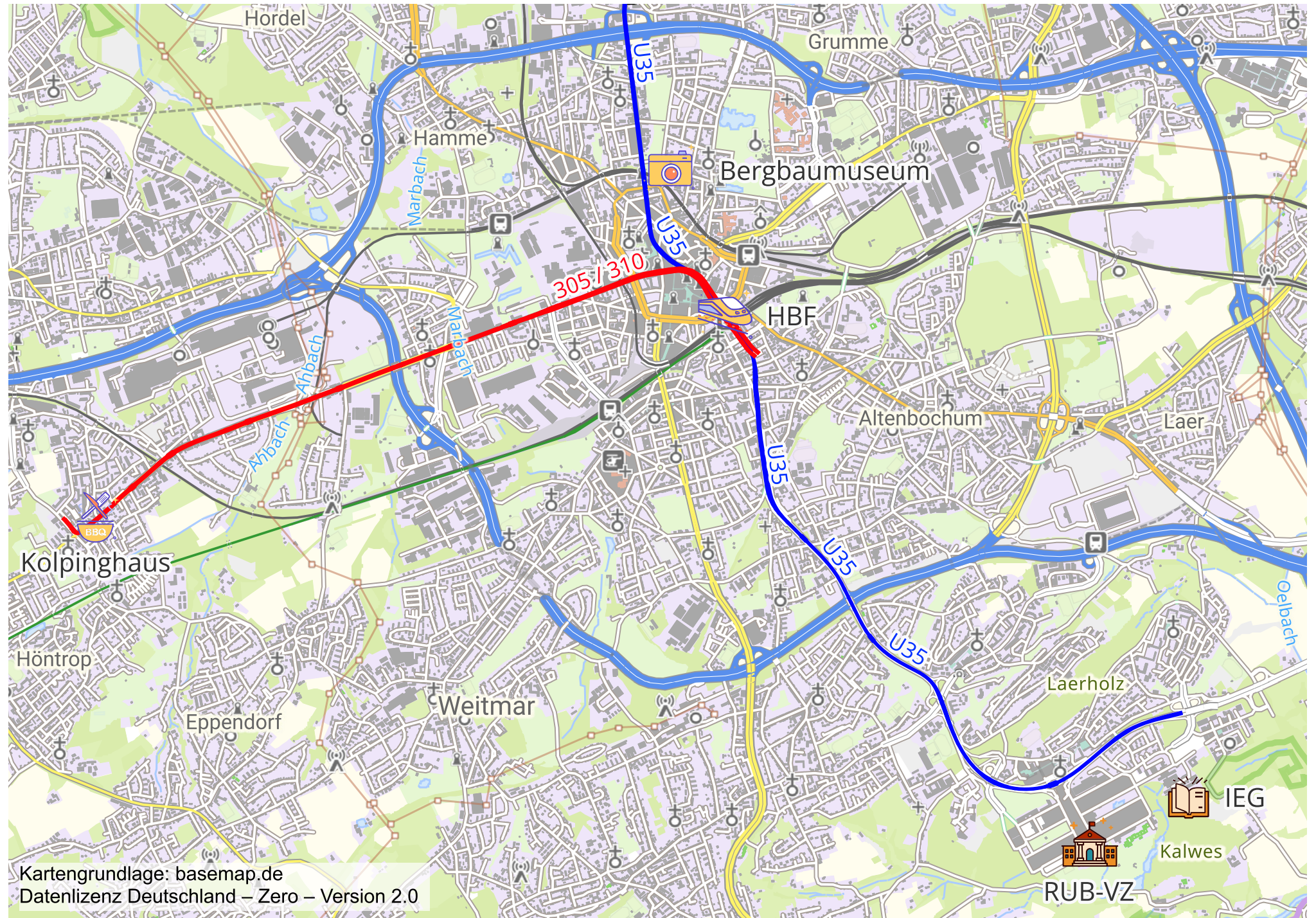
**RUB**

© 2022 Ruhr-Universität Bochum - Inhalt: Dezernat 5.I.4 (CAD) - Layout: Dezernat 5.I.3 (SC) - Aktualisierung: 07/2022



RUHR  
UNIVERSITÄT  
BOCHUM

[www.rub.de](http://www.rub.de)



# MIT INNOVATION & TEAMWORK HOCH HINAUS



## GEMEINSAM FÜR QUALITÄT!

- durch Forschung & Entwicklung
- durch modernste Technik
- durch geschultes Fachpersonal
- durch Teamwork

Bundesweit arbeiten über 40 Mitarbeiter\*innen aus der Geophysik & den Geowissenschaften eng zusammen. Die einzigartige Verbindung von Alltagsprojekten und innovativer Forschung & Entwicklung macht unsere Arbeit besonders.



## KOMM INS TEAM!

- Begleitung von Bachelor- & Masterarbeiten
- Praktikum/Werkstudentenjob
- Geo-Trainee-Programm
- Fort- & Weiterbildung mit der TAUBER-Akademie

### Interesse?

Sende uns eine Nachricht an [tgc@munition.de](mailto:tgc@munition.de) oder melde Dich unter +49 (0) 172 14 989 69.



35 Jahre Erfahrung in Rohstoffexploration, Geotechnik, Geothermie- und Grundwassererkundung



- ▼ **Aerogeophysik**  
Magnetik, Radiometrie, Gravimetrie  
G2D-EM (Drohnengeophysik)
- ▼ **Oberflächengeophysik**  
ERT, IP, HIRIP, Magnetik, Gravimetrie,  
MT, AMT, CSAMT, RMT, TDEM, FEM
- ▼ **Bohrlochgeophysik**  
Physikalische Eigenschaften,  
strukturgeologische Interpretation,  
Bohrlochvermessung und Bohrloch-EM



**terrateg services GmbH & Co. KG**

Schillerstraße 3, DE - 79423 Heitersheim

Tel.: +49 (0) 7634 50319 0

E-Mail: [sales@terrateg-geoservices.com](mailto:sales@terrateg-geoservices.com)

[www.terrateg-geoservices.com](http://www.terrateg-geoservices.com)

[LinkedIn](#) [Instagram](#)



Geotomographie  
Seismic Borehole Equipment  
for P-, SH- and SV-Waves



Besuchen Sie uns  
an unserem Stand  
auf der DGG2025  
in Bochum

[www.geotomographie.de](http://www.geotomographie.de)

# DGG 2025 TAGUNGSPROGRAMM – ÜBERSICHT

## SONNTAG, 23. FEBRUAR 2025

ab 18.00 Uhr Begrüßungsabend im Bergbaumuseum, Ausgabe der Tagungsunterlagen

## MONTAG, 24. FEBRUAR 2025

ab 08.00 Uhr	Registrierung
09.20–10.20 Uhr	Vorträge (S1, AG)
10.20–11.20 Uhr	Kaffeepause
11.20–13.00 Uhr	Vorträge (S1, VU, KD)
13.00–14.00 Uhr	Mittagspause
14.00–15.00 Uhr	Plenarvortrag S1
15.00–16.00 Uhr	Posterausstellung (S1, AG, KD, MG, VU) + Kaffeepause
16.00–17.30 Uhr	Eröffnungsveranstaltung mit Company Slam
17.30–19.00 Uhr	Eröffnung Firmenausstellung
ab 19.00 Uhr	studentischer Abend in Raum IC 03/149

## MITTWOCH, 26. FEBRUAR 2025

08.00–09.30 Uhr	Meet & Greet
09.00–13.00 Uhr	DGG Kolloquium Angewandte Geophysik
09.20–10.20 Uhr	Vorträge (SO, S3)
10.20–11.20 Uhr	Posterausstellung (SO, S3, BL) + Kaffeepause
11.20–13.00 Uhr	Vorträge (SO, S3)
13.00–14.00 Uhr	Mittagspause + Lunchseminar
14.00–15.00 Uhr	Plenarvortrag S3
15.00–16.00 Uhr	Vorträge (SO, GD)
16.00–17.00 Uhr	Posterausstellung (GT, PV, SO) + Kaffeepause
17.00–19.00 Uhr	Mitgliederversammlung
20.00–21.00 Uhr	öffentlicher Abendvortrag im Deutschen Bergbau-Museum

## DIENSTAG, 25. FEBRUAR 2025

09.00–10.20 Uhr	Vorträge (OG, MI)
10.20–11.20 Uhr	Posterausstellung (OG, MI, GO) + Kaffeepause
11.20–13.00 Uhr	Vorträge (OG, MI)
13.00–14.00 Uhr	Mittagspause + Firmenvorführung
14.00–15.00 Uhr	Plenarvortrag S2
15.00–16.00 Uhr	Vorträge (OG, S2)
16.00–17.00 Uhr	Posterausstellung (S2, OG, OS) + Kaffeepause
17.00–18.00 Uhr	Vorträge (OG, GO, OS, S2)
ab 19.00 Uhr	Gesellschaftsabend im Kolping-Haus Höntrop

## DONNERSTAG, 27. FEBRUAR 2025

9.00–10.20 Uhr	Vorträge (SO, SM, S4)
10.20–11.20 Uhr	Posterausstellung (S4, KI, SM) + Kaffeepause
11.20–13.00 Uhr	Vorträge (SO, KI, S4)
13.00–14.00 Uhr	Mittagspause + Lunch'n'Learn
14.00–15.00 Uhr	Plenarvortrag S4
15.00–16.00 Uhr	Abschlussveranstaltung mit Prämierung Poster und Vorträge

## FREITAG, 28. FEBRUAR 2025

8.30–16.00 Uhr	SEG-DGG Workshop (extra Anmeldung)
----------------	---------------------------------------



# Promoting scientific talents



Institute for  
Applied Geophysics

LIAG

## Become a member of our LIAG family!

- Exciting topics of societal importance
- A great combination of geophysical tools and methods
- A creative and non-hierarchical working space
- Interesting external and internal trainings in our LIAG graduate school
- Flexible working hours
- Spatial and technical integration into the Geozentrum Hannover
- Extensive social and recreational infrastructure of the state capital of Lower Saxony



Apply for open positions or do your master's thesis at LIAG!

More information on our website: [www.leibniz-liag.de/institut/karriere](http://www.leibniz-liag.de/institut/karriere)

Follow us on:

DMT

Engineering  
Performance

# SUMMIT X One

Unique Flexibility for Seismic Experts

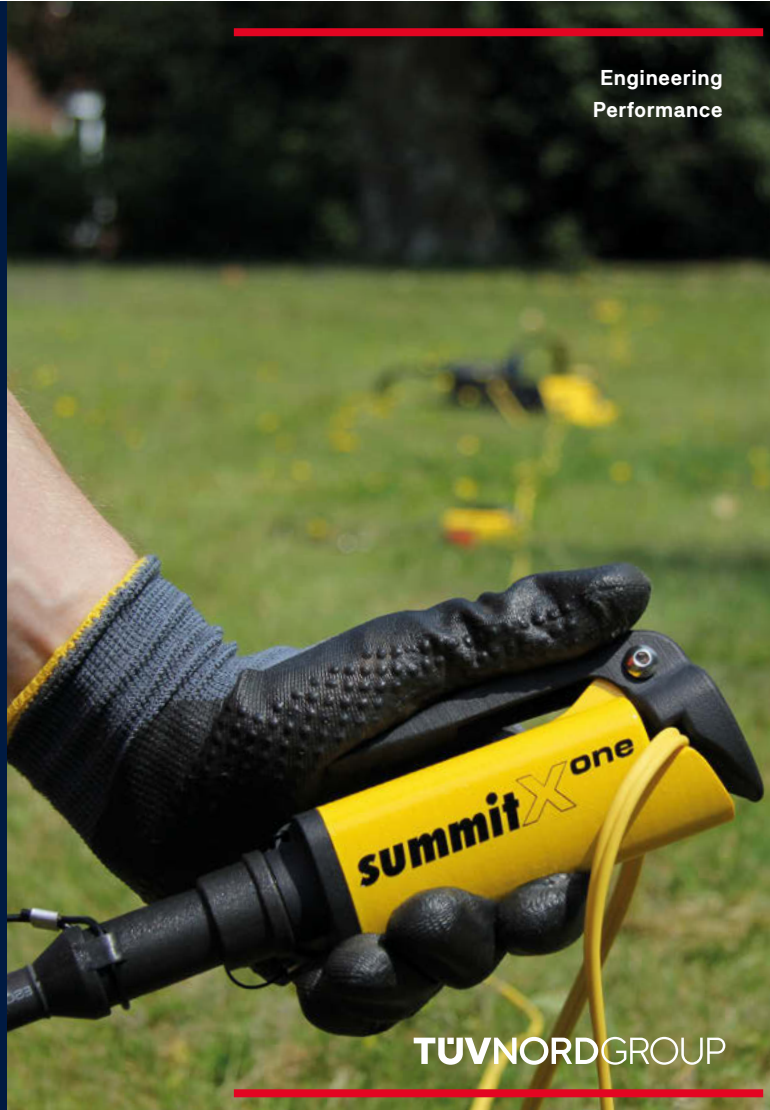
SUMMIT X One, the world's most flexible seismic acquisition system – combines the advantages of cableless and cable systems and represents the latest generation of DMT's long-standing SUMMIT product line of field seismographs.

#### System benefits:

- For 2D/3D seismic surveys
- Most flexible field deployment
- Fully scalable system
- Fast data transmission with online data control
- Highest productivity
- Easy field logistics
- Continous recording
- Only one battery for up to 50 single channels

„Set up and field handling with SUMMIT X One is very easy, flexible and fast. The system is reliable and data quality is of highest standard ...“

John Whiteford (Whiteford Geoservices Ltd)





## Mehr als 70 Jahre geophysikalische Dienste in Leipzig

geologische Interpretation  
& Modellierung

Datenbearbeitung



Gesellschaft für Geowissenschaftliche Dienste mbH

Bornaische Str. 120  
04279 Leipzig

Consulting

Planung & Durchführung  
geophysikalischer Feldmessungen

Digitalisierung &  
Aufbereitung

[www.geophysik-ggd.com](http://www.geophysik-ggd.com)



Wir gestalten die klimaneutralen  
Energiesysteme der Zukunft.

Fraunhofer-Einrichtung für Energieinfrastrukturen  
und Geotechnologien IEG

Forschung

Geothermie

Entwicklung



Besuchen Sie uns auf unserem Stand und online auf [www.ieg.fraunhofer.de](http://www.ieg.fraunhofer.de)

## DGG 2024 – PROGRAMM

› Montag 24. Februar 2025 ..... S. 31–35 ↗

› Dienstag 25. Februar 2025 ..... S. 35–42 ↗

› Mittwoch 26. Februar 2025 ..... S. 43–49 ↗

› Donnerstag 27. Februar 2025 ..... S. 50–54 ↗

## Schwerpunktsession – Saal 2a

### 09:20–10:20 O-S1 Rekonstruktion der Dynamik des tiefen Erdinnern über geologische Zeiträume

Moderation: C. Weber, Münster

#### 09:20–09:40 O-S1-01 Influence of Pressure on the Curie Temperature of Titanomagnetite

S.-M. Platzer, S. A. Gilder

*Ludwig-Maximilians-Universität München, Earth and Environmental Sciences, Munich*

#### 09:40–10:00 O-S1-02 Global characteristics of geomagnetic field reversals and excursions

M. Korte, A. N. Mahgoub, S. Shinu

*Deutsches GeoForschungsZentrum GFZ, Potsdam*

#### 10:00–10:20 O-S1-03 Palaeomagnetic secular variation at mid latitude: preliminary results from Vogelsberg (15–18 Ma) and Lausitz (29–32 Ma)

F. Lhuillier<sup>1</sup>, Y. Chi<sup>1</sup>, S. Hahn<sup>1</sup>, A. C. Manarcescu<sup>1</sup>, M. N. Putri<sup>1</sup>, J. Büchner<sup>2</sup>

<sup>1</sup>*Ludwig-Maximilians-Universität, Geophysik, München, Germany,*

<sup>2</sup>*Senckenberg Museum für Naturkunde, Görlitz*

## Oral – Saal 3

### 09:20–10:20 O-AG AG - Airborne Geophysics / Fernerkundung

Moderation: H. Sudhaus, Karlsruhe

#### 09:20–09:40 O-AG-01 Post-disaster impact assessment over urban environments by fusion of earth observation data

O. Stein<sup>1</sup>, H. Sudhaus<sup>2</sup>, A. Muhuri<sup>3</sup>

<sup>1</sup>*Institut für Geowissenschaften an der Christian-Albrechts-Universität zu Kiel, Aero- und Satellitengeophysik, Kiel, Germany*, <sup>2</sup>*Karlsruhe Institute of Technology (KIT), Geophysical Institute, Karlsruhe, Germany*, <sup>3</sup>*Geographisches Institut an der Christian-Albrechts-Universität Kiel, Earth Observation and Modelling, Kiel*

#### 09:40–10:00 O-AG-02 Efficient Large-Scale 3D Subsurface Imaging Using Semi-Airborne Electromagnetics

S. Nazari<sup>1</sup>, R. Rochlitz<sup>1</sup>, A. Thiede<sup>2</sup>, M. Schiffler<sup>3</sup>, C. Walther<sup>4</sup>, A. Steuer<sup>4</sup>, P. Yogeshwar<sup>5</sup>, M. Becken<sup>2</sup>, T. Günther<sup>6</sup>

<sup>1</sup>*LIAG Institute For Applied Geophysics, Hannover, Germany*, <sup>2</sup>*Institute for Geophysics, University of Münster, Münster, Germany*, <sup>3</sup>*Leibniz Institute of Photonic Technology, Jena, Germany*, <sup>4</sup>*Federal Institute for Geosciences and Natural Resources (BGR), Hannover, Germany*, <sup>5</sup>*University of Cologne, Cologne, Germany*, <sup>6</sup>*Technische Universität Bergakademie Freiberg, Freiberg*

#### 10:00–10:20 O-AG-03 Interferometric radar satellite and in-situ well time-series reveal groundwater extraction rate changes in urban and rural Afghanistan

N. Kakar<sup>1</sup>, S. Metzger<sup>2</sup>, T. Schöne<sup>1</sup>, M. Motagh<sup>3</sup>, H. Waizy<sup>4</sup>, N. A. Nasrat<sup>4</sup>, F. Amelung<sup>5</sup>, M. Lazecky<sup>6</sup>, B. Bookhagen<sup>7</sup>

<sup>1</sup>*GFZ Helmholtz-Zentrum für Geoforschung, Globales Geomonitoring und Schwerefeld, Potsdam, Germany*

<sup>2</sup>*GFZ Helmholtz-Zentrum für Geoforschung, Lithosphärenodynamik, Potsdam, Germany*, <sup>3</sup>*GFZ Helmholtz-Zentrum für Geoforschung, Fernerkundung und Geoinformatik, Potsdam, Germany*, <sup>4</sup>*Kabul Polytechnic University, Faculty of Geology and Mines, Kabul, Afghanistan*, <sup>5</sup>*University of Miami, Departement of Marine Geosciences, Miami, United States of America*, <sup>6</sup>*University of Leeds, COMET, School of Earth and Environment, Leeds, United Kingdom*, <sup>7</sup>*Universität Potsdam, Fernerkundung und Geomorphologie, Potsdam*

### 10:20–11:20 Kaffeepause

## Schwerpunktsession – Saal 2a

<b>11:20–12:20 O-S1</b>	<b>Rekonstruktion der Dynamik des tiefen Erdinnern über geologische Zeiträume</b>
	Moderation: S.-M. Platzer, München
11:20–11:40	O-S1-04
	<b>Effects of Rheological Parameters on the Stability of Thermochemical Piles and Plumes</b>
	<u>H. W. Sitte, C. Weber, C. Stein, U. Hansen</u>
	<i>Universität Münster, Institut für Geophysik, Münster</i>
11:40–12:00	O-S1-06
	<b>Double diffusive finger convection in the core: The contribution from experiments</b>
	<u>A. Rosenthal, A. Tilgner</u>
	<i>Universität Göttingen, Göttingen</i>
12:00–12:20	
	<b>Core material penetrating the mantle as one cause for dense CMB structures? (Cancelled)</b>
	<u>C. Stein, U. Hansen</u>
	<i>Institut für Geophysik, Universität Münster, Münster</i>

## Oral – Saal 3

<b>11:20–12:40 O-VU</b>	<b>VU - Vulkanologie</b>
	Moderation: M. Hensch, Freiburg
11:20–11:40	O-VU-01
	<b>Observation of electric phenomena associated with eruptions of Strokkur Geyser, Iceland</b>
	<u>J. Börner<sup>1</sup>, M. Hort<sup>1</sup>, D. Peppel<sup>2</sup>, M. Scheunert<sup>1</sup>, C. Schneider<sup>2</sup>, K. Spitzer<sup>1</sup></u>
	<sup>1</sup> TU Bergakademie Freiberg, Institut für Geophysik und Geoinformatik, Freiberg, Germany, <sup>2</sup> Universität Hamburg, Institut für Geophysik, Hamburg
11:40–12:00	O-VU-02
	<b>TEM at breathtaking heights: Imaging the shallow fumarolic system of Lastarria volcano, Chile</b>
	<u>T. Vondenhoff<sup>1</sup>, B. Blanco-Arrué<sup>2</sup>, J. Roas-Domingo<sup>1</sup>, B. Tezkan<sup>1</sup>, D. Diaz<sup>3</sup>, P. Yogeshwar<sup>1</sup></u>
	<sup>1</sup> Institute für Geophysik und Meteorologie, Universität zu Köln, Köln, Germany, <sup>2</sup> LIAF Institute for Applied Geophysics, Hannover, Germany, <sup>3</sup> Department of Geophysics, University of Chile, Santiago, Chile
12:00–12:20	O-VU-03
	<b>Onshore seismic monitoring of submarine Kavachi volcano reveals vigorous eruptive activity</b>
	<u>G. Rümpker<sup>1,2</sup>, C. Roga<sup>3</sup>, A. Kaviani<sup>1</sup>, F. Limberger<sup>1</sup>, L. Bitzan<sup>1</sup>, P. Laumann<sup>1</sup>, C. Tatapu<sup>3</sup>, J. Gwali<sup>3</sup>, T. Manker<sup>1</sup>, C. Vehe<sup>3</sup></u>
	<sup>1</sup> Goethe-Universität Frankfurt, Frankfurt, Germany, <sup>2</sup> Frankfurt Institute for Advanced Studies, Frankfurt, Germany, <sup>3</sup> Ministry of Mines, Energy and Rural Electrification, Geological Survey Division, Honiara, Solomon Islands
12:20–12:40	O-VU-04
	<b>The nature of volcanic tremor at Oldoinyo Lengai volcano, Tanzania</b>
	<u>M. C. Reiss<sup>1</sup>, D. Roman<sup>2</sup>, C. Caudron<sup>3</sup>, P. Hering<sup>4</sup></u>
	<sup>1</sup> Gutenberg Universität Mainz, Institut für Geowissenschaften, Mainz, Germany, <sup>2</sup> Carnegie Science, Washington, United States of America, <sup>3</sup> Université Libre de Bruxelles, G-Time, Brüssel, Belgium, <sup>4</sup> Igem, Bingen

## Oral – Saal 4

<b>11:20–12:20 O-KD</b>	<b>KD - Kampfmitteldetektion</b>
	Moderation: T. Wunderlich, Kiel
11:20–11:40	O-KD-01
	<b>Der DGG Arbeitskreis Kampfmitteldetektion – Erste Erfolge, laufende Projekte und Ziele für die Zukunft</b>
	<u>J.-P. Schmoldt<sup>1</sup>, T. Wunderlich<sup>2</sup>, P. Gödickmeier<sup>3</sup>, A. Fahl<sup>4</sup>, DGG-Arbeitskreis Kampfmitteldetektion</u>
	<sup>1</sup> Niedersächsisches Landesamt für Bau und Liegenschaften (NLBL), Referat BL 37, Hannover, Germany,
	<sup>2</sup> Christian-Albrechts-Universität, Institut für Geowissenschaften, Angewandte Geophysik, Kiel, Germany,
	<sup>3</sup> SENSYS Sensorik & Systemtechnologie GmbH, Bad Saarow, Germany, <sup>4</sup> KampfmittelService B&E GmbH, Würzburg

11:40–12:00	O-KD-02	<b>Aktuelle Entwicklungen bei der Detektion von marinen Munitionsaltlasten am GEOMAR</b> <u>M. Seidel, M. Keller</u> <i>GEOMAR Helmholtz-Zentrum für Ozeanforschung Kiel, DeepSea Monitoring, Kiel</i>
12:00–12:20	O-KD-03	<b>Elektromagnetik im Bohrloch – Projektbeispiel Grasbrook, Hamburg</b> <u>O. Geisler</u> <i>EGGERS Kampfmittelbergung GmbH, Tangstedt</i>
<b>13:00–14:00</b>		<b>Mittagspause</b>

## Schwerpunktsession – Saal 2a

### 14:00–15:00 O-S1-PV REVEAL: Data-adaptive global full-waveform inversion

English      Moderation: S. Gilder, München

A. Fichtner

*ETH Zurich, Department of Earth & Planetary Sciences, Zürich, Switzerland*

### 15:00–16:00 Kaffeepause

## Poster – Saal 2b

### 15:00–16:00 P1

#### Poster S1, AG, KD, MG, VU

Moderation: H. Sudhaus, Karlsruhe (AG), M. Hensch, Freiburg (VU), T. Wunderlich, Kiel (KD), V. Schlindwein, Bremerhaven (MG)

- P-S1-01      **Lower mantle 3-D density structure from joint inversion of gravity and normal mode data**  
W. Szwilus  
*CAU Kiel, Kiel*
- P-S1-02      **Investigation of the D'' reflector with short epicentral distances**  
J. Pahlings, C. Thomas  
*Universität Münster, Institut für Geophysik, Münster*
- P-S1-03      **Determination of <em>X</em>KS splitting parameters in the lowermost mantle beneath Siberia**  
F. Dorn, M. I. F. Dillah, Y. Fröhlich, J. R. R. Ritter  
*Karlsruhe Institute of Technology, Geophysical Institute (GPI), Karlsruhe*
- P-S1-04      **Determination of <em>X</em>KS splitting parameters in the Earth's lowermost mantle beneath the North Atlantic**  
M. Dillah, F. Dorn, Y. Fröhlich, J. Ritter  
*Karlsruher Institut für Technologie, Geophysics, Karlsruhe*
- P-S1-05      **On the influence of the solidification mechanism on magma ocean dynamics**  
C. Maas, U. Hansen  
*Universität Münster, Institut für Geophysik, Münster*
- P-S1-06      **Magneto-rotating double-diffusive convection in stable layers at the top of Earth's core**  
C. Weber, S. Stellmach  
*University of Münster, Institut of Geophysics, Münster*
- P-KD-01      **Kampfmitteldetektion mittels Bohrloch-Georadar - Verfahren. Unterschiede zwischen Reflexions- und Tomographie-Sondierungen**  
J.-P. Schmoldt, S. Kroll, S. Gremmler  
*Niedersächsisches Landesamt für Bau und Liegenschaften (NLBL), Referat BL 37, Hannover and others*
- P-KD-02      **Evaluating Ground Penetrating Radar (GPR) Capabilities for UXO Detection: Influence of Target Characteristics, Antenna Frequency, and Survey Design**  
O. Shata, R. Linck, J. Schmoldt, S. Gremmler, A. Stele  
*Ludwig-Maximilians-University, Department of Earth and Environmental Sciences, Geophysics, Munich and others*

P-KD-03	<b>Testing multi-receiver FD-EMI sensors on UXO targets: a controlled experiment.</b> <u>J. Guillemotteau, T. Wunderlich, J.-P. Schmoldt</u> <i>Universität Potsdam, Institut für Geowissenschaften, Potsdam and others</i>
P-MG-01	<b>Aktueller Stand der Umsetzung des Geologiedatengesetzes im marinen Bereich - Schwerpunkt „Seismische Messungen“ in der AWZ</b> <u>M. Breitzke</u> , GeoDG-Team der BGR <i>Bundesanstalt für Geowissenschaften und Rohstoffe, Hannover</i>
P-MG-02	<b>Offshore freshened groundwater exploration – a new playground for marine geophysics</b> <u>K. Schwalenberg</u> <i>Bundesanstalt für Geowissenschaften und Rohstoffe, B1.4 Marine Rohstoffexploration, Hannover</i>
P-MG-03	<b>Grundwassererkundung im Übergangsbereich von Land zum Meer in der Bucht von Antalya, Türkei</b> <u>E. Erkul, J. Hoffmann, S. Fischer, I. Yolcubal, A. Haroon, P. Yogeshwar, E. Sen, W. Rabbel, A. Sener, J. Schneider von Deimling, B. Tezkan, E. Peksen, A. Micallef, E. Gasimov, I. Kaplanvural, F. Gross, L. Sander, S. Baris</u> <i>University of Kiel, Institute of Geosciences, Kiel and others</i>
P-MG-04	<b>Gravity and Heat flow density measurements in the New Ireland Basin, Papua New Guinea</b> <u>I. Heyde, P. A. Brandl, R. Zitoun</u> <i>Bundesanstalt für Geowissenschaften und Rohstoffe, Marine Rohstofferkundung, Hannover and others</i>
P-MG-05	<b>OBS array for offshore monitoring of Mount Etna: Evaluation of array-derived event localizations</b> <u>H. Zimmer, K. Hannemann, M. Urlaub, C. Thomas, Y. Ren</u> <i>GEOMAR Helmholtz Centre for Ocean Research Kiel, Kiel and others</i>
P-AG-01	<b>Semi-Airborne Electromagnetic Survey for Deep Structural Mapping in a Complex Geological Setting</b> <u>M. Bayat, T. Günther, S. Nazari, M. Ronczka</u> <i>LIAG Institute for Applied Geophysics, Hannover and others</i>
P-VU-01	<b>Three-Dimensional Inversion of Magnetotelluric Data from Mt. Ruapehu, New Zealand</b> <u>P. Semper, T. Bertrand, G. Caldwell, W. Heise, M. Scheunert, K. Spitzer</u> <i>TU Bergakademie Freiberg, Institut für Geophysik und Geoinformatik, Freiberg and others</i>

## Event – Saal 2a

16:00–17:30      **Eröffnungsveranstaltung ↗**

## Event – Saal 1

17:30–19:00      **Eröffnung der Firmenausstellung ↗**

## Event – Extern

19:00–23:59      **Studentischer Abend ↗**

## DIENSTAG, 25. FEBRUAR 2025

### Oral – Saal 3

09:00–10:20 O-MI

#### MI - Modellierung / Imaging

Moderation: M. Boxberg, Aachen

09:00–09:20 O-MI-01

#### Das Thüringer Becken: Einblick in die Temperaturverteilung und Fluidodynamik durch dreidimensionale numerische Simulationen

A. Schulz, N. Kukowski

*Institut für Geowissenschaften, Friedrich-Schiller-Universität Jena, Allgemeine Geophysik, Jena*

09:20–09:40 O-MI-02

#### WBGeo – Workbench for Digital Geosystems: Leveraging Open Source Tools for Modular and Exchangeable Workflow Components

J. von Harten<sup>1</sup>, A. Lügges<sup>2</sup>, F. Wellmann<sup>1</sup>, B. Rumpe<sup>2</sup>

<sup>1</sup>RWTH Aachen University, Chair of Computational Geoscience, Geothermics and Reservoir Geophysics, Aachen, Germany, <sup>2</sup>RWTH Aachen University, Software Engineering Department of Computer Science 3, Aachen

09:40–10:00 O-MI-03

#### Integrating geophysical structure-based inversion with implicit geological modeling

A. Balza Morales<sup>1</sup>, A. Forderer<sup>2</sup>, F. Wellmann<sup>3</sup>, F. Wagner<sup>1</sup>

<sup>1</sup>RWTH Aachen University, Geophysical imaging and monitoring, Aachen, Germany, <sup>2</sup>RWTH Aachen University, Geotechnical engineering and institute of geomechanics and underground technology, Aachen, Germany, <sup>3</sup>RWTH Aachen University, Computational geoscience, geothermics and reservoir geophysics, Aachen

10:00–10:20 O-MI-04

#### Petrophysically and structurally coupled joint inversion

H. Söding<sup>1,2</sup>, F. Wagner<sup>2</sup>, H. Maurer<sup>1</sup>

<sup>1</sup>ETH Zürich, Department of Earth and Planetary Sciences, Zürich, Switzerland, <sup>2</sup>RWTH Aachen, Geophysical Imaging and Monitoring, Aachen

### Event – Tagungsraum 2

09:00–13:00

#### Vorstandssitzung

Oral

Saal 2a

09:20–10:20 O-OG

#### OG - Oberflächennahe Geophysik

Moderation: M. Müller-Petke, Hannover

09:20–09:40 O-OG-01

#### Effekte von dreidimensionalen Widerstands-Verteilungen auf die Inversion von zweidimensionalen Geoelektrik-Messungen – Herausforderungen und Lösungsansätze am Beispiel eines küstenparallelen Messprofils am Strand von Konyaaltı (Antalya, Türkei)

S. L. Fischer<sup>1</sup>, E. Erkul<sup>1</sup>, E. Pekşen<sup>2</sup>, I. Kaplanvural<sup>2</sup>, W. Rabbel<sup>1</sup>, J. Hoffmann<sup>3</sup>

<sup>1</sup>Christian-Albrechts-Universität zu Kiel, Kiel, Germany, <sup>2</sup>Kocaeli Üniversitesi, Mühendislik Fakültesi, Izmit, Turkey, <sup>3</sup>Alfred-Wegener-Institut Helmholtz-Zentrum für Polar- und Meeresforschung - AWI Sylt, List

09:40–10:00 O-OG-02

#### Geophysical Monitoring of Infiltration Processes in a Managed Artificial Recharge Pond Part A

A. Prayag<sup>1</sup>, T. Dahlin<sup>1</sup>, P. Hedblom<sup>1</sup>, Y. Abu Jaish<sup>1</sup>, P. Jonsson<sup>1</sup>, M. Rossi<sup>1</sup>, K. Hägg<sup>2</sup>, T. Martin<sup>1</sup>

<sup>1</sup>Lund University, Engineering Geology, Lund, Sweden, <sup>2</sup>Sydvatten AB, Malmö, Sweden

10:00–10:20 O-OG-03

#### Geophysical Monitoring of Infiltration Processes in a Managed Artificial Recharge Pond Part B

A. Prayag<sup>1</sup>, T. Dahlin<sup>1</sup>, P. Hedblom<sup>1</sup>, Y. Abu Jaish<sup>1</sup>, P. Jonsson<sup>1</sup>, M. Rossi<sup>1</sup>, K. Hägg<sup>2</sup>, T. Martin<sup>1</sup>

<sup>1</sup>Lund University, Engineering Geology, Lund, Sweden, <sup>2</sup>Sydvatten AB, Lund, Sweden

10:20–11:20

#### Kaffeepause

## Poster – Saal 2b

**10:20–11:20 P2**

### **Poster OG, MI, GO**

Moderation: F. Wagner, Aachen (MI), A. Rudloff, Potsdam (GO), M. Müller-Petke, Hannover (OG)

- P-OG-02 **FD-EMI electrical conductivity imaging with a multi-frequency source and decametric spacings: first test and comparison with ERT**

J. Guillemoteau, J. Tronicke

*Universität Potsdam, Institut für Geowissenschaften, Potsdam*

- P-OG-04 **ERT monitoring to observe saltwater intrusion at the Luneplate/Bremerhaven**

B. Blanco-Arrué, M. Müller-Petke, A. Kunicki, S. Julius, K. Seiter

*LIAG-Institut für Angewandte Geophysik, FB 1.2 Geophysikalische Erkundung/Monitoring, Hannover and others*

- P-OG-06 **Exploring the potential of using GPR to investigate the soil-plant continuum of maize crops**

L. Lärm, F. Bauer, L. Weihermüller, J. Rödder, H. Vereecken, J. Vanderborght, J. van der Kruk, A. Schnepf, A. Klotzsche

*Forschungszentrum Jülich, Institute of Bio- and Geoscience: Agrosphere (IBG-3), Jülich*

- P-OG-08 **NMR relaxation of peat soils at laboratory and field scale**

G. T. Beisembina, T. Splith, S. Costabel, T. Hiller, M. Müller-Petke

*Federal Institute for Geosciences and Natural Resources, BGR, Groundwater and Soil Science, Berlin and others*

- P-OG-10 **Geophysikalische Beiträge zur multidisziplinären Rekonstruktion des Bleichesee in der Egeraue in Nördlingen, Süddeutschland**

M. Pohle, M. Bauckholt, E. Zvara, S. Pejdanović, I. O. Nießen, L. Werther, P. Kühn, C. Zielhofer, U. Werban  
*Helmholtz-Zentrum für Umweltforschung GmbH - UFZ, Leipzig and others*

- P-OG-12 **Revealing hidden polygonal networks in saline alluvial sediments in the Atacama Desert using ground-penetrating radar**

P. Schwarze, J. Igel, B. Arrué Blanco, C. Sager, A. Airo, J. Feige

*Universidad de Chile, Departamento de Geofísica, Facultad de Ciencias Físicas y Matemáticas, Santiago, Chile and others*

- P-OG-14 **Erkundung von Lagerungsdefekten und Hohlräumen im Bereich von Entwässerungssystemen mittels Georadar**

M. Lorenzen, D. Grundke, M. Bücker

*Institut für Geophysik und extraterrestrische Physik, TU Braunschweig, Braunschweig and others*

- P-OG-16 **Geologische Eis-Wärme-Speicher – Reflexionsmessungen mittels Bohrlochgeoradar als Methode zur Abbildung von Gefrier-Tauzyklen in oberflächennahen Aquiferen**

A. Burzik, P. Jung, M. Pohle, G. Hornbruch, A. Dahmke, U. Werban

*Helmholtz-Zentrum für Umweltforschung - UFZ, Leipzig and others*

- P-OG-18 **Beispiele für die Detektion von Feuchtigkeit in Mauerwerk mittels Thermografie**

Y. E. Esel, N. Isik, S. Jahani, D. Schulte-Kortnack, E. Erkul, D. Köhn, T. Meier

*Deutsche Bundesstiftung Umwelt - DBU, Osnabrück and others*

- P-OG-20 **Comparing Attenuation-Based Methods for Sediment Classification from Sub-Bottom Profiling**

M. Ibrahimli, A. Schenk

*Karlsruher Institut für Technologie, Institut für Photogrammetrie und Fernerkundung, Karlsruhe*

- P-OG-22 **Landscape reconstruction of the Hebros delta**

M. Thorwart, W. Rabbel, H. Brückner, A. Dan, C. Karadima, D. Terzopoulou, S. Baris, D. Caka

*Kiel University, Institute for Geoscience, Kiel and others*

- P-OG-24 **Determination of Air Bubble Concentration in Fluids with Ultrasound: An Experimental Approach**

J. Calderon, M. Dormann, T. Branß, J. Aberle, M. Balcewicz, E. Saenger

*Hochschule Bochum, Bochum and others*

- P-OG-26 **Rover-gestützte Geomagnetik**

B. Jacobsen, J. Börner, P. Treichel, T. Planitzer, S. Min, R. Pena, K. Spitzer

*TU Bergakademie Freiberg, Freiberg and others*

P-MI-01	<b>Towards a time-domain Gauss-Newton algorithm for elastic multi-parameter full-waveform inversion</b> <u>S. S. Keßler, T. Bohlen</u> <i>Geophysikalisches Institut, KIT, Karlsruhe</i>
P-MI-02	<b>2D Near-Surface Elastic Full Waveform Inversion Using Synthetic Data from Traffic-Induced Moving Sources</b> <u>C. He, T. Bohlen, J. Chen</u> <i>Karlsruhe Institute of Technology, Geophysics Institute, Karlsruhe and others</i>
P-MI-03	<b>2D Viscoacoustic Full Waveform Inversion (FWI) for Imaging CO<sub>2</sub> sequestration of the Sleipner Field North Sea</b> <u>E. Anthony, T. Bohlen</u> <i>Geophysical Institute (GPI), Karlsruhe Institute of Technology (KIT), Germany, Karlsruhe</i>
P-MI-04	<b>Full Waveform Inversion for Sparse Parameter Spaces with a Gaussian Process Emulator</b> <u>G. El Fatih, M. S. Boxberg, F. M. Wagner</u> <i>RWTH Aachen University, Geophysical Imaging and Monitoring, Aachen</i>
P-MI-05	<b>Parallel Ensemble-Kalman-Inversion using Gaussian Random Fields</b> <u>R.-U. Börner</u> <i>TU Bergakademie Freiberg, Institut für Geophysik und Geoinformatik, Freiberg</i>
P-MI-06	<b>Time-lapse petrophysical joint inversion of seismic refraction and electrical resistivity permafrost monitoring data</b> <u>F. Wagner, J. Klahold, C. Hilbich, C. Hauck</u> <i>RWTH Aachen University, Geophysical Imaging and Monitoring (GIM), Aachen and others</i>
P-MI-07	<b>WaterSim – Modellierung des gekoppelten Fluid und Wärmetransports am Beispiel des Saaletals</b> <u>A. Schulz, N. Kukowski</u> <i>Institut für Geowissenschaften, Friedrich-Schiller-Universität Jena, Allgemeine Geophysik, Jena</i>
P-MI-08	<b>Investigation of salt deformation processes using a newly developed 3D two-way coupled DEM-FEM simulation technique</b> <u>D. Behrens, G. Bartzke, K. Huhn-Frechers</u> <i>Marum, Bremen</i>
P-MI-09	<b>Fractal-dimensional flow surrounding hydraulic dipoles</b> <u>F. Mumand, V. Jimenez Martinez, J. Renner</u> <i>Ruhr-Universität Bochum, Institut für Geologie, Mineralogie und Geophysik, Bochum</i>
P-GO-01	<b>Mit Raspberry-Pi Magnetometer junge Menschen früh für die Geowissenschaften begeistern</b> <u>J. Dielmann, A. Busse, A. Grayver, A. Wennmacher, R. Bergers</u> <i>Institut für Geophysik und Meteorologie, University of Cologne, Köln</i>
P-GO-02	<b>Aufbau eines Raspberry-Shake-Seismometernetzwerkes an Schulen in Sachsen</b> <u>O. Hellwig, S. Buske</u> <i>Institut für Geophysik und Geoinformatik / TU Bergakademie Freiberg, Freiberg</i>

## Oral – Saal 2a

11:20–13:00 O-OG

### OG – Oberflächennahe Geophysik

A. Klotzsche, Jülich

11:20–11:40 O-OG-04

### Investigation of groundwater salinity and seawater intrusion in northern Kuwait using transient electromagnetics

S. Burberg<sup>1</sup>, P. Yogeshwar<sup>1</sup>, B. Tezkan<sup>1</sup>, I. M. Ibraheem<sup>1</sup>, F. Bou-Rabee<sup>2</sup>, M. Duane<sup>2</sup>

<sup>1</sup>*University of Cologne, Institute of Geophysics and Meteorology, Cologne, Germany*, <sup>2</sup>*Kuwait University, Department of Earth and Environmental Sciences, Kuwait City, Kuwait*

11:40–12:00	O-OG-05	<b>Spatio-temporal salinity dynamics of a coastal aquifer on Spiekeroog island</b> N. Skibbe <sup>1</sup> , T. Günther <sup>2</sup> , M. Müller-Petke <sup>1</sup> <sup>1</sup> LIAG-Institut für Angewandte Geophysik, FB 1.2 Geophysikalische Erkundung/ Monitoring, Hannover, Germany, <sup>2</sup> TU Bergakademie Freiberg, Institut für Geophysik und Geoinformatik, Freiberg
12:00–12:20	O-OG-06	<b>MoreSpin: a non-invasive soil humidity sensor based on SNMR</b> T. Splitth <sup>1</sup> , G. T. Beisembina <sup>2</sup> , S. Costabel <sup>2</sup> , M. Müller-Petke <sup>1</sup> <sup>1</sup> LIAG Institute for Applied Geophysics, Hanover, Germany, <sup>2</sup> Federal Institute for Geosciences and Natural Resources, Berlin
12:20–12:40	O-OG-07	<b>Geoelectrical monitoring of soil moisture in hugelcultures</b> N. Müller <sup>1</sup> , J. Hoppenbrock <sup>1,2</sup> , F. Feldmann <sup>2</sup> , M. Bücker <sup>3</sup> <sup>1</sup> TU Braunschweig, Institut für Geophysik und Extraterrestrische Physik, Braunschweig, Germany, <sup>2</sup> Julius Kühn-Institut, Institut für Pflanzenschutz in Gartenbau und urbanem Grün, Braunschweig, Germany, <sup>3</sup> Christian-Albrechts-Universität zu Kiel, Institut für Geowissenschaften, Kiel
12:40–13:00	O-OG-08	<b>Enhancing Groundwater Exploration with Constrained Inversion of Reflection Seismic and Electrical Resistivity Data</b> N. Alaei <sup>1</sup> , H. Buiness <sup>1</sup> , T. Günther <sup>1,2</sup> , T. Eckardt <sup>3</sup> , B. Stiller <sup>4</sup> , R. Pechnig <sup>5</sup> , G. Gabriel <sup>1</sup> <sup>1</sup> LIAG institute for applied geophysics, Hannover, Germany, <sup>2</sup> Technische Universität Bergakademie Freiberg, Freiberg, Germany, <sup>3</sup> terratec geophysical services GmbH & Co. KG, Heitersheim, Germany, <sup>4</sup> Hamburg Wasser(HW), Hamburg, Germany, <sup>5</sup> Geophysica Beratungsgesellschaft mbH, Aachen

## Oral – Saal 3

11:20–12:40	O-MI	<b>MI - Modellierung / Imaging</b> Moderation: F. Wagner, Aachen
11:20–11:40	O-MI-05	<b>Gauß-Newton Full Waveform Inversion for Acoustic Media</b> K. He <i>Karlsruher Institut für Technologie, Geophysikalisches Institut, Karlsruhe</i>
11:40–12:00	O-MI-06	<b>Developing regional velocity models: Data, Methodology and Insights from the TUNB Velo 2.0 Project</b> C. Schimschal <sup>1</sup> , J. Ziesch <sup>1</sup> , F. Bense <sup>2</sup> <sup>1</sup> Landesamt für Bergbau, Energie und Geologie (LBEG), Hannover, Germany, <sup>2</sup> Bundesanstalt für Geowissenschaften und Rohstoffe (BGR), Hannover
12:00–12:20	O-MI-07	<b>EM Tensor Measurements for deep mapping of geology while drilling</b> A. Hartmann <sup>1</sup> , U. Peikert <sup>1</sup> , M. Linke <sup>1</sup> , Y. Antonov <sup>1</sup> , G. Dyatlov <sup>1</sup> , W. Fernandes <sup>1</sup> , H. Andersson <sup>2</sup> <sup>1</sup> Baker Hughes, Celle, Germany, <sup>2</sup> Baker Hughes, Stavanger, Norway
12:20–12:40	O-MI-08	<b>Transient electromagnetics and electrical resistivity tomography joint inversion using a novel approximated 2D transient electromagnetics inversion scheme</b> A. Jaron <sup>1</sup> , P. Yogeshwar <sup>2</sup> , A. Kemna <sup>3</sup> , F. Wagner <sup>1</sup> , T. Günther <sup>4</sup> <sup>1</sup> RWTH Aachen, Division of Earth Sciences and Geography, Aachen, Germany, <sup>2</sup> University of Cologne, Institute of Geophysics and Meteorology, Köln, Germany, <sup>3</sup> University of Bonn, Institute of Geosciences, Bonn, Germany, <sup>4</sup> TU Bergakademie Freiberg, Faculty of Earth Sciences, Geotechnics and Mining, Freiberg
13:00–14:00		<b>Mittagspause</b>

## Event – Extern

13:00–14:00	<b>Firmenvorführung</b> Moderation: C. Finger, Bochum
-------------	--

## Schwerpunktsession–Saal 2a

**14:00–15:00 O-S2-PV** **Lessons learned from microseismic monitoring of induced seismicity at megaton-scale CCS sites**  
English

Moderation: R. Harrington, Bochum

B. Goertz-Allmann

*NORSAR, Kjeller, Norway*

## Oral – Saal 2a

**15:00–16:00 O-OG** **OG - Oberflächennahe Geophysik**

Moderation: A. Klotzsche, Jülich

15:00–15:20 O-OG-09 **Novel developments of the 2.5D GPR full-waveform inversion for high resolution subsurface imaging**

D. Hoven, J. van der Kruk, H. Vereecken, A. Klotzsche

*Forschungszentrum Jülich GmbH, Institute of Bio- and Geoscience: Agrosphere (IBG-3), Jülich*

15:20–15:40 O-OG-10 **Using crosshole GPR to monitor the impact of maize roots and nitrate fertilizer on the soil-plant continuum**  
**Using crosshole GPR to monitor the impact of maize roots and nitrate fertilizer on the soil-plant continuum**

S. Schiebel, L. Lärm, F. Bauer, A. Schnepf, H. Vereecken, A. Klotzsche

*Forschungszentrum Jülich, Institut für Bio- und Geowissenschaften: Agrosphäre (IBG-3), Jülich*

15:40–16:00 O-OG-11 **Resonance Seismometry – a tool for near-surface cavity mapping in an arms control context**  
M. Joswig, M. Walter, R. Häfner

*Sonica GbR, Tübingen*

## Plenarvortrag – Saal 3

**15:00–16:00 O-PV** **Did this really happen? – Inclusive Geophysics**

Moderation: S. Donner, Hannover

L. Perez-Dias

*University of Oxford, United Kingdom*

## Schwerpunktsession – Saal 4

**15:00–16:00 O-S2** **S2 - Induzierte Seismizität**

Moderation: R. Harrington, Bochum

15:00–15:20 O-S2-01 **Seismic Event Discrimination with Vision Transformers: Advancing Model Explainability**

V. Kasburg<sup>1</sup>, M. van Laaten<sup>1</sup>, M. Zehner<sup>2</sup>, J. Müller<sup>1</sup>, N. Kukowski<sup>1</sup>

<sup>1</sup>*Friedrich-Schiller-Universität Jena, Institut für Geowissenschaften, Jena, Germany,*

<sup>2</sup>*Friedrich-Schiller-Universität Jena, Institut für Geographie, Jena*

15:20–15:40 O-S2-02 **A template-matching approach for simultaneous earthquake detection and localization using DAS data**

N. Boitz, W. Tegtow, S. Shapiro

*Freie Universität Berlin, Geowissenschaften - Geophysik, Berlin*

15:40–16:00 O-S2-03 **Relative Moment Tensors Rejuvenated: A Recent Approach to Resolve the Source Mechanism of Small Earthquakes**

W. Bloch<sup>1,2</sup>, D. Drolet<sup>3</sup>, A. Plourde<sup>4</sup>, M. Bostock<sup>3</sup>, V. Oye<sup>1</sup>

<sup>1</sup>*NORSAR, Applied Seismology, Kjeller, Norway*, <sup>2</sup>*GFZ Deutsches GeoForschungs Zentrum, Dynamik der Lithosphäre, Potsdam, Germany*,

<sup>3</sup>*The University of British Columbia, Vancouver, Canada*,

<sup>4</sup>*National Resources Canada, Dartmouth, Canada*

**16:00–17:00**

**Kaffeepause**

## Poster – Saal 2b

16:00–17:00 P3

### Poster S2, OG, OS

Moderation: D. Essing, Bochum (S2), T. Martin, Lund (OG), M. Isken, Potsdam (OS)

P-S2-01

#### **Induced seismicity in Germany during the last decade - an overview and update**

T. Plenefisch, M. Bischoff, G. Hartmann, U. Wegler

*Bundesanstalt für Geowissenschaften und Rohstoffe (BGR), B4.3, Hannover and others*

P-S2-02

#### **Estimating the effect of induced seismicity at the Earth's surface – case studies based on the geothermal projects Graben-Neudorf and Wörth in the Upper Rhine Graben**

P. Hering, N. Medinger, S. Abe, L. Küperkoch, H. Deckert

*Institut für Innovation, Transfer und Beratung gGmbH, Institut für geothermisches Ressourcenmanagement (igem), Bingen*

P-S2-03

#### **Explanation of Flooding-induced Seismicity - a combined approach from relocation of microseismicity and geomechanical numerical modelling**

M. Rische, T. Niederhuber, B. Müller, K. D. Fischer, W. Friederich

*Ruhr Universität Bochum, Institut für Geologie, Mineralogie und Geophysik (GMG), Bochum and others*

P-S2-04

#### **Lessons learned and challenges from AI-based seismic monitoring in a high noise-level area: the Weisweiler case**

S. Carrasco, M. P. Roth, R. M. Harrington, X. Chen, C. Finger, M. Dietl, M. Zeckra

*Ruhr University Bochum, Bochum and others*

P-S2-05

#### **Seismic Phase Picking for Induced Seismicity with Deep-Learning**

J. Heuel, V. Maurer, M. Frietsch, A. Rietbrock

*Karlsruher Institut für Technologie, Geophysikalisches Institut, Karlsruhe and others*

P-S2-06

#### **Match Filter Detection Routine with Synthetic Templates using 1D velocity model - aiming to detect the induced seismicity- test site: West Bohemia/Vogtland**

E. Kaldy, T. Fischer

*Charles University, Faculty of Science, Institute of Hydrogeology, Engineering Geology and Applied Geophysics, Prague, Czech Republic*

P-S2-07

#### **Locating Seismic Tremors Through Matched Field Processing Algorithm**

K. Karimi, T. Fischer

*Charles University, Faculty of Science, Prague, Czech Republic*

P-S2-08

#### **A coupled numerical model for the simulation of induced seismicity**

S. Abe, P. Hering, H. Deckert

*Institut für geothermisches Ressourcenmanagement, Bingen*

P-OG-01

#### **Small-scale geoelectrical monitoring of water transport processes at tree sites**

L. Schirra, J. Hoppenbrock, M. Beyer, M. Gerchow, S. Iden, M. Bücker

*Institut für Geophysik und extraterrestrische Physik, Technische Universität Braunschweig and others*

P-OG-03

#### **Detection of saltwater intrusion in a coastal aquifer in Qingdao, China using TEM and DCR**

P. Perez-Gamboa, P. Yogeshwar, W. Mörbe, B. Tezkan, Y. Li, L. Ming

*Universität zu Köln, Institut für Geophysik und Meteorologie, Köln and others*

P-OG-05

#### **Characterisation of a Palsa near Aidejávri/Norway with Electrical Resistivity Tomography**

I. Burger, R. Schulz, S. Westermann, A. Hördt

*TU Braunschweig, Institute of Geophysics and Extraterrestrial Physics, Braunschweig and others*

P-OG-07

#### **Erprobung eines skalierbaren elektromagnetischen Induktionssystems (SELMA-RB) für landwirtschaftliche Anwendungen**

M. Dick, E. Zimmermann, A. Mester, P. Wüstner, M. Ramm, B. Scherer, J. Bernard, J. A. Huisman, C. Brogi, S. Dogar, G. Natour

*Institut für Technologie und Engineering (ITE), Forschungszentrum Jülich GmbH, Jülich and others*

P-OG-09

#### **Evaluation of compaction measures on liquefaction susceptible dumps by means of surface-NMR**

T. Hiller, S. Costabel, G. Erdmann, E. Schönfeldt

*Bundesanstalt für Geowissenschaften und Rohstoffe, Cottbus and others*

P-OG-11	<b>Mit Georadar auf der Suche nach Sedimentumlagerungen zur Ostseesturmflut vom 20.10.2023</b> <u>M. Scharnweber, A. Knies, E. Erkul, T. Wunderlich, C. Winter</u> <i>Institut für Geowissenschaften CAU, Kiel</i>
P-OG-13	<b>Vergleich aktiver und passiver seismischer Messungen am Deich des Tümlauer Koogs (Dithmarschen)</b> <u>F. Al Tawashi, D. Köhn, C. Weidle, L. Wiesenberge, D. Wilken, R. Kirsch, T. Meier</u> <i>Geowissenschaften, Geophysik, Kiel and others</i>
P-OG-15	<b>Erkundung von Bahnstrecken mithilfe eines 3D Georadar-Arraysystems.</b> <u>N. Allroggen, T. Junghans, D. Hofmann</u> <i>DB E&amp;C, Georadar (I.TV-N-U-R), Bremen</i>
P-OG-17	<b>Einbau geophysikalischer Sensoren zur Rissdetektion an einem Demonstrationsbauwerk</b> <u>L. I. Pascharat, C. Friedrich, S. Schennen, F. Mielentz, U. Effner, H. Stolpe, M. Behrens, M. Sobiesiak, K. Plenkers, T. Fischer</u> <i>Bundesgesellschaft für Endlagerung mbH (BGE), Peine and others</i>
P-OG-19	<b>Investigation of Hydrodynamics in Carbonate Rock with Ground Penetrating Radar</b> <u>A. Rieß, P. Dietrich</u> <i>Helmholtz Zentrum für Umweltforschung - UFZ, Monitoring und Erkundungstechnologien, Leipzig and others</i>
P-OG-21	<b>Transient Electromagnetic Investigation of Sediment Deposits in the Yungay Claypan, Atacama Desert, Chile</b> <u>J. Dielmann, B. Blanco Arrué, B. Tezkan, A. Airo, P. Yogeshwar</u> <i>Institut für Geophysik und Meteorologie, University of Cologne, Köln and others</i>
P-OG-23	<b>Determination of Allowable Bearing Pressure for Geotechnical Engineering by Combining P- and S-Wave Seismic Refraction Data</b> <u>E. G. Nwaka, P. Dietrich</u> <i>Helmholtz Centre for Environmental Research – UFZ, Department of Monitoring and Exploration Technologies, Leipzig and others</i>
P-OG-25	<b>Determination of Air Bubble Concentration in Fluids with Ultrasound: A numerical approach</b> <u>M. Dormann, J. Calderon, S. Humpert, M. Balcewicz, E. H. Saenger</u> <i>Bochum University of Applied Sciences, Bochum and others</i>
P-OS-01	<b>Working towards a software package for Optimized Experimental Design for Electrical Resistivity Tomography</b> <u>N. Menzel, S. Uhlemann, F. M. Wagner</u> <i>RWTH Aachen, Geophysical Imaging and Monitoring, Aachen and others</i>

## Oral – Saal 2a

17:00–18:00	O-OG	<b>OG - Oberflächennahe Geophysik</b>
		Moderation: W. Rabbel, Kiel
17:00–17:20	O-OG-12	<b>Investigating the shallow subsurface at the Wiechert earthquake station in Göttingen with passive and active seismic measurements</b> <u>M. Hobiger<sup>1</sup>, T. Plenefisch<sup>1</sup>, B. Goebel<sup>1</sup>, M. Bischoff<sup>2</sup>, M. Napp<sup>2</sup>, S. Donner<sup>1</sup></u> <sup>1</sup> <i>Bundesanstalt für Geowissenschaften und Rohstoffe (BGR), Erdbebendienst des Bundes, Hannover, Germany</i> , <sup>2</sup> <i>Landesamt für Bergbau, Energie und Geologie (LBEG), Niedersächsischer Erdbebendienst, Hannover</i>
17:20–17:40	O-OG-13	<b>Geophysical Methods for Near-Surface Exploration in Seismic Microzonation Studies in Venezuela and Ecuador</b> <u>M. Schmitz</u> <i>Universidad Central de Venezuela, Departamento de Geofísica, Caracas, Venezuela</i>
17:40–18:00	O-OG-14	<b>Potential Field Data Indicate a Candidate Location for Parent Impact Crater of Australasian Tektites</b> <u>K. Karimi<sup>1</sup>, G. Kletetschka<sup>1</sup>, J. Mizera<sup>2</sup>, V. Meire<sup>1</sup>, V. Strunga<sup>2</sup></u> <sup>1</sup> <i>Charles University, Faculty of Science, Prague, Czech Republic</i> , <sup>2</sup> <i>Czech Academy of Sciences, Prague, Czech Republic</i>

## Oral – Saal 3

17:00–18:00	O-GO/OS	<b>GO / OS Geophysik in der Öffentlichkeit und im Wandel der Zeit / Open Source in Forschung und Lehre</b> Moderation: W. Friederich, Bochum
17:00–17:20	O-GO/OS-01	<b>Ist Isaac Newtons PRINCIPIA von 1687 auch eine Methodologie der heutigen Geophysik?</b> <u>J. Fertig</u> <i>Geophysik, Burgwedel</i>
17:20–17:40	O-GO/OS-02	<b>20 Jahre nach der Tsunami-Katastrophe im Indischen Ozean – Was haben wir gelernt?</b> <u>A. Rudloff<sup>1</sup>, J. Lauterjung<sup>1</sup>, A. Babeyko<sup>1</sup>, A. Strollo<sup>1</sup>, F. Tilmann<sup>1,2</sup></u> <sup>1</sup> <i>GFZ Helmholtz-Zentrum für Geoforschung, Potsdam, Germany</i> , <sup>2</sup> <i>Freie Universität Berlin, Institut für Geologische Wissenschaften, Berlin</i>
17:40–18:00	O-GO/OS-03	<b>EPOS – The European Plate Observing System and flagship projects Geo-INQUIRE and DT-GEO: opportunities for building communities and promoting openness in geoscience data</b> <u>F. Tilmann<sup>1</sup>, F. Cotton<sup>1</sup>, A. Strollo<sup>1</sup>, A. Babeyko<sup>1</sup>, J. Quinteros<sup>1</sup>, A. Gabriel<sup>2,3</sup>, H. Igel<sup>2</sup>, C. Hadzioannou<sup>4</sup></u> <sup>1</sup> <i>GFZ Helmholtz-Zentrum für Geoforschung, Potsdam, Germany</i> , <sup>2</sup> <i>Ludwig-Maximilians-Universität München, Department für Geo- und Umweltwissenschaften, München, Germany</i> , <sup>3</sup> <i>UC San Diego, Scripps Institution of Oceanography, La Jolla, United States of America</i> , <sup>4</sup> <i>Universität Hamburg, Fachbereich Erdsystemwissenschaften, Hamburg</i>

## Schwerpunktsession – Saal 4

17:00–18:00	O-S2	<b>S2 - Induzierte Seismizität</b>
17:00–17:20	O-S2-04	<b>Improving Seismic Monoitoring performance using Posthole and Borehole Instrumentation</b> <u>S. Uhlmann</u> <i>IGM GmbH, Überlingen</i>
17:20–17:40	O-S2-05	<b>AI-based Acoustic emission monitoring and detection from decameter-scale fluid injection tests in clay rock at the URL Tournemire, France</b> <u>T. Förster<sup>1,2</sup>, C. Böse<sup>2</sup>, R. Giese<sup>2</sup>, K. Plenkers<sup>3</sup>, P. Dick<sup>4</sup>, G. Zimmermann<sup>5</sup></u> <sup>1</sup> <i>Technische Universität Berlin, Berlin, Germany</i> , <sup>2</sup> <i>Helmholtz-Zentrum Potsdam Deutsches GeoForschungsZentrum, 4.2 wissenschaftliches Bohren und Geomechanik, Potsdam, Germany</i> , <sup>3</sup> <i>GMuG - Gesellschaft für Materialprüfung und Geophysik, Bad Nauheim, Germany</i> , <sup>4</sup> <i>Institut de Radioprotection et de Sûreté Nucléaire (IRSN), Fontenay-aux-Roses, France</i> , <sup>5</sup> <i>Helmholtz-Zentrum Potsdam Deutsches GeoForschungsZentrum, 4.3 Geoenergie, Potsdam</i>
17:40–18:00	O-S2-06	<b>Insights and highlights from the multi-sensor microseismic surface monitoring at the field-scale EGS laboratory Utah FORGE</b> <u>P. Niemz<sup>1</sup>, G. Petersen<sup>2</sup>, J. Rutledge<sup>3</sup>, K. Pankow<sup>1</sup>, K. Whidden<sup>1</sup></u> <sup>1</sup> <i>University of Utah, Seismograph Stations, Salt Lake City, United States of America</i> , <sup>2</sup> <i>GFZ Postdam, Erdbeben- und Vulkanphysik, Postdam, Germany</i> , <sup>3</sup> <i>Santa Fe Seismic LLC, Santa Fe, United States of America</i>

## Event – Extern

19:00–23:59	<b>Gesellschaftsabend   Conference Dinner</b>
-------------	---

## MITTWOCH, 26. FEBRUAR 2025

### Tagungsraum 2

08:00–09:30      Meet & Greet ↗

### Oral – Saal 2a

09:20–10:20	O-SO	<b>SO - Seismologie</b> Moderation: T. Dahm, Potsdam
09:20–09:40	O-SO-01	<b>Earthquake Location Imaging (ELI) for single-well Distributed Acoustic Sensing using Wavefield Classification</b> <u>A. Komeazi</u> , G. Rümpker <i>Goethe Universität Frankfurt, Frankfurt am Main</i>
09:40–10:00	O-SO-02	<b>Using dark fiber-optic cables to support geothermal exploration using passive seismic methods</b> <u>J. Pätzl</u> <sup>1</sup> , A. Yates <sup>1</sup> , C. Caudron <sup>1,2</sup> , J. Govoorts <sup>1,3,4</sup> <sup>1</sup> <i>Université libre de Bruxelles, Brussels, Belgium</i> , <sup>2</sup> <i>WEL Research Institute, Wavre, Belgium</i> , <sup>3</sup> <i>Royal Observatory of Belgium, Seismology and Gravimetry, Brussels, Belgium</i> , <sup>4</sup> <i>Université de Mons, Mons, Belgium</i>
10:00–10:20	O-SO-03	<b>QEST - An inversion code to separately estimate the frequency dependence and the depth dependence of intrinsic attenuation and scattering attenuation of seismic shear waves</b> <u>M. van Laaten</u> , <u>U. Wegler</u> <i>Friedrich-Schiller-Universität Jena, Jena</i>

### Oral – Saal 3

09:20–10:20      DGG-Kolloquium ↗

### Schwerpunktsession – Saal 4

09:40–10:20	O-S3	<b>S3 - Tektonische Geodäsie</b> Moderation: E. Korkolis, Bochum
09:40–10:00	O-S3-01	<b>Predicting baseline changes between GNSS stations from stacks of wrapped InSAR interferograms</b> <u>K. Cökerim</u> , E. Latypova, J. Bedford <i>Ruhr-Universität Bochum, Tektonische Geodäsie, Bochum</i>
10:00–10:20	O-S3-02	<b>The influence of GNSS network processing choices on the appearance of tectonic transient displacements</b> <u>J. Bedford</u> <sup>1</sup> , ERC TectoVision research team <sup>1,2</sup> <sup>1</sup> <i>RUB, Bochum, Germany</i> , <sup>2</sup> <i>GFZ, Potsdam</i>
10:20–11:20		<b>Kaffeepause</b>

**10:20–11:20 P4**

**Poster S3, BL, SO**

J. Bedford, Bochum (S3), E. Saenger, Bochum (BL), T. Meier, Kiel (SO)

P-BL-01 **Physical Properties of Rock Cuttings vs. Borehole Data: An Overview of Ongoing Research**

A. Serje Gutierrez, M. Balcewicz, E. H. Saenger

*Bochum University of Applied Sciences, Bochum and others*

P-BL-02 **Permittivity Determination of Rock Cuttings: An Overview of Ongoing Research**

N. Kerkmann, M. Siegert, N.-A. Kouamo Keutchafo, E. H. Saenger

*Fraunhofer IEG, Bochum and others*

P-BL-03 **Borehole-scale geothermal reservoir characterisation of structures and rock properties for the development of a geothermal-grade georadar tool. (Cancelled)**

M. Chatziliadou, A. Shakas

*Fraunhofer IEG, Reservoir Geophysics, Bochum and others*

P-BL-04 **Current Status of a Geological Segmentation for Rotondo Granite**

N.-A. Kouamo Keutchafo, M. Balcewicz, M. Siegert, E. H. Saenger

*Bochum University of Applied Sciences, Bochum and others*

P-BL-05 **Modification of the SDR equation for permeability prediction**

Z. Zhang, A. Weller

*Technische Universität Clausthal, Clausthal-Zellerfeld*

P-BL-06 **Influence of mineralogy and microstructure on the electrical properties of crustal rocks: insights from the DIVE Project in the Ivrea-Verbano Zone**

H. Mansouri, S. Tholen, V. Toy, F. Hawemann

*Johannes Gutenberg-Universität Mainz and others*

P-BL-07 **Fracture network characterization by structural geological analysis and periodic pumping tests in borehole SB1.1 of the Bedretto Underground Laboratory for Geosciences and Geoenergies, Switzerland**

F. Karim, S. Edem, S. Danaei, J. Renner

*Ruhr-Universität Bochum, Institut für Geologie, Mineralogie und Geophysik, Bochum*

P-BL-08 **Fracture detection on acoustic borehole televiewer images: Exploring various image processing approaches**

S. Danaei, J. Renner

*Ruhr-Universität Bochum, Institut für Geologie, Mineralogie und Geophysik, Bochum*

P-S3-01 **Seismicity vs. slip with Foamquake analog modelling subduction experiments.**

E. Latypova, F. Corbi, G. Mastella, F. Funiciello, J. Bedford

*Ruhr-Universität Bochum, Institute for Geology, Mineralogy and Geophysics, Bochum and others*

P-S3-02 **Geodetic Aspects of the Seismically Active Mt. Hochstaufen (Germany) – Space-borne and Ground-based InSAR Measurements**

A. Schlömer, J. Wassermann, S. Metzger

*LMU München, Department of Earth and Environmental Sciences, München and others*

P-S3-03 **The Geophysical Instrument Pool Potsdam (GIPP) – now with GNSS component**

B. Wawrzinek, C. Haberland, O. Ritter, B. Männel, C. Krawczyk

*GFZ Helmholtz Centre for Geosciences, Potsdam and others*

P-SO-01 **A dataservice for precomputed seismic noise cross-correlations functions**

J. Lehr, C. Sens-Schönfelder, A. Heinloo, J. Quinteros

*Geoforschungszentrum Potsdam*

P-SO-03 **Seismic noise field investigations at the EMR gravitational wave telescope candidate site**

D. Becker, C. Hammer, C. Hadzioannou

*Universität Hamburg, Institut für Geophysik, Hamburg*

P-SO-05	<b>Rayleigh-wave Ambient Noise Analysis for the OHANA Experiment in the Northeast Pacific</b>  <u>G. Laske</u> , G. Atkisson, J. A. Collins, D. K. Blackman  <i>Scripps Institution of Oceanography, Institute of Geophysics and Planetary Physics - 0225, La Jolla, United States of America and others</i>
P-SO-07	<b>Seismic signals associated with plume events and inner crater collapses during the 2021 Geldingadalir eruption</b>  <u>A. Joachim</u> , S. Heimann, E. P. S. Eibl, L. Rees, M. Dwars, É. Á. Gudnason, T. Ágústsdóttir, G. P. Hersir, T. Winder, N. Rawlinson, T. Fischer, J. Doubravová, J. Burjánek, O. D. Lamb  <i>University of Potsdam, Institute for Geosciences, Potsdam and others</i>
P-SO-09	<b>Seismicity of the High-Altitude Volcano Ojos del Salado</b>  <u>L. Murray-Bergquist</u> , <u>M. Thorwart</u> , A. Garcia Pina, C. Ulloa, J. van Ginkel, R. Wessels, L. van Huisstede, S. Rebolé Canals, A. Beniest  <i>Vrije Universiteit Amsterdam, Amsterdam, Netherlands and others</i>
P-SO-11	<b>Deciphering plausible driving mechanisms of swarms in the western Peloponnese (Greece) using earthquake clustering and statistical properties</b>  <u>S. Ahmadnia</u> , D. Essing, R. M. Harrington, G. M. Bocchini  <i>Ruhr-Universität Bochum, Institut für Geologie, Mineralogie und Geophysik, Bochum</i>
P-SO-13	<b>A repeating earthquake catalog for Northern Chile</b>  <u>J. Folesky</u> , J. Kummeow, L. J. Hofman  <i>Freie Universität Berlin, Geophysik, Berlin and others</i>
P-SO-15	<b>Heterogene seismische Anisotropie in der Erdkruste und Auswirkungen auf XKS-Splittinganalysen</b>  <u>M. Kaus</u> , J. P. Kruse, A. Kaviani, G. Rümpker  <i>Goethe-Universität Frankfurt, Institut für Geowissenschaften, Frankfurt am Main</i>
P-SO-17	<b>Seismologische Überwachung im Freistaat Sachsen: Migration des Sachsen-Netzes SXNET von der Universität Leipzig an die TU Bergakademie Freiberg</b>  C. Alexandrakis-Zieger, F. Hänel, F. Käßner, S. Funke, R. Voigt, M. Korn, L. Sonnabend, <u>S. Buske</u>  <i>TU Bergakademie Freiberg, Institute of Geophysics and Geoinformatics, Freiberg and others</i>
P-SO-19	<b>Illuminating Subsurface Dynamics During Injection and Production Restart in Deep Geothermal Wells Using Fiber-Optic Distributed Dynamic Strain Sensing</b>  <u>J. Hart</u> , C. Wollin, A. Andy, T. Ledig, T. Reinsch, C. Krawczyk  <i>GFZ Helmholtz-Zentrum für Geoforschung, Potsdam and others</i>

## Oral – Saal 2a

**11:20–13:00 O-SO**

### SO - Seismologie

Moderation: K. D. Fischer, Bochum

11:20–11:40 O-SO-04 **Investigation of seismicity in the Eifel region, using data from the Eifel Large-N Network**

P. Laumann<sup>1</sup>, H. Zhang<sup>1</sup>, M. P. Isken<sup>1</sup>, G. Petersen<sup>1</sup>, P. Büyükkapınar<sup>1</sup>, T. Dahm<sup>1</sup>, B. Schmidt<sup>2</sup>

<sup>1</sup>GFZ Potsdam, Section 2.1, Potsdam, Germany, <sup>2</sup>Geological Survey of Rhineland-Palatinate, State Seismological Service, Mainz

11:40–12:00 O-SO-05 **The upper crustal structure of the Eifel volcanic region, southwest Germany from local earthquake tomography using Large-N seismic network data**

H. Zhang, C. Haberland, T. Dahm, M. P. Isken, P. Laumann, P. Büyükkapınar

Helmholtz Centre Potsdam GFZ German Research Centre For Geosciences, Potsdam

12:00–12:20 O-SO-06 **What crustal magmatic reservoirs lie beneath the East Eifel volcanic fields? Clues from the Eifel Large-N passive seismic experiment**

T. Dahm<sup>1,2</sup>, H. Zhang<sup>1</sup>, P. Laumann<sup>1</sup>, P. Büyükkapınar<sup>1</sup>, M. Isken<sup>1</sup>, S. Heimann<sup>2</sup>

<sup>1</sup>Helmholtzzentrum für Geowissenschaften GFZ, Potsdam, Germany, <sup>2</sup>Universität Potsdam, Institut für Geowissenschaften, Potsdam

12:20–12:40	O-SO-07	<b>Automatic ML Catalogs in Action: Mapping Iceland's Volcanic Activity in High Detail</b> M. Isken <sup>1</sup> , T. Fischer <sup>2</sup> , T. Dahm <sup>1</sup> , P. Hrubcová <sup>3</sup> , J. Vlček <sup>2</sup> , J. Doubravová <sup>3</sup> , J. Burjánek <sup>3</sup> , E. Á. Guðnason <sup>4</sup> , T. Agustsdóttir <sup>4</sup> <sup>1</sup> GFZ Potsdam, Potsdam, Germany, <sup>2</sup> Charles University, Prague, Czech Republic, Faculty of Science, Prague, Czech Republic, <sup>3</sup> Academy of Sciences, Institute of Geophysics, Prague, Czech Republic, <sup>4</sup> Iceland GeoSurvey, ISOR, Reykjavik, Iceland
12:40–13:00	O-SO-08	<b>Linking seismicity, dyke and graben formation: a case study from the Reykjanes Peninsula</b> <u>T. J. Fischer</u> <sup>1</sup> , J. Vlček <sup>1</sup> , P. Hrubcová <sup>2</sup> , A. Lomax <sup>3</sup> <sup>1</sup> Charles University, Faculty of Science, Applied geophysics, Praha, Czech Republic, <sup>2</sup> Geophysical Institute, Academy of Science, Praha, Czech Republic, <sup>3</sup> ALomax Scientific, Mouans-Sartoux, France

## Oral – Saal 3

11:20–12:50	<b>DGG-Kolloquium ↗</b>
-------------	-------------------------

## Schwerpunktsession – Saal 4

11:20–12:20	O-S3	<b>S3 - Tektonische Geodäsie</b> Moderation: J. Bedford, Bochum
11:20–11:40	O-S3-03	<b>Aseismic creep of the Katouna–Stamna Fault, observed by satellite geodesy, field evidence and structural analysis</b> J. Szrek <sup>1</sup> , S. Crosetto <sup>2</sup> , G. Gomba <sup>3</sup> , <u>S. Metzger</u> <sup>2</sup> <sup>1</sup> École Normale Supérieure, Geowissenschaften, Paris, France, <sup>2</sup> GFZ Helmholtz-Zentrum für Geoforschung, Lithosphärenodynamik, Potsdam, Germany, <sup>3</sup> Deutsches Zentrum für Luft und Raumfahrt, SAR Signalverarbeitung, Wessling
11:40–12:00	O-S3-04	<b>Analysis of the Pütürge Segment at the East Anatolian Fault between the large 2020 and 2023 Earthquakes</b> A. Kuntze <sup>1</sup> , <u>H. Sudhaus</u> <sup>2</sup> <sup>1</sup> CAU Kiel, Satelliten- und Aerogeophysik, Kiel, Germany, <sup>2</sup> Karlsruhe Institut für Technologie, Geophysikalisches Institut, Karlsruhe
12:00–12:20	O-S3-05	<b>Deformation Monitoring on Laacher See by GNSS</b> <u>Z. Deng</u> <sup>1</sup> , M. Ramatschi <sup>1</sup> , T. Dahm <sup>2</sup> <sup>1</sup> GeoForschungsZentrum Potsdam, Geodesy, Potsdam, Germany, <sup>2</sup> GeoForschungsZentrum Potsdam, Physics of Earthquakes and Volcanoes, Potsdam

## Event – Saal 4

12:50–14:00	<b>Lunchseminar ↗</b>
13:00–14:00	<b>Mittagspause</b>

## Schwerpunktsession – Saal 2a

14:00–15:00	O-S3-PV	<b>Continental scale strain mapping with GNSS: hydrological signals and seismotectonic implications</b> English Moderation: J. Bedford, Bochum <u>E. Serpelloni</u> Istituto Nazionale di Geofisica e Vulcanologia di Bologna, Sezione di Bologna, Bologna, Italy
-------------	---------	---

## Oral – Saal 2a

15:00–16:00 O-SO

### SO – Seismologie

Moderation: M. Bischoff, Hannover

15:00–15:20 O-SO-09

#### Sustainable preservation of analogue seismic data in Germany – Digitization test and reference earthquake source parameters.

G. Kulikova<sup>1</sup>, F. Krueger<sup>2</sup>, C. Hadzioannou<sup>3</sup>

<sup>1</sup>UP Transfer GmbH at the University of Potsdam, Potsdam, Germany, <sup>2</sup>University of Potsdam, Institute of Geosciences, Potsdam, Germany, <sup>3</sup>University of Hamburg, Institute of Geophysics, Hamburg

15:20–15:40 O-SO-10

#### The Collm Archive - Preserving the legacy of several generations of Observatory members for future generations.

L. Sonnabend<sup>1</sup>, P. Buchholz<sup>2</sup>, G. Vogt<sup>3</sup>, S. Wendt<sup>2</sup>, T. Duteloff<sup>3</sup>

<sup>1</sup>Sächsisches Landesamt für Umwelt Landwirtschaft und Geologie, Abteilung Geologie / Referat 102 Geologische Kartierung und Geophysik, Freiberg, Germany, <sup>2</sup>Universität Leipzig, Leipzig, Germany,

<sup>3</sup>Sächsisches Landesamt für Umwelt Landwirtschaft und Geologie, Abteilung Geologie / Referat 101 Geologisches Archiv, Freiberg

15:40–16:00 O-SO-11

#### Development of a unified earthquake catalog for the Vogtland/West Bohemia swarm region for the investigation of the geometry of the crustal brittle-ductile boundary

A. Olivar-Castaño<sup>1</sup>, M. Ohrnberger<sup>1</sup>, P. Büyükkapınar<sup>2</sup>, T. Dahm<sup>2</sup>, J. Doubravová<sup>3</sup>, T. Fischer<sup>4</sup>, J. Wasserman<sup>5</sup>, U. Wegler<sup>6</sup>, S. Wendt<sup>7</sup>

<sup>1</sup>Universität Potsdam/Institut für Geowissenschaften, Potsdam, Germany, <sup>2</sup>GFZ Deutsches GeoForchungsZentrum, Potsdam, Germany, <sup>3</sup>Czech Academy of Sciences/Institute of Geophysics, Prague, Czech Republic, <sup>4</sup>Charles University, Prague, Czech Republic, <sup>5</sup>Ludwig-Maximilian Universität München, Department für Geo- und Umweltwissenschaften, München, Germany, <sup>6</sup>Friedrich-Schiller Universität Jena/Institut für Geowissenschaften, Jena, Germany, <sup>7</sup>Universität Leipzig/Institut für Erdsystemwissenschaft und Fernerkundung, Leipzig

## Oral – Saal 3

15:00–16:00

### Open Session – aktuelle Geo-Ereignisse

Moderation: K. D. Fischer, Bochum

## Oral – Saal 4

15:00–16:00 O-GD

### GD – Geodynamik / Tektonophysik

Moderation: N. Kukowski, Jena

15:00–15:20 O-GD-01

#### The role of proto-thrusts in strain accumulation along the segmented deformation front at the northern Cascadia subduction zone, Canada

W. Schäfer, M. Riedel, G. Crutchley, H. Kopp

GEOMAR Helmholtz-Zentrum für Ozeanforschung Kiel, Dynamik des Ozeanbodens - Marine Geodynamik, Kiel

15:20–15:40 O-GD-02

#### 2-D Crustal Modelling of the Mérida Andes - Venezuela Using Wide-Angle Seismic and Gravity Data

L. A. Yegres Herrera<sup>1</sup>, M. Schmitz<sup>2</sup>, J. Ávila-García<sup>3</sup>, F. Rondón<sup>4</sup>, A. GIAME Seismic Working Group<sup>4</sup>

<sup>1</sup>CICESE, Sismología, Ensenada, Mexico, <sup>2</sup>Universidad Central de Venezuela, Departamento de Geofísica, Caracas, Venezuela, <sup>3</sup>UNAM, Instituto de Geofísica, Ciudad de México, Mexico, <sup>4</sup>FUNVISIS, Departamento de Geofísica, Caracas, Venezuela

15:40–16:00 O-GD-03

#### Seismic Sequences in the Western Peloponnese: Unveiling Active Deformation Within and Beyond the Aegean microplate

D. Essing, G. M. Bocchini, M. P. Roth, R. M. Harrington

Ruhr-Uni Bochum, Bochum

16:00–17:00

### Kaffeepause

## Poster – Saal 2b

16:00–17:00 P5

### Poster GT, PV, SO

Moderation: D. Kreith, Braunschweig (GT), M. Bücker, Kiel (PV), T. Plenefisch, Hannover (SO)

P-SO-02

#### **On the quantification of ambient seismic noise amplitudes**

C. Sens-Schönfelder

*Deutsches GeoForschungsZentrum Potsdam, Potsdam*

P-SO-04

#### **Monitoring temporal seismic velocity changes in the western Bohemian Massif area using cross-correlation of ambient noise**

S. Mandal, T. Fischer, B. Růžek

*Charles University, Institute of Hydrogeology, Engineering Geology and Applied Geophysics,, Prague, Czech Republic and others*

P-SO-06

#### **Full-waveform modeling and ML-based tomography of volcanic edifices**

R. Medappil Pinatt, G. Rümpker, A. Komeazi, F. Limberger

*Goethe-University Frankfurt, Institute of Geosciences, Frankfurtand others*

P-SO-08

#### **Investigating Magmatic Processes in the Reykjanes Peninsula Through Seismic Velocity Monitoring: Vp/Vs Ratio and Shear Wave Velocity Variations During Volcanic Eruptions**

A. Masihi, T. Fischer

*Charles University, Faculty of Science, Prague, Czech Republic*

P-SO-10

#### **The cascade of events triggering a teleseismic week-long monochromatic signal**

A. Carrillo-Ponce, S. Heimann, G. Petersen, T. R. Walter, S. Cesca, T. Dahm

*GFZ German Research Centre for Geosciences, Potsdamand others*

P-SO-12

#### **Modeling historical earthquakes to quantify the Coulomb Failure Stress changes leading up to the 2023 Kahramanmaraş, Türkiye earthquake sequence**

C. Fockenberg, A. Verdecchia, G.-M. Bocchini, R. M. Harrington

*Institut für Geologie, Mineralogie und Geophysik, Bochum*

P-SO-14

#### **Out of the box or own model for ML phase picking at local (GRSN) and teleseismic distances (IMS)?**

A. Steinberg, K. Stammer, C. Ramos, G. Hartmann, P. Gaebler, T. Plenefisch, B. Goebel

*Bundesanstalt für Geowissenschaften und Rohstoffe (BGR), Erdbebendienst des Bundes, Kernwaffenteststopp, Hannover*

P-SO-16

#### **The SIEGFRIED passive seismological network**

M. Dietl, M. P. Roth, S. Carrasco, S. Neugebauer, N. Fazlibašić, C. Finger

*Fraunhofer IEG, Bochumand others*

P-SO-18

#### **Seismische Ereignisse in der südwestlichen Ostsee – Harmonisierung des deutschen und dänischen Ereigniskatalogs**

J. Horrmann, C. Weidel, T. Meier

*Christian-Albrechts-Universität zu Kiel, Kiel*

P-SO-20

#### **Fiber-optics-based observational platforms for investigating the urban subsurface: the InDySE Project**

V. Rodríguez Tribaldos, L. Pinzón Rincón, C. Krawczyk, P. Martínez-Garzón, M. Bohnhoff

*GFZ Helmholtz Centre for Geosciences, Geophysical Imaging, Potsdamand others*

P-GT-01

#### **Assessing the influence of high-resolution topography and radiogenic heat production on geothermal heat flow in Northeast Greenland**

J. Gehrig, J. Freienstein, C. Carter, G. Hüttner, O. Eisen, V. Helm, S. Franke, W. Szwilus, J. Ebbing

*Institut für Geowissenschaften CAU Kiel, Kieland others*

P-GT-02

#### **Untersuchung von Fehlstellen in der Hinterfüllung von Erdwärmesonden**

E. Berrios Amador, C. Gerhards, R.-U. Börner, K. H. Zschoke

*TU Bergakademie Freiberg, Freibergand others*

- P-GT-03      **Numerical Simulations of thermal data from a privately used Borehole Heat Exchanger**  
E. Pilgermann, A. Hördt, C. Virgil  
*TU Braunschweig, Institut für Geophysik und Extraterrestrische Physik, Braunschweig*
- P-PV-01      **Crossing the scales and disciplines – petrological and geophysical investigations of hydrogen source rocks in the Münchberg Massif, NE Bavaria**  
M. Bagge, P. Klitzke, M. Hasch, N. Koglin, A. Ruppel, J.-F. Goldmann, A. Löwer  
*Federal Institute for Geosciences and Natural Resources (BGR), Hannover and others*
- P-PV-02      **Geoelectrical Monitoring of Soil Moisture Dynamics in Plant Ecosystems**  
J. Hoppenbrock, M. Beyer, M. Gerchow, A. Iraheta, M. W. Strohbach, M. Bücker  
*Julius Kühn-Institut, Institute for Plant Protection in Horticulture and Urban Green, Braunschweig and others*

### Event – Saal 2a

17:00–19:00      **DGG-Mitgliederversammlung**

### Plenarvortrag – Extern

20:00–21:00    O-AV      **Öffentlicher Abendvortrag**

## DONNERSTAG, 27. FEBRUAR 2025

### Oral – Saal 2a

**09:00–10:20 O-SO**

#### **SO – Seismologie**

Moderation: S. Donner, Hannover

09:00–09:20 O-SO-12

##### **Rapid detection of small signal-to-noise ratio seismic events using fast time-reverse imaging**

C. Finger

*Fraunhofer IEG, Bochum*

09:20–09:40 O-SO-13

##### **Microseismic activity in the Eastern Alps: Seismic sequences, rupture mechanisms, and active faults**

G. Petersen<sup>1</sup>, L. Hofman<sup>2</sup>, J. Kummerow<sup>2</sup>, S. Cesca<sup>1</sup>

<sup>1</sup>*GFZ German Research Centre for Geosciences, Potsdam, Germany*, <sup>2</sup>*Freie Universität, Berlin*

09:40–10:00 O-SO-14

##### **Using 3D dynamic rupture simulations to probe the effects of source-station geometry and fault-zone architecture on spectral corner frequency**

M. Roßbach<sup>1</sup>, N. Schliwa<sup>2</sup>, R. M. Harrington<sup>1</sup>, A.-A. Gabriel<sup>3</sup>, E. S. Cochran<sup>4</sup>

<sup>1</sup>*Ruhr-Universität Bochum, Institut für Geologie, Mineralogie und Geophysik, Bochum, Germany*,

<sup>2</sup>*Ludwig-Maximilians-Universität München, München, Germany*, <sup>3</sup>*University of California, San Diego, United States of America*, <sup>4</sup>*United States Geological Survey, Pasadena, United States of America*

10:00–10:20 O-SO-15

##### **Microstructural evidence of episodic deformation at hypocentral depth recorded by fault rocks**

L. M. Beiers<sup>1,2</sup>, C. A. Trepmann<sup>2</sup>, F. Dellefant<sup>2,3</sup>

<sup>1</sup>*Hochschule Bochum, Reservoir Geophysics, Bochum, Germany*, <sup>2</sup>*Ludwig-Maximilians-Universität München, Department für Geo- und Umweltwissenschaften, München, Germany*,

<sup>3</sup>*Ludwig-Maximilians-Universität München, Department für Kulturwissenschaften und Altertumskunde, München*

### Oral – Saal 3

**09:00–10:20 O-SM**

#### **SM – Seismik**

Moderation: S. Wadas, Hannover

09:00–09:20 O-SM-01

##### **Wie Wellenforminversion die seismische Abbildungsmöglichkeiten erweitert: Projekt Chatseis**

T. Burschil<sup>1</sup>, D. Köhn<sup>2</sup>, M. Körbe<sup>3</sup>, J. Großmann<sup>4</sup>, G. Gabriel<sup>3,5</sup>, G. Firla<sup>6</sup>, C. Schmalfuß<sup>6</sup>, M. Fiebig<sup>6</sup>

<sup>1</sup>*Bundesanstalt für Geowissenschaften und Rohstoffe, B3.2, Hannover, Germany*,

<sup>2</sup>*Christian-Albrechts-Universität zu Kiel, Kiel, Germany*,

<sup>3</sup>*LIAG-Institut für Angewandte Geophysik, Hannover, Germany*,

<sup>4</sup>*Bayerisches Landesamt für Umwelt, Hof, Germany*, <sup>5</sup>*Leibniz Universität Hannover, Germany*,

<sup>6</sup>*Universität für Bodenkultur Wien (BOKU), Wien, Austria*

09:20–09:40 O-SM-02

##### **Integration of borehole and 2D seismic processing velocities for velocity modeling in Schleswig-Holstein**

D. Schindler

*Landesamt für Umwelt des Landes Schleswig-Holstein, Geologischer Dienst Schleswig-Holstein, Flensburg*

09:40–10:00 O-SM-03

##### **Seismic site characterization for the Low-Seismic-Lab (Lausitz area)**

O. Günaydin, F. Hloušek, M. Muhalanga, H. Näser, S. Buske

*TU Freiberg, Institute of Geophysics and Geoinformatics, Freiberg*

10:00–10:20 O-SM-04

##### **Bearbeitung und Analyse der 3D-Seismik Daten im Bereich der Asse-Salzstruktur (Niedersachsen)**

N. Kühne<sup>1</sup>, L. Bräunig<sup>1</sup>, F. Hlousek<sup>1</sup>, S. Buske<sup>1</sup>, H. Ding<sup>2</sup>, M. Scholze<sup>2</sup>

<sup>1</sup>*TU Bergakademie Freiberg, Institut für Geophysik und Geoinformatik, Freiberg, Germany*,

<sup>2</sup>*Bundesgesellschaft für Endlagerung, Peine*

## Schwerpunktsession – Saal 4

**09:00–10:20 O-S4**

### **S4 - Induzierte Polarisation**

Moderation: Katrin Breede, Clausthal-Zellerfeld

09:00–09:20 O-S4-01

#### **Is it possible to assess the quality of carbonates using IP?**

N. Klitzsch, L. Ahrensmeier

*RWTH Aachen University, CG<sup>3</sup> Aachen*

09:20–09:40 O-S4-02

#### **Kann IP bei der Permeabilitätsabschätzung helfen?**

A. Weller<sup>1</sup>, L. Slater<sup>2</sup>

<sup>1</sup>*Technische Universität Clausthal, Clausthal-Zellerfeld, Germany,*

<sup>2</sup>*Rutgers University, Newark, United States of America*

09:40–10:00 O-S4-03

#### **Influence of particle-particle interaction on the spectral induced polarization response of conducting and non-conducting particles**

D. Kreith<sup>1</sup>, J. Wentzki<sup>1</sup>, B. Brömer<sup>1</sup>, A. Haji<sup>1</sup>, M. Bücker<sup>1,2</sup>

<sup>1</sup>*Technische Universität Braunschweig, Institut für Geophysik und Extraterrestrische Physik, Braunschweig, Germany*, <sup>2</sup>*Christian-Albrechts-Universität Kiel, Institut für Geophysik, Kiel*

10:00–10:20 O-S4-04

#### **Implications of an additional surface capacitance for the understanding of electrode polarization**

M. Bücker<sup>1</sup>, F. Keiser<sup>2</sup>, D. Kreith<sup>2</sup>, K. Breede<sup>3</sup>, Z. Zhang<sup>3</sup>, A. Weller<sup>3</sup>

<sup>1</sup>*Universität Kiel, Kiel, Germany*, <sup>2</sup>*Technische Universität Braunschweig, Braunschweig, Germany*,

<sup>3</sup>*Technische Universität Clausthal, Clausthal*

**10:20–11:20**

### **Kaffeepause**

## Poster – Saal 2b

**10:20–11:20 P6**

### **Poster S4, KI, SM**

Moderation: M. Halisch, Hannover (S4), S. Buske, Freiberg (S4), M. Joswig, Tübingen (KI), S. Buske, Freiberg (SM)

P-S4-01

#### **Zeta-potential and spectral induced polarization measurements on municipal solid waste matrices at different ionic strengths**

A. Rahmani, M. Halisch, A. Mellage

*University of Kassel, Civil and Environmental Engineering, Kassel and others*

P-S4-02

#### **Dielectric Spectroscopy Measurements of Martian analogue Bentonite Soil Sample**

L. Zimmermann, S. Garland, A. Lorek, J. H. Börner

*TU Bergakademie Freiberg, Institut für Geophysik und Geoinformatik, Freiberg and others*

P-S4-03

#### **Numerical simulation of polarization mechanisms of frozen soil at the pore scale**

F. Keiser, A. Hördt

*TU Braunschweig, Institut für Geophysik und extraterrestrische Physik, AG Hördt, Braunschweig*

P-S4-04

#### **High-Frequency Induced Polarization (HFIP) for quantitative ice content estimation in a Palsa at Aidejavri (Norway)**

R. Schulz, I. Burger, A. Pischke, S. Westermann, A. Hördt

*Institut für Geophysik und Extraterrestrische Physik, Angewandte Geophysik, Braunschweig and others*

P-S4-05

#### **A novel approach to determine temperature correction coefficients for complex conductivity monitoring data**

A. M. Mansfeld, J. Hase, A. Kemna

*Institut für Geowissenschaften / Universität Bonn, Geophysik, Bonn*

P-S4-06

#### **Evaluierung einer neuartigen Anregungssignalform für Spektrale IP Messungen.**

T. Radic

*Radic Research, Berlin*

P-S4-07

#### **Accurate model inference and uncertainty quantification in complex resistivity imaging**

J. Hase, A. Kemna

*Institut für Geowissenschaften / Universität Bonn, Geophysik, Bonn*

P-S4-08	<b>Spectral Induced Polarization on metallic spheres</b> <u>K. Breede, D. Kreith, Z. Zhang, M. Bücker, A. Weller</u> <i>Institute of Geotechnology and Mineral Resources, Clausthal University of Technology, Clausthal-Zellerfeld and others</i>
P-KI-01	<b>Machine learning approach for heading error correction of drone-borne magnetic measurements</b> <u>C. Paul, V. Schmidt</u> <i>Universität Münster, Institut für Geophysik, Münster</i>
P-KI-02	<b>DeepONets applied to DC resistivity problems</b> <u>S. Weit, K. Spitzer, O. Rheinbach</u> <i>Technische Universität Bergakademie Freiberg, Institut für Geophysik und Geoinformatik, Freiberg and others</i>
P-SM-01	<b>Anisotropic anelastic Fresnel-Volume-Migration of the Asse 3D seismic data set</b> <u>N. Kühne, F. Hlousek, S. Buske, L. Bräunig, V. Becker, M. Scholze</u> <i>TU Bergakademie Freiberg, Institute of Geophysics and Geoinformatics, Freiberg and others</i>
P-SM-02	<b>A 3D high-resolution velocity model of the Asse salt structure (Lower Saxony)</b> <u>L. Bräunig, N. Kühne, F. Hloušek, S. Buske, V. Becker, M. Scholze</u> <i>TU Bergakademie Freiberg, Institut für Geophysik und Geoinformatik, Freiberg and others</i>
P-SM-03	<b>Reflection seismic imaging at the Asse salt structure from in-mine seismic recordings of a 3D surface seismic survey</b> <u>F. Hlousek, N. Kühne, L. Bräunig, S. Buske, M. Scholze</u> <i>TU Bergakademie Freiberg, Institut für Geophysik und Geoinformatik, Freiberg and others</i>
P-SM-04	<b>Seismic Exploration for the Emerging Lunar Industry</b> <u>O. Cornelius, D. Solis, P. Koch, J. de Freitas</u> <i>IMENSUS UG (haftungsbeschränkt), Stuttgart</i>
P-SM-05	<b>Velocity modeling in Schleswig-Holstein as part of the TUNB Velo 2.0 project</b> <u>D. Schindler, A. Omlin, F. Hese, C. Liebermann</u> <i>Landesamt für Umwelt des Landes Schleswig-Holstein, Geologischer Dienst Schleswig-Holstein, Flensburg</i>
P-SM-06	<b>Enhanced S-Wave Seismic Imaging for Near-Surface Applications</b> <u>S. H. Wadas</u> <i>LIAG-Institut für Angewandte Geophysik, Forschungsabteilung 1 - Geophysikalische Erkundung, Hannover</i>
P-SM-07	<b>Erkundung eines potenziellen Wärmespeichers im Untergrund durch Scherwellenreflexionsseismik</b> <u>P. Leineweber, R. Kirsch, C. Janout, L. Wicka, R. Mecking, G. Druivenga</u> <i>Geosym GmbH, Hannover and others</i>

## Oral – Saal 2a

11:20–12:40	<b>O-SO</b>	<b>SO - Seismologie</b> Moderation: W. Friederich, Bochum
11:20–11:40	O-SO-16	<b>An Image and Slab Model of the Northern Chilean Subduction Zone Forearc from P and PP Receiver Functions</b> <u>W. Bloch<sup>1,2</sup>, B. Schurr<sup>2</sup>, X. Yuan<sup>3</sup>, F. Tilmann<sup>3</sup>, C. Faccenna<sup>2</sup></u> <sup>1</sup> NORSAR, Applied Seismology, Kjeller, Norway, <sup>2</sup> GFZ Deutsches GeoForschungs Zentrum, Dynamik der Lithosphäre, Potsdam, Germany, <sup>3</sup> GFZ Deutsches GeoForschungs Zentrum, Seismologie, Potsdam
11:40–12:00	O-SO-17	<b>AdriaArray – a passive seismic experiment to explore geodynamic drivers of plate deformation and geohazards in the Central Mediterranean</b> <u>T. Meier<sup>1</sup>, P. Kolinsky<sup>2</sup></u> <sup>1</sup> CAU Kiel, Institut für Geowissenschaften, Kiel, Germany, <sup>2</sup> Czech Academy of Sciences, Prague, Czech Republic

12:00–12:20	O-SO-18	<b>Seismic Analysis and Remote Sensing Precursors of the February 13, 2024 Çöpler Gold Mine Landslide in Erzincan, Eastern Turkey</b>  <u>P. Büyükkapınar</u> <sup>1</sup> , A. Carrillo-Ponce <sup>1</sup> , H. Tanyas <sup>2</sup> , M. B. Munir <sup>2</sup> , E. Karasozen <sup>3</sup> , D. Ertuncay <sup>4</sup> <sup>1</sup> GFZ, Potsdam, Germany, <sup>2</sup> University of Twente, Enschede, Netherlands, <sup>3</sup> University of Alaska Fairbanks, Alaska, United States of America, <sup>4</sup> The Seismological Research Center - OGS, Udine, Italy
12:20–12:40	O-SO-19	<b>Elephant activity patterns in a zoo setting: a pilot study using co-located seismic and infrasound measurements</b>  <u>F. Limberger</u> <sup>1</sup> , G. Rümpker <sup>1</sup> , T. Spengler <sup>2</sup> , M. Becker <sup>2</sup> <sup>1</sup> Goethe-University Frankfurt, Institute of Geosciences, Frankfurt, Germany, <sup>2</sup> Opel-Zoo, Education and Research, Kronberg im Taunus

## Oral – Saal 3

11:20–13:00	O-KI	<b>KI Verfahren der Geophysik</b> Moderation: J. Heuel, Karlsruhe
11:20–11:40	O-KI-01	<b>‘Pattern recognition for earthquake detection’ - 40 years research in AI-based seismology</b> <u>M. Joswig</u> <i>Sonicona GbR, Tübingen</i>
11:40–12:00	O-KI-02	<b>SonoDet+: a new, AI-based multi-trace approach for seismic event identification</b> <u>M. Joswig</u> , R. Häfner <i>Sonicona GbR, Tübingen</i>
12:00–12:20	O-KI-03	<b>Utilizing Neural Operators for Seismic Travel Time Approximation and Inversion in Anisotropic 3D Media</b> <u>B. Paulwitz</u> , S. Buske, F. Hloušek, V. Raj <i>TU Bergakademie Freiberg, Freiberg</i>
12:20–12:40	O-KI-04	<b>Machine-learning-based picking of DAS data for cross-well tomography</b> <u>N. Boitz</u> <sup>1</sup> , A. Stork <sup>2</sup> , T. Fechner <sup>3</sup> , U. Ködel <sup>3</sup> , S. Mackens <sup>3</sup> <sup>1</sup> Freie Universität Berlin, Geowissenschaften - Geophysik, Berlin, Germany, <sup>2</sup> Silixa Ltd., Elstree, Hertfordshire, United Kingdom, <sup>3</sup> Geotomographie GmbH, Neuwied
12:40–13:00	O-KI-05	<b>Mit Hilfe automatischer Hyperbeldetektion und Geschwindigkeitsbestimmung zum 3D Modell und verbesserter (archäologischer) Interpretation</b> <u>T. Wunderlich</u> <sup>1,2</sup> , B. S. Majchczack <sup>1,3</sup> , D. Wilken <sup>1,2,3</sup> , M. Segschneider <sup>4</sup> , W. Rabbel <sup>1,2,3</sup> <sup>1</sup> Christian-Albrechts-Universität zu Kiel, Institut für Geowissenschaften, Kiel, Germany, <sup>2</sup> Christian-Albrechts-Universität zu Kiel, SFB1266 - Scales of Transformation, Kiel, Germany, <sup>3</sup> Christian-Albrechts-Universität zu Kiel, Exzellenzcluster ROOTS, Kiel, Germany, <sup>4</sup> NihK—Institute for Historical Coastal Research, Wilhelmshaven

## Schwerpunktsession – Saal 4

11:20–12:20 O-S4

### S4 – Induzierte Polarisation

Moderation: M. Halisch, Hannover

11:20–11:40 O-S4-05

#### High-frequency spectral induced polarisation to image permafrost features in Storflaket, Abisko, Northern Sweden

M. Sugand, A. Hördt

*TU Braunschweig, Braunschweig*

11:40–12:00 O-S4-06

#### Spectral induced polarization (SIP) as a non-invasive tool for tracking microbial dynamics: Insights from *<em>Shewanella oneidensis MR-1</em>* cell suspensions and alginate bead-packed column reactors

D. Amarawardana<sup>1</sup>, A. Mellage<sup>1</sup>, C. M. Smeaton<sup>2</sup>

<sup>1</sup>Universität Kassel, Civil and Environmental Engineering, Kassel, Germany, <sup>2</sup>School of Science and the Environment, Memorial University of Newfoundland, Newfoundland, Canada

12:00–12:20 O-S4-07

#### Towards Sustainable Cement Compositions: Exploring the Effects of Clinker Substitutes with NMR and Induced Polarization

S. Munsch<sup>1</sup>, L. Grobla<sup>1</sup>, W. Schmidt<sup>2</sup>, S. Kruschwitz<sup>1,3</sup>

<sup>1</sup>Bundesanstalt für Materialforschung und -prüfung, Zerstörungsfreie Prüfung, Berlin, Germany,

<sup>2</sup>Bundesanstalt für Materialforschung und -prüfung, Baustofftechnologie, Berlin, Germany,

<sup>3</sup>Technische Universität Berlin, Zerstörungsfreie Baustoffprüfung, Berlin

## Event – Saal 4

12:50–14:00

### Lunch'n Learn ↗

13:00–14:00

### Mittagspause

## Schwerpunktsession – Saal 2a

14:00–15:00 O-S4-PV

### Beyond Boundaries: Advancing Induced Polarization in Challenging Geophysical Contexts

English

Moderation: M. Halisch, Hannover

J. Börner

*Technische Universität Bergakademie Freiberg,  
Institut für Geophysik und Geoinformatik, Freiberg, Germany*

## Event – Saal 2a

15:00–16:00

### Abschlussveranstaltung mit Prämierung Poster und Vorträge

## Event – Saal 2a

16:00–17:00

### DGG-Vorstandssitzung

# Abstracts 2025

<b>S1–S4 Plenarvorträge .....</b>	<b>56–59</b>
<b>S1 – Rekonstruktion der Dynamik des tiefen Erdinnern über geologische Zeiträume</b>	
VORTRÄGE .....	60
POSTER .....	63
<b>S2 – Induzierte Seismizität</b>	
VORTRÄGE .....	67
POSTER .....	70
<b>S3 – Tektonische Geodäsie</b>	
VORTRÄGE .....	77
POSTER .....	81
<b>S4 – Induzierte Polarisation</b>	
VORTRÄGE .....	84
POSTER .....	90
<b>AG – Airborne Geophysics / Fernerkundung</b>	
VORTRÄGE .....	95
POSTER .....	97
<b>BL – Wissenschaftliches Bohren / Logging / Gesteins- und Mineralphysik</b>	
POSTER .....	98
<b>GD – Geodynamik / Tektonophysik</b>	
VORTRÄGE .....	104
<b>GO / OS</b>	
– Geophysik in der Öffentlichkeit und im Wandel der Zeit /	
Open Source in Forschung und Lehre	
VORTRÄGE .....	106
POSTER .....	109
<b>GT – Geothermie / Radiometrie</b>	
POSTER .....	111
<b>KD – Kampfmitteldetektion</b>	
VORTRÄGE .....	113
POSTER .....	115
<b>KI – KI Verfahren der Geophysik</b>	
VORTRÄGE .....	117
POSTER .....	120
<b>MG – Marine Geophysik</b>	
POSTER .....	121
<b>MI – Modellierung / Imaging</b>	
VORTRÄGE .....	125
POSTER .....	130
<b>OG – Oberflächennahe Geophysik</b>	
VORTRÄGE .....	136
POSTER .....	145
<b>PV – Potentialverfahren</b>	
POSTER .....	163
<b>SM – Seismik</b>	
VORTRÄGE .....	165
POSTER .....	167
<b>SO – Seismologie</b>	
VORTRÄGE .....	172
POSTER .....	185
<b>VU – Vulkanologie</b>	
VORTRÄGE .....	198
POSTER .....	201

### O-S1-PV

#### REVEAL: Data-adaptive global full-waveform inversion

A. Fichtner

*ETH Zurich, Department of Earth & Planetary Sciences, Zürich, Switzerland*

We present REVEAL, a transversely isotropic full-waveform inversion (FWI) model of the Earth's crust and mantle that assimilates more than 6 million three-component seismograms, including all body- and surface wave phases. REVEAL resolves previously unknown large-scale features that challenge the standard interpretation of global tomographic Earth models in terms of thermally dominated mantle convection.

The construction of REVEAL rests on the combination of stochastic mini-batch optimisation and wavefield-adapted spectral-element meshes. While the former exploits redundancies in the dataset, the latter reduces the cost of wavefield simulations by lowering the effective dimension of the numerical grid. As a consequence, the average cost of an iterative model update is only around 0.62 % of a standard update that uses the complete dataset in combination with a cubed-sphere-type mesh. We calculated 3-D synthetic seismograms using a GPU-accelerated spectral-element wave propagation solver that accounts for anelasticity, topography, bathymetry, ocean loading, and ellipticity. The ensemble of methodological improvements allows us to incorporate 6,005,727 three-component waveforms from 2366 earthquakes and to perform 305 quasi-Newton iterations; an order of magnitude more than all previous global-scale FWI models. For a diverse range of wave paths, REVEAL explains complete seismograms at 30 s period that have not been included in the inversion.

Tomographic models are paramount to unravel the Earth's interior dynamics. Most previous studies found positive wave speed anomalies that spatially correlate with the expected locations of subducted slabs. This correlation has been widely applied in plate reconstructions and geodynamic modelling. Thanks to the unprecedented amount of data included in REVEAL, the model resolves numerous previously undetected positive wave speed anomalies in the lower mantle. Many of these anomalies are situated below major oceans and continental interiors, with no geologic record of subduction, such as beneath the western Pacific Ocean. Moreover, we find no statistically significant correlation of positive anomalies in REVEAL and past subduction. This suggests more diverse origins for large-scale anomalies in Earth's lower mantle, unlocking FWI as an indispensable tool for mantle exploration.

### O-S2-PV

#### **Lessons learned from microseismic monitoring of induced seismicity at megaton-scale CCS sites**

**B. Goertz-Allmann**

*NORSAR, Kjeller, Norway*

For carbon capture and storage (CCS) to be widely accepted as an effective climate mitigation technology at the necessary scale (gigaton), ensuring seal integrity of the storage reservoir is crucial. This is especially important during the active injection phase when reservoir pressure increases. However, monitoring also needs to continue for a long time after injection has ceased.

Microseismic monitoring is one of the most cost-effective remote sensing techniques for this task. It offers real-time insights into the dynamic reservoir behaviour and allows to deduce pressure and stress changes caused by injection activities. The detection and precise location of tiny microseismic events can reveal developing fluid migration pathways, and thus allow the identification of potential leaks before they occur. However, even small seismic events can raise concerns among local communities. Continuous monitoring and transparent reporting of seismic activity at CCS sites can foster public trust, demonstrating that seismicity risks are being actively managed and that the integrity of the seal is being verified.

An effective passive seismic monitoring system must detect all relevant microseismic events while minimizing false negatives. Seismological source parameters are essential for understanding the stress conditions in the reservoir, providing valuable input for engineering decisions. A critical aspect of this process is the accurate determination of event focal depths, which is necessary for associating seismic events with the industrial activities being monitored. This is an important consideration when designing monitoring networks.

We evaluate various monitoring technologies, including surface and borehole geophones, and Distributed Acoustic Sensing (DAS), based on their ability to meet the key requirements outlined above. Comparison of lessons learned from microseismic monitoring at different megaton-scale CCS sites reveal what information is most important to resolve, and at what scale, in order to be of value for storage operations. We also highlight the importance of advanced signal and array processing techniques to reduce event detection thresholds while discussing the advantages and disadvantages of various sensor technologies.

### O-S3-PV

#### **Continental scale strain mapping with GNSS: hydrological signals and seismotectonic implications**

**E. Serpelloni**

*Instituto Nazionale di Geofisica e Vulcanologia di Bologna, Sezione di Bologna, Bologna, Italy*

The increasing availability of Global Navigation Satellite System (GNSS) data from both geophysical and non-geophysical continuously operating networks has advanced the use of ground deformation measurements to study active geophysical processes on land, ice, and in the atmosphere. GNSS has become an essential tool in Earth science and the assessment of natural and anthropogenic geohazards, enabling the monitoring and analysis of phenomena such as earthquakes, tsunamis, volcanoes, mountain formation, aquifers, sea level changes, glaciers, ice sheets, mantle flow, terrestrial water storage, and water vapor, among others.

Across the European plate and the broader Euro-Mediterranean region, GNSS networks managed by research institutions, national and regional agencies, and private companies offer relatively uniform spatial coverage. Meanwhile, modern computational infrastructures enable the analysis of vast GNSS datasets, producing geodetic products that are revolutionizing the modeling and visualization of active Earth processes.

In this talk, I will provide an overview of the European GNSS infrastructure and demonstrate how it enables the mapping of tectonic strain rates and vertical ground deformation at a continental scale. I will also explore three key applications made possible by dense GNSS ground deformation datasets, focusing on tectonic strain-rate mapping and seismic hazard implications, time-dependent deformation and fault dynamics, and hydrological drought monitoring.

Although GNSS geodesy is widely used to address these issues, its application in the slowly deforming or stable regions of the complex Africa-Eurasia plate boundary remains limited. Nevertheless, it is expected to play a pivotal role in geohazard mitigation across the Euro-Mediterranean region in the coming years.

### O-S4-PV

#### Beyond Boundaries: Advancing Induced Polarization in Challenging Geophysical Contexts

J. Börner

*Technische Universität Bergakademie Freiberg, Institut für Geophysik und Geoinformatik, Freiberg*

Induced polarization (IP) has moved beyond its traditional role in mineral exploration to become a critical tool for investigating complex fluid-dominated geophysical environments. Such environments range from the lithosphere and hydrosphere to the cryosphere and planetary bodies, and are prominent in applications such as geohazards - e.g. volcanic systems -, energy transition - e.g. underground gas storage -, or climate change impacts - e.g. permafrost destabilization. Basic research and application of IP in such contexts is challenging due to for example extreme thermodynamic conditions, physicochemical reactivity, or time-dynamic, non-stationary processes. The fundamentals of IP rock properties and their influencing factors will be discussed, as well as the measurement of IP effects in the laboratory and in the field, addressing technical, interpretation and modeling challenges. Case studies will highlight the utility and implementation of IP, e.g. in underground CO<sub>2</sub> storage and volcanic hydrothermal systems. Future advances will be discussed, including technological innovations and interdisciplinary integration that will push the boundaries of IP applications in geophysics.

## S1 – Rekonstruktion der Dynamik des tiefen Erdinnern über geologische Zeiträume

### Vorträge

#### O-S1-01

#### Influence of Pressure on the Curie Temperature of Titanomagnetite

**S.-M. Platzer, S. A. Gilder**

*Ludwig-Maximilians-Universität München, Earth and Environmental Sciences, Munich*

Titaniferous oxides are the most abundant magnetic minerals in the Earth's crust and serve as its primary carriers of remanent magnetization. However, knowing how pressure influences titanomagnetite's magnetic properties, and in particular the Curie temperature ( $T_c$ ), remains poorly known. In this study we used a moissanite anvil cell to investigate the effects of pressure on synthetic  $\text{Fe}_{2.18}\text{Ti}_{0.82}\text{O}_4$ , which has a Curie temperature ( $T_c$ ) of -40°C and is therefore paramagnetic at room temperature. Pressure was stepwise increased to 9.3 GPa and then stepwise decreased back to ambient conditions. Rubies placed in the center and edge of the cell determined the average pressure and pressure gradient using fluorescence spectroscopy. At each pressure step, the acquisition of a back-field isothermal remanent magnetization up to saturation (SIRM) was measured. SIRM and the coercivity of remanence ( $B_{cr}$ ) serve as proxies to identify the pressure-induced paramagnetic to ferrimagnetic transition. Starting at ~4 GPa, the sample began to exhibit a measurable remanent magnetization. By 9.3 GPa,  $B_{cr}$  reached 50 mT with a 60-fold increase in SIRM compared to its initial value. Notably, the magnetic response is perfectly reversible upon decompression. Using SIRM and  $B_{cr}$  to constrain the pressure needed to cross the paramagnetic to ferrimagnetic transition suggests that  $dT_c/dP$  is  $14.3 \pm 4^\circ\text{C}/\text{GPa}$  and  $16.1 \pm 3^\circ\text{C}/\text{GPa}$ , respectively. We relate the pressure induced change in  $T_c$  to a reduction in lattice constant, thereby making  $dT_c/dP$  predictable for any composition of titanomagnetite. For example, pure magnetite at 30 GPa (ca. 800 km depth inside the Earth) would have a  $T_c$  of 1030°C, which could be relevant if magnetite was brought to mantle depths in a relatively cool subducted slab of oceanic crust.

#### O-S1-02

#### Global characteristics of geomagnetic field reversals and excursions

**M. Korte, A. N. Mahgoub, S. Shinu**

*Deutsches GeoForschungsZentrum GFZ, Potsdam*

The geomagnetic field, generated in Earth's outer core, varies continuously and has experienced several polarity reversals throughout Earth's history. The field loses its dipole dominated structure during these events and displays a complex and multipolar morphology at Earth's surface for several decades to millennia. Moreover, intervals of stable polarity are interrupted by short geomagnetic excursions, where extreme changes of geomagnetic field direction are found globally or regionally. Reversals and excursions are also characterized by drops of geomagnetic dipole moment and globally weak field intensities. Both the physics underlying magnetic field polarity changes in Earth's deep interior and their influences on Earth's environment and our habitat are not well understood.

We introduce our ongoing project that aims at better understanding the relation between reversals and excursions and the underlying processes in the geodynamo process that cause these events. We use existing global paleomagnetic field reconstructions of a few excursions

and the last reversal, the Matuyama-Brunhes ca. 780 000 years ago, to compare properties such as the rates of dipole decay and recovery or field morphology during the events. Moreover, we are working on the first global reconstruction of the Gauss-Matuyama reversal that occurred about 2.6 million years ago to include a second full reversal in our comparisons.

## O-S1-03

### Palaeomagnetic secular variation at mid latitude: preliminary results from Vogelsberg (15–18 Ma) and Lausitz (29–32 Ma)

F. Lhuillier<sup>1</sup>, Y. Chi<sup>1</sup>, S. Hahn<sup>1</sup>, A. C. Manarcescu<sup>1</sup>, M. N. Putri<sup>1</sup>, J. Büchner<sup>2</sup>

<sup>1</sup>Ludwig-Maximilians-Universität, Geophysik, München,

<sup>2</sup>Senckenberg Museum für Naturkunde, Görlitz

The geomagnetic field, generated by a dynamo in the Earth's fluid outer core, is of prime importance to shield the biosphere and the telecommunication satellites from the solar wind. Modelled in first approximation by a geocentric axial dipole, it experiences spontaneous fluctuations (often referred to as palaeosecular variation, PSV) in its direction, intensity and polarity as a result of the chaotic activity of the geodynamo. Over geological timescales, the amplitude of these fluctuations can additionally be modulated by internal causes (e.g. spontaneous bifurcations of the geodynamo) or external triggers (e.g. changes in the thermal boundary conditions imposed by the mantle on the core) in a disputable fashion. To better understand how changes in PSV amplitude and reversal frequency are linked during the Cainozoic, we propose to investigate the palaeomagnetism of three of the largest volcanic fields in Germany—Vogelsberg (15–18 Ma), Lausitz (29–32 Ma) and Hocheifel (35–44 Ma)—which each consist of more than 100 eruptions centres.

In this contribution, we present preliminary palaeomagnetic results based on a collection of ~2000 cores (162 cooling units) from Vogelsberg and ~1000 cores (83 cooling units) from Lausitz, acquired during six field campaigns conducted from 2021 to 2023. We drilled 8–10 cores per cooling unit to average out within-unit variability. These cores were oriented using a Pomeroy fixture, with sun readings in 95% of the cases to minimise orienting uncertainties due to local magnetic anomalies. We determined individual palaeodirections from alternating field demagnetisation, supplemented by thermal demagnetisation on 2–3 samples per unit to ascertain the robustness of the remanence. After a careful removal of the correlated and transitional directions, we derived two robust estimates of the dispersion of the virtual geomagnetic poles—a proxy representative of the state of the geodynamo—at 15–18 Ma and 29–32 Ma, to be compared with results previously obtained at low latitude from Ethiopia.

## O-S1-04

### Effects of Rheological Parameters on the Stability of Thermochemical Piles and Plumes

H. W. Sitte, C. Weber, C. Stein, U. Hansen

Universität Münster, Institut für Geophysik, Münster

Beneath Africa and the Pacific, large low seismic velocity provinces have been identified, extending thousands of kilometers in width and several hundred kilometers in height. While the origin and exact nature of these structures is still an open question, it is likely that the latter can be constrained to be thermochemical. Furthermore, the LLSVPs are long-lived and stable, being at their present-day location for several hundreds of million years.

We use 2D Cartesian, thermochemical convection models to numerically study the effect of rheological parameters on the temporal and spatial stability of chemical pile structures forming at the lower boundary of our simulations, representing the core-mantle boundary (CMB). Increasing the top (by a larger yield stress) or bottom viscosity (by a larger depth- or composition-dependent viscosity contrast) yields a general increase in the stability of thermochemical piles, with global effects being more stabilizing than local ones. The larger viscosity reduces the strength of the convective flow and increases the time until the chemical material is completely entrained into the mantle. Hence, melt would result in quick entrainment. This can be counterbalanced by an appropriate combination of rheological parameters. Likewise, the convective vigor is reduced by a thermal expansivity decreasing with depth, also stabilizing the piles. The convective flow does not only affect the life time of the thermochemical piles but also their size. Structures in our simulations are between 1500 km and 7000 km wide and 80 km up to 950 km high. The largest heights, however, only occur when the piles are squeezed together.

Furthermore, we find that piles and plumes are mutually dependent. On the one hand, large plumes are anchored by thermochemical piles, with plumes located in the center of the latter. On the other hand, plumes pull along chemical material into the ambient mantle deforming the piles. During dynamical processes, such as the merge of structures, plumes also occur at the edges of piles before striving toward the center.

To summarize, we find that large and stable thermochemical structures can form in mantle evolution models. Following the magma ocean period chemically distinct material at the CMB is subjected to the convective mantle flow deforming this primordial layer. Under appropriate combinations of rheological parameters, this can result in large thermochemical piles that survive several hundred million years.

## **O-S1-05**

### **Core material penetrating the mantle as one cause for dense CMB structures?**

**C. Stein, U. Hansen**

*Institut für Geophysik, Universität Münster, Münster*

A variety of distinct structures are seismically detected at the Earth's core-mantle boundary (CMB). In numerical studies often the scenario of a primordial layer (as remnant of the magma ocean) is assumed, for which excess density and mass are ad hoc prescribed. In these models, thermochemical structures form within the convecting mantle. Alternatively, the observation of tungsten deficits in some ocean island basalts and the abundance of other highly siderophile elements in the mantle led to the thought of a possible interaction between the mantle and the core. A number of laboratory experiments suggest interaction mechanisms between the iron-rich, oxygen under-saturated core and (Mg,Fe)O mantle crystals.

We numerically adapted one of this ideas by applying a chemical gradient between the modelled mantle and the modelled core to study the infiltration of dense material into the chemically depleted mantle. In our 2D Cartesian models a chemically dense layer develops self-consistently at the base of the modelled mantle. Core material penetrates the mantle mainly by a diffusive chemical influx in the areas where slabs spread over the bottom boundary. Like in the primordial layer scenario, slabs sweep the dense material aside to form thermochemical piles beneath rising plumes. While laboratory experiments mostly suggest that the amount of penetrated material is too low to explain the observed structures at the CMB, our simulations reveal that the process of chemical diffusion is strongly affected by the mantle convection.

Comparing both scenarios, we find that the primordial layer scenario can explain the large

low seismic velocity provinces (LLSVPs). The scenario of core-mantle interaction instead typically forms smaller piles which are maybe more suited to explain the smaller, but denser ultra-low velocity zones (ULVZs). Due to the constant chemical influx, the latter structures are more long-lived and due to their higher density also spatially more stable. This would be in agreement with plate reconstruction models that suggest a spatial and temporal stability in the last 300 Myrs. Additionally, the convection-assisted entrainment of dense core material could allow for this material to be detected at the surface in ocean island basalts.

## **O-S1-06**

### **Double diffusive finger convection in the core: The contribution from experiments**

**A. Rosenthal, A. Tilgner**

*Universität Göttingen, Göttingen*

There are reasons to assume that parts of the outer core are thermally stably stratified while the release of light elements due to crystallization of the inner core maintains a destabilizing compositional stratification. Heat and ions diffuse at different rates so that double diffusive convection is possible in the outer core. The combination of stabilizing thermal and destabilizing compositional stratification leads to finger convection in which convection occurs in slender elongated cells aligned with the direction of gravity.

The electrodeposition cell is one of only two known systems which allow us to investigate double diffusive convection in laboratory experiments in a steady state. This talk will present the information that can be extracted from experiments concerning the structure of the fingers and their transport properties. Finger thickness, flow velocities and ion fluxes obey simple scaling laws in parts of

the parameter space. The flow may split into layers resulting in so called staircases. The consequence of staircase formation, as well as of global rotation and their impact on the dynamo process are the subject of current experiments.

## **S1 – Rekonstruktion der Dynamik des tiefen Erdinnern über geologische Zeiträume**

### **Poster**

## **P-S1-01**

### **Lower mantle 3-D density structure from joint inversion of gravity and normal mode data**

**W. Szwilus**

*CAU Kiel, Kiel*

The density structure within Earth's lowermost mantle is a crucial component for understanding its thermo-chemical nature and thereby its dynamics. While a wide array of seismological techniques can provide insight into the mantle, resolving density remains a challenge, due to its relatively weak impact on seismic wave propagation compared to changes in seismic velocity.

Gravity data are sensitive to the density structure, but are notoriously non-unique.

In this presentation, the focus will be on a joint inversion of satellite gravity data with normal modes with high sensitivity to the lower most mantle.

Due to mantle convection, the gravity response of density anomalies differs from a purely 'Newtonian' kernel and contains contributions from the deformed surface and CMB. As a result, the radial viscosity distribution enters as an additional unknown.

In this contribution, the density models from a trans-dimensional joint inversion of normal mode and satellite gravity data for different viscosity scenarios will be presented and compared in terms of their dynamical implications.

## **P-S1-02**

### **Investigation of the D" reflector with short epicentral distances**

**J. Pahlings, C. Thomas**

*Universität Münster, Institut für Geophysik, Münster*

The Earth's lowermost mantle is a region that shows many different structures, such as thermal changes, scatters and ancient slabs. One of these features is the D" reflector, which can be found in many studies but is not always visible. The reflector lays at a depth of around 2605km. However, it is still unknown whether the reflector is a global or a local feature, and neither is its origin. Studies show that the reflector possibly comes from a phase change of perovskite to post-perovskite or the existence of ancient slabs. To study the reflector, I used ray theory to analyse earthquakes around Japan and the eastern Russian coast with the seismic array of Kyrgyzstan. The events showed a clear reflection of the D" reflector for PdP-, SdS-, PdS- and SdP-reflections. A positive polarity was visible for all cases, indicating an increase in velocity across the reflector. My results fit the tomographic inversion of the area, showing a high-velocity zone for the area of reflection. I tried to calculate the depth of the reflector, which led to false results due to out-of-plane reflections that generated false travel time differences. Therefore, future studies should focus on modelling the reflection coefficient and calculating the depth using a more reliable method.

## **P-S1-03**

### **Determination of XKS splitting parameters in the lowermost mantle beneath Siberia**

**F. Dorn, M. I. F. Dillah, Y. Fröhlich, J. R. Ritter**

*Karlsruhe Institute of Technology, Geophysical Institute (GPI), Karlsruhe*

Within the Priority Program 2404 "Reconstructing the Deep Dynamics of Planet Earth over Geologic Time" (DeepDyn) we investigate possible seismic signatures at geomagnetic high-latitude flux lobes (HLFL). The focus is on four target regions on the northern hemisphere: Siberia, Canada, North Atlantic and Indonesia. While Siberia and Canada show the HLFLs, the North Atlantic region should be the location of a third postulated HLFL, but this area has no intense-flux signal in the magnetic field. The region beneath Indonesia is characterized by an area of intense magnetic flux that changes direction and moves westwards over time. We aim to understand whether mineralogy or seismic structures (i.e., thermal constraints) could cause these different magnetic signatures at the core mantle boundary (CMB). This is done by combining two approaches: seismic anisotropy (KIT) and seismic reflections (University of Münster) near the CMB.

The observation of shear wave splitting (SWS) is an unambiguous indication of seismic anisotropy in the Earth's interior and, thus, of deep geodynamic deformation processes. We measure the SWS of SKS, SKKS, and PKS (jointly referred to as XKS) phases and determine

the splitting parameters, the fast polarization direction  $\varphi$  and the delay time  $\delta t$ , using both the energy-minimization and the rotation-correlation methods. Especially, we search for phase pair SWS discrepancies, i.e., between SKS and SKKS phases, as they are a clear indication for a lowermost mantle (LMM) contribution to the splitting signal.

This poster focuses on the HLFL beneath Siberia. We present SWS measurements and pairs of XKS phases recorded at different seismic stations in Northern Europe and Asia that sample the LMM beneath Siberia. For the target region beneath the North Atlantic, see the poster by Dillah et al. (2025).

## **P-S1-04**

### **Determination of XKS splitting parameters in the Earth's lowermost mantle beneath the North Atlantic**

**M. Dillah, F. Dorn, Y. Fröhlich, J. Ritter**

*Karlsruher Institut für Technologie, Geophysics, Karlsruhe*

Shear-Wave Splitting (SWS) is an indication of seismic anisotropy along the ray path of the shear wave. When traveling through the Earth's interior, splitting discrepancies between SKS-PKS-SKKS (jointly referred to as XKS) phases can be used as an indication of anisotropy that is occurring in the Lower Most Mantle (LMM).

In the DFG Priority Program 2404 "Reconstructing the Deep Dynamics of Planet Earth over Geologic Time" (DeepDyn), we investigate target regions associated with geomagnetic High-Latitude Flux Lobes (HLFL) on the northern hemisphere, especially in the LMM beneath Siberia, the North Atlantic, Canada and Indonesia. The North Atlantic region is suggested to be the third HLFL beside Siberia and Canada. But unlike Siberia and Canada that show HLFLs, the North Atlantic region does not show intense-flux signal in the magnetic field. Understanding whether mineralogy or seismic structures could cause these different magnetic signatures at the core mantle boundary (CMB) is the purpose of the program. This is done by combining two approaches: seismic anisotropy (KIT) and seismic reflections (University of Münster) near the CMB.

In this study, we measure the SWS of XKS phases and determine the splitting parameters using the energy minimization and the rotation-correlation methods for our target region in North Atlantic. We focus on SKS-SKKS phase pairs and separate between discrepant and non-discrepant pairs based on the observation type in our target region, by measuring SWS and XKS phases recorded at seismic stations in Europe, Asia, and North America that sample LMM beneath North Atlantic.

This poster focuses on the target region in the LMM beneath the North Atlantic. For the target region beneath Siberia, see the poster by Dorn et al. (2025).

## **P-S1-05**

### **On the influence of the solidification mechanism on magma ocean dynamics**

**C. Maas, U. Hansen**

*Universität Münster, Institut für Geophysik, Münster*

During a later stage of Earth's accretion, approximately 4.5 billion years ago, impacts of Mars-sized bodies created a deep terrestrial magma ocean of global extent on proto-Earth. Once core formation is complete, the magma ocean begins to solidify. However, the solidification

mechanism and the location where crystallization initiates remain unclear and are subjects of debate. One widely accepted model posits that solidification begins at the bottom of the magma ocean (e.g., Andrault et al., 2011; Miller et al., 1991b). Contrarily, laboratory experiments conducted under high-pressure and temperature conditions suggest two alternate scenarios: Solidification may also commence at the top of the magma ocean (e.g., Mosenfelder et al., 2007) or at mid-depth (e.g., Mosenfelder et al., 2009; Stixrude et al., 2009; Boukare et al., 2015). The latter might yield a deep molten layer, referred to as a basal magma ocean, at the core-mantle boundary, which could potentially endure chemically and thermally isolated from the remaining mantle for an extended period (Labrosse et al., 2007).

This study models these three distinct solidification styles (bottom-up, top-down, mid-depth) and examines their impact on the dynamics and evolution of a convecting magma ocean through computational simulations. Determining whether the magma ocean solidifies from the bottom up, top down, or in a mid-outward manner holds paramount significance for Earth's evolution, influencing factors such as the level of differentiation and the initial conditions governing the advent of plate tectonics. Furthermore, the dominant mechanism and its timing could bear crucial implications for the ensuing evolution of the mantle and the distribution of geochemical trace elements.

## **P-S1-06**

### **Magneto-rotating double-diffusive convection in stable layers at the top of Earth's core**

**C. Weber, S. Stellmach**

*University of Münster, Institut of Geophysics, Münster*

The geomagnetic field is produced by thermochemical convection in the fluid outer core of the Earth. Since the top 80-300 km of the outer core of the Earth are likely stably stratified, large-scale Rayleigh-Bénard convection is hindered in this region. Instead, such stable density stratification might allow for small-scale double-diffusive convection (DDC). We analytically investigate the two types of DDC (fingering and oscillatory) with linear stability analysis. Both types of DDC could occur at core conditions up to a certain strength of stratification, fingers more readily than the oscillatory type. The influence of rotation and of the geomagnetic field dampen the growth of both double-diffusive convection patterns. Direct numerical simulations with the 3D spectral code PADDI are used to extend the results of the linear stability analysis into the non-linear regime.

## S2 – Induzierte Seismizität

### Vorträge

#### O-S2-01

#### **Seismic Event Discrimination with Vision Transformers: Advancing Model Explainability**

**V. Kasburg<sup>1</sup>, M. van Laaten<sup>1</sup>, M. Zehner<sup>2</sup>, J. Müller<sup>1</sup>, N. Kukowski<sup>1</sup>**

<sup>1</sup>*Friedrich-Schiller-Universität Jena, Institut für Geowissenschaften, Jena,*

<sup>2</sup>*Friedrich-Schiller-Universität Jena, Institut für Geographie, Jena*

To this date, the multitude of events recorded in seismic networks are often manually discriminated by experts into different origin types, such as earthquakes, quarry blasts, or induced events. Although in recent studies, deep learning algorithms, in particular Convolutional Neural Networks (CNNs), have demonstrated their ability to efficiently and accurately discriminate types of seismic events, their application for automated seismic event discrimination remains limited so far. This is partly due to the lack of globally applicable models that achieve high precision for local seismic networks, the limited data available for fine-tuning the Deep Learning (DL) models, and the lack of sufficient explainability of the decision-making of these black-box models.

In this contribution, we investigate the application of Vision Transformers (ViTs) as an innovative approach to automate the discrimination of seismic events. To evaluate their potential in terms of discrimination accuracy and explainability, we applied them to different types of seismic events of anthropogenic origin, focusing on the particularly challenging task of discriminating between quarry blasts and induced or mining events. For this purpose, we used data from the Seismic Network of the Ruhr-University Bochum (RuhrNet) and the Thuringian Seismic Network (TSN).

Our results demonstrate that ViTs are capable of analyzing the entire spectrogram of a seismic event coherently, providing better generalizability in pattern recognition compared to CNNs. Furthermore, in addition to its high discrimination accuracy, the attention weights of ViTs offer insight into the black-box DL model and provide a plausible explanation for its decision-making process.

#### O-S2-02

#### **A template-matching approach for simultaneous earthquake detection and localization using DAS data**

**N. Boitz, W. Tegtow, S. Shapiro**

*Freie Universität Berlin, Geowissenschaften – Geophysik, Berlin*

Subsurface fluid operations including hydraulic fracturing (HF), enhanced geothermal systems (EGS), and carbon capture and storage (CCS) typically induce microseismic events that can be used to evaluate the success of the treatment. For this, thorough microseismic monitoring is needed. In recent years, distributed acoustic sensing (DAS) has proved to be a cost-effective and long-lasting alternative to monitoring using borehole geophones. Modern DAS registrations record the seismic wavefield in terms of strain or strain rate with a high spatial and temporal (up to several kHz) resolution. This results in large amounts of data that cannot be reviewed by analysts and the need for efficient algorithms for automatic data processing. In microseismic processing usually the first step is event detection within the continuous recordings. For this, we use a 2D template-matching approach. We select the

recording of a microseismic event in space and time and cross-correlate this template with the continuous recordings. If the cross-correlation value exceeds a certain threshold, we declare an additional event as detected. We apply this methodology to induced seismicity from the hydraulic fracturing test site 2, where seismicity is recorded using one vertical and one horizontal fiber and several downhole geophones. Previous works using classical detection methods found significantly fewer events in the DAS data than in the geophone recordings. Using the template-matching approach, we detect several hundred additional events per fracturing stage. As a side product of the template-matching, we obtain the position of the apex of the arrival-time hyperbola and the arrival-time of the stronger S-wave at both fibers. For the specific dataset geometry, we can directly derive north and depth locations using the travel-time hyperbolas. Using the earliest S-wave arrival times at both fibers, we invert for the full 3D location and origin time for each event. This is possible even for events, where P-wave arrivals are too weak to be visible in the data. The detection and localization procedure works fully automatically and is quick enough for real-time monitoring. The detected event signatures can be further used to estimate event magnitudes and mechanisms.

## **O-S2-03**

### **Relative Moment Tensors Rejuvenated: A Recent Approach to Resolve the Source Mechanism of Small Earthquakes**

**W. Bloch<sup>1,2</sup>, D. Drolet<sup>3</sup>, A. Plourde<sup>4</sup>, M. Bostock<sup>3</sup>, V. Oye<sup>1</sup>**

<sup>1</sup>*NORSAR, Applied Seismology, Kjeller, Norway,*

<sup>2</sup>*GFZ Deutsches GeoForschungs Zentrum, Dynamik der Lithosphäre, Potsdam,*

<sup>3</sup>*The University of British Columbia, Vancouver, Canada,*

<sup>4</sup>*National Resources Canada, Dartmouth, Canada*

The seismic moment tensor is an invaluable quantity to understand earthquake source processes. It delivers a point source representation of the energy radiated by a seismic event. The calculation of absolute moment tensors is a data-intensive and often cumbersome task. This is even more critical for small earthquakes, where the requirement to model the seismic waveform at high frequencies hampers inclusion of moment tensor information in studies of micro-seismicity.

We here present a recent approach to compute *relative* moment tensors for clustered seismicity tied to a reference moment tensor. It takes advantage of the similarity in subsurface Green's functions for closely spaced events, facilitating accurate moment tensor calculations, especially for small earthquakes. Specifically, we combine measurements of relative waveform amplitudes on common stations using seismogram principal components with an algebraic formulation to simultaneously invert the relative amplitudes for moment tensors. Our algorithms are implemented in the Python programming language and available via GitHub (<https://github.com/wasjabloch/reIMT>) with the aim to develop a re-usable research-grade software package.

We compute relative moment tensors for clusters of fore- and aftershock seismicity recorded during a sequence of strong earthquakes in the Pamir highlands of Central Asia. The test data set features seismicity in the magnitude range between ~1 and 7.2 on a multitude of tectonic structures. 33 moment tensors are known from conventional absolute full-waveform inversion and allow for the validation of our results. For this data set, the new approach allows us to lower the magnitude threshold for moment tensor calculation from 4 to ~1.5.

## **O-S2-04**

### **Improving Seismic Monitoring performance using Posthole and Borehole Instrumentation**

**S. Uhlmann**

*IGM GmbH, Überlingen*

In recent years, the number of induced seismic monitoring projects has significantly increased, particularly in densely populated regions. However, finding suitable surface sites remains a challenge.

To address this, an increasing number of stations are being deployed in subsurface configurations, such as Posthole or Borehole installations.

This work examines the technical specifications, performance benefits, and potential limitations of deploying broadband seismometers in subsurface environments.

## **O-S2-05**

### **AI-based Acoustic emission monitoring and detection from decameter-scale fluid injection tests in clay rock at the URL Tournemire, France**

**T. Förster<sup>1,2</sup>, C. Böse<sup>2</sup>, R. Giese<sup>2</sup>, K. Plenkers<sup>3</sup>, P. Dick<sup>4</sup>, G. Zimmermann<sup>5</sup>**

<sup>1</sup>*Technische Universität Berlin, Berlin,*

<sup>2</sup>*Helmholtz-Zentrum Potsdam Deutsches GeoForschungsZentrum, 4.2 wissenschaftliches Bohren und Geomechanik, Potsdam,*

<sup>3</sup>*GMuG - Gesellschaft für Materialprüfung und Geophysik, Bad Nauheim,*

<sup>4</sup>*Institut de Radioprotection et de Sûreté Nucléaire (IRSN), Fontenay-aux-Roses, France,*

<sup>5</sup>*Helmholtz-Zentrum Potsdam Deutsches GeoForschungsZentrum, 4.3 Geoenergie, Potsdam*

The Tournemire Underground Research Laboratory (URL) is located in a Mesozoic marine basin on the southern border of the French Massif Central, at the western limit of the Causse du Larzac. The URL consists of a century-old railway tunnel and several recent galleries (excavated in 1996, 2003, 2008, and 2024) that cross a Toarcian shale formation. Research conducted at Tournemire aims to acquire methodological and phenomenological knowledge on claystones similar to those found at Bure, where Andra could establish a radioactive waste disposal facility. One of the recent studies developed at Tournemire is the so-called CHENILLE-experiment, where the coupled behavior of thermo-hydro-mechanical properties is tested. In the experiments, a pre-heated rock interval in a fault core and a damage zone (DZ) are hydraulically stimulated with gas and water injections. Optical fiber cables enable the monitoring of temperature along heater boreholes with high resolution. The seismic activity is recorded by an In-situ acoustic emission (AE) network consisting of 12 AE sensors spanning the injection interval and two movable hydrophones. The sensors cover an interval of about five meters of width and depth and three meters of height. The sensors are capable to record seismic waves in the frequency range 1 kHz to 100kHz. Continuous waveform recording is performed for twelve months with a sampling rate of 200 kHz. Amounting to 500 GB data per day, data management and processing is one of the challenges faced in the dataset.

This passive seismic dataset of seven months of the pre-injection and injection phase is processed and evaluated by several python- and MATLAB-scripts. A simple short-time-average/long-time-average (STA/LTA) coincidence python triggering script extracts short event files to be classified. Event classification is achieved by a specifically trained convolutional neural network (CNN), as human labor is out of scale for the data size. Several adaptations of the triggering parameters and training of the CNN revealed over 20.000

acoustic emission events from 14.12.2023 until 25.07.2024 with a significant increase in activity during the injection experiment, especially in the DZ. To determine the influence of temperature and pressure, natural occurring seismicity of the pre-injection phase is compared to seismicity rates during the hydraulic stimulation experiments. The correlation of seismic activity to the temporal evolution of temperature and pressure is shown.

## **O-S2-06**

### **Insights and highlights from the multi-sensor microseismic surface monitoring at the field-scale EGS laboratory Utah FORGE**

**P. Niemz<sup>1</sup>, G. Petersen<sup>2</sup>, J. Rutledge<sup>3</sup>, K. Pankow<sup>1</sup>, K. Whidden<sup>1</sup>**

<sup>1</sup>*University of Utah, Seismograph Stations, Salt Lake City, United States of America,*

<sup>2</sup>*GFZ Postdam, Erdbeben- und Vulkanphysik, Postdam,*

<sup>3</sup>*Santa Fe Seismic LLC, Santa Fe, United States of America*

Enhanced geothermal systems (EGS) are one of the cornerstones for the transition into a sustainable future of energy production. Large-scale experiments and pilot projects have increased our knowledge regarding the seismic response of the subsurface to high-pressure fluid injections. We present an overview of the recent experimental phases at Utah FORGE (Frontier Observatory for Research in Geothermal Energy, Utah, USA) monitored with a multi-sensor seismic surface network. Surface networks are much more cost-effective than downhole monitoring setups. With recent, machine-learning-based advances in location and detection algorithms, we are able to compile high-resolution microseismic catalogs for periods without downhole monitoring at Utah FORGE, allowing for imaging of continued fracture growth during the circulation experiments in 2023.

In subsequent reservoir stimulations in 2024, we took advantage of the increased azimuthal coverage from a temporary, large-N nodal geophone deployment to study moment tensors with a focus on non-double-couple components. Such components reflect volumetric changes and tensile opening/closing. If resolved reliably, these components are key for interpreting larger-scale processes in EGS, such as developing a rather simple hydraulic fracture or activating complex fracture networks mainly driven by slip along preexisting faults and fractures. Utah FORGE is an excellent test environment exploring these subsurface processes and their resolution limits.

## **S2 – Induzierte Seismizität**

### **Poster**

## **P-S2-01**

### **Induced seismicity in Germany during the last decade - an overview and update**

**T. Plenefisch<sup>1</sup>, M. Bischoff<sup>2</sup>, G. Hartmann<sup>1</sup>, U. Wegler<sup>3</sup>**

<sup>1</sup>*Bundesanstalt für Geowissenschaften und Rohstoffe (BGR), B4.3, Hannover,*

<sup>2</sup>*Landesamt für Bergbau, Energie und Geologie (LBEG), Hannover,*

<sup>3</sup>*Friedrich-Schiller-Universität Jena, Institut für Geowissenschaften, Jena*

The Federal Seismic Survey at BGR routinely evaluates seismic events in Germany and neighbouring countries on a daily basis. The results are supplemented by the outcomes of

the seismological agencies of the federal states of Germany and German universities and stored in an event database and in the German earthquake catalogue, which is complete for earthquakes with magnitudes  $ML \geq 2$ .

Furthermore, the events are classified as natural earthquakes, induced earthquakes, or explosions (mostly quarry blasts). A considerable number of the events are induced earthquakes. They originate from stress changes due to human activity in the subsurface. The main causes of the induced events are coal mining, potash salt mining, natural gas extraction and geothermal energy.

We describe the characteristics of the associated seismicity for the different mining regions in Germany. In contrast to natural seismicity characterized by long-term tectonic processes, the number and strength of induced seismicity can be strongly dependent on rather short-term temporal and spatial changes following the mining process.

The seismicity in coal mining regions, e.g., decreased coinciding with the shutdown of coal mining, whereas seismic activity in geothermal or natural gas fields show different behavior, increasing or decreasing depending on the location. Additionally, the latter both types of induced seismicity show remarkable peculiarities in their temporal behavior. Seismic events still occur with a delay after a geothermal power plant was shut down. Seismic activity can start even several years after the start of extraction in a new natural gas field.

We show the temporal course of induced seismicity over the last 10 years in dependence on the distinct extraction types, compare it with the previous decades and discuss the main features. In addition, we also investigate the magnitude-frequency relationship and the energy release of the induced earthquakes. We determine these parameters regarding their originators as well as in relation to those of natural earthquakes.

## **P-S2-02**

### **Estimating the effect of induced seismicity at the Earth's surface – case studies based on the geothermal projects Graben-Neudorf and Wörth in the Upper Rhine Graben**

**P. Hering, N. Medinger, S. Abe, L. Küperkoch, H. Deckert**

*Institut für Innovation, Transfer und Beratung gGmbH, Institut für geothermisches Ressourcenmanagement (igem), Bingen*

Minimizing the occurrence of noticeable seismicity is a key aspect to increase the public acceptance of geothermal energy production in Germany. This requires a fundamental understanding of the subsurface response to pressure changes at reservoir depths, as well as a precise estimation of the impact of associated induced seismicity at the Earth's surface. The interdisciplinary research projects RESTLESS and DEKAPALATIN, both funded by the *Bundesministerium für Wirtschaft und Klimaschutz (BMWK)*, are dedicated to investigate those aspects in the framework of the geothermal projects Graben-Neudorf and Wörth in the Upper Rhine Graben. Here, THM simulations will be used to simulate the temporal and spatial distribution of seismic events in response to pressure changes and within the regional tectonic setting. Additionally, the source mechanisms of those events will serve as input signals to perform 3D full waveform simulations and predict maximum surface velocity amplitudes (peak ground velocity values, PGV) in the target areas.

The accuracy of the PGV-estimates strongly depends on the quality of the seismic velocity model used in the 3D waveform simulations. In particular, near surface velocity structures can have a significant impact on PGV values as they may lead to amplification due to resonance effects (site effects). To get a more detailed image of the shallow subsurface we collected H/V measurements and used array measurements to calculate dispersion curves. The results

of the H/V measurements show that the thick sediments in the Upper Rhine Graben do not feature significant velocity contrasts at depths that are relevant to induced seismicity. We further used 1D inversion tools to obtain seismic velocity profiles from the dispersion curves. The profiles are used to calibrate the uppermost part of the 3D velocity model, which is setup using a regional velocity model as well as information from 3D seismic explorations. Going forward, the derived velocity models will be used to estimate PGV values for different operational scenarios of the power plants. They can later be compared with possibly occurring seismicity in the operating phase.

## P-S2-03

### Explanation of Flooding-induced Seismicity - a combined approach from relocalization of microseismicity and geomechanical numerical modelling

M. Rische<sup>1</sup>, T. Niederhuber<sup>2</sup>, B. Müller<sup>2</sup>, K. D. Fischer<sup>1</sup>, W. Friederich<sup>1</sup>

<sup>1</sup>Ruhr Universität Bochum, Institut für Geologie, Mineralogie und Geophysik (GMG), Bochum,

<sup>2</sup>Karlsruhe Institute of Technology, Institut für Angewandte Geowissenschaften (AGW), Karlsruhe

Monitoring seismicity in the Ruhr coal mining has long been the task of the RUB Seismological Observatory. In active mining, the water level was lowered by continuous pumping to enable safe mining. Observed seismicity could be closely correlated with the mining operations. Since the closure of the mines, controlled flooding of the mines has begun.

Within the project FloodRisk we investigate the relationship between mine water level rise, regional and local stresses, and induced seismicity. The seismological database is based on the recordings of a network of up to 30 short-period seismic stations installed by the Ruhr University in the area of the former Bergwerk Ost, which had the highest seismicity in the Ruhr region during active mining. The stations cover an area of around 160 km<sup>2</sup> and are spaced 0.5 to 3.5 km apart and enabled continuous monitoring.

Since the start of flooding in 2019, over 2600 induced events have been recorded. A prerequisite for the interpretation of seismicity is a localization of the events that is as detailed as possible. The application of a relative earthquake location procedure reduced the location uncertainty significantly and enabled the investigation of the spatial and temporal evolution of earthquake clusters due to the rise of the mine water level. The resulting pattern of seismicity has been compared with known underground structures. We detect concentrations of microseismicity about 300 m below the already flooded deepest mine level, especially in sections below the main pillars.

Based on the regional state of stress we performed 3D numerical geomechanical modeling of stress in the mine. Four generic models with increased complexity were developed to study the influence of interacting factors like pillar width, depth levels and subsurface morphology. We used transient simulations calculating results for the flooding period between October 2019 (-1123 m), and June 2024 (-738 m) as well as a static calculation based on the final flooding level of -600 m. The model aims to predict the temporal and spatial occurrence of critical stress concentrations within collieries during flooding. This helps to identify the locations and orientations of faults that could be reactivated, as indicated by negative DMF values. The zones of potential fault reactivation occur at a depth of ca. 300 m below the pillars and thus corresponds to observed seismicity.

## Lessons learned and challenges from AI-based seismic monitoring in a high noise-level area: the Weisweiler case

S. Carrasco<sup>1</sup>, M. P. Roth<sup>1</sup>, R. M. Harrington<sup>1</sup>, X. Chen<sup>1</sup>, C. Finger<sup>2</sup>, M. Dietl<sup>2</sup>, M. Zeckra<sup>3</sup>

<sup>1</sup>Ruhr University Bochum, Bochum,

<sup>2</sup>Fraunhofer IEG, Bochum,

<sup>3</sup>Earthquake Observatory Bensberg, University of Cologne, Cologne

The Lower Rhine Embayment (LRE) is one of Germany's most seismically active regions, where historical records provide evidence for a total of nine Ms > 5 earthquakes in the region near Aachen. The extensional faulting system hosts a moderate seismicity rate with regional mean slip rates of approximately 0.1 mm/yr on a set of normal faults that offer many possible conduits for fluid circulation along the general NNW strike direction. The combination of comparatively high permeability near the fault zone and a profitable geotherm also makes the LRE an ideal target for geothermal energy production. In the context of the SIEGFRIED project (see poster by Dietl et al.), creating a high-resolution earthquake catalog to quantify background seismicity and study the active structures in the region is necessary to ensure safe and economical energy production. Nevertheless, the comparatively high average noise level above 1 Hz in the LRE (primarily of anthropogenic origin) hinders classical automated earthquake detection routines, particularly for low-magnitude events (M<0.5)

Here, we implemented an AI-based workflow to monitor seismicity in the LRE, near the Weisweiler town. We denoise the continuous recordings using a decoder-autoencoder denoiser (Heuel et al., 2022). We then pick P- and S-phases using PhaseNet (Zhu et al., 2018), and associate picks using PyOcto (Münchmeyer, 2024) with a local velocity model based on Reamer & Hinzen (2004). The parameters involved in the localization workflow are then tuned by comparing the AI-catalog (this work) to the earthquake catalog built by the Earthquake Observatory Bensberg (BNS). We detect 93 events between July 2021 and December 2021, of which 46 were reported by BNS (~50% of the AI-catalog), 20 are newly detected events (~20%), and 27 correspond to quarry blasts (~30%). Our workflow overlooked 11 events reported by BNS, but we were able to recover them by relaxing parameters at the expense of a higher false detection rate (>40 times the true detections if the smallest events are intended).

We will present possible improvements to this workflow (e.g., a dynamic associator that is based on available stations for spatially and temporally heterogeneous deployments), the need for visual inspection due to anthropogenic sources and potentially mislocated, low-magnitude events, and, augmentation of seismic data using DAS recordings, as well as a preliminary interpretation of the newly detected seismic sources.

## **Seismic Phase Picking for Induced Seismicity with Deep-Learning**

**J. Heuel<sup>1</sup>, V. Maurer<sup>2</sup>, M. Frietsch<sup>1</sup>, A. Rietbrock<sup>1</sup>**

<sup>1</sup>*Karlsruher Institut für Technologie, Geophysikalisches Institut, Karlsruhe,*

<sup>2</sup>*ES Geothermie, Strasbourg, France*

Over the last years, several seismological data sets and deep-learning picking models for artificial intelligence (AI) applications in seismology have been published and are easily accessible and trainable through the Python toolbox SeisBench. Most of these data sets contain earthquakes recorded at local, regional and teleseismic distances, with only limited data in the low magnitude close distance region. As a result, applying current published models to induced seismicity data leads to only a few events being detected and deep learning pickers are not able to outperform well-established workflows in seismology. Combining different trained deep-learning picking models using e.g. a semblance-based ensembler, has only shown limited improvement in event detection. Therefore, it is necessary to build up a new data set for induced seismicity to train AI deep-learning pickers.

In our study, we gathered approximately 180 000 three component seismic waveforms from around 42 000 different seismic events to train PhaseNet for induced seismicity. Compared to existing data sets, our data set contains more events with low signal-to-noise ratios and low magnitudes. Furthermore, some windows contain multiple events whereas previous PhaseNet models were mainly trained on single events in a time window. We tested different approaches to obtain the best model for detecting induced seismicity. First, we applied transfer learning by fine tuning existing PhaseNet models by, loading the previously published weights and continuing the training with the new data set. Second, we trained PhaseNet from scratch employing data augmentation techniques to enlarge our data set artificially and enhance model generalizability. In addition, we included noise samples to reduce the number of false picks.

We validated our deep-learning phase picking models on continuous data from a geothermal site in Rittershoffen (France). Our new model outperforms both transfer-learned and existing models. The newly created seismicity catalogue contains more events than those published by the agencies, but all events that have already been published are included in our catalogue. To further reduce false positives, we also combined our new model with existing models using a semblance-based ensembler. We show that training PhaseNet with noise samples reduces the number of false picks tremendously, which helps in the end to reduce the number of false detections.

## **P-S2-06**

### **Match Filter Detection Routine with Synthetic Templates using 1D velocity model - aiming to detect the induced seismicity- test site: West Bohemia/Vogtland**

**E. Káldy, T. Fischer**

*Charles University, Faculty of Science, Institute of Hydrogeology, Engineering Geology and Applied Geophysics, Prague, Czech Republic*

Match filter detection routine is a very powerful instrument allowing detecting micro-earthquakes with waveform amplitudes at and below the noise level (Gibbons & Ringdal, 2006, Beaucé, Frank, et al., 2017). It requires knowledge of a template waveform and it recognizes only the earthquakes of similar pattern - nearby location and similar focal mechanism. Therefore this detection method is not used in regions without previously detected earthquakes. But already some studies show that synthetic templates are performing as well (Chamberlain & Townend, 2018). Our research is driven by the following questions: To which level, can a synthetic waveform perform as a template for match filter detection routine? Especially when a set of synthetic temples is used, varying in locations and mechanisms. Our test site is West Bohemia / Vogtland region (Czech Republic), where the natural seismicity is monitored both by Neural Network (Doubravková & Horálek, 2019) and amplitude based PEPiN (Káldy & Fischer, 2024) detector. The aim is to use it for monitoring an uprising enhanced geothermal system (EGS) in Litoměřice, Czech Republic.

Preliminary results from West Bohemia.

## **P-S2-07**

### **Locating Seismic Tremors Through Matched Field Processing Algorithm**

**K. Karimi, T. Fischer**

*Charles University, Faculty of Science, Prague, Czech Republic*

Matched Field Processing (MFP) is gaining popularity in seismology for locating seismic sources with coherent signals and tremors. Although this method performs well in identifying many types of anomalous sources, there is ongoing debate regarding the optimal form of the replica vectors used in its algorithm. This research discusses the most suitable choice of replica vectors and applies the improved algorithm to seismic data related to the flow of injected water through a created fracture inside a borehole.

The accuracy of MFP depends on the velocity model of the area under investigation. The essence of this approach lies in finding a replica vector (synthetic signals at all geophones) that closely resembles the measured vector (measured signals at all geophones). This similarity is quantified using the Bartlett Beamformer (BB), a metric where  $0 \leq BB \leq 1$ . BB reaches its maximum value when the projection of the replica vector onto the measured vector is maximized. In this methodology, each node of a 3D grid, dividing the half-space into smaller cubes, is considered as a potential location for the seismic source. The algorithm iterates over these nodes, and the one with the maximum BB value is selected as the optimal estimate for the seismic source location. For each velocity model, the maximum BB occurs at a different depth, underscoring the importance of an accurate velocity model.

We implemented an improved MFP algorithm on an array within a pilot geothermal borehole (PVGT-LT1) in Litoměřice, located in northwestern Czech Republic. This borehole samples 800 meters of Paleozoic and Mesozoic sediments overlying a crystalline basement. Recovery tests revealed the low hydraulic conductivity of the zone ( $10^{-11} \text{ m/s}$ ). The study involved two phases of water injection into the borehole: first, a permeable fracture was created at a depth

of 880 meters through water injection. Seven months later, the second injection operation was performed on the same borehole. The observations showed that the fracture was still preserved.

Evaluation of MFP on modeled data demonstrates that incorporating waveform attenuation into the replica vector yields more accurate results than other waveforms, such as Rayleigh waves or body waves with only phase information. Therefore, this type of replica vector was applied for examination of seismic characteristics due to the created fracture.

## P-S2-08

### A coupled numerical model for the simulation of induced seismicity

S. Abe, P. Hering, H. Deckert

*Institut für geothermisches Ressourcenmanagement, Bingen*

The risk of induced seismicity is one of the major issues controlling the public acceptance of energy production from deep geothermal reservoirs. One possibility to quantify and potentially reduce this risk is the use of numerical methods to simulate the expected induced seismicity before the development and operation of a geothermal power plant.

The key mechanism causing induced seismicity in geothermal reservoir is the reactivation of existing faults as a result of effective stress changes on the fault planes caused by changes to pore pressure and temperature in the reservoir. To efficiently simulate the induced seismicity in response to these pressure and temperature changes a thermo-hydraulic reservoir model is combined with a dynamic fault model based on fault slip calculations using rate and state dependent friction laws. The reservoir model is implemented using a Finite Difference (FD) calculation of pore fluid flow and the associated conductive and advective heat transport. The dynamic fault model is based on a modified implementation of the RSQSim approach proposed by Richards-Dinger and Dieterich (2012). This approach enables the efficient simulation of the stick-slip dynamics of faults while discretising only the fault plane itself (in 2D) and does not require a full 3D discretisation of the surrounding material. Fault creep can also be included, depending on the frictional properties of the faults. The thermo-hydraulic reservoir model and the dynamic fault model are coupled using two different mechanisms: The pore pressure in the reservoir model is used to calculate changes in the effective normal stress at the faults. This is achieved directly by obtaining the local pore pressure in the reservoir model at the location of each fault patch. Additionally, the stress changes on the fault due to poro- and thermoelastic effects are calculated. For this purpose expansion / contraction of the rock in a given volume element of the reservoir model due to temperature changes or poroelastic effects are translated into the equivalent displacement of the surfaces of that volume element and the resulting stress change at each fault patch is calculated using a Boundary Element (BEM) approach.

This approach enables the simulation of induced seismicity in geothermal reservoirs using realistic geometries and fault properties. Uncertainties in the input data can be taken into account using ensemble modeling.

ms, such as Rayleigh waves or body waves with only phase information. Therefore, this type of replica vector was applied for examination of seismic characteristics due to the created fracture.

## S3 – Tektonische Geodäsie

### Vorträge

#### O-S3-01

#### **Predicting baseline changes between GNSS stations from stacks of wrapped InSAR interferograms**

**K. Cökerim, E. Latypova, J. Bedford**

*Ruhr-Universität Bochum, Tektonische Geodäsie, Bochum*

Monitoring ground displacements is critical for understanding tectonic processes, strain accumulation, and seismic hazards. GNSS networks provide highly accurate measurements with minimal atmospheric noise, their coverage is often limited, leaving significant gaps in regions with sparse or no stations. InSAR (Interferometric Synthetic Aperture Radar) offers extensive spatial coverage but is more susceptible to atmospheric noise compared to GNSS measurements. Previous studies have shown the capabilities of various deep learning approaches to separate the noise in InSAR interferograms and attain displacement on the scale of millimeters. By combining InSAR interferograms with machine learning, we aim to bridge this gap and provide a robust method for estimating relative ground displacements between two points, especially across fault lines. This study presents a proof-of-concept approach using a convolutional neural network (CNN) to predict displacement changes between GNSS stations, leveraging the spatial and temporal information contained in InSAR stacks.

The CNN model was trained on a dataset comprising stacks of wrapped InSAR interferograms from Japan and GNSS stations as anchor points within these scenes to assess the ground displacement. For each InSAR scene, we generated training samples by applying a sliding window approach to extract localized subsets of the data, considering all possible GNSS station pair (NC2) combinations within the window. These samples were used to predict changes in distance between GNSS stations. The model's performance was evaluated by comparing predicted displacements to observed displacements between GNSS stations. Our results demonstrate that even with a relatively small dataset and a simple CNN architecture, the model effectively predicts relative ground displacements between GNSS station pairs. The predictions exhibit strong agreement with observed GNSS measurements, showcasing the model's ability to extract meaningful displacement information from InSAR interferograms. This proof-of-concept approach highlights the potential for scaling the method to larger datasets and more complex architectures. Enhanced models could provide valuable tools for assessing ground displacements or strain rates in regions with sparse or no GNSS coverage.

## **O-S3-02**

### **The influence of GNSS network processing choices on the appearance of tectonic transient displacements**

**J. Bedford<sup>1</sup>, ERC TectoVision research team<sup>1,2</sup>**

<sup>1</sup>RUB, Bochum, <sup>2</sup>GFZ, Potsdam

GNSS displacement time series are nowadays routinely processed and distributed for many regions globally. For most earthquake researchers, Precise Point Positioning (PPP) data are sufficient for estimating coseismic displacements, postseismic signals, and general interseismic trends. However, when the aim is to understand the subtle accelerations related to ongoing processes on plate interfaces, more care needs to be given to the processing strategy.

For the most tectonically active plate boundaries, various research groups provide network solutions. In contrast to PPP, where positions are obtained independently for each station, network processing aims to preserve the inner geometry of the stations in the tectonic region of interest. In theory, network processing should result in more accurate relative motions of surface displacements, making such a strategy more appropriate for studies of 2<sup>nd</sup> order features in the time series (i.e. tectonic transients).

In this presentation I will show some ongoing analysis of different network solutions in Japan and Cascadia. For different network solutions at the same location and time span, we should ideally be capturing the same underlying tectonic processes, however we see different spatiotemporal features in the station trajectories that depend on the differences in the processing strategies. The challenge to the tectonic geodesy community is to figure out why these time series can vary so much and which features are most likely to be of a tectonic origin. One approach is to fit the observed signals with analytic models for elastic dislocation to see if the motions make sense from a fault slip perspective. Another approach is to experiment ourselves with parameters of the network processing to understand their impact of the appearance of transients. The presentation will conclude with our current recommendations for network processing to preserve real tectonic transients and minimize the appearance of artifactual transients that derive from certain processing choices.

## **O-S3-03**

### **Aseismic creep of the Katouna–Stamna Fault, observed by satellite geodesy, field evidence and structural analysis**

**J. Szrek<sup>1</sup>, S. Crosetto<sup>2</sup>, G. Gomba<sup>3</sup>, S. Metzger<sup>2</sup>**

<sup>1</sup>École Normale Supérieure, Geowissenschaften, Paris, France,

<sup>2</sup>GFZ Helmholtz-Zentrum für Geoforschung, Lithosphärenodynamik, Potsdam,

<sup>3</sup>Deutsches Zentrum für Luft und Raumfahrt, SAR Signalprozessierung, Wessling

The left-lateral, NW-trending Katouna–Stamna Fault in Western Greece marks the NE-boundary of the Ionian Islands-Acarnania block. The Global Navigation Satellite System (GNSS) displacement field shows significant fault activity and the fault is thought to creep, given the minimal seismicity in the area. To better understand the current kinematics of the Katouna–Stamna Fault, we integrated full-coverage surface displacement rates derived from 7-yr-long Interferometric Synthetic-Aperture Radar (InSAR) time-series with the GNSS rates, field observations and structural analyses. We aligned the InSAR surface rates in a fixed-Eurasia reference frame (spanned by the GNSS) and decomposed them into East and

Up rates. Fault-perpendicular rate profiles show a rate drop of 7 mm/yr in East and ~3 mm/yr in Up direction over a distance of only one kilometer, which clearly confirming the assumption of fault creep.

We designed a distributed slip model spanned by triangular and rectangular fault patches embedded in an elastic half-space to validate the geodetic observations. The best-fitting model reveals a transition from pure left-lateral movement at the southeastern end of the fault (where a half-graben forks off towards ESE) to oblique motion with a normal component at the northwestern end. Maximum sinistral creep of up to 11 mm/yr is observed at 1-8 km depth in the southeastern part, respectively, of up to 7 mm/yr at 2-6 km depth in the northwestern part. In addition, this latter accommodates normal creep of up to 5 mm/yr. Field evidence indicates complex fault kinematics with multiple deformation phases. We found proof of ductile deformation of gypsum and calcite recrystallization, suggesting influence of fluids, and possibly pressure solution creep as a key element of the fault's aseismic behavior.

## **O-S3-04**

### **Analysis of the Pütürge Segment at the East Anatolian Fault between the large 2020 and 2023 Earthquakes**

**A. Kuntze<sup>1</sup>, H. Sudhaus<sup>2</sup>**

<sup>1</sup>*CAU Kiel, Satelliten- und Aerogeophysik, Kiel,*

<sup>2</sup>*Karlsruhe Institut für Technologie, Geophysikalisches Institut, Karlsruhe*

The major East Anatolian Fault zone (EAF) separating the Anatolian and Arabian plates has shown an increased seismic activity in the current century. The most recent severe earthquake has been the Mw 7.8 Kahramanmaraş earthquake on 6th February 2023. Surface rupture and aftershocks reveal coseismic faulting along the three westernmost segments EAF up to the Pütürge segment. To the east, beyond the 2023 northeastern rupture tip, only three years earlier in January 2020, the Mw 6.8 Sivrice event had ruptured a an at most ~60 km part of the Pütürge segment with a northeast to southwest directivity. We have analyzed in detail the part of the EAF where these two large ruptures seemingly touch to better understand, if there has been a continuous seismic release of stress or if a persisting part remained unbroken. In the latter case, stress release has yet to happen seismically or is accommodated aseismically, e.g. through fault creep.

We used surface displacements data based on InSAR (radar interferometry), SAR pixel offset and GNSS data, partly together with seismic waveforms, to image the rupture planes of the Kahramanmaraş and Sivrice earthquakes at depth. Additionally we investigated the aftershocks in the focus area at the Pütürge segment between the two main rupture areas. We join these data in a Bayesian Optimization of a finite pseudo-dynamic seismic rupture model, applying implementations of the open-source Pyrocko toolbox. For the very large 2023 Kahramanmaraş earthquake we reduced the modeling to the northeastern end the rupture and modeled the remaining part based on a published fault slip model. For the 2020 Sivrice earthquake we optimized the entire rupture area.

We found that between the two large earthquakes on the Pütürge segment there is indeed an approximately 20 km long seismic gap. Reported creep in this part of the fault is not observed for the period from 2016 to 2022 based on InSAR time series data provided by DLR. Also a recent M6 earthquake in this region but off the EAF by several kilometers could indicate that this part on the fault is not relaxed, but rather that there is a strong asperity hampering rupture.

## Deformation Monitoring on Laacher See by GNSS

Z. Deng<sup>1</sup>, M. Ramatschi<sup>1</sup>, T. Dahm<sup>2</sup>

<sup>1</sup>*GeoForschungsZentrum Potsdam, Geodesy, Potsdam,*

<sup>2</sup>*GeoForschungsZentrum Potsdam, Physics of Earthquakes and Volcanoes, Potsdam*

The intracontinental volcanic systems located west and north of the Alps, including the Massif Central and the Eifel, are among the youngest Quaternary volcanic fields in Central Europe. They are characterized by extensive distributed basaltic fields containing hundreds of cinder cones and maars, with episodic volcanic activity dating back approximately 700 thousand years. The plumbing system beneath remains active, and recent signs of incipient unrest have been detected. Despite this, the transcrustal magmatic system has not yet been imaged using advanced geophysical techniques. The Eifel region, however, is ideally suited for the application and testing of new models of transcrustal magma transport and storage, which can provide insights into volcanic hazards and potential eruption scenarios.

A recent study by Hensch et al. (2019) revealed that the Laacher See Volcano (LSV), one of three explosive eruptive centers in the East Eifel with a VEI=VI eruption occurring 13,000 years ago, is experiencing volcanic deep low-frequency (DLF) earthquakes between 10 and 43 km depth. These earthquakes are associated with the unrest of magmatic fluids or magmas. The unrest activity began in 2013 and continues to the present day, with the latest events recorded in August 2022. A recent local seismic tomography study (Zhang et al., submitted), using a comprehensive dataset from a large-N passive seismic experiment, shows a large significant velocity anomaly beneath the LSV that extends from the surface to a depth of about 12 km. The anomaly may represent the residual magmatic reservoir of the last eruption, which may still be susceptible to fluid inflow and uplift today.

The Eifel volcanic fields experience noticeable uplift measured by GNSS today, possibly driven by upper mantle upwelling with a diameter of approximately 200 km, and ongoing magmatic processes at the crust mantle boundary. To better understand these geological dynamics, we build up a dense GNSS network in the East Eifel in collaboration with our partners. We present preliminary analysis for the dense GNSS network since 2022 and discuss unusual local transients which may be related to the ascent of magmatic fluids or CO<sub>2</sub>.

## S3 – Tektonische Geodäsie

### Poster

#### P-S3-01

#### **Seismicity vs. slip with Foamquake analog modelling subduction experiments.**

**E. Latypova<sup>1</sup>, F. Corbi<sup>2</sup>, G. Mastella<sup>3</sup>, F. Funiciello<sup>4</sup>, J. Bedford<sup>5</sup>**

<sup>1</sup>Ruhr-Universität Bochum, Institute for Geology, Mineralogy and Geophysics, Bochum,

<sup>2</sup>Istituto di Geologia Ambientale e Geoingegneria - CNR c/o Dipartimento di Scienze della Terra, Sapienza Università di Roma, Roma, Italy,

<sup>3</sup>Sapienza University of Rome, Earth Sciences, Roma, Italy,

<sup>4</sup>Università "Roma TRE", Dipartimento di Scienze, Laboratory of Experimental Tectonics, Italy,

<sup>5</sup>Ruhr-Universität Bochum, Institute for Geology, Mineralogy and Geophysics, Bochum

Seismic and geodetic networks are essential tools for studying subduction tectonics, though they face several challenges. Available geophysical data are limited for instance by noise, sparse station coverage, offshore monitoring challenges, and data gaps.

Scaled seismotectonic models have become useful in filling these observational gaps. Such models can reproduce hundreds of analog seismic cycles in a few minutes of experimental time with the advantage of known and controlled boundary conditions.

Here we present experimental results from the Foamquake 3D seismotectonic model, which simulates megathrust subduction earthquakes. In our study, we used a high-frequency camera (as a geodetic network) to record model surface deformation at 50 Hz and a network of 5 three-component accelerometers (as a seismic network) located on the model surface to characterise seismic deformation at 1 kHz. Using accelerometer data, we identified the hypocenter locations of seismic events. To analyse the camera data, we employed Particle Image Velocimetry (PIV), an image analysis technique allowing us to depict surface displacement data. This method allowed having the analog of a dense, homogeneously distributed geodetic network spanning updip to scaled depths.

This data is a key to unravel the seismic cycles of subduction megathrust earthquakes since these areas are typically under-monitored in natural subduction zones as usually located offshore.

Here we show how the joint study of seismicity and slip in a laboratory setting can work together. We identify, cluster, and localise laboratory earthquakes based on both the PIV and accelerometer data.

Our analysis primarily focuses on investigating the nucleation of laboratory earthquakes and characterizing the spatial and temporal relationships between seismic and aseismic fault slip, a crucial aspect for understanding the behavior of natural faults.

## **Geodetic Aspects of the Seismically Active Mt. Hochstaufen (Germany) – Space-borne and Ground-based InSAR Measurements**

**A. Schrömer<sup>1</sup>, J. Wassermann<sup>1</sup>, S. Metzger<sup>2</sup>**

<sup>1</sup>*LMU München, Department of Earth and Environmental Sciences, München,*

<sup>2</sup>*GFZ Potsdam, Potsdam*

The Mt. Hochstaufen region, located in the Northern Alps, is one of the few areas in Germany with significant microseismic activity. For centuries the area has experienced single earthquakes with magnitudes up to M3.2, as well as irregular swarm-type sequences. While most of the swarms occurred during summer and were often accompanied by heavy precipitation, a direct correlation between seismicity and water infiltration into the mountain was suggested. However, a swarm in 2019 characterized by numerous high-magnitude earthquakes occurred without significant synchronous rainfall, and another earthquake cluster occurred in winter 2022 when the surface was snow-covered. These irregularities indicate that strong precipitation and tectonic background stress alone cannot fully explain the unusually high seismicity in this region.

To investigate the complete set of driving forces, seismological, meteorological, and geodetic observations of the last decade were analysed. Here, we focus on the results from space-borne and ground-based Interferometric Synthetic Aperture Radar (InSAR) measurements. Ground-based InSAR data, collected from three line-of-sights around Mt. Hochstaufen, revealed significant displacements of natural reflectors on the mountain slopes. The results indicate the opening of prominent fractures on both flanks of the mountain and subsidence of the Bad Reichenhaller basin west of the Saalach River. To analyze the long-term regional deformation, four year long time-series from the European Ground Motion Service collected by the Sentinel-1 satellite mission were used. These data revealed significant vertical velocity variations on Mt. Hochstaufen, with negligible movement on the northern flank contrasting with subsidence exceeding 5 mm/year on the southwestern slopes near the summit. This region coincides with the concentration of relocated earthquakes.

Seasonal effects dominate the time series of individual reflectors on the mountain. After suppressing these effects no clear correlation between the displacement time-series and earthquake occurrences could be identified. To further investigate displacement patterns, the time-series were clustered and compared with geological maps. The comparison reveals that cluster boundaries align with transitions between distinct geological units, such as the boundary between „Wettersteinkalk“ and „Alpiner Muschelkalk,“ or with known fault lines.

## **The Geophysical Instrument Pool Potsdam (GIPP) – now with GNSS component**

**B. Wawerzinek<sup>1</sup>, C. Haberland<sup>1</sup>, O. Ritter<sup>1</sup>, B. Männel<sup>1</sup>, C. Krawczyk<sup>1,2</sup>**

<sup>1</sup>*GFZ Helmholtz Centre for Geosciences, Potsdam,*

<sup>2</sup>*Technische Universität Berlin, Institute for Applied Geosciences, Berlin*

Geophysical field observations are making an essential contribution to research of the Earth structure and the ongoing processes since a long time. To support temporary field experiments - in addition to permanent monitoring networks and observatories - the "Geophysical Instrument Pool Potsdam" (GIPP) at the "GFZ Helmholtz Centre for Geosciences" provides mobile seismic and magnetotelluric recorders and sensors. The land stations of the "German Pool for Amphibious Seismology" (DEPAS) are also managed at the GIPP. As a new feature, in fall 2024, the GIPP was expanded to include a GNSS component.

This research infrastructure facility is open to all academic applicants (research institutes, universities, etc.; national and international), and the instruments are made available free of charge following a transparent application and evaluation procedure ([www.gfz-potsdam.de/gipp](http://www.gfz-potsdam.de/gipp)). The applications are evaluated by an external steering committee. The instruments are used in experiments on a wide range of topics, including earth structure, geodynamics, earthquakes, geo-resource exploration, volcano monitoring, soil investigations and much more. Since its foundation around 30 years ago, the GIPP has supported almost 500 geoscientific projects (approx. 20 to 40 per year). The devices are in high demand and overbooking regularly occurs. A major part of our work is related to the development of innovative hardware (i.e. digital recorders) and software. In addition we operate a data repository to archive the collected data.

Today the seismological part of the GIPP consists of more than 1000 digital recorders, 250 broadband sensors, numerous geophones and the necessary accessories. We also provide instruments for controlled source experiments (autonomous nodes and cable based system). For magnetotelluric experiments, > 50 real-time data-loggers, >150 induction coils, >500 electrodes as well as a large number of cables and accessories are available. The GNSS component consists of 50 compact, mobile units. Possible applications range from atmospheric research to tectonic targets.

## S4 – Induzierte Polarisation

### Vorträge

#### O-S4-01

##### **Is it possible to assess the quality of carbonates using IP?**

**N. Klitzsch, L. Ahrensmeier**

*RWTH Aachen University, CG<sup>3</sup>, Aachen*

Carbonate rock, i.e. limestone and dolomite, is often used as building material and construction aggregate, but also in industrial processes, e.g. in metallurgy and glass production. For many applications, the mineralogical purity of the carbonate rock, i.e. its calcium carbonate or dolomite content, is crucial. For carbonate deposits overlain by unconsolidated sediments, minerals can infiltrate into the carbonate's fracture network. These are mainly clay minerals as they are easily transported by water and can therefore infiltrate particularly well. As a result, they influence the mineralogical composition of the mined carbonate. To meet the purity requirements, one would like to assess the purity of the carbonate, at least qualitatively, before mining.

For the exploration of carbonate deposits electrical resistivity tomography (ERT) is a commonly used method that benefits from the high contrast between the resistivity of unconsolidated sediment and carbonate. ERT is however applied for the spatial delineation between overburden and carbonate rock, but not for assessing the quality of the latter. We investigate whether the induced polarization (IP) method can be used for assessing the purity of carbonates. Specifically, we test the hypothesis that the imaginary conductivity and normalized chargeability are correlated with the clay content of the carbonate. This correlation is expected because the clay content determines the carbonates inner surface area and its cation exchange capacity (CEC). These two variables in turn correlate with the mentioned IP parameters.

To test our hypothesis, we measured two IP profiles in a dolomite quarry and obtained samples from the underlying wall. On these samples, we measured CEC and SIP. Additionally, we determined the clay mineral content of selected samples using the XRD analyses. We will present the results of this study, in particular whether IP measurements can be utilized to assess the quality of carbonates.

#### O-S4-02

##### **Kann IP bei der Permeabilitätsabschätzung helfen?**

**A. Weller<sup>1</sup>, L. Slater<sup>2</sup>**

<sup>1</sup>*Technische Universität Clausthal, Clausthal-Zellerfeld,*

<sup>2</sup>*Rutgers University, Newark, United States of America*

Die Permeabilität von Gesteinsformationen wird durch die beiden Parameter Porosität und Porengröße entscheidend beeinflusst. Die Porosität ist über die Archie-Gleichung mit dem Formationsfaktor verbunden, der sich aus geoelektrischen Messungen gewinnen lässt. Allerdings muss dabei der Einfluss der Grenzflächenleitfähigkeit berücksichtigt werden. Der Zugang zur Porengröße erfolgt über die auf das Porenvolumen normierte innere Oberfläche  $S_{\text{por}}$ . Für einige Gesteinsformationen wurden empirische Beziehung zwischen  $S_{\text{por}}$  und dem Imaginärteil der elektrischen Leitfähigkeit oder auch der normierten Aufladbarkeit gefunden. Eine Vielzahl von Modellen zur Permeabilitätsabschätzung basiert

auf Potenzfunktionen sowohl vom Formationsfaktor als auch von einem IP-Parameter. Die für die Parameter verwendeten Exponenten variieren für verschiedene Gesteinsformationen. Die Variationen in den Exponenten lassen sich auf die für die einzelnen Formationen ermittelten Zusammenhänge zwischen Porosität und Porengröße zurückführen. Für viele Festgesteinsformationen bleibt der Formationsfaktor der entscheidende Parameter für die Permeabilitätsabschätzung. Der Exponent variiert für die von uns untersuchten Formationen zwischen -1 (Mudstone) und -8 (Araba Formation). Die Einbindung von IP-Parametern verbessert die Permeabilitätsabschätzung nur geringfügig. Bei Lockergesteinen, die oft nur eine geringe Variation im Formationsfaktor zeigen, ist die Einbeziehung von IP-Parametern erforderlich.

Die Untersuchungen an verschiedenen Gesteinsformationen haben deutlich gezeigt, dass es kein universelles Modell zur Permeabilitätsabschätzung gibt. Mit den Ergebnissen von petrophysikalischen Untersuchungen können die formationsspezifischen Modelle bereitgestellt werden. Dabei kann auch die Frage beantwortet werden, ob die Einbeziehung von IP-Parametern die Qualität der Permeabilitätsabschätzung verbessert.

## O-S4-03

### Influence of particle-particle interaction on the spectral induced polarization response of conducting and non-conducting particles

D. Kreith<sup>1</sup>, J. Wentzki<sup>1</sup>, B. Brömer<sup>1</sup>, A. Haji<sup>1</sup>, M. Bücker<sup>1,2</sup>

<sup>1</sup>Technische Universität Braunschweig, Institut für Geophysik und Extraterrestrische Physik, Braunschweig,

<sup>2</sup>Christian-Albrechts-Universität Kiel, Institut für Geophysik, Kiel

Spectral induced polarization (SIP) assesses the frequency-dependent complex electrical conductivity. The frequency-dependency is caused by polarization processes taking place at the scale of single mineral grains in the subsurface. Mechanistic micro-scale models help understanding measured complex-conductivity spectra and relating them to relevant petrophysical parameters.

Most polarization models assume simple geometries consisting of one single particle embedded in an electrolyte solution. However, particles in real geological materials are surrounded by other nearby particles, leading to a mutual influence on the electrical field around the particles and thus on the expected polarization response. This interaction is neglected in most mechanistic models, which limits their applicability when comparing modeled with measured SIP data.

We extend existing numerical models of single particles by adding a second particle in order to investigate the effect of possible particle-particle interactions on the SIP response. We consider different relative positions of two spherical particles and vary the distance between them.

Our treatment covers the two limiting cases of (i) infinite and (ii) vanishing particle conductivity. These two cases represent the two most important polarization mechanisms in the SIP frequency range. An infinite particle conductivity corresponds with the electrode polarization around metallic grains. On the other hand, the polarization of the different parts of the electrical double layer covering the surface of non-conductive particles, such as sand and clay particles, plays an important role for hydro-geophysical applications of the SIP method.

For the case of non-conductive particles, the polarization amplitude decreases when the particles are aligned parallel to the electrical field, while the polarization strength decreases with the spheres being aligned perpendicular to the electrical field. Both effects vanish when

the distance between the particles becomes larger. For the case of two perfectly conducting spheres aligned parallel to the electrical field, an additional polarization at higher frequencies depending on the distance between the particles can be observed.

Based on the results, it is possible to gain deeper insight into the influence of particle-particle interaction on the SIP response of densely packed granular materials.

## **O-S4-04**

### **Implications of an additional surface capacitance for the understanding of electrode polarization**

**M. Bücker<sup>1</sup>, F. Keiser<sup>2</sup>, D. Kreith<sup>2</sup>, K. Breede<sup>3</sup>, Z. Zhang<sup>3</sup>, A. Weller<sup>3</sup>**

<sup>1</sup>*Universität Kiel, Kiel,*

<sup>2</sup>*Technische Universität Braunschweig, Braunschweig,*

<sup>3</sup>*Technische Universität Clausthal, Clausthal*

The process of electrode polarization causes the largest chargeability values in induced polarization (IP) measurements. Before the recent diversification of IP applications, the strong electrode polarization response of metal-bearing mineral grains was the primary target of IP field measurements for the longest time of the existence of the method. It is even more surprising that there are still many open questions regarding the underlying physical processes at the scale of individual grains or pores.

In this contribution, we briefly review old and new experimental data as well as long-known and more recent micro-scale polarization models. We arrive at the conclusion that there is no comprehensive analytical model that can explain the variety of relations  $\tau \propto f^b$  between the relaxation time  $\tau$  assessed by spectral IP measurements and the fluid conductivity  $f$ , with observed exponents  $0.5 < b < 1$ .

Motivated by recent empirical models deduced from laboratory measurements, we integrate an additional surface capacitance – apart from the diffuse-layer capacitance(s) already considered in earlier micro-scale models – into a simple diffuse-layer electrode polarization model. Depending on the ratio between diffuse-layer capacitance and the new surface capacitance, values of the exponent  $0.5 < b < 1$  are obtained.

The additional capacitance could, e.g., be associated with the capacitance of the Helmholtz layer (or the distance of closest approach of ions to the surface), the capacitance of an additional diffuse layer building up within the solid (e.g., when the solid is a semi-conductor), thin non-conducting coatings of the metallic surface (e.g., oil films or paint), or a combination of various capacitances.

While the nature of the additional capacitance is not yet clear, the proposed model is the first that can explain the broad variety of relaxation time-fluid conductivity relations observed in experimental data based on the simple and physically meaningful assumption of an additional surface capacitance.

## **High-frequency spectral induced polarisation to image permafrost features in Storflaket, Abisko, Northern Sweden**

**M. Sugand, A. Hördt**

*TU Braunschweig, Braunschweig*

The geoelectrical method of High-frequency induced polarisation (HFIP) can detect the presence of ice in the subsurface, as its characteristic dielectric relaxation occurs in frequency ranges of 1 kHz to 100 kHz. Through further petrophysical modelling, it is also possible to quantify volumetric ice content. A two-component mixture model, with one component as ice and the second as the surrounding matrix, has been used to quantify ice content in recent field surveys. The model incorporates ice relaxation to describe the high-frequency polarisation and includes a constant phase shift model to explain the low-frequency polarisation occurring due to relaxation of the electrical double layer.

Results from HFIP field measurements at Storflaket mire, a peatland permafrost site in Northern Sweden, are presented. An HFIP dataset ranging from 1 Hz to 230 kHz was collected along a 12-metre two-dimensional profile. The dataset is inverted as independent frequencies, after which the spectral results are compiled to obtain the inverted resistivities and phase shift. This inversion approach avoids assuming any relaxation, thus yielding the true subsurface spectra. The two-component model is then fitted to these inverted spectra to obtain the volumetric ice content. The model includes several free parameters: for the ice component, these comprise DC resistivity and relaxation time; for the matrix component, these include matrix conductivity, low-frequency phase shift, and matrix permittivity. Additionally, the model exponent,  $k$ , describes how the ice and matrix components are mixed.

The volumetric ice content results are validated against ice content measured from a permafrost core extracted along the profile. The results show excellent agreement. Furthermore, two of the free model parameters show particularly interesting trends. The model exponent,  $k$ , increases with increasing ice content. This could mean that the geometrical arrangement of ice and matrix depends on the ice content itself. The matrix permittivity, which in theory allows for solid matrix identification, shows elevated values ( $\approx 60$ ) for unfrozen peat in ice-poor or ice-free zones. In ice-rich zones (>20% ice content), the values are even higher ( $>80$ ), suggesting the matrix permittivity may be capturing additional complexities not yet fully understood. These findings contribute to understanding the induced polarisation in permafrost peatlands, which is an underexplored area from a geophysical perspective.

## **Spectral induced polarization (SIP) as a non-invasive tool for tracking microbial dynamics: Insights from *Shewanella oneidensis* MR-1 cell suspensions and alginate bead-packed column reactors**

**D. Amarawardana<sup>1</sup>, A. Mellage<sup>1</sup>, C. M. Smeaton<sup>2</sup>**

<sup>1</sup>*Universität Kassel, Civil and Environmental Engineering, Kassel,*

<sup>2</sup>*School of Science and the Environment, Memorial University of Newfoundland, Newfoundland, Canada*

Spectral induced polarization (SIP) is a geophysical technique that has shown promise for non-invasively monitoring microbial growth and metabolic activity in porous media. A growing body of literature has linked the presence of bacteria and their growth to SIP signals. However, open questions remain regarding the contribution of biomass density vs. activity. Do bacteria simply need to be present in porous media or do they also have to be metabolically active to be detected with SIP? Moreover, studies in cell suspensions, that is, without porous media, have proven difficult to reproduce. The latter has contributed to an open debate about the source of microbially driven signals, either stemming from cells themselves, or sediment-microbe interactions. Here, we aim to address both knowledge gaps and provide evidence of cell-driven microbial polarization while also addressing the complexities of running "in-suspension" experiments. To that end we investigated the SIP response, focusing on imaginary conductivity ( $\sigma''$ ) signals, of *Shewanella oneidensis* MR-1 in two experimental configurations: (1) cell suspensions and (2) non-polarizing alginate bead-packed reactors. In static cell suspension experiments, we observed spectral responses between 0.1 to 10 Hz, during the first 24 hours, gradually shifting to frequencies below 0.1 Hz over time with changes in magnitudes and decreasing data reliability with increasing incubation time. In bead-packed reactors, we observed a distinct frequency-dependent behaviour (0.01-1 Hz) across different phases of microbial growth. Microbial activity and concentrations were monitored using adenosine triphosphate (ATP) and optical density (OD), respectively. Our results show a correlation ( $R^2= 0.90$ ,  $R^2= 0.80$ ; ATP and OD respectively) between  $\sigma''$  and both microbial growth and activity. Our measured  $\sigma''$  signals reach a maximum during maximum growth (i.e., log phase) and activity, then decrease during stationary and death phases. Although the presence of cells in suspension was detectable, obtaining reliable signals proved challenging, which we attribute to the settling of microbial cells and aggregation. Moreover, the growth media-infused bead-packed columns yielded high phase shifts of 15 mrad. Our findings from both experiments unequivocally link signals to the presence and growth of cells and provide a strong base to further develop SIP as a quantitative indicator of microbial dynamics in biogeochemically active systems.

## Towards Sustainable Cement Compositions: Exploring the Effects of Clinker Substitutes with NMR and Induced Polarization

S. Munsch<sup>1</sup>, L. Grobla<sup>1</sup>, W. Schmidt<sup>2</sup>, S. Kruschwitz<sup>1,3</sup>

<sup>1</sup>Bundesanstalt für Materialforschung und -prüfung, Zerstörungsfreie Prüfung, Berlin,

<sup>2</sup>Bundesanstalt für Materialforschung und -prüfung, Baustofftechnologie, Berlin,

<sup>3</sup>Technische Universität Berlin, Zerstörungsfreie Baustoffprüfung, Berlin

The reduction of clinker content in cement is a key strategy to lower the CO<sub>2</sub> footprint of the cement industry. In the recently approved composite cements of class CEM II, a significant portion of the clinker (up to 50 %) can already be replaced. A promising option in this context is the so-called LC<sup>3</sup> (Limestone Calcined Clay Cement), which offers exciting alternatives especially for countries with large clay deposits. To ensure the performance and durability of such binders, understanding hydration processes and the role of the used supplementary cementitious materials (SCMs) is crucial.

The authors present findings from two independent studies: a master thesis and a round-robin experiment conducted within a RILEM Technical Committee. Both studies investigate cementitious materials incorporating SCMs using advanced characterization techniques. The master thesis focuses on early hydration processes during the first 100 hours using Nuclear Magnetic Resonance relaxometry (NMR), providing detailed insights into microstructural development, hydrogen bonding, and water mobility. In contrast, the round-robin experiment explores hydration and durability over a longer timeframe of 3 to 91 days using induced polarization (IP) to study bulk conductivity and its changes with age. For all investigated mixtures—including pure Ordinary Portland (CEM I), Portland Limestone Cement (CEM II) including blends with calcined clay and fly ash—heat flow calorimetry serves as a reference method to monitor hydration progress during the early stages.

This approach allows a comprehensive understanding of the effects of SCMs on hydration, combining short-term and long-term perspectives while leveraging complementary techniques. Preliminary results demonstrate a significant increase in NMR T<sub>2</sub> relaxation times with the addition of fly ash, accompanied by a strong reduction in the free water component. Concurrently, early IP measurements reveal a steady increase in impedance with sample age, particularly pronounced in mixtures containing calcined clay. These findings underline the potential of NMR and IP to evaluate hydration and durability-related properties in cementitious systems with reduced clinker content.

## S4 – Induzierte Polarisation

### Poster

#### P-S4-01

#### **Zeta-potential and spectral induced polarization measurements on municipal solid waste matrices at different ionic strengths**

**A. Rahmani<sup>1</sup>, M. Halisch<sup>2</sup>, A. Mellage<sup>1</sup>**

<sup>1</sup>*University of Kassel, Civil and Environmental Engineering, Kassel,*

<sup>2</sup>*LIAG Institute for Applied Geophysics (LIAG), Hannover*

Recent advances in the application of spectral induced polarization (SIP) highlight its effectiveness as a proxy for monitoring ion exchange processes, for example during controlled desorption of ammonium from municipal solid waste (MSW). Natural soils and sediments as well as MSW contain substantial amounts of solid organic material that (1) contributes to sorption sites and (2) to surface charge and thereby to polarization/ charge storage. Moreover, the strong contribution of organic matter to SIP signals has been highlighted by studies in organic-rich sediments, which showed a correlation between total organic carbon (TOC) and imaginary conductivity. The mechanisms of polarization in organic matrices, however, remain understudied and yet poorly understood. Here, we present results from a preliminary investigation where we measured the zeta-potential and SIP response of porous matrices of clean sand, MSW and an MSW-sand mixture at different ionic strengths. Our results show clean sand has fewer reactive surface sites than MSW, which is highly reactive due to its organic-rich composition. In the MSW-sand mixture, MSW reactivity is reduced by sand. SIP data confirms this, with an imaginary conductivity of around 0.005 S/m for sand and the sand-MSW mixture, compared to 0.015 S/m for MSW only. We aim to build on our findings and systematically investigate SIP responses over a broad range of organic matter contents, focusing on joint geophysical and surface charge characterization. We seek to refine the interpretation of SIP signals collected in organic-rich solid matrices, and thereby improve the method's quantitative applicability to (e.g.) characterize zones of high organic content in the subsurface and improve our understanding of the underlying polarization mechanisms that shape these signatures.

#### P-S4-02

#### **Dielectric Spectroscopy Measurements of Martian analogue Bentonite Soil Sample**

**L. Zimmermann<sup>1</sup>, S. Garland<sup>2</sup>, A. Lorek<sup>2</sup>, J. H. Börner<sup>1</sup>**

<sup>1</sup>*TU Bergakademie Freiberg, Institut für Geophysik und Geoinformatik, Freiberg,*

<sup>2</sup>*Deutsches Zentrum für Luft- und Raumfahrt, Institut für Planetenforschung, Berlin*

#### **Dielectric Spectroscopy Measurements of Martian analogue Bentonite Soil Sample**

The planet Mars holds a particular fascination for us, as it is a potential future habitat. However, for the time being, our focus remains on Earth, which is the only known location where life exists. All known forms of life require water as a basic necessity. Therefore, the discovery of significant quantities of water or ice on Mars would represent a breakthrough in scientific knowledge.

Given that the Martian atmosphere consists mostly of CO<sub>2</sub> the gas was used for the measurements. The sample utilised is bentonite, due to its resemblance to the Martian soil. This contribution uses dielectric spectroscopy to investigate the influence of CO<sub>2</sub> on the dielectric properties of a bentonite soil sample with varied water content.

Dielectric spectroscopy measurements were conducted at the Institute of Planetary Research of the DLR using a parallel plate capacitor system in a Mars simulation chamber. The capacitor is constructed to incorporate a gas gap above a soil sample, allowing soil/atmosphere interactions to be studied. The capacitance was measured under different atmospheric humidities in the frequency range 10 Hz to 1.1 MHz.

The capacitance was found to be dependent on the gas (air or CO<sub>2</sub>) and its humidity. It was observed that lower gas humidity generally leads to lower capacities. This was observed in both air and CO<sub>2</sub> measurements. The resulting curve can be modelled with a Cole-Cole formula.

## P-S4-03

### Numerical simulation of polarization mechanisms of frozen soil at the pore scale

F. Keiser, A. Hördt

TU Braunschweig, Institut für Geophysik und extraterrestrische Physik, AG Hördt, Braunschweig

Permafrost is a common feature in the polar and high alpine regions of the world. Given the current challenges posed by global warming, the monitoring and understanding of permafrost is not only of local interest but also of global importance. The degradation of permafrost can result in the release of large amounts of greenhouse gases and the destabilization of the ground, which can lead to landslides and other natural hazards.

One possible method to investigate Permafrost is High-Frequency Induced Polarization (HFIP), a geophysical method that is used to investigate the electrical properties of the subsurface in the frequency range between 1 Hz and 230 kHz. In contrast to conventional electrical resistivity tomography, HFIP is sensitive to charge storage and has been used to infer the presence of ice in the subsurface.

Unlike most other materials, the electrical permittivity of ice exhibits a significant drop in the frequency range around 10 kHz. The frequency-dependence of permittivity causes a characteristic ice peak in the phase spectrum of the HFIP response, which has been observed both in field and laboratory measurements. In the past, this so-called "Ice Peak" has been used to infer the presence of ice in the subsurface and to estimate the ice content. The estimation is normally based on a 2-component weighted power law model that considers ice as one medium and the mixture of minerals and fluid water as the second medium. While the model had some success in field scale applications, its accuracy has not been investigated in great detail. As a macroscopic model, it cannot consider the specific polarization processes and in particular potential interaction between different mechanisms, such as ice polarization and double layer polarization, which might effect ice content estimates.

The goal of this work is to develop a mechanistic model that can describe the polarization mechanisms and SIP response of (partly) frozen porous media. In a first step, we use the COMSOL Multiphysics software to numerically simulate the polarization response on a pore scale. We use a simplified geometry of a mostly frozen pore surrounded by a matrix. While the bulk of the pore space is filled with ice, there is a small unfrozen water film at the pore walls due to the surface effects. We consider both Stern and diffuse layers at both the ice-water and water-matrix interfaces and conduct parametric studies to investigate the effect on the SIP response of the sample.

## **P-S4-04**

### **High-Frequency Induced Polarization (HFIP) for quantitative ice content estimation in a Palsa at Aidejavri (Norway)**

**R. Schulz<sup>1</sup>, I. Burger<sup>1</sup>, A. Pischke<sup>1</sup>, S. Westermann<sup>2</sup>, A. Hördt<sup>1</sup>**

<sup>1</sup>*Institut für Geophysik und Extraterrestrische Physik, Angewandte Geophysik, Braunschweig,*

<sup>2</sup>*Department of Geosciences, Oslo, Norway*

High-Frequency Induced Polarization (HFIP) is a non-invasive geophysical method that extends conventional induced polarization (IP) techniques by broadening the measurement frequency range up to 230 kHz. This allows the characterization of the frequency-dependent electrical conductivity of water ice, enabling quantitative estimates of ice content in permafrost environments. HFIP measurements at the field scale are challenged by electromagnetic (EM) coupling effects, including cable-to-cable coupling and induction within the subsurface. Addressing these challenges helps to achieve reliable data and accurate interpretations.

In this study, HFIP was employed to investigate a palsa, a permafrost-cored hill, situated in a peat mire in Aidejavri. The HFIP dataset was pre-processed to mitigate EM coupling effects, ensuring that the derived measurements reflect the true polarization response of the subsurface. The processed data were inverted using a two-component dielectric mixture model to get spatially resolved estimates of ice content across the surveyed transects.

To support the HFIP findings, complementary geophysical methods, including electrical resistivity tomography (ERT) and ground-penetrating radar (GPR), were applied in the same area. ERT provides additional insight into the permafrost's lateral extent and resistivity contrasts. GPR is useful to find the upper boundary of the frozen subsurface. Together, these methods provide a broad subsurface overview, while HFIP uniquely quantifies ice content, making it essential for palsa characterization.

This study demonstrates that HFIP, when combined with robust pre-processing techniques to remove coupling effects, is a reliable tool for ice-rich permafrost investigations. The dataset from Aidejavri contributes to advancing the understanding of palsa structures. By comparing it with repetitive measurements in future it is planned to derive the palsa's vulnerability to climatic changes.

## **P-S4-05**

### **A novel approach to determine temperature correction coefficients for complex conductivity monitoring data**

**A. M. Mansfeld, J. Hase, A. Kemna**

*Institut für Geowissenschaften / Universität Bonn, Geophysik, Bonn*

Many geophysical monitoring measurements are subject to periodical yet uncontrollable changes in the ambient temperature, such as the diurnal temperature cycle. Relations between complex electrical conductivity and temperature have been studied in the past and can be employed to correct gathered time series for temperature effects. However, these corrections rely on the knowledge of material-specific properties, which may not be available during practical laboratory- or field applications. Furthermore, when working with heterogeneous geological materials, finding a representative mean correction coefficient for a given representative elementary volume is non-trivial. Complexity increases further if we consider spectral data, as the electrical conductivity's imaginary part of each polarization

process has a unique dependency on temperature. We propose making use of the periodical component of temperature changes, in order to identify the temperature-driven change of the measured signal and compensate for it during data processing.

For monitoring data sets affected by a periodical change in temperature, a Fourier transform of the complex conductivity time series yields a maximum in amplitude at the frequency corresponding to the period of the temperature cycle. In our approach, we optimize the choice of hyperparameters for the temperature correction by minimizing the amplitude of the Fourier spectrum at this frequency. In contrast to a filtering approach, the fitted temperature compensation model not only corrects for periodical changes in temperature but also compensates for non-periodical changes. In this case study, we show the results of our approach for the temperature correction of the complex electrical conductivity of a rock sample, as well as shifts in the peak relaxation time of a SIP-monitoring data set, using a simple Arrhenius type temperature relationship. With the help of this approach, we can significantly improve the overall interpretation of the data with regard to underlying processes. The principle behind this approach of recovering temperature correction coefficients could be applied to temperature correction models or other cyclical sources of change.

## **P-S4-06**

### **Evaluierung einer neuartigen Anregungssignalform für Spektrale IP Messungen.**

**T. Radic, Radic Research, Berlin**

Die Spektrale IP Methode grenzt sich von der Zeitbereichs IP nicht durch die Verwendung sinusförmiger Anregungssignale ab, sondern durch die Zeitreihenanalyse im Frequenzbereich.

Wir haben uns daher die Frage gestellt, ob alternative Anregungssignalformen evtl. Vorteile gegenüber Sinusförmigen bieten.

Transmitter zur Erzeugung sinusförmiger Anregungssignale für Spektrale IP Messungen weisen nämlich einige Nachteile gegenüber solchen für rechteckförmigen Pulse auf:

- Technisch aufwendiger und daher teurer in der Fertigung.
- Erzeugen Abwärme. Kühlmaßnahmen erhöhen Gewicht und Volumen.
- Produzieren ~40% geringere effektive Stromamplitude. Geringere Messgenauigkeit ist die Folge. Es stellt sich somit die Aufgabe zu evaluieren, ob der Einsatz rechteckförmiger, anstelle von sinusförmiger Anregungssignale, für Spektrale IP Messungen zu gleichwertigen oder gar besseren Ergebnissen führt. Da wir dies in der Vergangenheit bereits für einfache rechteckförmige Anregungssignale zeigen konnten (Radic, 2016), lag unser aktueller Fokus auf der Frage, ob sich die Messfortschrittssteigerung, die sich mit überlagerten sinusförmigen Anregungssignalen einstellt, auch mit geeigneten komplexeren rechteckförmigen Pulsfolgen realisieren lässt. Angeregt durch eine Publikation von Yang et al. (2021) haben wir eine rechteckförmige Pulsfolge berechnet die im Spektrum 4 Frequenzen mit nahezu gleicher effektiver Amplitude aufweist. Zudem sind die Frequenzen logarithmisch äquidistant mit dem Faktor 2 verteilt angeordnet. Unser Poster zeigt anhand von realen Vergleichsmessungen an polarisierten Gesteinsproben, dass die neue Pulsfolge erfolgreich hohen Messfortschritt mit größerer Messgenauigkeit kombiniert. Das positive Ergebnis könnte zudem den Weg zu kompakteren und genaueren vielkanaligen SIP Feldmessinstrumenten ebnen.

RADIC, T. (2016), Wie gut sind rechteckförmige Signale für Spektrale IP Messungen geeignet? Poster und Abstract im Tagungsband (ISSN 0344-7251) zur 76. DGG Jahrestagung, Münster.

YANG, Y. et al (2021), Energy distribution and effective components analysis of  $2^n$  sequence pseudo-random signal. DOI: 10.1016/S1003-6326(21)65641-8, ScienceDirect.

## P-S4-07

### Accurate model inference and uncertainty quantification in complex resistivity imaging

J. Hase, A. Kemna

*Institut für Geowissenschaften / Universität Bonn, Geophysik, Bonn*

Induced polarization measurements are a valuable tool for the geoelectric characterization of the subsurface. They are increasingly applied in disciplines across earth sciences. As applications become more quantitative, it is necessary that the applied imaging techniques keep pace with the demand for accuracy and uncertainty quantification. In our work we developed a novel probabilistic framework for the analysis of induced polarization measurements by means of complex resistivity imaging. By using complex probability distributions, the approach accounts for individual errors of real and imaginary data parts, independently regularizes real and imaginary parts of the complex model, and accounts for cross-sensitivities resulting from the complex forward calculation. We show that complex resistivity data, with real and imaginary parts being subject to different errors, can be fitted adequately by a maximum a posteriori (MAP) model, determined efficiently by means of Gauss-Newton optimization, using independent regularization for the conductivity magnitude and phase of the inferred subsurface model. However, due to the non-linearity of the geoelectric forward calculation, the isolated information gained from the estimation of the MAP model is not sufficient to perform an accurate global uncertainty quantification. To overcome the limitations of the inversion by means of Gauss-Newton, we create a representative sample of the posterior model distribution by using Hamiltonian Monte Carlo (HMC) sampling. HMC is a Markov chain Monte Carlo algorithm with the ability to incorporate the sensitivity information available for the complex resistivity imaging problem into an efficient random walk through the model space. The algorithm succeeds in creating a converged sample of the posterior model distribution, as indicated by evaluation of the potential scale reduction factor. The sample allows us to evaluate integral estimators of interest, such as the mean model, correlations between parameters, and the posterior covariance matrix. We instigate the validity of the locally approximated uncertainties, estimated on the basis of the MAP model, by comparing them to the results obtained by HMC. The introduced probabilistic framework and its solutions by means of optimization and HMC sampling provide an improved basis for model inference and uncertainty quantification in the context of complex resistivity imaging.

## P-S4-08

### Spectral Induced Polarization on metallic spheres

K. Breede<sup>1</sup>, D. Kreith<sup>2</sup>, Z. Zhang<sup>3</sup>, M. Bücker<sup>4</sup>, A. Weller<sup>1</sup>

<sup>1</sup>*Institute of Geotechnology and Mineral Resources, Clausthal University of Technology, Clausthal-Zellerfeld,*

<sup>2</sup>*Institute of Geophysics and Extraterrestrial Physics, TU Braunschweig, Braunschweig,*

<sup>3</sup>*Institute of Geotechnology and Mineral Resources, Clausthal University of Technology, Geosciences, Clausthal-Zellerfeld,*

<sup>4</sup>*Institute of Geosciences, University of Kiel, Kiel*

Spectral Induced Polarization measurements were conducted on metallic spheres with varying electrical conductivity of the saturating fluid. We used spheres of stainless steel, copper, brass, and aluminum with a diameter of 12 mm. For each experiment, a single metallic sphere was fixed by a 3D-printed holder in the center of the measurement cell that has been filled by a sodium chloride solution. The complex electrical spectra were recorded

starting with a fluid conductivity of 200 mS/m, which is consecutively reduced in steps of 25 mS/m until a final electrical conductivity of 25 mS/m is reached. Afterwards, the measurements were repeated with increasing fluid conductivity. For 200 mS/m, a distinct phase peak occurs at a frequency of about 200 Hz. As predicted by theory, the peak shifts to lower frequencies with reducing electrolyte conductivity. However, due to redox reactions between the electrolyte and the surfaces of metallic spheres, we observe slight changes in the phase spectra between the first and the repeated measurements. This shift depends on the metal type of the sphere and the staying time of the sphere in the solution. The strongest shifts could be observed for aluminum and brass. Obviously, visible alterations of the surface color of the spheres cause remarkable changes in the spectra of the imaginary part of electrical conductivity. For aluminum a great shift of the peak of the imaginary part of electrical conductivity by a factor of 20 to lower frequencies by comparable phase values could be observed between first and repeated measurements, while for brass, a shift by a factor of about three to higher frequencies and smaller phase values was observed.

## AG – Airborne Geophysics / Fernerkundung

### Vorträge

#### O-AG-01

### **Post-disaster impact assessment over urban environments by fusion of earth observation data**

O. Stein<sup>1</sup>, H. Sudhaus<sup>2</sup>, A. Muhuri<sup>3</sup>

<sup>1</sup>Institut für Geowissenschaften an der Christian-Albrechts-Universität zu Kiel, Aero- und Satellitengeophysik, Kiel,

<sup>2</sup>Karlsruhe Institute of Technology (KIT), Geophysical Institute, Karlsruhe,

<sup>3</sup>Geographisches Institut an der Christian-Albrechts-Universität Kiel, Earth Observation and Modelling, Kiel

Following natural disasters that affect large regions, it is critical to rapidly assess the spatial distribution of damage to identify areas where people are most affected and where assistance is urgently needed. Coherence loss in interferometric synthetic aperture radar (InSAR) data can serve as an effective indicator of damage to buildings and infrastructure. This study focuses on the impact of the February 2023 earthquake in southeastern Turkey, using data from the Sentinel-1 (C-band) and COSMO-SkyMed (X-band) radar missions. We analyze urban areas near the rupture of the particularly the cities of Kahramanmaraş, Osmaniye, and Gaziantep. To create a damage map, the coherence of an interferogram before the event and an interferogram which spans the event is calculated. A significant loss of coherence in the coseismic interferograms indicates substantial change on the ground, which we use as a proxy for damage. However, the relationship between coherence loss and damage is complex and indirect.

In order to refine our interpretation, we incorporate high-resolution optical imagery from the Maxar satellite, building maps, and, where available, damage assessments provided by civil engineers. We also examine how terrain and surface conditions, as well as variations in spatial resolution and radar wavelength, influence the method's accuracy. Specifically, we compare Sentinel-1 data with a spatial resolution of 12 x 14 m to COSMO-SkyMed data, which have a higher resolution of 3 x 3 m.

We observe that, our damage proxy maps, when combined with other data sources, can provide crucial insights for estimating risks to people and infrastructure in the aftermath of a disaster.

## **Efficient Large-Scale 3D Subsurface Imaging Using Semi-Airborne Electromagnetics**

**S. Nazari<sup>1</sup>, R. Rochlitz<sup>1</sup>, A. Thiede<sup>2</sup>, M. Schiffler<sup>3</sup>, C. Walther<sup>4</sup>, A. Steuer<sup>4</sup>, P. Yogeshwar<sup>5</sup>,  
M. Becken<sup>2</sup>, T. Günther<sup>6</sup>**

<sup>1</sup>*LIAG Institute For Applied Geophysics, Hannover,*

<sup>2</sup>*Institute for Geophysics, University of Münster, Münster,*

<sup>3</sup>*Leibniz Institute of Photonic Technology, Jena,*

<sup>4</sup>*Federal Institute for Geosciences and Natural Resources (BGR), Hannover,*

<sup>5</sup>*University of Cologne, Cologne,*

<sup>6</sup>*Technische Universität Bergakademie Freiberg, Freiberg*

Semi-airborne electromagnetic (SAEM) surveying represents an efficient method for deep three-dimensional subsurface imaging as it combines the advantages of fast airborne magnetic field registration with grounded dipoles extended on the surface, exciting strong pulsed currents. The combined inversion of overlapping flight patches (i.e. transmitters with associated flight areas) in one modelling domain is essential to avoid artifacts and to achieve sufficient resolution. Already a limited number of patches allocates large memory resources of high-performance computers (e.g. 3 TB in our case) and leads to runtimes in the range of days. Therefore, methods are needed to efficiently create large scale 3D models by some sort of model segmentation strategy.

We present a new approach as follows:

1. Create one super-mesh including all patches with a target resolution.
2. Run single-patch inversion on each patch to evaluate data quality and consistency.
3. Subdivide patches into super-patches of 2-3 patches depending on overlapping area.
4. Perform inversion of subsets. As an example, Tx5, Tx6 and Tx7 form one subset,  
where Tx' refers to individual transmitters used in specific survey patches.
5. Interpolate results of subsets to super-mesh and combine overlapping results by using a  
coverage-weighted mean of all results.
6. Grow/exchange patches to subsets and invert with starting model interpolated from  
super-mesh.

We applied this new approach to a data set acquired during our 2022 campaign in the western Upper Harz Mountains, covering around 130 km<sup>2</sup> and including 11 flight patches.

Upper Harz Mountains is a region rich in Zn-Pb-(Cu) ores.

Our findings include mapped conductive structures aligned with the known fault strike directions and fault-induced displacements affecting conductive structures. We have identified anomalies that, although not following the mineralization network, correlate with the tectonic and anticlinal axes, indicating possible strata-bound conductors. The alignment of structural features correlates with the orientation of fold axes, and the main faults correlate with local mineralization patterns, emphasizing the role of faulting in the distribution of mineral deposits.

## **O-AG-03**

### **Interferometric radar satellite and in-situ well time-series reveal groundwater extraction rate changes in urban and rural Afghanistan**

**N. Kakar<sup>1</sup>, S. Metzger<sup>2</sup>, T. Schöne<sup>1</sup>, M. Motagh<sup>3</sup>, H. Waizy<sup>4</sup>, N. A. Nasrat<sup>4</sup>, F. Amelung<sup>5</sup>, M. Lazecky<sup>6</sup>, B. Bookhagen<sup>7</sup>**

<sup>1</sup>*GFZ Helmholtz-Zentrum für Geoforschung, Globales Geomonitoring und Schwerefeld, Potsdam,*

<sup>2</sup>*GFZ Helmholtz-Zentrum für Geoforschung, Lithosphärenrendynamik, Potsdam,*

<sup>3</sup>*GFZ Helmholtz-Zentrum für Geoforschung, Fernerkundung und Geoinformatik, Potsdam,*

<sup>4</sup>*Kabul Polytechnic University, Faculty of Geology and Mines, Kabul, Afghanistan,*

<sup>5</sup>*University of Miami, Departement of Marine Geosciences, Miami, United States of America,*

<sup>6</sup>*University of Leeds, COMET, School of Earth and Environment, Leeds, United Kingdom,*

<sup>7</sup>*Universität Potsdam, Fernerkundung und Geomorphologie, Potsdam*

Worldwide, population growth, climate change, and a lack of infrastructure result in increased water demand and unsustainable groundwater exploitation. We present cases of urban and rural Afghanistan, where countrywide 7-yr-long Sentinel-1 radar-interferometric time-series exhibit significant regional subsidence. The cultural centres of Kabul, Ghazni, Helmand, Farah, Baghlan, and Kunduz, for example, subside by more than  $\sim 5 \pm 0.1$  cm/yr. Of particular focus to us were Kabul capital city and the growing agricultural sector of rural Ghazni. In Kabul, we compared spatiotemporal subsidence patterns to water table heights and precipitation. In Ghazni, we monitored the transition from ancient to modern irrigation techniques by mapping solar-panel arrays as a proxy for electrical water pumping and by evaluating the vegetation index as a proxy for agricultural activity. In Kabul, ground subsidence is largest near the city center with a 6-yr total of  $31.2 \pm 0.5$  cm, but it's the peripheral wells of the Kabul basin that exhibit highest water-table drops. In Ghazni, with a 7-yr total of  $77.8 \pm 0.5$  cm of subsidence, the rates are dramatically accelerating since 2018, when barren land was transformed into farmland at great extent and traditional irrigation was replaced by electrical water pumps to tap groundwater. As a result, m-wide and km-long desiccation cracks appeared in the area with the highest irrigation volume and subsidence. These dramatic cases present only a fraction of similar processes all around the world.

## **AG – Airborne Geophysics / Fernerkundung**

### **Poster**

## **P-AG-01**

### **Semi-Airborne Electromagnetic Survey for Deep Structural Mapping in a Complex Geological Setting**

**M. Bayat<sup>1</sup>, T. Günther<sup>2</sup>, S. Nazari<sup>1</sup>, M. Ronczka<sup>1</sup>**

<sup>1</sup>*LIAG Institute for Applied Geophysics, Hannover,*

<sup>2</sup>*TU Bergakademie Freiberg, Institut für Geophysik und Geoinformatik, Freiberg*

In the framework of the GeoMetEr project, aimed at assessing the suitability and informative value of various geophysical methods, including Electromagnetics (EM), we conducted a semi-airborne EM (SAEM) survey in Lower Saxony. The surveys utilized long grounded transmitters and airborne receiver instruments, carried by a helicopter and drone, including induction coil magnetometers and SQUID sensors, combining the strengths of ground-based and airborne techniques. Given the limited investigation depth of purely airborne methods and

local-scale electrical resistivity tomography (ERT), SAEM was employed to explore deeper structures within the study area, located at the north of Schneeberg. The area features multiple fractures with varying orientations, dominated by the Roter Kamm fault zone—a normal fault with observed thicknesses up to 100 m and a documented dip of 65–70° NE.

The inversion has been done using custEM and pyGIMLI software packages. Preliminary inversion results identified resistivity anomalies aligning with the expected location of the Roter Kamm fault, despite challenges posed by noise sources such as a power line, a railway, and buried infrastructures.

These findings validate the potential of the inversion method for resolving fault zones at greater depths compared to conventional pure airborne and ERT techniques. Additionally, the inversion tool demonstrated strong capability in managing complex survey geometries and enhancing interpretation accuracy. This study contributes to a deeper understanding of the Roter Kamm fault zone, refining the regional geological model by providing updated insights into the fault's geometry, and resistivity properties.

## BL – Wissenschaftliches Bohren / Logging / Gesteins- und Mineralphysik

### Poster

#### P-BL-01

### Physical Properties of Rock Cuttings vs. Borehole Data: An Overview of Ongoing Research

A. Serje Gutierrez<sup>1</sup>, M. Balcewicz<sup>1</sup>, E. H. Saenger<sup>1,2,3</sup>

<sup>1</sup>Bochum University of Applied Sciences, Bochum,

<sup>2</sup>Fraunhofer Research Institution for Energy Infrastructures and Geothermal Systems IEG, Bochum,

<sup>3</sup>Ruhr University Bochum, Bochum

Over the past few years, several scientific projects at Bochum University of Applied Sciences have developed new methods and procedures for determining the petrophysical properties of small rock samples. These workflows, which are part of Digital Rock Physics (DRP) and have been published in peer-reviewed journals, are based on the non-destructive testing of samples using X-ray computed tomography.

After the subsequent semi-automated segmentation - i.e. the identification of the pore space and different minerals in the 3D scan - the thermophysical, hydraulic and mechanical properties of the rock sample relevant for geothermal projects are calculated using numerical methods. The method can be applied to cuttings (drill cuttings produced during the drilling process). The method thus offers the possibility of determining the relevant rock parameters over the entire drilling section and without the use of expensive core drilling methods, which can save costs on one hand and significantly improve the database for the subsequent numerical simulation of the geothermal plant on the other.

We present the first results of the ongoing SimBoL-project. A selection of Carbonate cuttings were scanned with a high-resolution CT device. Those digital images were transformed into digital rock samples which are the basis of numerical simulations to determine the permeability, the heat conductivity and the mechanical rock properties. A first qualitative comparison with borehole data is presented.

## **Permittivity Determination of Rock Cuttings: An Overview of Ongoing Research**

**N. Kerkmann<sup>1,2</sup>, M. Siegert<sup>3</sup>, N.-A. Kouamo Keutchafo<sup>3</sup>, E. H. Saenger<sup>1,2,3</sup>**

<sup>1</sup>*Fraunhofer IEG, Bochum,*

<sup>2</sup>*Ruhr University Bochum, Bochum,*

<sup>3</sup>*Bochum University of Applied Sciences, Bochum*

As part of the European-funded GeoHEAT project, new methods for geothermal target prospecting are to be established, including a georadar probe to characterize geological structures. For the effective use of said probe, an accurate determination of the relative permittivity of the surrounding rock mass is of great importance. To make this process more time and cost efficient, we are investigating the possibility of quantifying this dielectric property using digital rock physics (DRP) and rock cuttings. Since the latter are produced as a by-product of exploratory drilling and therefore do not constitute an additional expense for the acquisition of samples. Here we want to present our latest developments and the current state of work.

For the numerical computation of the desired property, a sample is first scanned using computed tomography (CT). These images are then segmented by assigning different phases to the gray-scale intensities of the scanned sample. Afterwards, physical properties are assigned to individual material particles in the location-dependent volume. This pore-scale model can then be used to calculate the relative permittivity using a numerical solving algorithm. To optimize this approach, standardized cylindrical core samples are segmented. This involves the use of granite rock from the Bedretto Lab facilities located in Switzerland. To ensure the accuracy of the numerical estimates, the results are validated against laboratory measurements of the same rock type.

The acquisition of core samples is expensive, requires interruption of drilling and samples can only be taken for limited boreholes and depth sections. However, drilling usually produces cuttings that are transported to the surface with the drilling mud. In the next step, we therefore investigate the possibility of using these cuttings to determine the relative permittivity. We examine to what extent the accuracy of the results obtained suffers under this cost- and time-saving approach.

Preliminary results from the analysis of core samples show promising accuracy in estimating relative permittivity values using DRP. Investigating the use of rock cuttings as a substitute for cores represents a potential breakthrough in minimizing cost and time while ensuring reliable data. The results of our research could significantly improve the practical application of georadar probes and lead to more efficient geothermal exploration and a better understanding of the geology of the subsurface.

## P-BL-03

### Borehole-scale geothermal reservoir characterisation of structures and rock properties for the development of a geothermal-grade georadar tool.

M. Chatziliadou<sup>1</sup>, A. Shakas<sup>2</sup>

<sup>1</sup>Fraunhofer IEG, Reservoir Geophysics, Bochum,

<sup>2</sup>ETH Zürich, Department of Earth and Planetary Sciences, Zürich, Switzerland

High exploration costs are one of the main issues hindering more widespread installation of deep geothermal energy. To minimise pre-drilling exploration costs and maximise learning rates from exploratory drilling, a novel georadar probe will be developed in the EU-funded GeoHeat project. The aim of this probe is to operate under high temperature (up to 200 °C) and pressure (700 bar) conditions to allow its deployment in geothermal boreholes for a wide range of deep geological settings. To optimally analyse the results from the probe, it will be complemented with acoustic televiewer (ATV), digital rock physics models and drilling-induced micro-seismicity. This enables the characterisation up to 100 m around the borehole and will constrain a 3D fracture network model along with the permeability and seismic susceptibility of individual fractures.

In the upcoming years, we will work on the integration of the borehole scale evaluation of rock properties and structures. ATV logging is performed for geological structure mapping (e.g., fractures, bedding, lithologic contacts, foliation), characterising thin bedding, joints and fractures, mapping fracture depth and orientation, mapping rock units and contacts and determining stress field properties and orientations. X-ray diffraction (XRD) and X-ray fluorescence (XRF) analysis on cuttings and core samples are performed to obtain qualitative and quantitative elemental and mineral phase compositions. Transmitted-light microscopy on thin sections from cuttings and petrographical descriptions of the lithology are performed. The results will be calibrated and validated with XRD and XRF and available logs from different geothermal wells. Based on those results, a lithological and mineralogical description of the geothermal reservoir stratigraphy will be provided. These results serve as quality control to calibrate and extend the data from georadar, ATV and digital rock physics.

Here, we will present the planned strategy and first insights into the possible information gain from this multiscale integration. Ultimately, the final georadar-imaged fracture network model will contribute to reservoir performance and georisk assessment at new resolutions, inform statistical seismic risk models for long-term seismicity forecasting, and investigate promising borehole deviations and future placements that maximise the resource's productivity while minimizing risk.

## P-BL-04

### Current Status of a Geological Segmentation for Rotondo Granite

N.-A. Kouamo Keutchafo<sup>1</sup>, M. Balcewicz<sup>1</sup>, M. Siegert<sup>1</sup>, E. H. Saenger<sup>1,2,3</sup>

<sup>1</sup>Bochum University of Applied Sciences, Bochum,

<sup>2</sup>Fraunhofer Research Institution for Energy Infrastructures and Geothermal Systems IEG, Bochum,

<sup>3</sup>Ruhr University Bochum, Bochum

Digital Rock Physics (DRP) and its use of non-destructive methods have rapidly emerged as a potentially valuable source for advancing the fundamental understanding of geological formations. By contributing to the accurate characterization of reservoir properties and physical processes at the microstructural level, DRP can play a significant role in monitoring seismic hazards by providing physical characterizations of e.g., stressed, saturated, or fractured rocks at the pore scale.

The fundamental principle of DRP is „image-and-compute“, implemented through a structured five-step workflow. The process begins with the preparation of a high-resolution X-ray computed tomography image, followed by the tomographic reconstruction of the image by simple back-propagation techniques. It continues with the assessment and handling of artifacts, prior to the segmentation of individual phases. The final stage consists of solving physical equations to compute the desired properties, like thermal conductivity, permeability, and elastic properties.

A major challenge within this workflow lies in image segmentation, which assigns different phases to a gray-scale image, a critical step that profoundly influences subsequent analyses. Over the years, various segmentation techniques have been developed, ranging from global thresholding and local-adaptive methods to machine-learning or deep-learning-based segmentation methods. However, most studies rely on binary segmentation, simplifying rock samples into just two phases: pore and solid. This suboptimal approach neglects the complexity of the mineral phase in multiphase rock samples, thereby limiting the accuracy of property predictions or simulations.

This study presents a true geological segmentation process that enables multiphase segmentation by accounting for every distinct phase within a granitic reservoir sample. This method provides a robust and detailed representation of the rock's microstructure in a 3D volume, leading to significantly improved simulations of petrophysical properties. By enhancing segmentation accuracy, this geological-based approach represents an important step towards more precise geothermal reservoir assessments, contributing to sustainable energy solutions.

**Keywords:** Digital Rock Physics, Granite, Multiphase Segmentation, Petrophysical Properties, Geothermal Reservoir.

## **P-BL-05**

### **Modification of the SDR equation for permeability prediction**

**Z. Zhang, A. Weller**

*Technische Universität Clausthal, Clausthal-Zellerfeld*

Permeability prediction for reservoir rocks is still a challenge in geophysical exploration. Porosity and pore radius are the most relevant parameters used in models of permeability prediction. A variety of petrophysical experiments or logging tools provide reliable porosity values. The effective hydraulic radius  $r_{\text{eff}}$  controls the fluid flow through porous rocks with a certain pore radius distribution.

Nuclear magnetic resonance (NMR) relaxometry provides an estimate of porosity and a relaxation time distribution. The maximum or mean values of the relaxation time distribution are regarded as proxies for the effective hydraulic radius. The original Schlumberger-Doll Research (SDR) equation relates the weighted geometric mean of the transverse relaxation time and porosity to permeability. In the common form of SDR equation, the relaxation time is raised to the 2nd power and porosity to the 4th power.

We investigate the relationships between different characteristic relaxation times and  $r_{\text{eff}}$ . The weighted geometric mean, the weighted arithmetic mean and the weighted harmonic mean are tested for data from three different sandstone formations from Egypt, to see whether the different characteristic pore radii can be used as suitable proxies for  $r_{\text{eff}}$ .

In a further modification of the SDR equation, we replace the characteristic relaxation time by a characteristic pore radius. The best results are achieved with weighted harmonic mean that

proves to be a reliable proxy for the effective hydraulic radius. However, the transformation of relaxation time into pore radius requires the knowledge of the specific surface area for each sample to determine an individual value of surface relaxivity. We confirm the potential of the SDR equation in NMR applications. A careful calibration of the equation with suitable values for the prefactor and exponents will contribute to an improved permeability prediction.

## P-BL-06

### Influence of mineralogy and microstructure on the electrical properties of crustal rocks: insights from the DIVE Project in the Ivrea-Verbano Zone

H. Mansouri<sup>1,2</sup>, S. Tholen<sup>1</sup>, V. Toy<sup>1</sup>, F. Hawemann<sup>1</sup>

<sup>1</sup>Johannes Gutenberg-Universität Mainz,

<sup>2</sup>Ruhr-Universität Bochum, Institut für Geologie, Mineralogie und Geophysik, Bochum

Geophysical electrical surveys potentially offer valuable information on the distribution of fluids and economically important (semi-)conductive like graphite and sulfides, and tectonic processes. However, further advances in electrical imaging of rocks at depth are hindered by the lack of understanding of the relative contributions of paragenesis, fabric, and active processes to electrical conductivity, and lack of accurate measurements of relevant geological materials. The ICDP project DIVE (Drilling the Ivrea-Verbano ZonE) provides a unique opportunity to evaluate these parameters by combining samples and measurements from up to ~1 km depth with a wide range of geophysical surface surveys. The first 580 m deep DIVE drill core comprises lower crustal rocks consisting of metasediments (the so-called Kinzigites), calc-silicates and amphibolites with pegmatitic lenses. We collected 25 samples from these main lithologies to analyze fabric characteristics (e.g., foliation, grain size) and conductive phases using microscopy and computed tomography (CT). With impedance spectroscopy we then investigated the electrical properties of 15 samples of the main lithologies.

The electrical properties of these samples were measured under both dry and brine-saturated conditions (with salinities of 0.1 to 1 molarity) across a broad frequency range. Formation factor showed a weak relationship with porosity, indicating that conductivity variations are primarily controlled by sulfide and graphite content and their connections through saturated fluids, foliation, or microcracks. Overall, our measurements suggest the presence of graphite and sulfides in combination with either the presence of fracture networks or a strong foliation could explain electrical anomalies observed in the Ivrea-Verbano Zone.

## P-BL-07

### Fracture network characterization by structural geological analysis and periodic pumping tests in borehole SB1.1 of the Bedretto Underground Laboratory for Geosciences and Geoenergies, Switzerland

F. Karim, S. Edem, S. Danaei, J. Renner

Ruhr-Universität Bochum, Institut für Geologie, Mineralogie und Geophysik, Bochum

Enhanced Geothermal Systems (EGS) have gained significant attention in Europe in recent years as a response to climate change and the energy crisis. Fracture characterization within crystalline rocks is crucial for understanding EGS performance. This study presents the progress of research regarding structural analyses and periodic pumping tests (PPT) in the Bedretto Underground Laboratory for Geosciences and Geoenergies (BULGG), Switzerland. We combine structural geological measurements in the tunnel and log analysis for four vertical boreholes SB 1.1, 2.1, 3.1, and 4.1. Fracture sets trending NE-SW are dominant around SB 1.1, but absent in the other boreholes, where sets with NW-SE orientation, i.e., parallel to the tun-

nel, and N-S are prevalent. In each of the four boreholes, several fractures were induced during a previous hydro-fracturing campaign (Bröker and Ma, 2022). We performed a stress analysis on the traces of these induced fractures, which confirmed that the stress regime is predominately strike-slip but also suggests that the vertical stress is not strictly a principal stress. Extensive periodic pumping tests were performed in SB1.1 using a multi-packer probe allowing to target natural and induced fractures. We applied harmonic and square oscillations of injection and production flow rates with a range of periods from 100 to 100,000 s and different mean flow rates and flow-rate amplitudes. The protocols aim at constraining the hydro-mechanical properties of individual fractures and the fracture network surrounding SB1.1.

Bröker, K., Ma, X., 2022. Estimating the Least Principal Stress in a Granitic Rock Mass: Systematic Mini-Frac Tests and Elaborated Pressure Transient Analysis. *Rock Mech Rock Eng* 55, 1931–1954. <https://doi.org/10.1007/s00603-021-02743-1>

## P-BL-08

### Fracture detection on acoustic borehole televIEWer images: Exploring various image processing approaches

S. Danaei, J. Renner

*Ruhr-Universität Bochum, Institut für Geologie, Mineralogie und Geophysik, Bochum*

Geothermal systems play a crucial role in the energy transition, an alternative to conventional hydrocarbon combustion, as they can provide a renewable and environmentally sustainable source of energy. Hydraulic fracturing may enhance the efficiency of geothermal systems by inducing fractures around injectors. Monitoring the fracture process during hydraulic fracturing could provide necessary information to guide these operations. For this purpose, acoustic borehole televIEWers are commonly used because they capture high-resolution images of the borehole wall. In this work, we present a workflow to constrain the fracture process using borehole image logs obtained before and after the hydraulic fracturing operation. Our workflow starts by identifying pre-existing (natural) fractures from image logs before hydraulic fracturing. On the one hand, we explore different filter techniques on the images gained after the fracturing to enhance the detectability of induced fracture traces. On the other hand, we correct method-related contortions between the two sets of images, i.e., before and after stimulation, to allow for image subtraction. Ideally, the difference between the two images should produce the traces of the induced fracture. The developed techniques are applied to logs from two sites, the Reiche Zeche mine, Freiberg (Germany), and the Bedretto Underground Laboratory for Geosciences and Geoenergies (Switzerland). Our results indicate that all image processing filters enhance the detectability of pre existing fractures. Image subtraction is feasible and the difference images of before and after logs can serve as basis for fracture detection. The workflow presented will be integrated into the logging-while pumping concept followed in the DoPaTV project, funded by BMWK.

#### O-GD-01

#### **The role of proto-thrusts in strain accumulation along the segmented deformation front at the northern Cascadia subduction zone, Canada**

**W. Schäfer, M. Riedel, G. Crutchley, H. Kopp**

*GEOMAR Helmholtz-Zentrum für Ozeanforschung Kiel, Dynamik des Ozeanbodens - Marine Geodynamik, Kiel*

Earthquakes at subduction zones are among the most dangerous on Earth. This study focuses on the Cascadia continental margin off the west coast of Canada, where the oceanic Juan de Fuca plate subducts beneath the continental North American plate. This region is one of the areas of the world where a major subduction earthquake is expected in the foreseeable future. The last major earthquake occurred in 1700 A.D. as confirmed by records of a tsunami in Japan, over 7000 km away on the other side of the Pacific.

With this study we aim to determine the nature of upper plate compaction along the fragmented deformation front off Vancouver Island, focusing on the development of proto-thrusts (PT). Our database consists of high-resolution multichannel seismic (MCS) reflection data and coincident echosounder profiles acquired during the SO294 cruise of RV SONNE in 2022, as well as vintage MCS data.

We present the first systematic investigation of PTs on the northern Cascadia margin. The use of data spanning a wide frequency spectrum enables PTs to be imaged over their entire depth range from oceanic crust to the seafloor. Our high-frequency data enable fault offsets as small as 0.5 m to be resolved in the upper-most sedimentary record, thus yielding a broad representation of PT occurrence.

The data reveal a correlation between the characteristics of PTs and the vergence of the main frontal thrust of the accretionary prism. In the case of a landward verging main frontal thrust, the PT-zone is widest and PTs are of mixed vergence. In contrast, if the main frontal thrust is seaward verging, PTs are sparse and predominantly seaward verging.

Significant compaction from lateral compression seaward of the deformation front is recognized from velocity analyses of vintage MCS data in regions associated with PT development. A North-to-South intensification in this compaction-related velocity increase is observed, from ~15% up to a maximum of ~30%.

We also observe similar networks of PTs landward of the main frontal thrust. Their contribution to total shortening within the prism remains unknown, as well as the question of whether they are still active.

The effective combined shortening by PTs and lateral pore space compaction will be used in refining the regional geo-hazard model that currently overlooks these processes.

## **O-GD-02**

### **2-D Crustal Modelling of the Mérida Andes - Venezuela Using Wide-Angle Seismic and Gravity Data**

**L. A. Yegres Herrera<sup>1</sup>, M. Schmitz<sup>2</sup>, J. Ávila-García<sup>3</sup>, F. Rondón<sup>4</sup>, A. GIAME Seismic Working Group<sup>4</sup>**

<sup>1</sup>*CICESE, Sismología, Ensenada, Mexico,*

<sup>2</sup>*Universidad Central de Venezuela, Departamento de Geofísica, Caracas, Venezuela, 3UNAM,*

*Instituto de Geofísica, Ciudad de México, Mexico,*

<sup>4</sup>*FUNVISIS, Departamento de Geofísica, Caracas, Venezuela*

The Mérida Andes (MA) exemplify a key orogenic system formed by the tectonic interplay between the Caribbean and South American plates, marking the western boundary of the Maracaibo block, and the northern end of the North Andean Block. To elucidate the geodynamic processes shaping this region, we integrated wide-angle seismic and gravity data along a 380-kilometer profile crossing the MA from the Falcón basin to the Barinas-Apure basin. Seismic data from 11 controlled explosive sources, recorded by 480 Texan devices, revealed significant crustal variations. PmP reflections delineate a Moho discontinuity deepening from 29 km in the Falcón basin to a maximum of 53 km beneath the orogen, with a pronounced asymmetry of the crustal root displaced 10 km northwest of the topographic crest. Complementary gravity data, including 325 field measurements with GNSS-precision, were incorporated into high-resolution 2D forward models to constrain the density structure. Velocity and density models delineate five crustal layers reflecting the tectonic evolution of the region: surface Cenozoic sediments ( $V_p$ : 2–4 km/s), deeper Cretaceous sediments ( $V_p$ : 4–5 km/s), crystalline basement ( $V_p$ : 5.5–6.3 km/s, density: 2.78 g/cm<sup>3</sup>), lower crust ( $V_p$ : 6.5–7 km/s, density: 2.84 g/cm<sup>3</sup>), and lithospheric mantle ( $V_p$ : >7.7 km/s, density: 3.22 g/cm<sup>3</sup>). The results suggest an incipient type-A subduction of South America beneath the Maracaibo block, driven by the orogenic load of the MA and sedimentary dynamics in adjacent basins. This study highlights the integration of seismic and gravity data to unravel crustal-scale processes and offers new insights into the tectonophysics of active orogenic belts, with implications for understanding lithospheric deformation and plate interactions in complex geological settings.

## **O-GD-03**

### **Seismic Sequences in the Western Peloponnese: Unveiling Active Deformation Within and Beyond the Aegean microplate**

**D. Essing, G. M. Bocchini, M. P. Roth, R. M. Harrington**

*Ruhr-Uni Bochum, Bochum*

West of the Peloponnese, the Hellenic subduction system transitions from oceanic-continent to continent-continent collision resulting in a complex tectonic environment with a mix of thrust and strike-slip deformation. Extensional deformation inferred by earthquakes with normal-faulting mechanisms in the crust of the Aegean microplate adds additional complexity to the seismotectonic processes in the broader region. Part of the elastic energy release occurs seismically, resulting in frequent  $M>5$  earthquakes, occasionally with complex aftershock sequences. New geological and geodetic observations suggest that additional aseismic deformation occurs in the overriding plate, while a recent study provides evidence for significant aseismic deformation at the interface between the overriding and the subducting plate. Here we present new observations of seismic sequences in the western Peloponnese

and investigate their evolution in space, time, and size to interpret driving mechanisms. Specifically, we quantify their spatiotemporal distribution to investigate the consistency of fluid-diffusion as a driving mechanism, or test whether alternative deformation mechanisms need to be invoked.

We make use of a joint seismic network to build a high-resolution earthquake catalog. We will present several notable seismic sequences detailed with the new high-resolution catalog, including details of their spatial organization, spatiotemporal evolution, and statistical properties. Our set of qualitative and quantitative observations offer preliminary evidence of migration patterns consistent with aseismic-slip triggering in the Aegean microplate at shallow depths <10 km. Additionally, we offer a preliminary discussion of potential driving mechanisms behind other sequences, contributing to a better understanding of the deformation processes active in the region.

Our catalog is derived from a joint network that combines new data from eight broadband stations deployed by Ruhr University Bochum with 25 permanent seismic stations from the University of Patras, the National Observatory of Athens, and four temporary Adria Array stations. The unprecedented station density with interstation distances as small as 15 km and our automated workflow allows for a catalog that consists of ~20,000 events and a  $M_c \sim 1$  for the period from December 2023 to September 2024.

## GO / OS – Geophysik in der Öffentlichkeit und im Wandel der Zeit / Open Source in Forschung und Lehre

### Vorträge

#### O-GO/OS-01

#### Ist Isaac Newtons PRINCIPIA von 1687 auch eine Methodologie der heutigen Geophysik?

J. Fertig

Geophysik, Burgwedel

Im Vorwort zur *Principia [Philosophiae Naturalis Principia Mathematica]* richtet sich Newton an den Leser: „...Die gesamte Schwierigkeit der Physik scheint darin zu liegen, dass wir die Kräfte aus den „phaenominis“ der Bewegung aufspüren müssen und anschließend aus diesen Kräften die übrigen Naturerscheinungen herleiten müssen...“

So stellt Newton zunächst die Gesetze und Regeln auf, mit denen er später die gesicherten Beobachtungen erläutern und deren Ursachen mit seinem Gesetz der Schwere am Himmel und auf der Erde und deren Beziehungen untereinander erklären will. So ist für die Existenz einer allgemeinen Zentripetalkraft der Flächensatz notwendig. Die Form des Kraftgesetzes  $f(r)$  ergibt sich aus der Abhängigkeit vom mittleren Abstand  $a$  und Umlaufzeit  $T$  bei einer geschlossenen Bahn; für das  $1/r^2$ -Gesetz gilt das Verhältnis  $T^2 \sim a^3$  und umgekehrt. Diese Gesetz garantiert mit vorgegebenen Anfangswerten die Existenz von Kegelschnitten als Bahnkurven. Für eine in der Ebene elliptische Bahn, die nicht geschlossen ist, kann die Potenz im Abstandsgesetz modifiziert werden oder dieses durch eine Zusatzkraft ergänzt werden, um so das Bahnverhalten zu erklären. Newton versucht anders als Kepler, der vom Einkörperproblem ausgeht, über das Dreikörper-Problem im „merkwürdigen“ aber schwierigen Lehrsatz Nr. 66 in der *Principia* die Phänomene am Himmel und auf der Erde zu erklären. Dies gelingt ihm im Ansatz für die schwierige Bewegung des Mondes mit dessen *Variation*, der Drehung

der Apsiden der Planetenbahnen in ihren Bahnebenen und der Ableitung der gezeiten-erzeugenden Kräfte; und dies vorzugsweise allein mit geometrischen Mitteln! Insgesamt liefert Newton m.E. im auch eine **Methodologie** in der **Geophysik** wie sie im Studienführer von J. Bartels (1944) für die Geophysik als Aufgabe definiert wird: „*Die Geophysik erforscht die natürlichen physikalischen Erscheinungen auf der Erde, einschließlich der Wirkungen und Einflüssen, die von anderen Weltkörpern, insbesondere von der Sonne und vom Mond auf die Erde ausgeübt werden...*“

## O-GO/OS-02

### **20 Jahre nach der Tsunami-Katastrophe im Indischen Ozean – Was haben wir gelernt?**

A. Rudloff<sup>1</sup>, J. Lauterjung<sup>1</sup>, A. Babeyko<sup>1</sup>, A. Strollo<sup>1</sup>, F. Tilmann<sup>1,2</sup>

<sup>1</sup>GFZ Helmholtz-Zentrum für Geoforschung, Potsdam,

<sup>2</sup>Freie Universität Berlin, Institut für Geologische Wissenschaften, Berlin

Der zweite Weihnachtsfeiertag 2024 war der zwanzigste Jahrestag einer der größten Naturkatastrophen: der so genannte „Boxing Day Tsunami“ kostete fast 230.000 Menschen um den ganzen Indischen Ozean das Leben. Ursache war ein Megabeben vor der Nordküste Sumatras, welches den Meeresboden über 1.000 Kilometer bewegte. Mit einer Magnitude von 9,3 zählt es bis heute zu den stärksten je gemessenen Erdbeben weltweit.

Die globale Anteilnahme war angesichts des Ausmaßes und der Wirkung der Bilder enorm. Binnen einer Woche nach dem Ereignis bereiteten Forschende des GFZ, zusammen mit Kolleg:innen aus anderen Einrichtungen, ein Konzept für ein Frühwarnsystem vor, um das Ausmaß solcher Katastrophen künftig zu beschränken. Dieses wurde noch im Januar 2005 von der Bundesregierung bewilligt. Bis dahin hatte es lediglich im Pazifik Tsunami-Frühwarnsysteme von Japan und den USA gegeben.

Prinzipiell ist eine positive Bilanz des Einsatzes des Indonesischen Tsunami-Frühwarnsystems zu ziehen: Seit dem Ersteinsatz 2007 wurden mehrere Tausend Erdbeben analysiert und vor zahlreichen Tsunami erfolgreich gewarnt. Aber es gab auch einzelne Fehlschläge. Hier zeigte sich die Bedeutung von nicht-seismischen Quellen sowie der sogenannten letzten Meile.

Maßgeblich für den Erfolg war auch die Koordinierung durch die UNESCO ab 2005 mit diversen Arbeitsgruppen und Gremien, die zu Frühwarn- und Schutzprogrammen in der ganzen Welt geführt haben. Die Wissenschafts- und Kulturorganisation der Vereinten Nationen sorgt dafür, dass sich potenziell gefährdete Gemeinschaften und Regionen auf Tsunamivorwarnungen vorbereiten, indem sie Evakuierungen trainieren, Indigenes Wissen nutzen, Wissenstransfer z.B. in Schulen durchführen, etc.

Auch für den Wissens- und Technologietransfer kann eine positive Bilanz gezogen werden: Die maßgeblich vom GFZ entwickelte seismische Monitoring-Software „SeisComP“ wird seit 2009 sehr erfolgreich von der ausgründeten Firma gempa weiterentwickelt. Die Software wurde außerdem in viele der seither entwickelten Tsunami-Frühwarnsysteme übernommen.

Als übergeordnetes Ziel bleibt eine weitere Verbesserung der Tsunami-Frühwarnung, insbesondere auch für nicht-seismische Auslöser wie z.B. Hangrutschungen oder vulkanische Aktivität. Dies gilt sowohl für den Indischen Ozean, als auch für die Mittelmeerregion, wo das GFZ ebenfalls bereits seit 2005 engagiert ist.

## **EPOS – The European Plate Observing System and flagship projects Geo-INQUIRE and DT-GEO: opportunities for building communities and promoting openness in geoscience data**

**F. Tilmann<sup>1</sup>, F. Cotton<sup>1</sup>, A. Strollo<sup>1</sup>, A. Babeyko<sup>1</sup>, J. Quinteros<sup>1</sup>, A. Gabriel<sup>2,3</sup>,  
H. Igel<sup>2</sup>, C. Hadzioannou<sup>4</sup>**

<sup>1</sup>*GFZ Helmholtz-Zentrum für Geoforschung, Potsdam,*

<sup>2</sup>*Ludwig-Maximilians-Universität München, Department für Geo- und Umweltwissenschaften,  
München,*

<sup>3</sup>*UC San Diego, Scrippp Institution of Oceanography, La Jolla, United States of America,*

<sup>4</sup>*Universität Hamburg, Fachbereich Erdsystemwissenschaften, Hamburg*

EPOS is a European infrastructure consortium designed to integrate geoscientific data under FAIR principles. Its origins trace back over 20 years, building on successful data integration initiatives primarily in seismology through ORFEUS and EMSC. Approval for inclusion in the European roadmap EPOS in 2008 paved the way for significant funding through the EPOS Preparatory, Implementation and Sustainability Phase projects, which served to build its communities, software tools and governance. EPOS, formally founded as a European Research Infrastructure Consortium (ERIC) in 2018, remains the only ERIC in solid Earth geosciences. After a pilot phase, it became fully operational in 2023, offering access to diverse datasets (>800 TB), and nearly 300 services from hundreds of providers via its dedicated portal and thematic services. Currently, EPOS includes 19 member countries, with Germany participating as observer.

Arguably, the most significant impact has been to galvanise diverse communities for data sharing. Organised within *Thematic Core Services*, they include geomagnetic observatories, near-fault observatories, geological information & modelling, multi-scale laboratories, volcano observatories, satellite data, GNSS, anthropogenic hazards, tsunamis, and seismology. Some long-running frameworks, such as ORFEUS-EIDA (European Integrated Data Archive) in seismology, are now integrated into EPOS and have benefited enormously from the related projects. In other communities, e.g., near-fault observatories and multi-scale laboratories, unified data standards and open data sets were only enabled through EPOS.

Integration with ERICs is now mandatory in Horizon Europe infrastructure calls. Two flagship projects are Geo-INQUIRE, which opens up new geophysical datasets, workflows and software and provides training and transnational access to many key sites, and DT-Geo (Digital Twins for Geophysical Extremes), which integrates supercomputing and large scientific data sets for geophysical hazard analysis (earthquakes, tsunami, volcanoes). While German contributions to these projects are diverse, the presentation will focus on the development of standards and tools for sharing DAS data for traditional and cloud-computing workflows within the EIDA framework and in cooperation with Earthscope, and on the integration of physics-based simulations with empirical ground motion observations in providing multi-frequency assessment of expected accelerations in future earthquakes.

## GO / OS – Geophysik in der Öffentlichkeit und im Wandel der Zeit / Open Source in Forschung und Lehre

### Poster

#### P-GO-01

### Mit Raspberry-Pi Magnetometer junge Menschen früh für die Geowissenschaften begeistern

J. Dielmann, A. Busse, A. Grayver, A. Wennmacher, R. Bergers

*Institut für Geophysik und Meteorologie, University of Cologne, Köln*

Die Zukunft der Naturwissenschaften liegt in der Inspiration junger Menschen. Um das Interesse an diesen Disziplinen zu wecken, wurde das Projekt „*Magnetische Observatorien in Schulen*“ ins Leben gerufen.

Im Mittelpunkt dieses Projekts steht ein kostengünstiges und dennoch präzises 3-Komponenten-Magnetometer, dessen Sensoren in einem 3-D gedruckten Gehäuse montiert sind und welches von einem Raspberry-Pi gesteuert wird. Ein Python-Programm ermöglicht es, geomagnetische Stürme sowie Schwankungen im Erdmagnetfeld die durch Weltraumwetterereignisse verursacht werden, zu messen und darzustellen.

Seit April 2024 ist eines dieser Magnetometer im Einsatz am seismischen Observatorium in Bensberg, NRW, und zeichnet dort kontinuierlich Daten auf. Diese Daten werden mit denen von magnetischen Observatorien in Deutschland verglichen, um die Genauigkeit und Zuverlässigkeit des Systems zu validieren.

Das Projekt hat das Ziel, Schülerinnen und Schüler der Jahrgangsstufen 8 bis 13 für die Naturwissenschaften zu begeistern und ihnen die faszinierende Welt der Geophysik durch praktische Experimente und reale Anwendungen näherzubringen.

In Zusammenarbeit mit den Lehrkräften wird eine passende Herangehensweise entwickelt, um diese wissenschaftlichen Konzepte verständlich und spannend zu vermitteln. Das übergeordnete Ziel ist es, den Schülerinnen und Schülern die Funktionsweise eines Magnetometers und dessen Bedeutung in der Geophysik näherzubringen und eine neue Generation von jungen Wissenschaftlerinnen und Wissenschaftlern zu fördern.

#### P-GO-02

### Aufbau eines Raspberry-Shake-Seismometernetzwerkes an Schulen in Sachsen

O. Hellwig, S. Buske

*Institut für Geophysik und Geoinformatik / TU Bergakademie Freiberg, Freiberg*

Seit Herbst 2023 baut das Institut für Geophysik und Geoinformatik der TU Bergakademie Freiberg ein Netzwerk bestehend aus Raspberry-Shake-Erschütterungssensoren an Schulen auf. Mittlerweile umfasst das Netzwerk ca. 30 Stationen an sächsischen Schulen und eine Station im benachbarten Thüringen. Über die Online-Nutzeroberfläche unter dem Link <https://stationview.raspberryshake.org> besteht nahezu in Echtzeit Zugriff auf die Daten des Netzwerks sowie von mehr als 2500 weiteren, weltweit verteilten Stationen. Die Nutzeroberfläche stellt darüber hinaus einfach zu bedienende Datenbearbeitungs- und Analysewerkzeuge sowie Informationen zu aktuellen Erdbeben weltweit zur Verfügung. Somit ergibt sich

die Möglichkeit, das Seismometernetz und die damit gewonnenen Daten unkompliziert in den naturwissenschaftlichen Unterricht einzubinden und junge Menschen für diese Thematik zu begeistern. Die Messgeräte an den Schulen registrieren nicht nur die Erschütterungen, die durch den Schulbetrieb verursacht werden. Vor allem während der Nachtstunden, an Wochenenden und in der Ferienzeit sind auch stärkere, weltweit auftretende Erdbeben leicht zu erkennen, wie z.B. das Beben am 05.12.2024 vor der Küste Nordkaliforniens mit einer Momentenmagnitude von 7,0 oder das Magnitude-7,1-Beben in Tibet am 07.01.2025. Einige sehr ruhige Standorte, vorwiegend im Erzgebirge und im Vogtland, bieten dafür vergleichsweise gute Beobachtungsbedingungen. Neben den Fernbeben werden auch zahlreiche Nahbeben registriert. Darunter befinden sich Schwarmbeben in Westböhmen und im Vogtland, die sich zwischen März und Juli 2024 sowie im Januar 2025 ereigneten und von denen die stärksten Ereignisse Lokalmagnituden bis 2,5 erreichten. Daneben registriert das Netzwerk häufig auftretende Bergschläge mit Lokalmagnituden bis über 4 bei Lubin und Polkowice in Niederschlesien, die durch den Kupferschieferbergbau verursacht werden, der dort bis in eine Teufe von mehr als 1000 m stattfindet. Für Medienaufmerksamkeit sorgte der Einsturz der Carolabrücke in Dresden in der Nacht zum 11.9.2024. Da sich etwa 800 m von der Brücke entfernt am St.-Benno-Gymnasium Dresden auch eine unserer Raspberry-Shake-Stationen befindet, konnte der Zeitpunkt des Einsturzes mit 02:58:21 Uhr MESZ genau ermittelt werden. Der Abriss weiterer Brückenteile zwei Nächte später war dann sogar an weiteren Stationen des Netzwerks bis in 30 Kilometer Entfernung zu erkennen.

## **P-OS-01**

### **Working towards a software package for Optimized Experimental Design for Electrical Resistivity Tomography**

**N. Menzel<sup>1</sup>, S. Uhlemann<sup>2</sup>, F. M. Wagner<sup>1</sup>**

<sup>1</sup>*RWTH Aachen, Geophysical Imaging and Monitoring, Aachen,*

<sup>2</sup>*Universität Bremen, Fachgebiet Umweltgeophysik, Bremen*

The noninvasive monitoring of both static structures as well as dynamic transport processes in the subsurface through geophysical methods has gained increasing attention in recent decades. Electrical resistivity tomography (ERT) is particularly well-suited for this purpose due to its sensitivity to variations in fluid content and temperature. Optimizing the measurement layout for ERT is crucial when considering hazardous, static or moving subsurface targets since it ensures accurate characterization of subsurface features by maximizing image resolution and thereby minimizing risks. In particularly in sensitive environments, such as contaminated groundwater zones, radioactive waste repositories, unstable slopes or areas with unexploded ordnances, an optimized ERT array can enhance resolution and sensitivity to improve delineation and risk assessment. Additionally, for moving targets, such as groundwater plumes, tailored configuration schedules enable the detection of dynamic changes over time, supporting effective monitoring strategies.

Intensive research in the past decades yielded many different approaches to Optimized Experimental Design (OED) that share the goal of maximizing the information content of a dataset, while keeping the survey expenses to a minimum. Typically performed before field measurements, OED ensures efficient data acquisition and avoids additional steps. However, the process involves labor-intensive stages, from creating a subsurface model to generating hardware-compatible ERT acquisition schemes. This study introduces a comprehensive, modular software package for OED in ERT, streamlining the optimization process and producing acquisition templates with minimal input.

The software comprises four key components:

- 1) Input: Incorporates prior information, including target characteristics, geology, and subsurface flow simulations.
- 2) Masking: Uses focusing functions to prioritize critical areas, enhancing the cost-benefit ratio.
- 3) Optimization: Provides stochastic and deterministic algorithms for goal-specific ERT designs.
- 4) Export: Generates machine-readable schemes compatible with common ERT devices.

This modular design ensures flexibility across diverse applications, supports case-specific adaptations, and allows users to integrate custom algorithms under a permissive open-source license. By simplifying the OED process while enabling user-specific innovations, this tool enhances ERT measurement efficiency and adaptability.

## GT – Geothermie / Radiometrie

### Poster

#### P-GT-01

#### Assessing the influence of high-resolution topography and radiogenic heat production on geothermal heat flow in Northeast Greenland

J. Gehrig<sup>1</sup>, J. Freienstein<sup>1</sup>, C. Carter<sup>2</sup>, G. Hüttner<sup>1</sup>, O. Eisen<sup>2</sup>, V. Helm<sup>2</sup>, S. Franke<sup>2</sup>, W. Szwilus<sup>1</sup>, J. Ebbing<sup>1</sup>

<sup>1</sup>Institut für Geowissenschaften CAU Kiel, Kiel,

<sup>2</sup>Alfred Wegener Institut, Bremerhaven

Accurate estimates of geothermal heat flow are essential for understanding ice dynamics, with especially small-scale geothermal heat flow (GHF) being highly influential on those. Recent work also shows that the topography can have a significant influence on the resulting geothermal heat flow.

We want to present a fine scale GHF model for a ca. 65 km by 40 km large region within the North East Greenland Ice Sheet (NEGIS), including newly acquired airborne ice/ground penetrating radar (GPR) data (provided by AWI). This dataset allows us to incorporate high-resolution topography data to a 3D model and estimate the surface GHF.

We set up our 3D model with the python package pyGIMLi. Comparing results derived from high-resolution topography with models using constant or low-resolution data, we demonstrate the significant impact of topographic variability on estimated GHF in ice covered regions. Furthermore, small-scale variations of radiogenic heat production (RHP) with a correlation length scale between 10 km and 50 km have shown to strongly influence the pattern and amplitude of the resulting GHF. Thus, we also apply different maps for the radiogenic heat production, including constant values and small-scale variations, to further investigate the influence of such different RHP on the GHF when considering high-resolution topography.

Our work aims to give an insight into the factors that have a high influence in the estimated GHF and to reassess the need to include high resolution data and 3D modelling for estimating reliable high-resolution geothermal heat flow in Greenland.

## **P-GT-02**

### **Untersuchung von Fehlstellen in der Hinterfüllung von Erdwärmesonden**

**E. Berrios Amador<sup>1</sup>, C. Gerhards<sup>1</sup>, R.-U. Börner<sup>1</sup>, K. H. Zschoke<sup>2</sup>**

<sup>1</sup>*TU Bergakademie Freiberg, Freiberg,*

<sup>2</sup>*geoENERGIE Konzept GmbH, Freiberg*

Die Nutzung von Geothermie stellt eine vielversprechende Alternative zu fossilen Energieträgern im Rahmen der Energiewende dar. Um eine optimale Anbindung an das Grundgebirge sowie eine zuverlässige Abdichtung zu Grundwasserleitern sicherzustellen, ist die Kontrolle der Hinterfüllung von Erdwärmesonden (EWS) von besonderer Bedeutung. Während des Verpressvorgangs können durch Klüfte oder Grundwasserströmungen Fehlstellen in der Hinterfüllung entstehen. Aufgrund des geringen Durchmessers der Sondenrohre ist der Einsatz gängiger Messverfahren der Bohrlochgeophysik jedoch nur eingeschränkt möglich. Das Unternehmen geoENERGIE-Konzept GmbH hat das Messverfahren geo-Post-Grouting-Test (geoPGT) entwickelt, das in dieser Arbeit untersucht wurde. Die zentrale Forschungsfrage lautet, anhand welcher Parameter Fehlstellen durch Temperaturmessungen klassifiziert werden können. Hierzu wurde geoPGT mit etablierten Verfahren wie dem Kurz-Thermal-Response-Test (Kurz-TRT) und tiefenaufgelösten Temperaturprofilmessungen (T-log) verglichen. Ergänzend wurden synthetische Temperaturkurven mit der Software FEFLOW der DHI Group berechnet. Im Rahmen der vorgestellten Bachelorarbeit wurden Temperaturmessungen an einer bereits hinterfüllten Doppel-U-EWS in Freiberg, Deutschland, durchgeführt. Zur Interpretation der Messergebnisse wurde die EWS mithilfe der Finite-Elemente-Methode in FEFLOW modelliert und simuliert. Die synthetisch berechneten Temperaturprofile wurden anschließend mit den im Feld gemessenen Profilen verglichen. Die Ergebnisse zeigen, dass eine Klassifikation von Fehlstellen anhand von Temperaturprofilen nur eingeschränkt Rückschlüsse auf deren Dimension oder Art erlaubt. In zukünftigen Studien könnte das Messverfahren an weiteren EWS getestet werden. Darüber hinaus könnten etablierte Messverfahren der Bohrlochgeophysik, die speziell für die Anwendung in EWS angepasst sind, zu einer präziseren Klassifikation beitragen.

## **P-GT-03**

### **Numerical Simulations of thermal data from a privately used Borehole Heat Exchanger**

**E. Pilgermann, A. Hördt, C. Virgil**

*TU Braunschweig, Institut für Geophysik und Extraterrestrische Physik, Braunschweig*

In November of 2021 a Borehole Heat Exchanger (BHE) was installed on a private property. In two 100m deep boreholes double U-pipes circulates cold water, warming it by about 3 K. It is of interest whether the temperature of the surrounding ground could fall below 0°C during normal use as this would diminish the efficiency of the BHE. We used numerical simulation to determine the development of the temperature in the ground over time. The model approximates the borehole by a finite line source. The ground consists of clay. Its thermal properties can be taken from literature.

In a first step, we tried to validate the model using the heat extraction rates as input and the temperature calculated at the edge of the borehole as output. The temperature of the water leaving the pipes was used as a proxy for the average borehole temperature. In order for the simulated temperature to match the proxy data, the heat conductivity in the ground has to be significantly lower than that found in literature. Under this assumption, the results mostly

fit the proxy well, with the exception of a few time sections. The model was also validated using the so-called g-function, representing an analytical solution for a line-source heat extraction. In the next step, we simulated a long term use, which implies freezing is possible during normal use. As the assumption of a low thermal conductivity of Clay might be critical for the conclusiveness of the results, we examined the usage of the water temperature as a proxy for borehole temperature as a potential source of uncertainty. For this purpose, we used the same simulation on laboratory data previously obtained by other authors, which included measurements for the heat conductivity, the temperature of the water leaving the pipe and a temperature probe at the edge of the borehole. The simulated temperature differed by 1 K from the temperature at the edge of the borehole and by 10 K from the temperature of the water.

This suggests that the water temperature is unsuitable for comparison with the simulation output. As a result, the assumed heat conductivity is too low, causing unrealistic cooling of the ground. We conclude that finding the correct heat conductivity by matching simulation output with the water temperature is questionable. Using literature values for long-term predictions would likely provide more realistic long-term predictions.

## KD – Kampfmitteldetektion

### Vorträge

#### O-KD-01

### Der DGG Arbeitskreis Kampfmitteldetektion – Erste Erfolge, laufende Projekte und Ziele für die Zukunft

J.-P. Schmoldt<sup>1</sup>, T. Wunderlich<sup>2</sup>, P. Gödickmeier<sup>3</sup>, A. Fahl<sup>4</sup>, DGG-Arbeitskreis Kampfmitteldetektion

<sup>1</sup>Niedersächsisches Landesamt für Bau und Liegenschaften (NLBL), Referat BL 37, Hannover,

<sup>2</sup>Christian-Albrechts-Universität, Institut für Geowissenschaften, Angewandte Geophysik, Kiel,

<sup>3</sup>SENSYS Sensorik & Systemtechnologie GmbH, Bad Saarow,

<sup>4</sup>KampfmittelSERVICE B&E GmbH, Würzburg

Die Gefahren durch Kampfmittel aus vergangenen und aktuellen Kriegen und Konflikten ist ein globales Problem. Die Details der Problemlage an den jeweiligen Orten sind dabei abhängig von der Art der Kampfhandlungen aber auch den Umständen der Produktion, Transport und Entsorgung der Kampfmittel. Diese Details bestimmen die Anforderungen an die geophysikalischen Untersuchungen, die Wahl der Verfahren und die Einschränkungen bezüglich der Detektionsergebnisse. Für eine zielführende Beantwortung der damit verbundenen Fragestellungen, bedarf es intensiver Untersuchungen auf wissenschaftlichem Niveau.

Die Anforderungen an die geophysikalischen Detektionsverfahren in Deutschland unterscheidet sich dabei zum Teil signifikant von den Anforderungen in anderen Ländern.

Untersuchungen in anderen Ländern zielen oftmals auf Munition kleineren Kalibers, die von Infanterie und Artillerie eingesetzt werden, sowie auf verlegte Munition wie Minen und Sprengfallen. In Deutschland gilt das Augenmerk derzeit vor Allem den sogenannten Bombenblindgängern, wie die nicht explodierte Fliegerbomben aus der massiven Bombardierung Deutschland im zweiten Weltkrieg bezeichnet werden. Aus diesem Grund gibt es die Notwendigkeit eigene Studien durchzuführen. Gleichzeitig bietet sich hier der Wissenschaft die Möglichkeit ganz neue Erkenntnisse zu publizieren.

Der Arbeitskreis Kampfmitteldetektion der DGG wurde mit dem Ziel gegründet, zur Umsetzung dieses Ziels beizutragen. In den bisherigen Sitzungen und Workshops wurden

die Ziele des Arbeitskreises konkretisiert und Mitglieder aus den verschiedenen geophysikalischen Disziplinen sind dem Arbeitskreis beigetreten. Erste Erfolge des Arbeitskreises sind die Bereitstellung einer Referenzsammlung, die Veröffentlichungen aus dem Bereich der geophysikalischen Detektionsverfahren zusammenfasst, die Sammlung und Bereitstellung einer Liste an Themen für Abschlussarbeiten und die Einrichtung einer eigenen Session für Kampfmitteldetektion auf der DGG-Jahrestagung 2025. Außerdem wurden die ersten Leitfäden der primären Kampfmittel-Detektionsverfahren (Magnetik und GPR) fortgeschrieben und Wege für die Verbreitung der Ergebnisse des AKs in Wissenschaft, der Kampfmittelbranche und der Öffentlichkeit in Auge gefasst und Kontakt mit den jeweiligen Personen aufgenommen.

## **O-KD-02**

### **Aktuelle Entwicklungen bei der Detektion von marinen Munitionsaltlasten am GEOMAR**

**M. Seidel, M. Keller**

*GEOMAR Helmholtz-Zentrum für Ozeanforschung Kiel, DeepSea Monitoring, Kiel*

In der deutschen Nord- und Ostsee liegen schätzungsweise 1.6 Millionen Tonnen Altmunition, wobei der größte Teil davon nach dem Zweiten Weltkrieg absichtlich versenkt wurde.

Munition in Nord- und Ostsee birgt vielfältige Risiken für Mensch und Umwelt. Das Risiko ist abhängig von der Art und Dichte der Kampfmittelbelastung sowie der Form der Nutzung der Meeresgebiete, Ufer und Strände.

Im Rahmen unterschiedlicher Forschungsprojekte erfassen Wissenschaftler:innen des GEOMAR Helmholtz-Zentrum für Ozeanforschung Kiel seit 2016 die Verteilung dieser Altlasten aus dem Zweiten Weltkrieg,

untersuchen deren Auswirkungen auf die Umwelt und tragen zur Entwicklung von Möglichkeiten für die Bergung und Räumung bei.

Der Vortrag präsentiert aktuelle Entwicklungen und technologische Fortschritte bei der Detektion von marinen Munitionsaltlasten unter Verwendung moderner Tauchroboter sowie schiffsbasierter Sensoriken.

## **O-KD-03**

### **Elektromagnetik im Bohrloch – Projektbeispiel Grasbrook, Hamburg**

**O. Geisler**

*EGGERS Kampfmittelbergung GmbH, Tangstedt*

Die Elektromagnetik stellt neben der Geomagnetik als zusätzliches Sondierverfahren ein wertvolles Werkzeug bereit. Geomagnetische Überlagerungen durch geogene und anthropogene Einflüsse lassen sich oft durch die Anwendung des aktiven Verfahrens, der die Materialeigenschaft der Leitfähigkeit zugrunde liegt, auflösen. Beispielsweise können die störenden Signaturen von Fundamenten oder Bohrpfählen soweit reduziert werden, dass eine Beurteilung des Verdachts auf Bombenblindgänger möglich ist. Insbesondere wertvoll sind die Aussagen der Elektromagnetik zusammen mit der Geomagnetik für die Bewertung von Verdachtssubjekten. Mit dem eigens entwickelten Verfahren 4R-EM wird die Technologie der Elektromagnetik im Bohrloch angewendet und somit zur Erkundung in der Tiefe verfügbar. Am Projektbeispiel Grasbrook wird die Anwendung des Verfahrens 4R-EM im Rahmen eines

der größten Bohrlochprojekte zur Kampfmittelbergung Europas aufgezeigt. Im Herzen Hamburgs findet mit dem Entwicklungsprojekt HafenCity eine Umwandlung von gewerblichen Hafenflächen in einen Stadtteil urbanen Lebens und Arbeitens statt. Der Grasbrook stellt hier den Brückenschlag des Stadtteils nach Süden über die Elbe dar. Auf etwa 200.000 m<sup>2</sup> ehemaligen Flächen zum Stückgutumschlag entstehen Wohnungen, Gewerberäume und Parkanlagen. Im Vorwege wird die Fläche kampfmitteltechnisch untersucht, u. a. mit etwa 77.000 Bohrungen zur Tiefensorierung. Etwa 120.000 m<sup>2</sup> der Fläche sind ehemalige Wasserflächen und wurden bis zu einer Tiefe von 15 m unter Geländeoberkante untersucht. Es wird gezeigt, wie der Einsatz maschinengesteuerter Lafettenbohrtechnik und die Sondierung mit Elektromagnetik im Bohrloch (4R-EM) zur Effizienzsteigerung, v.a. im Bergeprozess, beigetragen haben.

## KD – Kampfmitteldetektion

### Poster

#### P-KD-01

### **Kampfmitteldetektion mittels Bohrloch-Georadar - Verfahren. Unterschiede zwischen Reflexions- und Tomographie-Sondierungen**

J.-P. Schmoldt<sup>1</sup>, S. Kroll<sup>1</sup>, S. Gremmler<sup>2</sup>

<sup>1</sup>Niedersächsisches Landesamt für Bau und Liegenschaften (NLBL), Referat BL 37, Hannover,

<sup>2</sup>Tauber Geo-Consult GmbH, Greven

Die Belastung durch Kampfmittel in Deutschland aufgrund zweier Weltkriege und der damit verbundenen Kampfhandlungen, Produktion, Transport und unsachgemäßer Entsorgung ist auch heute noch ein erhebliches Problem. Gerade von der nicht-explodierten Abwurfmunition aus der umfangreichen Bombardierung, den sogenannten Bombenblindgängern, geht eine große Gefahr für Menschen, Umwelt und schützenswerten Sachgütern aus. Die zielführende Detektion derartiger Bombenblindgänger ist daher ein wesentlicher Bestandteil der Kampfmittelräumung in Deutschland.

Georadar-Messungen sind prinzipiell in der Lage, Objekte im Untergrund zu detektieren, die in ihren physikalischen Eigenschaften Ähnlichkeit zu sprengkräftigen Kampfmitteln aus dem 2. Weltkrieg haben. Für Georadar-Messungen im Reflexions-Verfahren wurde diese Tauglichkeit bereits mehrfach nachgewiesen und das Verfahren wird vielfach in der Kampfmitteldetektion in Deutschland eingesetzt. Der Einsatz des Reflexions-Verfahrens erfolgt dabei sowohl an der Oberfläche als auch im Bohrloch.

Vergleichsweise neu ist der Einsatz des Georadars im Transmissions-Verfahren für die Kampfmitteldetektion. Im Falle von Bohrlochmessungen befinden sich beim Transmissions-Verfahren der Sender und der Empfänger in unterschiedlichen Bohrlöchern. Bei einer Messung wird üblicherweise der Sender in einer definierten Tiefe positioniert und der Empfänger wird vom unteren Ende des Bohrlochs an die Erdoberfläche gezogen, wobei kontinuierlich Daten aufgezeichnet werden. Der Untersuchungsbereich befindet sich dann zwischen den beiden Bohrlöchern. Wenn Transmissionsmessungen mehrfach wiederholt werden und dabei die Position von Sender und Empfänger variiert werden, so dass der Untersuchungsbereich aus verschiedenen Richtungen sondiert wird, dann spricht man vom Bohrloch-Georadar – Tomographie-Verfahren (Multi-Offset-Profil). Um die Zweckmäßigkeit des Verfahrens für die Kampfmitteldetektion zu bewerten, wurde von der Firma Tauber Geo-Consult GmbH eine Messreihe auf einem Testfeld des NLBL in der Nähe von Hannover durchgeführt. Die Ergebnisse dieser Messreihe werden bewertet und hier vorgestellt.

## P-KD-02

### Evaluating Ground Penetrating Radar (GPR) Capabilities for UXO Detection: Influence of Target Characteristics, Antenna Frequency, and Survey Design

O. Shata<sup>1</sup>, R. Linck<sup>1,2</sup>, J. Schmoldt<sup>3</sup>, S. Gremmler<sup>4</sup>, A. Stele<sup>2</sup>

<sup>1</sup>Ludwig-Maximilians-University, Department of Earth and Environmental Sciences, Geophysics, Munich,

<sup>2</sup>Bavarian State Dept. for Monuments and Sites (BLfD), Munich,

<sup>3</sup>Lower Saxony State Dept. for Construction and Real Estate, Hannover,

<sup>4</sup>Tauber Geo Consult, Greven

Ground Penetrating Radar (GPR) is widely used for detecting buried Unexploded Ordnance (UXO) and subsurface objects. This study investigates the influence of key survey parameters, like profile orientation, spacing, antenna frequency, and target properties on the detection performance of GPR in controlled test scenarios conducted on the Tauber-test site in Greven near Münster (Germany). Three grids with varying configurations and target types were surveyed to evaluate the detection efficiency.

The results highlight critical insights into GPR's capabilities and limitations. Targets at shallow depths ( $\leq 1\text{m}$ ) showed good detectability, when profile spacing and antenna frequencies were optimised, with metallic objects yielding stronger reflections compared to non-metallic ones. In addition, large enough targets were detected clearly. However, deeper targets ( $\geq 2.5\text{m}$ ), small targets and targets oriented in unfavourable way to the survey design were not resolved or at least clearly identified due to limitations of antennas, survey design or ground conditions, emphasising the need for supplementary geophysical methods. Profile orientation significantly affected detection accuracy, with perpendicular orientations producing sharper reflection hyperbolas. Dense profile spacing also improved resolution in complex environments with subsurface noise. Furthermore, it could be shown that based on the reflection signal polarity, a preliminary assumption on solid or air-filled objects can be drawn. This study underscores the importance of proper survey design, equipment calibration, and integration of geophysical methods for improving UXO detection reliability in diverse subsurface conditions. In addition, it highlights the importance of GPR method in UXO detection. It is an exceptionally reliable method for detecting medium to large UXO, but smaller targets or ammunition can remain undetected and extremely hard to be distinguished from other subsurface objects of natural and/or anthropogenic origin.

## P-KD-03

### Testing multi-receiver FD-EMI sensors on UXO targets: a controlled experiment.

J. Guillemoteau<sup>1</sup>, T. Wunderlich<sup>2</sup>, J.-P. Schmoldt<sup>3</sup>

<sup>1</sup>Universität Potsdam, Institut für Geowissenschaften, Potsdam,

<sup>2</sup>Christian-Albrechts-Universität zu Kiel, Institut für Geowissenschaften, Kiel,

<sup>3</sup>Niedersächsischen Landesamt für Bau und Liegenschaften, Hannover

A common approach to characterize buried metallic targets with electromagnetic induction data is to model them as secondary magnetic dipoles. The time domain electromagnetic induction (TD-EMI) method using transient source waveform is popular because it was once the only EMI technology capable to simultaneously measure several components of the magnetic field and at several locations, which is a critical information for the modelling of both the moment and the orientation of the targeted virtual magnetic dipoles. Modern multi-receiver frequency-domain (FD-EMI) instruments can nowadays fulfill the same task at

a high sampling rate. In this study, we tested several instruments and acquisition setups on controlled targets of different shapes, buried at different depths, and with different orientations. Our result shows that such parameters are indeed well detectable in the collected data sets. This opens the possibility to develop new modelling and acquisition strategies, which are specifically designed to help detection of unexploded ordnances (UXO) and other explosive remnants of war (ERW), e.g., by reducing false positives. That way, time and expenses of surveys can be reduced and resources optimized.

## KI - KI Verfahren der Geophysik

### Vorträge

#### O-KI-01

#### **'Pattern recognition for earthquake detection' - 40 years research in AI-based seismology**

**M. Joswig**

*Sonicona GbR, Tübingen*

Since the first presentation of AI-based approaches for seismogram processing ('pattern recognition detector and remote station dialog in a local seismic network' at AGU Fall Meeting 1985), much experience was gained for different AI approaches. They act on both non-parametric, sub-symbolic waveform data as well as parametric, symbolic bulletin information. Approaches range from pattern recognition and trained multi-layer perceptron as statistical classifiers to rule-based systems and unsupervised learning by, e.g., Kohonen nets. An important and often crucial step is signal/image preprocessing to reduce parameter dimensionality in the machine learning. While this was necessary in early days to cope with limited computational resources, it is still mandatory today if limited data sets should ensure machine learning without overfitting. Examples will demonstrate the achieved experience but also stress the limitations for specific research tasks.

#### O-KI-02

#### **SonoDet+: a new, AI-based multi-trace approach for seismic event identification**

**M. Joswig, R. Häfner**

*Sonicona GbR, Tübingen*

SonoDet was designed as single-trace detector to recognize patterns of spectral energy distribution in prewhitened, noise-adaptive f-t images, the sonograms. The first version evaluated the match to predefined contour patterns of (+,-,.) indicating energy, no-energy, and don't care. Later versions used complete spectral footprints of single events to compile the pattern base. The inherent pattern adaption scales each pattern's maximum energy to the actual energy spots under evaluation. This approach predicts which fractions of the initial pattern remain visible above noise – only these fractions are considered for calculation of pattern fit. SonoDet+ extends this scheme of pattern adaptation to all stations in a seismic network based on reference amplitudes of the nearest station. Coding now travel time delays, relative amplitude ratios, and spectral energy distributions gives unique footprints for each seismic region. The reduction to spectral matrices in sonograms results in a principal fuzziness that triggers pattern matches beyond the simple fit of cross correlation.

## **O-KI-03**

### **Utilizing Neural Operators for Seismic Travel Time Approximation and Inversion in Anisotropic 3D Media**

**B. Paulwitz, S. Buske, F. Hloušek, V. Raj**

*TU Bergakademie Freiberg, Freiberg*

The forward modelling as well as the inversion of seismic travel times plays an important role in different parts of seismic data analysis. First-arrival travel times are often computed with eikonal solvers and can be used e.g. within Kirchhoff-type pre-stack depth migration approaches or within travel time inversions to derive the corresponding P- or S-wave velocity models. However, both forward modelling and inversion are challenging tasks in the case of anisotropic media. This work investigates the usage of the Fourier Neural Operator (FNO) to approach this problem. With an eikonal solver, training datasets have been generated and a FNO was trained to approximate the forward modelling solution. It was adapted further to interpolate travel times on off-grid points. Its forward modelling performance in isotropic, vertically transversally isotropic and tilted transversally isotropic media has been investigated. The same trained Neural Operator was also used for inversion by freezing the weights and optimizing on the starting model parameters. Various tests have been performed on the ability to reliably predict travel times and to assess the inversion capabilities of the approach. Potential concerns of the methodology were discussed and analysed in detail, such as the assumption of a homogeneous source region in the eikonal solver that leads to significant difficulties when trying to approximate the numerical mapping with FNO. It was also shown how this issue can be reduced by applying a mask during training. The presented approach already yields promising results that are worth to be further refined and developed.

## **O-KI-04**

### **Machine-learning-based picking of DAS data for cross-well tomography**

**N. Boitz<sup>1</sup>, A. Stork<sup>2</sup>, T. Fechner<sup>3</sup>, U. Ködel<sup>3</sup>, S. Mackens<sup>3</sup>**

<sup>1</sup>*Freie Universität Berlin, Geowissenschaften - Geophysik, Berlin,*

<sup>2</sup>*Silixa Ltd., Elstree, Hertfordshire, United Kingdom,*

<sup>3</sup>*Geotomographie GmbH, Neuwied*

The rapid development of distributed acoustic sensing (DAS) over the past decade has led to its application in various seismic and geotechnical applications. For DAS, a fibre-optic cable is placed on the ground or in a borehole. An interrogator unit repeatedly sends laser pulses that are backscattered by small defects inside the cable. The change in the backscattered signal can be converted into the strain or strain rate in the rock surrounding the cable. DAS has been successfully used for vertical seismic profiling and monitoring of induced seismicity (hydraulic fracturing, enhanced geothermal systems, and CO<sub>2</sub> sequestration). However, there are few applications for cross-well seismic surveys published. For this, acoustic signals are generated in one borehole and recorded by a fibre or conventional geophones in a second borehole. Travel times between these two boreholes can be inverted into a velocity distribution within the subsurface. Arrival time picks from 3-component geophones for such settings are usually very accurate, whereas DAS registrations typically show a lower signal-to-noise ratio, and the quality additionally depends on the incidence angle and polarisation of the arriving wave. To overcome these challenges, we propose to train a convolutional neural network (CNN) using DAS registrations and arrival-time information from geophones installed in the same borehole. We applied this methodology to data from the Svelvik test site, where CO<sub>2</sub> was injected at shallow depths and migration of the gas was monitored using cross-well

tomography. We train the CNN on recorded baseline data (before the start of injection) and geophone picks. To increase the amount of training data, we also generate synthetic data using Convolutional Variational Autoencoders, which are routinely used for image generation but not very common in seismic applications. During training, the CNN learns to accurately detect first arrivals in the DAS data. For testing, we use the trained CNN to pick arrivals in the repeated measurements during the days of CO<sub>2</sub> injection. The pick accuracy is in the range of 0.1 milliseconds which is sufficient to detect the velocity changes caused by the CO<sub>2</sub> inside the subsurface. Next, we plan to train additional CNNs capable of picking SH- and SV-waves to increase the significance of the tomography. The presented methodology can be adapted and expanded for similar case studies.

## O-KI-05

### Mit Hilfe automatischer Hyperbeldetektion und Geschwindigkeitsbestimmung zum 3D Modell und verbesserter (archäologischer) Interpretation

T. Wunderlich<sup>1,2</sup>, B. S. Majchczack<sup>1,3</sup>, D. Wilken<sup>1,2,3</sup>, M. Segschneider<sup>4</sup>, W. Rabbel<sup>1,2,3</sup>

<sup>1</sup>Christian-Albrechts-Universität zu Kiel, Institut für Geowissenschaften, Kiel,

<sup>2</sup>Christian-Albrechts-Universität zu Kiel, SFB1266 - Scales of Transformation, Kiel,

<sup>3</sup>Christian-Albrechts-Universität zu Kiel, Exzellenzcluster ROOTS, Kiel,

<sup>4</sup>NihK—Institute for Historical Coastal Research, Wilhelmshaven

Hyperbeln in Radargrammen werden durch eine Vielzahl von kleinen Objekten im Untergrund verursacht. Aus der Form dieser Hyperbeln kann die Ausbreitungsgeschwindigkeit im Untergrund bestimmt werden, die für eine exakte Zeit-Tiefen-Umrechnung und Migration wichtig ist und auch Informationen über den Wassergehalt des Bodens liefert. Diese Bearbeitung kann automatisiert werden, indem im ersten Schritt das Deep-learning Netzwerk RetinaNet zur automatischen Hyperbeldetektion trainiert und auf alle GPR (Ground Penetrating Radar) Daten angewendet wird. Im nächsten Schritt wird dann mit Hilfe eines Schwellwerts, dem C3-Algorithmus (Column Connection Clustering) und einer Kurvenanpassung die Geschwindigkeit und der Apex-Punkt jeder automatisch detektierten Hyperbel bestimmt. Als Ergebnis kann ein geglättetes 3D-Geschwindigkeitsmodell erstellt werden. Die Kombination der Hyperbellokationen und des 3D-Geschwindigkeitsmodells mit Radargrammen und Zeitscheiben führt zu einer verbesserten archäologischen Interpretation durch (1) die korrekte Zeit-zu-Tiefen-Umrechnung durch Migration mit dem 3D-Geschwindigkeitsmodell, (2) die Erstellung von Tiefenscheiben, die der Topographie folgen, (3) die Auswertung der räumlichen Verteilung von Hyperbeln und (4) die Ableitung eines 3D-Wassergehaltsmodells der Fundstelle.

Als Anwendungsbeispiel zeigen wir die Ergebnisse des archäologischen Fundplatzes Goting auf Föhr. Auf der gesamten vermessenen Fläche von ca. 1,76 ha wurden 38490 Hyperbeln detektiert. Die Geschwindigkeiten im erzeugten 3D Modell variieren lateral und vertikal im Bereich von ca. 7 cm/ns bis 12 cm/ns. Die nach der Migration erstellten Tiefenscheiben parallel zur Oberfläche enthüllten die Reste eines Langhauses, was in den Zeitscheiben nicht sichtbar war. Lineare Anreihungen von Hyperbeln zeigen klar die Lage von verfüllten Gräben mit darin liegenden Steinen. Anhand des abgeleiteten 3D-Wassergehaltsmodells konnten wir die Mächtigkeit der archäologisch relevanten Schicht auf dem gesamten Gelände ermitteln. Diese Schicht enthält viel Humus und hat ein hohes Wasserrückhaltevermögen, was zu einem höheren Wassergehalt im Vergleich zum darunter liegenden, gut entwässerten Gletschermoränensand führt.

#### P-KI-01

### Machine learning approach for heading error correction of drone-borne magnetic measurements

C. Paul, V. Schmidt

*Universität Münster, Institut für Geophysik, Münster*

The use of drones for magnetic surveying has drastically increased in recent years. Among other things, this was made possible by the development of miniaturized optical pumped magnetometers (OPM). However, these magnetometers have a relatively large orientation-dependent heading error of several nanotesla, which is a major source of error especially for drone-borne surveys because of the strong and rapid changes in sensor orientation during flight. Thus, additional processing routines are required to compensate for such heading errors. These routines often use data from an inertial measurement unit (IMU), which is attached to the sensor platform. In this study, we present the application of an artificial neural network (ANN) for heading error correction of a miniature OPM suspended from an octocopter drone. A two-layer feed-forward ANN was trained to compute the magnetometer's individual heading error from IMU data, which can then be subtracted from the measured magnetic data. We tested different calibration flight patterns to acquire appropriate training data. Different combinations of input parameters and their effect on the heading error correction were tested. Overall, a combination of compass, gyroscope, and accelerometer data as input into the ANN yields good heading error correction results. An inclusion of attitude data of the drone further reduces the heading error, as additional interferences from the drone can be compensated. This procedure enables the reduction of the heading error of the miniaturized OPM below 100 picotesla, when good training data are available. The method was applied to field data from actual drone-borne magnetic surveys for archaeological prospection at the deserted town Blankenrode in North-Rhine Westphalia and a Gallo-Roman vicus in the Saarland. These results prove the effectiveness of the method.

#### P-KI-02

### DeepONets applied to DC resistivity problems

S. Weit<sup>1</sup>, K. Spitzer<sup>1</sup>, O. Rheinbach<sup>2</sup>

<sup>1</sup>*Technische Universität Bergakademie Freiberg, Institut für Geophysik und Geoinformatik, Freiberg,*

<sup>2</sup>*Technische Universität Bergakademie Freiberg, Institut für Numerische Mathematik und Optimierung, Freiberg*

As machine learning finds wide application in a variety of fields, potential scientific applications become of great interest. This includes physics applications, particularly the solving of PDEs.

Traditional Neural Network approaches often require excessive training data, are limited to a specific mesh or require retraining of the network for every new problem.

One promising approach lies in the utilization of Neural Operators, which, among other things, could allow for a reduction in computation time during problem solving compared to traditional numerical approaches in either forward or inverse problems while remaining reusable without retraining. Particularly DeepONets (achieved through the scalar product of the outputs of two separate Neural Networks) are a promising recent development. They predict a goal function at arbitrary coordinates based on an input function sampled at

discrete locations. Furthermore, their architecture allows for the use of automatic differentiation inherent to machine learning implementations to evaluate the PDE during training and evaluation. The resulting mesh-free physics informed forward operator can be used on arbitrary domains without an increase in necessary computational resources. We present the implementation and results of DeepONets applied to typical DC resistivity problems in comparison to traditional numerical solvers. The advantages and drawbacks of the approach with regard to DC resistivity problems will be discussed and potential use cases identified.

## MG – Marine Geophysik

### Poster

#### P-MG-01

### Aktueller Stand der Umsetzung des Geologiedatengesetzes im marinen Bereich - Schwerpunkt „Seismische Messungen“ in der AWZ

M. Breitzke, GeoIDG-Team der BGR

Bundesanstalt für Geowissenschaften und Rohstoffe, Hannover

Das Geologiedatengesetz (GeoIDG) ist am 30. Juni 2020 in Kraft getreten. Es löst das Lagerstättengesetz von 1934 ab und regelt die staatliche geologische Landesaufnahme, die Anzeige und Übermittlung geologischer Daten an die zuständigen Behörden sowie deren Pflichten zur dauerhaften Sicherung und öffentlichen Bereitstellung geologischer Daten. Der Anwendungsbereich erstreckt sich sowohl auf Daten, die den Behörden bereits vor Inkrafttreten des GeoIDG vorlagen („Altdaten“), als auch auf neu gewonnene geologische Daten. Zuständige Behörden sind die staatlichen geologischen Dienste der Länder für den „onshore“ Bereich sowie die Bundesanstalt für Geowissenschaften und Rohstoffe (BGR) für den „offshore“ Bereich der Ausschließlichen Wirtschaftszone (AWZ).

Dieses Poster gibt einen Überblick über den aktuellen Stand der Anzeige, Übermittlung und öffentlichen Bereitstellung der „Altdaten“ mit Schwerpunkt „Seismische Daten“ sowie der neu gewonnenen Daten.

Aktuell liegen „Altdaten“ von 168 2D- und 7 3D-seismischen Surveys vor, die in den 1970er – 2010er Jahren zur Exploration von Kohlenwasserstoffen gewonnen wurden. Dabei handelt es sich bei 28 2D- und 7 3D-Surveys um digitale prozessierte, teilweise auch um Rohdaten im SEG-Y/SEG-D Format. Ca. 50% dieser digitalen Daten (14 x 2D, 2 x 3D) wurden bereits qualitätskontrolliert und sind über eine Download-Webseite der BGR veröffentlicht, ergänzt um die Roh- und prozessierten Daten von 2 neuen 2D-/3D-Surveys der BGR.

Die analogen „Altdaten“ werden zurzeit im Rahmen der Digitalisierung des GZH-Archivs sukzessive eingescannt, ggf. auch digitalisiert und entsprechend den Regelungen des GeoIDG bereitgestellt.

Des Weiteren wurden seit Inkrafttretens des GeoIDG 52 neue geologische Untersuchungen in der AWZ angezeigt, wobei ein kontinuierlicher Anstieg von 4 Anzeigen in 2020 auf 17 Anzeigen in 2024 zu verzeichnen ist. Anzeigende Institutionen sind Forschungseinrichtungen, Behörden und industrielle Unternehmen, die Projekte zur geologischen Grundlagenforschung durchführen, als Auftraggeber für Projekte zur Flächenvoruntersuchung von Offshore Windparks fungieren und Neubearbeitungen von „Altdaten“ durchführen.

Die dabei gewonnenen Daten werden entsprechend den Fristen des GeOLDG veröffentlicht. Eine Sonderrolle nimmt dabei das BSH ein. Daten von 11 zentralen Flächenvoruntersuchungen für Offshore Windparks stehen über das PINTA Portal des BSH öffentlich zum Download bereit und sind per Link mit der Download-Webseite der BGR verknüpft.

## P-MG-02

### Offshore freshened groundwater exploration – a new playground for marine geophysics

K. Schwalenberg

*Bundesanstalt für Geowissenschaften und Rohstoffe, B1.4 Marine Rohstoffexploration, Hannover*

The exploration of offshore freshened groundwater has become an emerging field of research for marine geophysical methods in recent years. Offshore freshened groundwater (OFG) is considered as a water body with a salinity less than seawater (typical 34 psu, ~35 mS/cm) that is stored in near coastal sub-seafloor sediments and fractures. The OFG body may have formed during the last glacial maximum about 26-20k years ago when sea levels were around 100 m below todays and rainfalls caused the formation of near coastal aquifers. Evidence, mostly incidentally from drilling and submarine groundwater discharge, show that these aquifers still exist in seafloor sediments at many sites around the globe, typically within 50 km of the coastline down to water depths of 100m. They are considered to represent a hitherto largely unexplored and unused resource of freshened water. Open research questions address the lateral extent and volume of the OFG bodies and whether they are actively connected to an onshore aquifer thus subject to meteoric recharge, or if they are disconnected.

A number of recent field studies have shown the usefulness of combining marine seismic (providing structural information) and electromagnetic methods (sensitive to salinity contrasts) to detect and evaluate the presence of OFG bodies in various siliciclastic carbonate or volcanic settings. In this paper I will provide an overview of recent geophysical field studies by various institutions, instrumental aspects, and ongoing and planned research programs related to OFG exploration.

## P-MG-03

### Grundwassererkundung im Übergangsbereich von Land zum Meer in der Bucht von Antalya, Türkei

E. Erkul<sup>1</sup>, J. Hoffmann<sup>2</sup>, S. Fischer<sup>1</sup>, I. Yolcubal<sup>3</sup>, A. Haroon<sup>4</sup>, P. Yogeshwar<sup>5</sup>, E. Sen<sup>5</sup>, W. Rabbel<sup>1</sup>, A. Sener<sup>6</sup>, J. Schneider von Deimling<sup>1</sup>, B. Tezkan<sup>5</sup>, E. Peksen<sup>6</sup>, A. Micallef<sup>7</sup>, E. Gasimov<sup>6</sup>, I. Kaplanvural<sup>6</sup>, F. Gross<sup>1</sup>, L. Sander<sup>2</sup>, S. Baris<sup>6</sup>

<sup>1</sup>*University of Kiel, Institute of Geosciences, Kiel,*

<sup>2</sup>*Alfred-Wegener-Institute, Helmholtz Centre for Polar and Marine Research, Sylt,*

<sup>3</sup>*Istanbul Technical University, Department of Geological Engineering, Istanbul, Turkey,*

<sup>4</sup>*University of Hawaii, Hawaii Institute of Geophysics and Planetology, Honolulu, United States of America,*

<sup>5</sup>*University of Cologne, Institute of Geophysics and Meteorology, Cologne,*

<sup>6</sup>*Kocaeli University, Department of Geophysical Engineering, Izmit, Turkey,*

<sup>7</sup>*University of Malta, Marine Geology and Seafloor Surveying, Msida, Malta*

Die für ihre Badestrände bekannte Stadt Antalya im Süden der Türkei wurde auf mächtigen Travertin-Terrassen errichtet. Der karstische Aquifer sorgt für den Transport von beträchtlichen Mengen an Grundwasser aus dem Taurusgebirge ins Meer. Diese Situation stellt für die Stadt einen großen Vorteil dar, da reichlich Grundwasser vorhanden ist. In den vergangenen

20 Jahren hat sich die Einwohnerzahl der Stadt jedoch verdoppelt und der Grundwasserspiegel ist um mehr als 10 Meter gesunken. Dies hat unter anderem zu Erdfällen geführt. Der florierende Tourismus führte zu Kontaminationen des Grundwassers im Hinterland sowie auf dem Flughafengelände. Es ist von entscheidender Bedeutung, die Grundwasserquellen und die grundwasserführenden Schichten auf ihrem Weg vom Land zum Meer besser zu schützen. Dazu sind umfassende Kenntnisse der hydrogeologischen Eigenschaften des Untergrundes und eine entsprechende Modellbildung erforderlich.

Unser Beitrag widmet sich der Grundwassererkundung im küstennahen Übergangsbereich vom Land zum Meer unter Einsatz geophysikalischer und hydroakustischer Messungen. Die eingesetzten Methoden der Geoelektrik und der Elektromagnetik liefern Informationen über die Porenwassereigenschaften. Die Ergebnisse der Multibeam-Messungen dienen der hochauflösenden Kartierung der Meeresbodenmorphologie. In-situ Wassermessungen nahe der Meeresoberfläche, zusammen mit den aus den Multibeam-Daten abgeleiteten Wassertiefen, liefern wichtige Vorgaben für die Inversion der geoelektrischen Daten. Die Messungen wurden am Strand sowie im unmittelbaren küstennahen Bereich der Antalyabucht durchgeführt. Insgesamt konnten im Wasser ca. 130 Profilkilometer mit mobiler mariner Geoelektrik sowie Multibeam- und CTD-Messungen erfasst werden. An der Küste wurde auf einer Länge von ca. 4 km Elektromagnetik eingesetzt, abschnittsweise ergänzt durch Geoelektrik.

Die berechneten geoelektrischen Inversionsmodelle liefern an Land Informationen bis zu einer Eindringtiefe von ca. 30 m unter der Oberfläche und im küstennahen Wasserbereich bis ca. 20 m unter der Seebodenoberfläche. Die Ergebnisse lassen den Schluss zu, dass entlang des Badestrandes ein dispersiver Grundwasserfluss vorherrscht, während entlang der Steilküste der Grundwassertransport überwiegend in Rinnen erfolgt. Wir beobachten Fluss- und küstennahe Grundwasseraustritte in die Bucht sowie lokalisierte submarine Quellen. Die Quellen werden aus dem küstennahen Grundwasserleiter gespeist.

## **P-MG-04**

### **Gravity and Heat flow density measurements in the New Ireland Basin, Papua New Guinea**

**I. Heyde<sup>1</sup>, P. A. Brandl<sup>2</sup>, R. Zitoun<sup>2,3</sup>**

<sup>1</sup>Bundesanstalt für Geowissenschaften und Rohstoffe, Marine Rohstofferkundung, Hannover,

<sup>2</sup>GEOMAR Helmholtz-Zentrum für Ozeanforschung, Kiel,

<sup>3</sup>IMOS Integrated Marine Observing System, Battery Point, Australia

Cruise SO299 DYNAMET in summer 2023 from Townsville, Australia to Singapore aimed at studying the links between geodynamics (regional-scale plate tectonics, local structural geology and volcanism) and metallogeny with a special emphasis on the Aurich mineralisation on and in the vicinity of Lihir Island in the Tabar–Lihir–Tanga–Feni island chain. Gravity measurements were carried out with a sea gravimeter system KSS32-M continuously during the complete cruise. However, the data acquisition was running in the EEZ of Papua New Guinea and afterwards in international waters and was stopped before entering the EEZ of Indonesia. The free air gravity map of the main working area in the New Ireland Basin is dominated by the anomalies of the main topographic features. The minimum in the South reflects the extension of the Feni Deep. Towards New Ireland and the Islands of the Lihir Group the anomalies increase to values of up to +140 mGal. Local maxima correlate with bathymetric highs. Even small-scale structures like the New World Seamount are resolved in the gravity map. Towards North the gravity decreases rapidly with the increasing water depth approaching the Manus-Kilinailau Trench. Maps of Bouguer gravity and isostatic residual anomalies were developed subsequently.

For the heat flow density measurements the video controlled BGR "hard ground" probe was used, as it was intended to operate the probe in areas of low sediment coverage and/or consolidated volcanoclastic sediments. Measurements were conducted at 20 stations. Thermal conductivities were determined both in-situ and at sediment cores. The gravity corer stations were largely positioned at the sites of heat flow measurements to allow the correlation between heat flow, fluid chemistry, sedimentology, and mineralogy. The first 16 stations were measured along profiles South of Lihir. The values range from about  $27 \text{ mW/m}^2$  to more than  $3100 \text{ mW/m}^2$ . The highest value was measured at the foot of Mussel Ridge to the East of Edison Seamount. The sediment coverage there amounts to only about 1 m. Two stations were measured in the area of the Lihir deep, whereby rather homogeneous values of around  $70 \text{ mW/m}^2$  were found. The last two stations, west of New World Seamount and on the plain northeast of Lihir show similar values. Additional data of cruise SO94 were added. However, no further heat flow density data in the working area, e.g. from the database of the International Heat Flow Commission, could be found so far.

## P-MG-05

### OBS array for offshore monitoring of Mount Etna: Evaluation of array-derived event localizations

H. Zimmer<sup>1,2,3</sup>, K. Hannemann<sup>2</sup>, M. Urlaub<sup>1,3</sup>, C. Thomas<sup>2</sup>, Y. Ren<sup>1</sup>

<sup>1</sup>GEOMAR Helmholtz Centre for Ocean Research Kiel, Kiel,

<sup>2</sup>University of Münster, Münster,

<sup>3</sup>Kiel University, Kiel

Earthquake localization relies on a precise timing within a seismic array. The application of ambient noise cross-correlation as well as the analysis of teleseismic earthquakes allows the detection of timing issues, such as static time offsets or nonlinear time drift of individual stations. The latter cause an inaccurate determination of the earthquake epicenter and need to be eliminated in order to improve the localization method. This study provides insight into the ability to localize local earthquakes using a small-aperture OBS array offshore Sicily – five stations with interstation distances of up to a few kilometers, deployed for one year. A static time offset of 0.173 s and 0.678 s is determined for the stations OBS1 and OBS2. Correction of the individual time offsets is found to improve the accuracy of local earthquake location from deviations of tens of kilometers to just a few kilometers. Furthermore, it is shown that a sediment layer in the form of a sediment deposit in a canyon-like structure or as an additional layer on top, or rather a combination of both, is a suitable explanation for individual static time offsets of one or more stations. Depending on the model and the seismic velocity in the marine sediments, the determined sediment layer thickness varies between 0.4 km and 1.1 km for OBS1 and between 1.4 km and 4.2 km for OBS2. This is in good agreement with the expected depth of Mount Etna's basement in this region.

## MI – Modellierung / Imaging

### Vorträge

#### O-MI-01

#### **Das Thüringer Becken: Einblick in die Temperaturverteilung und Fliddynamik durch dreidimensionale numerische Simulationen**

**A. Schulz, N. Kukowski**

*Institut für Geowissenschaften, Friedrich-Schiller-Universität Jena, Allgemeine Geophysik, Jena*

Sedimentbecken sind bedeutende Ressourcenträger von Mineral- und Energielagerstätten, deren Entstehung wesentlich von der Temperaturverteilung und Fliddynamik in den jeweiligen Ablagerungsräumen beeinflusst wird. Daher ist ein tiefgehendes Verständnis der physikalischen Transportprozesse von entscheidender Bedeutung.

Numerische Simulationen ermöglichen es diese komplexen Systeme zu analysieren und Wissenslücken in Bereichen zu schließen in denen keine Datenakquisition durchgeführt wurde. In dieser Studie wurde auf der Basis eines geologischen Untergrundmodells und mit Hilfe moderner Simulationstechniken ein digitaler Zwilling des Thüringer Beckens erstellt, um den gekoppelten Wärme- und Fluidtransport experimentell zu erfassen. Ziel der Simulationen ist es mögliche Ursachen für Temperatur- bzw. Wärmestromanomalien zu ermitteln.

Zur Kausalitätsanalyse wurden Modellierungen durchgeführt, die das ungestörte regionale Temperaturfeld abbilden und durch diffusive Wärmetransportmechanismen bestimmt werden. Diese sind essenziell, um die thermischen Signaturen konduktiver und advektiver Prozesse zu untersuchen. Dazu wurden drei Modellumgebungen entwickelt, die die Mächtigkeitsverteilung des Zechsteins, die Tiefenlage der Grundgebirgsobergrenze, der Conrad-Diskontinuität und der Lithosphären-Asthenosphären Grenze einbeziehen. Diese wurden zudem mit variierenden thermophysikalischen Eigenschaften attribuiert. Ergänzend wurden weiterführende Simulationen durchgeführt, die den advektiven Wärmetransport berücksichtigen und in denen die hydraulischen Eigenschaften der Gesteine variieren.

Die Ergebnisse zeigen, dass insbesondere die advektiven Wärmetransportprozesse einen erheblichen Einfluss auf die Temperaturverteilung im Untergrund des Thüringer Beckens haben und eine zentrale Ursache für die beobachteten Temperaturanomalien darstellen. Nicht alle Anomalien konnten simulativ nachvollzogen werden. Insbesondere Störungszonen, die das Becken durchziehen, beeinflussen das Grundwasserströmungsverhalten und können somit eine mögliche Ursache für Veränderungen des thermischen Regimes darstellen.

#### O-MI-02

#### **WBGeo – Workbench for Digital Geosystems: Leveraging Open Source Tools for Modular and Exchangeable Workflow Components**

**J. von Harten<sup>1</sup>, A. Lügges<sup>2</sup>, F. Wellmann<sup>1</sup>, B. Rumpe<sup>2</sup>**

<sup>1</sup>*RWTH Aachen University, Chair of Computational Geoscience, Geothermics and Reservoir Geophysics, Aachen,*

<sup>2</sup>*RWTH Aachen University, Software Engineering Department of Computer Science 3, Aachen*

Open source tools and frameworks are increasingly indispensable in advancing the geosciences, providing transparency, fostering collaboration, and enhancing accessibility for a diverse community of researchers, educators, and practitioners. However, one common problem is that open source workflows are difficult to maintain – which often results in code

that can not be run anymore, some years after a project is completed. This is to a degree due to challenges such as code decay, interoperability limitations, and other technical barriers for non-specialist users, which often impede the adoption and sustainability of open source projects. Addressing these challenges is critical to promoting innovation and inclusivity in domains such as structural geology and geothermics.

With this contribution we present a digital workbench for geosystems developed within the project WBGeo, supported by BMBF through the program "Geoforschung für Nachhaltigkeit (GEO:N), Digitale Geosysteme: Virtuelle Methoden und digitale Werkzeuge für geowissenschaftliche Anwendungen". The workbench represents an integrated computational environment designed to optimize workflows encompassing structural geological modeling, meshing, process simulation, and visualization. Central to this framework is the utilization of both textual and graphical domain-specific languages, enabling users to define and manage workflows with enhanced clarity and accessibility. The defining feature of the workbench is its modular architecture, which facilitates the integration of interchangeable components for each stage of the workflow. These components leverage a diverse array of approaches sourced from a range of open source projects. For example, the structural modeling module supports multiple approaches, allowing users to systematically compare results. By employing standardized interface formats, the workbench ensures interoperability and mitigates the systemic risks associated with the obsolescence or failure of individual components.

The workbench enhances collaboration and reproducibility by harmonizing interface formats and providing users with the flexibility to experiment with various tools. This capability is particularly valuable in educational contexts, where students can explore alternative approaches without necessitating advanced coding expertise.

By emphasizing modularity and interoperability, this digital workbench establishes a robust framework for typical workflows in geothermal applications.

## O-MI-03

### Integrating geophysical structure-based inversion with implicit geological modeling

A. Balza Morales<sup>1</sup>, A. Forderer<sup>2</sup>, F. Wellmann<sup>3</sup>, F. Wagner<sup>1</sup>

<sup>1</sup>RWTH Aachen University, Geophysical imaging and monitoring, Aachen,

<sup>2</sup>RWTH Aachen University, Geotechnical engineering and institute of geomechanics and underground technology, Aachen,

<sup>3</sup>RWTH Aachen University, Computational geoscience, geothermics and reservoir geophysics, Aachen

Interpreting geophysical inversion results across diverse applications presents challenges, particularly when the resulting images from conventional smoothness-constrained inversions lack clear, distinct interfaces. The inclusion of prior information to guide the inversion process adds complexity, especially when those prior data carry their own uncertainties. This study explores methods to improve the representation of geological structures by integrating geophysical data with geological models. While current methods are typically either data-driven or model-driven, they often fail to fully leverage available data in a dynamic, unified geophysical model. We propose a novel framework that integrates geological models and geophysical data through structure-based inversion, which maintains geological realism while improving the imaging of sharp contrasts in geophysical models.

To address uncertainties in both the geometric structure and physical parameters, we implement a sequential inversion process. The first step resolves shifts in geological interfaces, and the second step inverts for geophysical parameters, using the updated

geometry as a constraint. The approach is implemented using open-source software frameworks, ensuring flexibility and adaptability to a wide range of geophysical scenarios.

We demonstrate the efficacy of our approach through synthetic cross-hole travel-time tomography examples and a field case study. Results show that our method successfully recovers subsurface interface geometries from geophysical data confirmed by interpolated borehole data. Furthermore, the method preserves layer heterogeneity, improving interpretability compared to other structure-based inversion approaches with constant layer properties. We anticipate that this method will be applicable to large-scale geophysical surveys and can be extended to a variety of scenarios and geophysical techniques.

## **O-MI-04**

### **Petrophysically and structurally coupled joint inversion**

**H. Söding<sup>1,2</sup>, F. Wagner<sup>2</sup>, H. Maurer<sup>1</sup>**

<sup>1</sup>*ETH Zürich, Department of Earth and Planetary Sciences, Zürich, Switzerland,*

<sup>2</sup>*RWTH Aachen, Geophysical Imaging and Monitoring, Aachen*

Tomographic techniques are essential for subsurface imaging and joint inversion methods offer a powerful approach to use multiphysical data sets for enhancing individual inversion results. Traditional joint inversion schemes often rely on either petrophysical or structural coupling.

Petrophysical joint inversion links parameters from different geophysical methods through a common petrophysical parameter space enabling a direct petrophysical interpretation. However, petrophysical relations, which are crucial for the success of this approach, are often uncertain and can vary spatially within the subsurface.

Structural joint inversions addresses this issue by promoting similar structural features across geophysical models commonly using cross-gradient constraints. While these methods ensure structural consistency, they do not honour petrophysical relations during the inversion. In our work, we propose a novel method that addresses spatially varying petrophysical relations. Our approach combines petrophysical coupling where valid relations hold and relaxes to structural coupling in regions of uncertain or contradictory relations. We demonstrate our methodology on a synthetic example and discuss an approach for automatic detection of regions with contradictory petrophysical relations.

## **O-MI-05**

### **Gauß-Newton Full Waveform Inversion for Acoustic Media**

**K. He**

*Karlsruher Institut für Technologie, Geophysikalisches Institut, Karlsruhe*

We present a Gauss-Newton full waveform inversion (FWI) method for acoustic media. This approach is based on the acoustic wave equation for forward modeling of wave propagation and the Gauss-Newton method for model updating to refine the subsurface properties. Both the forward simulation and the inversion are performed in the time domain. While the gradient method is widely used in FWI due to its simplicity and avoidance of large matrix computations, it often struggles to resolve the background velocity accurately. In contrast, the Gauss-Newton method provides higher resolution but is rarely used due to the computational challenges associated with the explicit calculation of the Jacobian and the approximate Hessian matrix. To address these challenges, we calculate the partial derivative field

(or Jacobian matrix) using virtual sources and the reciprocity principle. The partial derivative wavefields are explicitly obtained by convolving the forward wavefields, propagated from each source, with the reciprocal wavefields from each receiver. With numerical experiments, we show that the Gauss-Newton method achieves significantly higher resolution and faster convergence rates compared to the gradient method.

## O-MI-06

### Developing regional velocity models: Data, Methodology and Insights from the TUNB Velo 2.0 Project

C. Schimschal<sup>1</sup>, J. Ziesch<sup>1</sup>, F. Bense<sup>2</sup>

<sup>1</sup>Landesamt für Bergbau, Energie und Geologie (LBEG), Hannover,

<sup>2</sup>Bundesanstalt für Geowissenschaften und Rohstoffe (BGR), Hannover

During the TUNB (Tiefer Untergrund Norddeutsches Becken) project the State Geological Surveys of Schleswig Holstein, Lower Saxony, Mecklenburg Western Pomerania, Brandenburg and Saxony-Anhalt as well as the Federal Institute for Geoscience and Natural Resources (BGR) developed a comprehensive 3D structural model for the North German Basin. It consists of 13 geological horizons from Zechstein to Tertiary and important structural elements like salt domes and fault systems. The model is used for enhanced subsurface spatial planning, e.g. for CO<sub>2</sub> storage, nuclear waste disposal or geothermal projects.

In the follow-up TUNB Velo 2.0 project, the structural model is transformed into a volume model and parameterized with seismic velocities. The resulting velocity model enables to convert seismic data or geologic interpretations from time to depth domain and vice versa. Modelling approaches in Aspen SKUA and the initial velocity data differ between the project partners. For the velocities, borehole data (VSP and depth markers), seismic processing velocities and pre-existing large-scale velocity models provide the basis for modelling and QC. For the North German Basin, Jaritz et al. (1991) published a velocity model for Lower Saxony and Schleswig Holstein in which velocities increase linearly with depth by a dedicated gradient per layer. For the eastern federal states, Reinhardt (1988) published maps with empirical velocity functions for different layers and areas. These velocity models were checked with newer data and are used, adapted or newly developed.

Over the past year, the project partners focused on a shared pilot area to align the different methods and datasets. In the presentation, we will address the challenges and results, demonstrating that the difference in modelling approaches and initial velocities require a harmonisation along the borders to have a consistent, trans-border model. We will provide insights on modelling approaches, velocity considerations and border harmonisation methods.

#### References:

Reinhardt H.G. (1988) Überarbeitung regionale Laufzeitkurven Präzechstein (Stand September 8/88). VEB Geophysik Leipzig

Jaritz W., Best G., Hildebrand G., Jürgens U. (1991) Regionale Analyse der seismischen Geschwindigkeiten in Nordwestdeutschland. Geol Jahrb 45:23–57

## **O-MI-07**

### **EM Tensor Measurements for deep mapping of geology while drilling**

**A. Hartmann<sup>1</sup>, U. Peikert<sup>1</sup>, M. Linke<sup>1</sup>, Y. Antonov<sup>1</sup>, G. Dyatlov<sup>1</sup>, W. Fernandes<sup>1</sup>,  
H. Andersson<sup>2</sup>**

<sup>1</sup>*Baker Hughes, Celle,*

<sup>2</sup>*Baker Hughes, Stavanger, Norway*

Geosteering horizontal wells has been a long-standing practice, in particular where seismic uncertainty is large. Conventional logging-while-drilling EM tools detect remote layers several meters away from the wellbore, sufficient to place the wellbore accurately relative to a formation boundary. However, operators today want to understand the full reservoir architecture, and need deep mapping technology to do so.

An electromagnetic logging-while-drilling system has been designed to meet this requirement and map multiple boundaries up to 300 ft away from the wellbore. This is achieved by a modular design, placing transmitters and receivers spaced 10 m and 30 m apart in the drill-string. The system measures the full 9 component magnetic coupling tensor using the induction logging principle.

Data analysis is based on 1D- and 2D inversion of the acquired data. 1D algorithms are based on a semi-analytical solver coupled with a statistics-enhanced Levenberg-Marquart algorithm for inversion. 2D algorithms are based on a pixel-based FEM solver coupled with the same inversion engine. An inversion workflow combines both systems for near-realtime mapping of reservoir boundaries.

The system performance was modelled in order to define the needed system specifications. Frequencies, spacings, and coil dipole moments were defined based on the modeling. The system was then built and verified in the lab. It was then deployed in a test well in Germany. Data was compared to a previous generation logging tool, confirming the enhanced mapping capabilities of the system.

## **O-MI-08**

### **Transient electromagnetics and electrical resistivity tomography joint inversion using a novel approximated 2D transient electromagnetics inversion scheme**

**A. Jaron<sup>1</sup>, P. Yogeshwar<sup>2</sup>, A. Kemna<sup>3</sup>, F. Wagner<sup>1</sup>, T. Günther<sup>4</sup>**

<sup>1</sup>*RWTH Aachen, Division of Earth Sciences and Geography, Aachen,*

<sup>2</sup>*University of Cologne, Institute of Geophysics and Meteorology, Köln,* <sup>3</sup>*University of Bonn, Institute of Geosciences, Bonn,*

<sup>4</sup>*TU Bergakademie Freiberg, Faculty of Earth Sciences, Geotechnics and Mining, Freiberg*

Different geophysical prospecting techniques have specific advantages and disadvantages. Depending on the method, they are sensitive to different physical parameters, such as the electrical resistivity or density. But also methods that resolve the same physical parameter, may have different resolution characteristics, due to for example the specific source-receiver configuration. Similarly, the investigation depths can differ. To provide an improved subsurface image, measurements from different methods can be efficiently combined in a joint inversion (JI) process. Here we present a novel JI development based on the framework

pyGIMLi. We combine the loop source Transient Electromagnetic Method (TEM) and Electrical Resistivity Imaging (ERT) in hybrid joint inversion scheme. ERT is commonly collected in a 2D manner and has a superior lateral resolution, whereas TEM provides a much larger depth of investigation as well as has a superior layer resolution, particularly for conductors. However, TEM is usually collected comparably sparse and the multi dimensional inversion is extremely challenging. For weak 2D problems, more sophisticated quasi 2D approaches using for example laterally constrained inversion can be efficiently applied. However, until now there is no development that combines 2D ERT with 1D TEM in an inversion scheme. Our developed 2D-1D hybrid joint inversion approach is capable of handling 2D ERT data and integrating TEM soundings along a profile line, using a fast semi-analytic 1D TEM forward operator. For TEM, model columns are extracted below each sounding. A rather sparse pseudo 2D TEM Jacobian matrix is constructed and combined with the full 2D ERT Jacobian. To compensate for weak 2D effects and to include neighboring cells in the TEM response, a depth-dependent weighting function is used for material averaging. This also allows for an approximated 2D sensitivity calculation by laterally distributing the sensitivities across cells. This approach allows a smoothness constraint inversion. The cost-function is minimized incorporating a data term plus a 2D smoothness constraining functional using a step-wise cooling for the regularization parameter. Systematic synthetic modeling studies are carried out to evaluate the performance and assure an optimal model reconstruction. Our synthetics and field data studies demonstrate that the approach is applicable to both, single pseudo 2D TEM inversion as well as 2D hybrid joint inversion.

## MI – Modellierung / Imaging

### Poster

#### P-MI-01

### Towards a time-domain Gauss-Newton algorithm for elastic multi-parameter full-waveform inversion

S. S. Keßler, T. Bohlen

*Geophysikalisches Institut, KIT, Karlsruhe*

Until today, it remains challenging to reduce crosstalk between model parameters in multi-parameter full waveform inversion in elastic media. Several authors developed methods such as the truncated Newton approach to better account for possible parameter trade-offs compared to classical gradient methods. However, to reduce computational time, the product of the Hessian and the model update is only approximated in this case. Although computationally more time-consuming, the Gauss-Newton method can reduce crosstalk by applying the approximate Hessian matrix. Furthermore, the method is promising for fast convergence and has the potential to provide high resolution parameter models. This is especially important for the inversion of the mass density, which is often avoided by using empirical relations such as Gardner's relation to deduce the density from the velocity.

Based on existing work, we show how to derive formulas to calculate the Jacobian matrix of the seismic wavefield in a time-saving manner. The matrix is proved and used to calculate the gradient and the approximate Hessian matrix. Additionally, an insight into further work on a Gauss-Newton algorithm in the time-domain is provided.

## P-MI-02

### 2D Near-Surface Elastic Full Waveform Inversion Using Synthetic Data from Traffic-Induced Moving Sources

C. He<sup>1,2</sup>, T. Bohlen<sup>1</sup>, J. Chen<sup>2</sup>

<sup>1</sup>Karlsruhe Institute of Technology, Geophysics Institute, Karlsruhe,

<sup>2</sup>Chinese Academy of Sciences, Institute of Geology and Geophysics, Beijing, China

Traffic-induced seismic signals, generated by moving vehicles on roads or railways, represent an environmentally friendly and computationally efficient approach for reconstructing subsurface structures through Full Waveform Inversion (FWI). By modeling these signals as a series of time-delayed excitations, we apply passive viscoelastic FWI to synthetic data to recover near-surface S-wave and P-wave velocities as well as density models. We evaluate the performance of three source types: conventional fixed sources, cars at various speeds, and high-speed trains (HST). Numerical experiments demonstrate that traffic-induced moving sources achieve inversion accuracy comparable to fixed sources while significantly reducing computational costs. Slow-moving cars (e.g., 36 km/h) deliver the highest inversion accuracy due to reduced wavefield interference, whereas faster cars expedite computations but sacrifice accuracy. The HST source, moving at 360 km/h, provides an optimal balance between computational efficiency and accuracy. This research highlights key trade-offs among source speed, inversion accuracy, and computational efficiency. The moving-source approach shows substantial potential for large-scale and near-surface subsurface imaging, particularly in urban settings. However, challenges such as traffic route constraints, environmental noise, and source modeling complexities remain. Despite these challenges, traffic-induced moving-source FWI offers a practical and sustainable solution for seismic imaging and monitoring applications.

## P-MI-03

### 2D Viscoacoustic Full Waveform Inversion (FWI) for Imaging CO<sub>2</sub> sequestration of the Sleipner Field North Sea

E. Anthony, T. Bohlen

*Geophysical Institute (GPI), Karlsruhe Institute of Technology (KIT), Karlsruhe*

Most full-waveform inversion methods carried out to image CO<sub>2</sub> accumulation in the thin layers of the Sleipner Field have typically ignored the effect of attenuation. This oversight can lead to less accurate imaging and characterization of the CO<sub>2</sub>-bearing layers, as attenuation significantly impacts the amplitude and phase of seismic waves. Consequently, incorporating attenuation effects is crucial for improving the fidelity of subsurface models in such scenarios. To image both the velocity and attenuation of the CO<sub>2</sub> migration and accumulation of the Sleipner Field, we used the standard linear body theory which describes attenuation. This was used to derive a simplified viscoacoustic equation that characterizes amplitude attenuation and phase distortion. Unlike conventional equations that include memory variables, this simplified equation requires less memory during computation, making the implementation of attenuation compensation easier. The finite difference method is employed to solve the equations, with the attenuation terms addressed in the wavenumber domain and all other terms in the time-space domain. To stabilize the adjoint wavefield, robust regularization operators are applied to the wave equation, effectively eliminating the high-frequency components of numerical noise generated during the backward propagation of the viscoacoustic wavefield. Synthetic velocity models for pre-CO<sub>2</sub> and post-CO<sub>2</sub> injection scenarios in the Sleipner Field, North Sea, were generated. The results demonstrate that Full Waveform Inversion (FWI) can reconstruct the velocity and Q model of the Sleipner Field with enhanced resolution.

## P-MI-04

### Full Waveform Inversion for Sparse Parameter Spaces with a Gaussian Process Emulator

G. El Fatih, M. S. Boxberg, F. M. Wagner

RWTH Aachen University, Geophysical Imaging and Monitoring, Aachen

Ultrasound transmission measurements are a common technique to determine rock properties in the lab. The target parameters are typically P-wave and S-wave velocities ( $v_P$  and  $v_S$ ), as well as the quality factors ( $Q_P$  and  $Q_S$ ) that quantifies attenuation. Several methods have been proposed for determining these parameters. While the determination of P-wave velocity is typically straightforward, determining S-wave velocity and attenuation is problematic. Even when using S-wave transmitters, the recorded waveforms often show P-wave precursors that originate from conversions and prevent accurate determination of the direct S-wave onset. Simulations of wave propagation have been used to assist analysis, as they help identify different arrival phases in the waveforms. This has led to the idea of using full waveform inversion to determine the parameters. However, determining attenuation using full waveform inversion is also challenging. Assuming the rock sample is homogeneous, the inversion parameter space reduces drastically, consisting of only four parameters in total instead of four parameters per element in the numerical mesh. This led to the idea of using a Gaussian process emulator to solve the inverse problem. However, instead of emulating the waveforms, the emulator predicts the misfit between the measured and simulated waveforms. Starting with a few simulations to sample the parameter space and to create an initial prior of the misfit function, we then use an objective function that combines both the misfit itself—since the inversion aims for the lowest misfit values—and the uncertainty of the misfit function in terms of entropy, because the absolute minimum of the misfit function might be in an unsampled area of the parameter space. By iteratively adding more simulations in regions with low entropy and low misfit, we approach the global minimum of the misfit function. We demonstrate the effectiveness of this approach using both synthetic and real lab measurements.

## P-MI-05

### Parallel Ensemble-Kalman-Inversion using Gaussian Random Fields

R.-U. Börner

TU Bergakademie Freiberg, Institut für Geophysik und Geoinformatik, Freiberg

This study presents a parallel implementation of the Ensemble-Kalman-Inversion (EKI) algorithm, tailored for 2-D magnetotelluric (MT) inversion. We employ Gaussian Random Fields (GRF) for effective parametrization of the electrical conductivity.

In our numerical approach we utilized the Julia Finite Element package Gridap.jl which ensures accurate mapping of GRFs onto the Finite Element (FE) space.

Furthermore, we customized the Gridap.jl package to meet the specific requirements of 2-D MT modeling, resulting in the development of GridapMT.jl.

The EKI method is characterized by the following key features:

- **Derivative-Free Optimization:** EKI does not require the calculation of derivatives, making it suitable for complex or black-box forward models.
- **Ensemble-Based Approach:** The method uses a collection of ensemble members to explore the solution space, offering robustness against noise and uncertainties.

- **Embarrassingly Parallelizable:** The independent calculation of forward models and model updates for each ensemble member allows for straightforward parallelization, significantly enhancing computational efficiency.
- **Stable Convergence:** EKI converges stably to an approximate solution that accounts for the noise level in the data.
- **Flexibility in Parameter Space:** The method can handle large and complex parameter spaces, making it practical and easy to implement for various applications.

## P-MI-06

### Time-lapse petrophysical joint inversion of seismic refraction and electrical resistivity permafrost monitoring data

F. Wagner<sup>1</sup>, J. Klahold<sup>2</sup>, C. Hilbich<sup>3</sup>, C. Hauck<sup>3</sup>

<sup>1</sup>RWTH Aachen University, Geophysical Imaging and Monitoring (GIM), Aachen,

<sup>2</sup>University of Lausanne, Lausanne, Switzerland,

<sup>3</sup>University of Fribourg, Fribourg, Switzerland

Permafrost degradation is a global concern with significant ramifications, including the release of greenhouse gases from thawing soils and increased risks of rockfalls and landslides in alpine regions. High-resolution, non-invasive geophysical monitoring methods offer unique opportunities to observe permafrost dynamics. However, accurately quantifying pore-filling constituents—such as ice, water, and air content—using a single geophysical method is challenging due to ambiguous relationships between these constituents and their geophysical signatures. This difficulty is further exacerbated by unknown porosity distributions and uncertainties in petrophysical equations, which involve additional parameters often assumed to be spatially and temporally constant.

In this study, we introduce a methodology that employs petrophysical and temporal coupling in the inversion of geoelectrical and seismic refraction monitoring data. Petrophysical coupling enables the direct estimation of pore-filling constituents by honoring petrophysical relationships and ensuring physical plausibility through volumetric constraints. Temporal coupling differentiates between parameters assumed to be invariant within the monitoring period (e.g., porosity) and those expected to exhibit dynamic behavior (e.g., ice and liquid water contents). We demonstrate the advantages and limitations of this time-lapse joint inversion framework with synthetic experiments and field data from Norway. We conclude by highlighting necessary advancements, such as integrating additional geophysical methods, to enhance the reliability and robustness of geophysics-based ground ice estimation.

## P-MI-07

### WaterSim – Modellierung des gekoppelten Fluid und Wärmetransports am Beispiel des Saaletals

A. Schulz, N. Kukowski

Institut für Geowissenschaften, Friedrich-Schiller-Universität Jena, Allgemeine Geophysik, Jena

Wasser ist eine der wertvollsten Ressourcen der Erde, doch steigende Nachfrage, Umweltverschmutzung und Klimawandel gefährden weltweit Verfügbarkeit und Qualität. Der „Thüringer Wasser-Innovationscluster“ (ThWIC - [www.thwic.uni-jena.de](http://www.thwic.uni-jena.de)) entwickelt innovative und nachhaltige Lösungsansätze für den Umgang mit Wasser.

Das Ziel des Projektes WaterSim als Teil vom ThWIC ist es, die natürlichen Wassertransportprozesse im geologischen Untergrund zu visualisieren. Hierfür werden 4D-Simulationen des ge-

koppelten Fluid- und Wärmetransports durchgeführt, um Volumina, Strömungsraten und Verweildauern des Tiefengrundwassers abzuschätzen. Das Saaletal wurde als Untersuchungsgebiet gewählt, da seine geologischen Gegebenheiten für weite Teile Deutschlands und Mitteleuropas repräsentativ sind.

In diesem Beitrag wird der Fokus auf die Erstellung des Untergrundmodells sowie auf erste Simulationsergebnisse gelegt.

Das Modell umfasst den Großraum Jena mit einer Fläche von 40 mal 30 km und beinhaltet insgesamt 12 stratigraphische Einheiten, welche mit gesteinsphysikalischen Eigenschaften attribuiert wurden wie sie für das Thüringer Becken, an dessen östlichem Rand Jena liegt, typisch sind. Permeabilität und Wärmeleitfähigkeit wurden an Bohrkernproben aus dem Thüringer Becken mit einem TinyPerm 3 bzw. eines Thermoscaner bestimmt. Als

Randbedingungen flossen die Jahresschnittstemperaturen an der Oberfläche, der basale Wärmefluss und die radiogene Wärmeproduktion in die Simulationen ein.

Die Simulationen, durchgeführt mit dem frei verfügbaren und bereits adaptierten Code Pflotran ([www.pflotran.org](http://www.pflotran.org)), zeigen, welche stratigraphischen Einheiten den Fluidtransport dominieren, wo Maxima und Minima hinsichtlich der Fließgeschwindigkeit zu erwarten sind und wie der Fluidtransport das Temperaturfeld beeinflusst.

In späteren Projektphasen sollen durch Einbindung von Klimadaten, Pegelständen und Grundwasserförderraten als zeitabhängige Randbedingungen die Auswirkungen des „Global Change“, wie Wasserknappheit und extreme Wetterereignisse, sowie anthropogene Einflüsse simuliert werden. Dies bildet die Grundlage für gezielte Mitigationsmaßnahmen.

## P-MI-08

### Investigation of salt deformation processes using a newly developed 3D two-way coupled DEM-FEM simulation technique

D. Behrens, G. Bartzke, K. Huhn-Frehers

Marum, Bremen

Numerical process simulations have been successfully used in the past to gain a deeper insight into the deformation processes of crustal materials. However, it is still difficult to simulate the evolution of faults and thrusts in space and time within a sedimentary section that is fracturing under an increasing ice load. This is particularly the case when the brittle sediments are deposited on a thick, viscous salt bed. The dominant numerical simulation techniques, the Discrete Element Method (DEM) and the Finite Element Method (FEM), are still limited in simulating deformation processes in layered crustal sections composed of different rheologies, e.g. sediment-salt sequences.

A novel 3D two-way coupled DEM-FEM model, integrating ANSYS Rocky and ANSYS Mechanical via a Python interface, has been developed to study salt-sediment-ice interaction and sediment fracturing. To demonstrate the advantages of this new numerical approach, a simple basin model was used, consisting of a 1 km thick salt layer, a 2.6 km thick sediment cover, and spanning 60 km in length, with half of the profile covered by an ice load. Three different ice load cases of 2 km, 3 km and 4 km were tested. The basement beneath the salt and the side walls were assigned fixed boundaries, and deformation under gravity was simulated.

For the FEM salt layer, we used the Norton creep law with a density of 2200 kg/m<sup>3</sup> and creep constants of 1E-25 s<sup>-1</sup>·Pa<sup>-n</sup> and 3.3. The DEM simulated the sediment layer, generated from 52054 particles sized 75–85 m with a density of 2700 kg/m<sup>3</sup>. Sediments were modeled using hysteretic linear springs for normal forces and Coulomb-limited springs for tangential forces, with a damping ratio of 0.25, including static and dynamic friction. After each iteration step, the deformations in the DEM sediments caused by the ice load are applied to the FEM salt.

The resulting salt deformation is then ‘re-applied’ to the sediment before the ice load is increased in the next iteration step. This results in full coupling between salt and sediment. The simulation results of the three cases show that increasing ice load leads to increasing displacement in the salt layer, resulting in deeper propagation of sediment fractures, indicating a successful coupling approach. Reactivation of fractures is observed during modelling, indicating the dynamic formation of fault zones. The fracture angles range from -60° to 10° and are mainly determined by the material properties of the sediment.

## P-MI-09

### Fractal-dimensional flow surrounding hydraulic dipoles

F. Mumand, V. Jimenez Martinez, J. Renner

*Ruhr-Universität Bochum, Institut für Geologie, Mineralogie und Geophysik, Bochum*

Simultaneous operation of several boreholes tapping the same fluid resource is common. Specifically, in geothermal applications, operation of a pair of boreholes, one for production and one for injection, called a doublet, constitutes the most basic concept. Hydraulically, this scenario corresponds to a hydraulic dipole. Seasonal variations in flow rates and/or directions correspond to a periodic excitation of the dipole. Abstracting the real borehole operation as a periodic dipole affords the opportunity for analytical modeling. We use the generalized radial flow model presented by Barker (1988), which extends conventional radial (two-dimensional) flow by allowing the flow dimension to be fractal, i.e., anywhere between 1 (one dimensional or linear flow) and 3 (three-dimensional or spherical flow). It has been proposed that fractal descriptions are particularly apt for physical fields in highly heterogeneous media, such as fractured rocks. The dipole scenario is realized by superposing the two general solutions corresponding to the two boreholes at different locations operated with the same period but different amplitudes and phases in flow rate. As a side product, the dipole solution can be used to model planar constant pressure boundaries or no flow boundaries, a useful, symmetry breaking extension of the concentric shell models used so far. Hydraulic characterization of the system rests on two approaches, injectivity analysis that relates spectral characteristics of flow rate and pressure in one of the pumping wells, and interference analysis that compares pressures observed in monitoring wells and the pumping wells. In our analysis of the analytical solution, we focus on the effect of the simultaneous operation of the boreholes on their individual injectivity, i.e., the ratio between achieved flow rate and applied pumping pressure, and its dependence on flow dimension. Our approach has significant potential for both aquifer characterization and geothermal energy provision, as the analytical solution suggests that regulating the periodicity of the flow affects the injectivity of the boreholes.

Barker, J.A., 1988. A Generalized Radial Flow Model for Hydraulic Tests in Fractured Rock. Water Resources 24, 1796–1804.

#### O-OG-01

#### **Effekte von dreidimensionalen Widerstands-Verteilungen auf die Inversion von zweidimensionalen Geoelektrik-Messungen – Herausforderungen und Lösungsansätze am Beispiel eines küstenparallelen Messprofils am Strand von Konyaaltı (Antalya, Türkei)**

S. L. Fischer<sup>1</sup>, E. Erkul<sup>1</sup>, E. Pekşen<sup>2</sup>, I. Kaplanvural<sup>2</sup>, W. Rabbel<sup>1</sup>, J. Hoffmann<sup>3</sup>

<sup>1</sup>*Christian-Albrechts-Universität zu Kiel, Kiel,*

<sup>2</sup>*Kocaeli Üniversitesi, Mühendislik Fakültesi, Izmit, Turkey,*

<sup>3</sup>*Alfred-Wegener-Institut Helmholtz-Zentrum für Polar- und Meeresforschung - AWI Sylt, List*

Eine grundlegende Annahme bei der 2D-Inversion von Gleichstrom-Geoelektrik-Daten ist eine zweidimensionale Widerstands-Verteilung im Untergrund, die ausschließlich Variationen in Profilrichtung und in die Tiefe aufweist. Besonders im urbanen Raum oder in Gebieten mit komplexer Geologie ist diese Bedingung jedoch häufig nicht erfüllt. Falls die Änderungen des elektrischen Widerstands senkrecht zur Profilrichtung in 2D-Inversionen nicht berücksichtigt werden, kann es zu Verzerrungen der Inversions-Modelle kommen.

In dieser Studie werden solche Effekte am Beispiel eines küstenparallelen Profils untersucht, entlang dessen Geoelektrik-Messungen zur Untersuchung von Grundwasser-Austritten und Salzwasser-Intrusionen durchgeführt wurden. Aufgrund der Fragestellung und der starken (touristischen) Nutzung des Strandbereichs verläuft das Profil lediglich 20 m - 30 m entfernt von der Küstenlinie. Wegen der sehr niedrigen elektrischen Widerstände des Meerwassers von ca. 0.2 Ωm wird erwartet, dass die gemessenen Widerstände ab einer gewissen Auslagen-Länge scheinbar sinken, da ein Teil des elektrischen Stroms durch das Salzwasser fließt. Um die Auswirkungen der Nähe des Profils zur Küstenlinie zu quantifizieren, werden Vorwärtsmodellierungen unter Berücksichtigung der vorliegenden Geometrie und Bathymetrie vorgestellt. Außerdem werden Ergebnisse von 3D-Inversionen, die den Effekt des Meerwassers berücksichtigen, mit denen einfacher 2D-Inversionen verglichen.

Dabei stellt sich heraus, dass die Ergebnisse der 2D-Inversion im Vergleich zu denjenigen der 3D-Inversionen ab einer Tiefe von ca. 20 m um 50% - 70% niedrigere Widerstände aufweisen. Dies spiegelt den Effekt des Meerwassers wider, der zu einer Erniedrigung der scheinbaren Widerstände bei größeren Auslagen-Längen führt. Umgekehrt zeigen die 2D-Inversionsergebnisse um bis zu 100% höhere Widerstände in geringen Tiefen bis ca. 20 m, was höchstwahrscheinlich auf eine Kompensation der zu niedrigen Widerstände in größeren Tiefen zurückzuführen ist.

Für das beispielhafte Profil ist es also von großer Bedeutung, den Effekt des Meerwassers zu berücksichtigen. Dies ist mithilfe einer 3D-Inversion unter Einbeziehung von Bathymetrie, Topografie und Messgeometrie möglich.

Ein Ziel zukünftiger Untersuchungen ist es, zu zeigen, inwieweit das Küstenmodell während der Inversion vereinfacht und damit der Rechenaufwand verringert werden kann, ohne dass die Qualität der 3D-Inversion signifikant abnimmt.

## **O-OG-02**

### **Geophysical Monitoring of Infiltration Processes in a Managed Artificial Recharge Pond – Part A**

**A. Prayag<sup>1</sup>, T. Dahlin<sup>1</sup>, P. Hedblom<sup>1</sup>, Y. Abu Jaish<sup>1</sup>, P. Jonsson<sup>1</sup>, M. Rossi<sup>1</sup>, K. Hägg<sup>2</sup>, T. Martin<sup>1</sup>**

<sup>1</sup>*Lund University, Engineering Geology, Lund, Sweden,*

<sup>2</sup>*Sydvatten AB, Malmö, Sweden*

Within the EU *Blue Transition* project (<https://www.interregnorthsea.eu/blue-transition>), which focuses on an integrated approach to water and soil management in the context of climate change, one of our research areas is the geophysical monitoring of an artificial recharge pond. The primary goal of this work is to monitor water saturation and transport dynamics beneath the infiltration pond to better understand the infiltration process and to optimize the operation of water works. An additional objective is to explore the potential for monitoring biofilm growth in the sand filter.

To achieve this, a Direct Current Induced Polarization (DCIP) system has been installed at a Managed Aquifer Recharge (MAR) plant in southern Sweden. The system is deployed in and around an infiltration pond and consists of 416 electrodes distributed across three lines. Each electrode is a 10 cm x 10 cm stainless steel plate, buried in trenches at a depth of 0.4 meters. These electrodes are connected alternately to two parallel cables, which are spaced 0.7 meters apart. The system is based on a Terrameter LS2, featuring a 16x32 relay switch with built-in lightning protection, controlled via PC over a network. In addition, sensors for water conductivity, water level, and temperature have been installed. Periodically, 3D-GPR measurements are conducted to monitor the groundwater level horizon and to assist in the structural interpretation of the subsurface.

DCIP data is collected using a 100% duty cycle with 4s pulses in roll-along. Multiple-gradient array are used for measurements, as well as a pseudo pole-dipole array in which the farthest electrode in each spread serves as the „remote“ electrode. Reciprocal measurements are made for 10% of the data to allow for quantification of observation errors. In total, approximately 16,000 datapoints are measured daily. The data is transferred via SFTP to a server for processing and archiving.

Preliminary inversion of the apparent resistivity and integral chargeability data has yielded excellent fits, with mean residuals below 1%. The sandy sediments above the groundwater level show resistivities above 1 kΩm, which decrease to a few hundred Ωm in the saturated zone which reflects variations in sediment grain size. Where the line is near the neighbouring water-filled infiltration pond, a sharp increase in the resistivity interface is observed, corresponding to a rise in groundwater level. The chargeability in this area is relatively low.

## **O-OG-03**

### **Geophysical Monitoring of Infiltration Processes in a Managed Artificial Recharge Pond – Part B**

**A. Prayag<sup>1</sup>, T. Dahlin<sup>1</sup>, P. Hedblom<sup>1</sup>, Y. Abu Jaish<sup>1</sup>, P. Jonsson<sup>1</sup>, M. Rossi<sup>1</sup>, K. Hägg<sup>2</sup>, T. Martin<sup>1</sup>**

<sup>1</sup>*Lund University, Engineering Geology, Lund, Sweden,*

<sup>2</sup>*Sydvatten AB, Lund, Sweden*

The Vombverket water supply facility in southern Scania, Sweden, operates 54 infiltration ponds as part of its Managed Aquifer Recharge (MAR) system, a vital component of the region's water infrastructure. Each pond features a 1-meter-thick layer of washed sand overlying well-sorted glaciofluvial sediments. However, infiltration processes at the pond scale are inadequately understood, posing challenges as population growth, industrial and agricul-

tural demands, and climate change drive the need for increased MAR system production. To address these gaps, a pilot pond was studied using advanced geophysical monitoring techniques. The study integrated a Direct Current Resistivity (DC) system, sensors for water conductivity, soil moisture, and temperature, alongside periodic Ground Penetrating Radar (GPR) surveys. These methods captured temporal and spatial variations in water content and unsaturated zone changes during infiltration.

Sandy sediments above the groundwater table exhibited high resistivity values exceeding  $1 \text{ k}\Omega\text{m}$ , while saturated zones displayed lower resistivity, ranging from a few hundred  $\Omega\text{m}$ . Time-lapse resistivity data, calculated by subtracting baseline values from seasonal measurements, revealed infiltration dynamics, where water initially concentrated in localized areas before spreading. Profiles such as the South-North Pond (SNP) and West-East Pond (WEP) lines demonstrated significant infiltration patterns tied to groundwater movement and soil characteristics.

GPR surveys (170 MHz) provided 3D subsurface models, identifying groundwater levels at depths of 4–6 meters. Reflections highlighted geological material variations related to sediment grain size. The two geophysical methods indicated similar results, showing consistent groundwater levels and infiltration patterns.

These findings enhance the understanding of MAR system infiltration, forming a basis for optimizing efficiency. Future work will estimate soil hydrological properties and incorporate findings into hydrogeological models, supporting sustainable water management strategies. This approach addresses increased water demand and mitigates climate change impacts in Scania.

## **O-OG-04**

### **Investigation of groundwater salinity and seawater intrusion in northern Kuwait using transient electromagnetics**

**S. Burberg<sup>1</sup>, P. Yogeshwar<sup>1</sup>, B. Tezkan<sup>1</sup>, I. M. Ibraheem<sup>1</sup>, F. Bou-Rabee<sup>2</sup>, M. Duane<sup>2</sup>**

<sup>1</sup>*University of Cologne, Institute of Geophysics and Meteorology, Cologne,*

<sup>2</sup>*Kuwait University, Department of Earth and Environmental Sciences, Kuwait City, Kuwait*

This study employs a geophysical investigation using 1D transient electromagnetics (TEM) to assess the spatial distribution of saline groundwater in northeastern Kuwait, a region chosen for significant future urban development. For this purpose, 63 TEM soundings were measured along a regional profile spanning 75 km as well as spatially covering a local area near the Subiya coast. The TEM soundings were measured in a coincident loop configuration with a 50 m x 50 m layout. The regional profile extends from the coast of Kuwait Bay in the south to Abdali, a farm area near the freshwater fields of Al-Raudhatain, in the north.

The TEM data were inverted using Marquardt-Levenberg and Occam inversion techniques to obtain 1D resistivity models of the subsurface. These models reveal significant variations in groundwater resistivity eventually related to salinity. Decreased subsurface resistivity is observed closer to the coast and at greater depths. In contrast, the northern region, near the Abdali farms and Al-Raudhatain freshwater fields, exhibits larger resistivities and obviously fresher groundwater at depth.

By correlating the resistivity models with previous studies on total dissolved solids (TDS), the presence of highly saline groundwater in the coastal zone ( $\text{TDS} > 10,000 \text{ mg/l}$ ) and relatively fresh to brackish groundwater in the Abdali farm area was confirmed. These findings highlight the potential for saltwater intrusion, particularly in coastal areas, and provide valuable insights for sustainable water resource management and urban development planning in the region.

## **O-OG-05**

### **Spatio-temporal salinity dynamics of a coastal aquifer on Spiekeroog island**

**N. Skibbe<sup>1</sup>, T. Günther<sup>2</sup>, M. Müller-Petke<sup>1</sup>**

<sup>1</sup>*LIAG-Institut für Angewandte Geophysik, FB 1.2 Geophysikalische Erkundung/Monitoring, Hannover,*

<sup>2</sup>*TU Bergakademie Freiberg, Institut für Geophysik und Geoinformatik, Freiberg*

Coastal aquifers at the transition zone between freshwater and saltwater show large salinity contrasts. Salinity is a key parameter to understand coastal groundwater flow dynamics and consequently geochemical and microbial processes in subterranean estuaries. Within the project DynaDeep, we apply geophysical and hydrogeological methods accessing either bulk or fluid conductivity to monitor the temporal and spatial salinity changes. Investigation area is a high-energy beach on the North Sea Island of Spiekeroog.

A unique dataset has been acquired since 2022, covering a 2D transect from the dune base to the low water line including strong topographic changes over the seasons. We use electrical resistivity tomography (ERT) to get access to 2D distributions in a six-week cycle. Additionally, continuous monitoring is carried out using a saltwater monitoring system (SAMOS) down to a depth of 20 meters located at the high-water line. Direct push (DP) data at various locations and EC values from fluid samples gathered via DP provide high-resolution 1D information. In three multi-level wells (6, 12, 18, and 24 meters depth) we log the fluid EC and temperature and take samples on a regular basis.

For a dense dataset between January and March 2023 we compare the applied EC methods in detail and found a general agreement after suitable calibration and temperature correction. We furthermore derive a formation factor model for the conversion to salinity. We use a combined inversion of the ERT data (salinity inversion) with the additional data aiming for fluid EC directly under the assumption of this temporally fixed formation factor model. In contrast to standard inversion techniques where often artefacts around formation changes are observed, this allows for a naturally occurring smooth transition of salinities over the different geological units. We found this to be critical when analyzing the spatial and temporal changes in comparison with the available non-ERT data. Furthermore, additional data are included in the inversion process in a joint inversion scheme.

As a result, we present the new algorithm and show salinity distributions based on the combined dataset along with the temporal dynamics of the dataset for the ERT campaigns and compare them to all available EC data.

## **O-OG-06**

### **MoreSpin: a non-invasive soil humidity sensor based on SNMR**

**T. Splith<sup>1</sup>, G. T. Beisembina<sup>2</sup>, S. Costabel<sup>2</sup>, M. Müller-Petke<sup>1</sup>**

<sup>1</sup>*LIAG Institute for Applied Geophysics, Hanover,*

<sup>2</sup>*Federal Institute for Geosciences and Natural Resources, Berlin*

Soil humidity is a critical parameter for many biological, chemical and hydrological processes in the soil. While there are many methods to determine soil moisture, most of them are either invasive or measure soil moisture indirectly. In the latter case, a calibration becomes necessary, which can be difficult because of the heterogeneity that can be found in many soils. Recently, efforts have been made to apply the surface nuclear magnetic resonance (SNMR) method to soil moisture. SNMR is a non-invasive method that can directly detect water content and is commonly used to characterize aquifers in the subsurface. For this purpose, surface coils are utilized to transmit an excitation pulse at the local Larmor frequency and to detect the NMR response from the water in the subsurface. For the

application of SNMR to soil moisture, the method needs to be extended with prepolarization. Because of the short relaxation times that are expected in soils, it also becomes necessary to shorten the duration of the resonant pulses of the SNMR method and increase the pulse amplitude instead.

Both, the prepolarization (and especially its switch-off) and the short pulses of high amplitude introduce new challenges to the modelling of the acquired data. We improved the forward modelling operator accordingly by introducing a numerical solver for the Bloch-equations. This allows us to account for the so-called Bloch-Siegert-effect, a phenomenon known to cause apparent "ghost" aquifers in SNMR inversion results if not considered properly. Test measurements obtained on water-filled pallet boxes verify the improved forward models. We conducted a numerical parameter study to optimize the field setup (configuration of transmitter coil, receiver coil and prepolarization coil) regarding the resolution capabilities of the method. A case study on a peatland near Gnarrenburg, where we performed measurements on peat and mineral soil, demonstrates the applicability of the PP-SNMR method and the improved modelling. The short relaxation times still pose a major challenge which, however, can be overcome by further improvements of the receiving electronics and the measurement scheme.

## **0-OG-07**

### **Geoelectrical monitoring of soil moisture in hugelcultures**

N. Müller<sup>1</sup>, J. Hoppenbrock<sup>1,2</sup>, F. Feldmann<sup>2</sup>, M. Bücker<sup>3</sup>

<sup>1</sup>TU Braunschweig, Institut für Geophysik und Extraterrestrische Physik, Braunschweig,

<sup>2</sup>Julius Kühn-Institut, Institut für Pflanzenschutz in Gartenbau und urbanem Grün, Braunschweig,

<sup>3</sup>Christian-Albrechts-Universität zu Kiel, Institut für Geowissenschaften, Kiel

Climate change is leading to extreme weather conditions, such as droughts and intense rainfall. These conditions affect soil water content and pose challenges for plant cultivation. One promising possibility to attain profitable harvests is through hugelcultures. Hugelculture (translated from German as „mound culture“) is a gardening practice that involves creating raised beds using decaying wood and organic matter. Such hugelcultures are expected to promote storage of water in their wooden core, which is thought to supply plants with water during drought periods and store larger amounts of water during heavy rainfall.

We use Electrical Resistivity Tomography (ERT) to monitor soil moisture dynamics of three hugelcultures located in two gardens in Braunschweig. The cultures differ in age, size, and orientation. In each bed, we installed ERT profiles with 0.2 m electrode spacing as well as Time Domain Reflectometry (TDR) sensors at depths between 20 and 70 cm for complementary soil moisture information. We recorded weekly ERT measurements between June and October 2023. TDR sensors continuously recorded soil moisture and temperature during the same period, providing high temporal resolution.

To examine the effects of irrigation strategies, one hugelculture was irrigated daily for 30 minutes using a sprinkler, while the other two were occasionally watered manually. To simulate heavy rainfall, we conducted an additional irrigation test, during which one of the beds was irrigated for 4 hours.

The inversion of individual ERT measurements indicates the presence of conductive zones of 20 to 50  $\Omega\text{m}$  within the hugelcultures, suggesting the presence of water reservoirs. Lateral variations in resistivity were observed, likely related to different exposures to the sun and irrigation. Time-Lapse-Inversions of the irrigation test showed that water gradually saturates the entire hugelculture. It took approximately three hours for water to reach the maximum depth of 0.75 m.

Our ERT monitoring results highlight the existence of low-resistivity zones, which we interpret as persistent water reservoirs. The irrigated hugelculture showed more homogeneous resistivity values, whereas the other two cultures showed stronger variations. Upon comparing these results and since all three beds had the same good harvests, we conclude that intensive watering is unnecessary. Our findings provide valuable insights for optimizing hugelculture systems in the context of water management.

## **O-OG-08**

### **Enhancing Groundwater Exploration with Constrained Inversion of Reflection Seismic and Electrical Resistivity Data**

**N. Alaei<sup>1</sup>, H. Buness<sup>1</sup>, T. Günther<sup>1,2</sup>, T. Eckardt<sup>3</sup>, B. Stiller<sup>4</sup>, R. Pechnig<sup>5</sup>, G. Gabriel<sup>1</sup>**

<sup>1</sup>*LIAG institute for applied geophysics, Hannover,*

<sup>2</sup>*Technische Universität Bergakademie Freiberg, Freiberg,*

<sup>3</sup>*terrateg geophysical services GmbH & Co. KG, Heitersheim,*

<sup>4</sup>*Hamburg Wasser(HW), Hamburg,*

<sup>5</sup>*Geophysica Beratungsgesellschaft mbH, Aachen*

Groundwater resources are essential, yet their exploration faces increasing challenges from climate change and competing demands. In regions like northern Germany, where geological complexity and limited prior knowledge impede traditional exploration methods, a non-invasive and cost-effective strategy is critical. To address these challenges, we propose an advanced approach combining seismic and Electrical Resistivity Tomography (ERT) methods. This methodology integrates compressional and shear wave seismic with geoelectric techniques to create accurate 3D geological models, thus enhancing groundwater assessment and management decisions. We will refine this integration by developing new workflow integration techniques such as constrained inversion, joint inversion, and full waveform inversion. Currently, we focus on constrained inversion, using seismic interfaces to guide ERT for precise subsurface imaging.

We conducted a comprehensive geophysical survey in Hamburg-Sülldorf, an area characterized by a complex sequence of Quaternary sands, gravels, silts, clays, and tills, as well as deep Miocene mica clays. This geology presents a challenging yet ideal test environment for our methods. Two 2D seismic profiles were acquired, employing both P-wave and S-wave techniques, and were complemented by ERT profiles. Additionally, a new groundwater well was drilled, and geophysical logging was conducted. In this abstract, we present results from our north-south profile, encompassing two test boreholes (ABBAU12 and R108), which extends 1008 meters and 747 meters using P-wave and S-wave techniques, respectively. Concurrently, a 950-meter ERT profile was measured from south to north. Results from an additional profile will be presented in a future presentation.

The results demonstrate that the integration of seismic and ERT methods, implemented with PyGIMLi, provides significant improvements in imaging subsurface conditions. The constrained inversion approach, guided by seismic horizons, successfully delineates geological layers with high resolution which align well with lithological data from boreholes, enabling more accurate interpretation of the subsurface structure. These findings underscore the value of integrating seismic and ERT techniques for advancing groundwater resource assessments in geologically complex areas.

## **O-OG-09**

### **Novel developments of the 2.5D GPR full-waveform inversion for high resolution subsurface imaging**

**D. Hoven, J. van der Kruk, H. Vereecken, A. Klotzsche**

*Forschungszentrum Jülich GmbH, Institute of Bio- and Geoscience: Agrosphere (IBG-3), Jülich*

Imaging the critical zone is crucial for understanding the complex dynamics of flow and transport processes from the surface to deeper subsurface and groundwater. Soil functions, such as water buffering and filtration, are vital for sustaining life. However, imaging the critical zone with high spatial resolution remains challenging because of heterogenous and complex subsurface structures (e.g. high and low hydraulic conductivity and porosity zones) and soil water content variability. Ground-penetrating radar (GPR) full-waveform inversion (FWI) offers high-resolution characterization of permittivity and electrical conductivity of the subsurface, thereby improving imaging of such small-scale structures. Here, we introduce a novel 2.5D GPR FWI that incorporates realistic 3D geometries in forward modeling. Using the 3D finite-difference solver gprMax, we can now model air- and water-filled boreholes, finite-length antennas, and complex geometries. Subgridding allows for localized finer grid cells, improving computational efficiency and enabling more accurate representations of subsurface properties. This innovation represents a significant advancement in GPR FWI. In order to demonstrate the benefits of this approach, we present two synthetic case studies.

In the first case study, we create an aquifer model that includes structures with high contrasts in terms of permittivity and electrical conductivity and has high-angle data caused by a short borehole offset. Both features are challenging for traditional 2D crosshole inversions and cause artefacts and errors. By incorporating boreholes and antenna models, our 2.5D approach resulted in more accurate reconstructions than conventional ray-based and 2D FWI. This is particularly the case for high-contrast structures. Since many processes are taking place on small scales, we test the potential of this novel 2.5D FWI using higher frequency GPR data acquired around a lysimeter, which is a PVC cylinder with a diameter of 1m filled with soil material. The 3D geometry of such a lysimeter causes wave types that cannot be adequately modeled using 2D GPR FWI. For the test, we positioned the antennae at the side walls of the lysimeters and generated synthetical GPR data for a heterogenous soil model. Our 2.5D GPR FWI achieved sub-decimeter reconstruction resolution using the high-frequency data and the results show strong agreement between reconstructed and observed data, capturing multiple wave types in lysimeter setups.

## **O-OG-10**

### **Using crosshole GPR to monitor the impact of maize roots and nitrate fertilizer on the soil-plant continuum**

**S. Schiebel, L. Lärm, F. Bauer, A. Schnepf, H. Vereecken, A. Klotzsche**

*Forschungszentrum Jülich, Institut für Bio- und Geowissenschaften: Agrosphäre (IBG-3), Jülich*

Non-invasive imaging of the soil-plant continuum is crucial for precision agriculture, particularly for managing natural resources such as groundwater and soil. This study demonstrates the potential of crosshole ground-penetrating radar (GPR) to monitor soil water variations below maize crop and the effect of soil nitrate concentrations on GPR data. In 2023, time-lapse GPR measurements were conducted during a maize growing season using 200 MHz and 500 MHz borehole systems at the upper minirhizotron facility in Selhausen. The facility features horizontal rhizotubes arranged in three columns, allowing GPR and

root measurements at depths between 0.1 m and 1.2 m. GPR data were collected weekly using horizontal zero-offset profiling (ZOP) at five depths between 0.2 m and 1.2 m, while root images were obtained at all six available depths. Variations in soil water content and root presence are known to be primarily related to relative permittivity variability, while we expected variations in soil nitrate concentrations to affect soil electrical conductivity and thus GPR signal amplitude. Standardized processing methods were used to determine the relative permittivity of the time-lapse GPR data. The GPR signal amplitude was analyzed by calculating the envelope of each trace and identifying its maximum to differentiate areas of varying conductivity and soil nitrate concentration. In addition, the permittivity and maximum envelopes were trend corrected to reduce static and dynamic effects on the signals and allow for time-lapse comparison. Trend-corrected permittivity results showed increased variability over time to depths of 0.8 m, correlating with increased root presence, while maximum envelopes correlated with increased root presence only at 0.2 m. The 500 MHz data improved the reconstruction of small-scale features within the soil when both data were compared along the rhizotube, but did not show the same correlation. Preliminary results indicated that varying soil nitrate concentrations affected electrical conductivity and GPR signal amplitude along the rhizotubes, with both frequencies showing reduced maximum envelopes in areas of higher soil nitrate concentration. These results highlight the potential of GPR as a non-invasive tool to accurately map root zones and assess spatial variations in soil nitrate concentrations, thereby enhancing precision agriculture practices and promoting sustainable crop management.

## **O-OG-11**

### **Resonance Seismometry – a tool for near-surface cavity mapping in an arms control content**

**M. Joswig, M. Walter, R. Häfner**

*Sonicona GbR, Tübingen*

Resonance Seismometry is the – slightly misleading – name for passive seismic approaches defined in the Comprehensive Test Ban Treaty (CTBT) of UN. The technique shall narrow down the search area for underground nuclear explosions (UNE) during On-Site Inspection to some 10 m to position the final drilling investigations. Different research teams have proposed approaches to evaluate scatter effects caused by the underground cavity and/or rubble zone. These approaches work in time or frequency domain, using remote seismic events or ambient noise as source signal. Results are presented for studies of UNE Tiny Tot at the former Nevada Test Site NTS and the Rotmoos cavities, Austrian Alps.

## **O-OG-12**

### **Investigating the shallow subsurface at the Wiechert earthquake station in Göttingen with passive and active seismic measurements**

**M. Hobiger<sup>1</sup>, T. Plenefisch<sup>1</sup>, B. Goebel<sup>1</sup>, M. Bischoff<sup>2</sup>, M. Napp<sup>2</sup>, S. Donner<sup>1</sup>**

<sup>1</sup>*Bundesanstalt für Geowissenschaften und Rohstoffe (BGR), Erdbebendienst des Bundes, Hannover,*

<sup>2</sup>*Landesamt für Bergbau, Energie und Geologie (LBEG), Niedersächsischer Erdbebendienst, Hannover*

The Wiechert earthquake station in Göttingen is the oldest existing seismograph station in the world, recording earthquakes since 1903. The modern broadband seismometer station GTTG was installed there in 2003 as part of the German Regional Seismic Network (GRSN).

Recordings of regional earthquakes show a strong amplification of the horizontal signals between 1 and 5 Hz, with a maximum around 3 Hz. This amplification indicates the presence of softer layers overlying the harder seismic bedrock at the site. In order to investigate this site effect in more detail, we performed different geophysical measurements.

A passive seismic array recorded ambient seismic vibrations for about 2.5 hours to retrieve the dispersion curves of Love and Rayleigh waves. For the locations of each of the 20 three-component seismic sensors, the H/V ratio and the Rayleigh wave ellipticity were also retrieved. Furthermore, two rotational seismometers were integrated into the array.

In addition to the passive measurements, an active seismic measurement was performed by dropping the Mintrop ball, a steel sphere of about 4 tons, from a height of about 14 m. The evaluation of the different measurements is still ongoing. The goal of the experiment is the deduction of a representative 1-dimensional shear-wave velocity profile for the near-surface underground structure beneath the broadband station GTTG.

## **0-OG-13**

### **Geophysical Methods for Near-Surface Exploration in Seismic Microzonation Studies in Venezuela and Ecuador**

**M. Schmitz**

*Universidad Central de Venezuela, Departamento de Geofísica, Caracas, Venezuela*

Seismic microzonation studies is a vital tool for mitigation of seismic risk in urban areas, especially in developing countries experiencing rapid population growth. Besides regional seismic hazard due to proximity to active faults, local soil conditions often play a determining role in controlling ground shaking. Integrating local soil characterization into urban planning can significantly reduce building damage and loss of lives. Geophysical methods, combined with geological and geotechnical studies, provide essential insights into near-surface configurations. Their application varies depending on geological settings, targeting features like sedimentary basin depth and geometry, and the quality of the uppermost soil layers (e.g., Vs30) that influence shaking amplification and hazards such as soil liquefaction and landslides. Here, we highlight examples from different cities in Venezuela and the city of Portoviejo in Ecuador, conducted by collaborative working groups. Space constraints and urban regulations increasingly favor ambient noise-based methods over traditional active-source techniques, as these are cost-effective and environmentally friendly. Basin geometry and depth are effectively mapped using gravimetric surveys (for basin geometry) and seismic noise measurements (for the generation of 1-D shear velocity soil profiles) from individual or array measurements. Seismic-noise-based methods enable the determination of fundamental soil periods and, with adequate recording durations, the inversion of Rayleigh wave dispersion and ellipticity curves to derive 1-D shear velocity profiles down to the seismic basement. For near surface exploration, passive methods have increasingly replaced active seismic techniques with sources as sledgehammer or explosives. Using standard 48-channel seismographs, acquisition geometries and logistics remain similar, but advanced processing methods such as ReMi (Refraction Microtremor) and iMASW (interferometric MASW) provide more robust results, taking advantage mainly of surface waves within the seismic noise. Measurement grid density, typically between 300–500 m, is adapted to geological and geotechnical conditions at urban scales. Seismic microzonation results should be used for urban planning or specific engineering indications in county ordinances in complement to national seismic building codes.

## **O-OG-14**

### **Potential Field Data Indicate a Candidate Location for Parent Impact Crater of Australasian Tektites**

**K. Karimi<sup>1</sup>, G. Kletetschka<sup>1</sup>, J. Mizera<sup>2</sup>, V. Meire<sup>1</sup>, V. Strunga<sup>2</sup>**

<sup>1</sup>*Charles University, Faculty of Science, Prague, Czech Republic,*

<sup>2</sup>*Czech Academy of Sciences, Prague, Czech Republic*

Meteorite impacts on Earth can generate natural glasses called tektites, formed by melting of target material. These ejecta are transported to distant strewn fields. Four main tektite fields on Earth have been identified so far: Central European (moldavites), Australasian (indochinites, philippinites, australites), North American (georgiaites, bediasites), and West African - Ivory Coast (ivorites). Among them, the parent crater of the largest, Australasian tektites, remains debated. Spanning over one-sixth of Earth's surface, its likely location was initially proposed in Southeast Asia, where tektite abundance is highest. However, an alternative theory suggests an arid region in Northwest China as the source, based on discrepancies in geochemistry and lack of analogies with other strewn fields.

Gravity and magnetic data have proven effective for studying large-scale impact structures, revealing variations in morphology and mineral composition. These methods often precede detailed evaluations of potential impact sites. To explore the proposed Northwest China site, we analyzed gravity aspects—parameters reflecting density and morphological variations in the bedrock—combined with magnetic data to uncover complementary insights.

Our analysis revealed features typical of impact craters. The gravity data show: (1) a cavity-like structure with a ~100 km diameter, displaying a strong negative anomaly surrounded by a positive anomaly rim; (2) preferred parallel alignments suggesting zones susceptible to shock waves; and (3) truncation of the local fault system near the suggested site. The magnetic data confirms a strong anomaly, indicating the presence of highly magnetic minerals within the hypothetical crater.

Joint gravity-magnetic analysis suggests these magnetic materials form an extensive, thin melt pool of highly magnetic minerals, likely created ~0.8 Ma ago. The solidification of this melt likely occurred after the Brunhes-Matuyama geomagnetic reversal. Together, these findings strengthen the case for the proposed site as the parent crater of the Australasian tektites, warranting further investigation.

## **OG – Oberflächennahe Geophysik**

**Poster**

## **P-OG-01**

### **Small-scale geoelectrical monitoring of water transport processes at tree sites**

**L. Schirra<sup>1,2</sup>, J. Hoppenbrock<sup>1,3</sup>, M. Beyer<sup>2</sup>, M. Gerchow<sup>2,3</sup>, S. Iden<sup>2</sup>, M. Bücker<sup>1,4</sup>**

<sup>1</sup>*Institut für Geophysik und extraterrestrische Physik, Technische Universität Braunschweig,*

<sup>2</sup>*Institut für Geoökologie, Technische Universität Braunschweig,*

<sup>3</sup>*Institut für Pflanzenschutz in Gartenbau und urbanem Grün, Julius Kühn-Institut, Braunschweig,*

<sup>4</sup>*Institut für Geowissenschaften, Christian-Albrechts-Universität zu Kiel, Kiel*

A reliable water supply is crucial for the health and vitality of trees and directly impacts the ecosystem services they provide. With ongoing climate change, water availability in Central Europe is expected to decrease especially during the summers, increasing the risk of drought

stress and threatening forest health. Therefore, knowledge on soil water availability and the effects of tree and site characteristics on the processes of soil water flow will help to develop adaptation and mitigation strategies for forest ecosystems. This contribution aims to assess water flow dynamics using geoelectrical measurements, with a focus on infiltration and hydraulic redistribution at tree sites.

Electrical resistivity tomography (ERT) offers a non-invasive means for studying soil moisture dynamics by detecting changes in subsurface resistivity. To capture water flow processes at tree sites accurately, a high spatial resolution is required.

We use a surface ERT setup with 5 cm electrode spacing and a total length of approximately 1.2 m to monitor water flow induced by small-scale infiltration experiments. We invert the resulting dataset using a time-lapse inversion approach implemented in pyGIMLi and incorporate soil moisture data from Frequency Domain Reflectometry (FDR) and Time Domain Reflectometry (TDR) sensors at various depths for validation.

Our results demonstrate the potential of small-scale ERT for monitoring infiltration processes at shallow depths (decimeter range). By comparing the inversion results with measured hydraulic conductivities, the time-lapse inversion of our geoelectrical datasets combining Wenner and Dipole-Dipole configurations was found to be most effective for assessing the propagation of the moisture front during infiltration. However, the maximum investigation depth was limited to approximately 30 cm due to the limited total length of the ERT setup, which resulted in incomplete imaging of the infiltration at greater depths.

In upcoming work, these small-scale ERT setups will be applied at forest trees to investigate the hydraulic redistribution of water by trees, with the aim of providing insights into this process which might be one component for increasing water availability and improving the resilience of forest ecosystems.

## **P-OG-02**

### **FD-EMI electrical conductivity imaging with a multi-frequency source and decametric spacings: first test and comparison with ERT**

**J. Guillemoteau, J. Tronicke**

*Universität Potsdam, Institut für Geowissenschaften, Potsdam*

In contrast to electric dipoles as used for electric resistivity tomography (ERT), magnetic dipoles do not require coupling with ground in practice. This makes electromagnetic induction (EMI) methods employing coils for both source and receiver (loop-loop mode) popular to efficiently survey large areas as used, for example, in airborne surveying since decades. For sensing the first 50-100 m of the subsurface in an efficient manner, motorized time-domain EMI strategies have been recently developed. Here, we explore the capabilities of ground-based frequency-domain EMI (FD-EMI) for exploring near-surface environments. For this, we have performed FD-EMI measurements across a dipping clay layer embedded in a sandy background environment. Our surveying strategy includes several spacings and several source frequencies using both z- and x-components and a high lateral sampling along the profile. We compare the inversions result with the result of co-located ERT surveying. This experiment shows that the FD-EMI conductivity image obtained with a laterally constrained 1D inversion approach is comparable to the ERT resistivity model obtained using a standard 2D inversion approach. Our results motivate the development of a full 2D inversion method in order to maximize the lateral resolution of the FD-EMI conductivity image.

## **P-OG-03**

### **Detection of saltwater intrusion in a coastal aquifers in Qingdao, China using TEM and DCR**

**P. Perez-Gamboa<sup>1</sup>, P. Yogeshwar<sup>1</sup>, W. Mörbe<sup>1</sup>, B. Tezkan<sup>1</sup>, Y. Li<sup>2</sup>, L. Ming<sup>2</sup>**

<sup>1</sup>*Universität zu Köln, Institut für Geophysik und Meteorologie, Köln,*

<sup>2</sup>*Ocean University of China, College of Marine Geo-sciences, Qingdao, China, People's Republic of*

Saltwater intrusion (SWI) is a major concern for freshwater reservoirs in coastal areas, especially those supporting agricultural activities. During July and August 2024, geophysical surveys were conducted at Silver Beach, Qingdao, China, to investigate subsurface freshwater reservoirs and their potential vulnerability to saltwater intrusion. A total of 61 transient electromagnetic (TEM) stations with a loop size of  $25 \times 25$  m were deployed along the shore and complemented by direct current resistivity (DCR) measurements. In addition, we collected water samples from nearby wells.

A large portion of the data shows significant distortion, such as sign reversals or oscillating transient decay. To identify potential noise sources due to the urban setting, we analyzed the data in a spatial context. Less distorted data, usable for further imaging, were interpreted with conventional 1D inversion schemes to characterize subsurface resistivity structures. Along Silver Beach, we clearly identified a zone of increased conductivity related to SWI, comparable to the DCR results. Eventually, a joint inversion framework shall be used to integrate the TEM and DCR data to improve model resolution and differentiation between freshwater and saline zones.

## **P-OG-04**

### **ERT monitoring to observe saltwater intrusion at the Luneplate/Bremerhaven**

**B. Blanco-Arrué<sup>1</sup>, M. Müller-Petke<sup>1</sup>, A. Kunicki<sup>2</sup>, S. Julius<sup>3</sup>, K. Seiter<sup>3</sup>**

<sup>1</sup>*LIAG-Institut für Angewandte Geophysik, FB 1.2 Geophysikalische Erkundung/ Monitoring,*

*Hannover,*

<sup>2</sup>*Leibniz Universität Hannover, Institut für Geologie, Hannover,*

<sup>3</sup>*Geological Service in Bremen, University of Bremen, Bremen*

The Luneplate area is a particularly sensitive region to saltwater intrusion, located in the southern part of Bremerhaven. The western area of the Luneplate is a natural protected area, while the eastern part is used for agriculture. Recently, part of the agriculturally used land is being developed for industrial use, i.e., a green economy part is currently built. This change in land use likely changes the water management in the area. In particular, groundwater recharge is expected to decrease due to limited infiltration, which is planned to be compensated by artificial rainwater recharge that is collected at the economy park.

Within the EU-Interreg project Blue Transition, dealing with the climate impact on soil and groundwater management, the Luneplate area serves as one out of sixteen pilot regions. To observe changes in the saltwater-freshwater boundary, possible interactions with the Weser River, which flows into the North Sea, and the potential existence of clay lenses affecting rainwater infiltration, we perform electrical resistivity tomography (ERT) measurements across several profiles twice per year since the beginning of 2024. Additionally, to supplement the ERT findings and improve the resolution of the resistivity distribution's lateral extension at shallow depths, Electromagnetic Induction (EMI) surveys were conducted to generate conductivity maps between the ERT profiles. Various boreholes were used to correlate and analyze the ERT data.

We show the first measurements conducted in the project. Generally, the ERT images align well with the geological characteristics of Luneplate, help to asses potential infiltration strategies and show the current state of saltwater intrusion. However, some of the near-surface structures may be caused by 3D structures that are not well captured by the ERT profiles. The EMI results clearly assign these structures to clay lenses and enable mapping their lateral extend.

With the ongoing building of the economy part, ERT measurements will continue to observe potential changes in the saltwater intrusion caused by land-sealing and the success of the planned infiltration.

## P-OG-05

### Characterisation of a Palsa near Aidejávri/Norway with Electrical Resistivity Tomography

I. Burger<sup>1</sup>, R. Schulz<sup>1</sup>, S. Westermann<sup>2</sup>, A. Hördt<sup>1</sup>

<sup>1</sup>TU Braunschweig, Institute of Geophysics and Extraterrestrial Physics, Braunschweig,

<sup>2</sup>University of Oslo, Department of Geosciences, Oslo, Norway

Palsas are peat covered mounds mainly found in subpolar peat mires. They contain a frozen core that is protected from thawing during summer by the insulating capacity of the overlying dry peat. They appear in discontinuous permafrost areas and are subject to degradation caused by environmental changes like global warming.

Knowledge of the internal structure of a palsa can provide insights into previous and present environmental conditions. The high electrical resistivity of ice and frozen peat makes it possible to distinguish permafrost from its unfrozen surroundings.

Five profiles were measured with Electrical Resistivity Tomography (ERT) on a palsa near Aidejávri/Norway in May 2024. The palsa is located at the edge of a permafrost peat plateau and has a convoluted shape inside a 70 x 40 m rectangle. The height of the palsa was 401.3 m in UTM and 2.7 m compared to the current height of the nearby stream, which was the lowest measured elevation. A lot of cracks could be seen in the palsa surface, and it was surrounded by several ponds. Of the measured profiles four lead directly over the palsa. They all have two-meter electrode spacings and the Wenner-configuration was used for measurements. A 25-electrode setup was used for two profiles, while 50 were used for the other three. Additionally, the conductivity was measured in all the ponds surrounding the palsa.

The data was inverted using pyGIMLI - an open-source library for multi-method modelling and inversion in geophysics. GPS data was extrapolated and included into the dataset. Every pseudo section was inverted separately. Additionally, all the data was inverted together to form a 3D result. The main features are consistent between the 2D and 3D models while the 2D-models exhibit larger resistivity contrasts. Absolute resistivity values range from 100 to 20,000  $\Omega\text{m}$ . Values are low beneath ponds while there are high resistivity areas under the palsa and adjacent peat plateau. Further from the surface the high resistivity areas seem to connect and deviate from the overlying structures.

## **P-OG-06**

### **Exploring the potential of using GPR to investigate the soil-plant continuum of maize crops**

**L. Lärm, F. Bauer, L. Weihermüller, J. Rödder, H. Vereecken, J. Vanderborght, J. van der Kruk, A. Schnepf, A. Klotzsche**

*Forschungszentrum Jülich, Institute of Bio- and Geoscience: Agrosphere (IBG-3), Jülich*

The soil-plant continuum plays a vital role in regulating key processes that impact plant performance and agricultural productivity. Understanding these processes is becoming increasingly important as climate change affects agricultural systems. Diverging techniques like agrogeophysics and crop science are currently used to investigate individual components of the soil-plant continuum at contrasting scales. However, since these components influence each other, integrated methods combining methods like ground penetrating radar (GPR) with root imaging and modelling techniques are needed. First, a study examined the impact of row crops like maize on horizontal variability in GPR-derived permittivities and root volume fraction. Factors like soil type, water treatment, and atmospheric conditions were found to influence this. A statistical analysis method was developed to visualize the trend-corrected spatial permittivity deviation, allowing correlation between permittivity variability and root volume fractions. Second, numerical modeling showed roots had a greater impact on GPR signals than above-ground shoots. A new approach to derive available soil water was presented, demonstrating that neglecting the root phase in petrophysical mixing models overestimates soil water content. Third, horizontal crosshole GPR-derived soil water contents were combined with a hydrological model to estimate soil hydraulic parameters for winter wheat. This sequential hydrogeophysical inversion was first used for a one-dimensional averaged case, then upscaled to estimate pseudo three-dimensional spatially distributed parameters for a dual-porosity Mualem-van-Genuchten model.

## **P-OG-07**

### **Erprobung eines skalierbaren elektromagnetischen Induktionssystems (SELMA-RB) für landwirtschaftliche Anwendungen**

**M. Dick<sup>1</sup>, E. Zimmermann<sup>1</sup>, A. Mester<sup>1</sup>, P. Wüstner<sup>1</sup>, M. Ramm<sup>1</sup>, B. Scherer<sup>1</sup>, J. Bernard<sup>1</sup>, J. A. Huisman<sup>2</sup>, C. Brogi<sup>2</sup>, S. Dogar<sup>2</sup>, G. Natour<sup>1,3</sup>**

<sup>1</sup>*Institut für Technologie und Engineering (ITE), Forschungszentrum Jülich GmbH, Jülich,*

<sup>2</sup>*Institut für Bio- und Geowissenschaften - Agrosphäre (IBG-3), Forschungszentrum Jülich GmbH, Jülich,*

<sup>3</sup>*Fakultät für Maschinenwesen (ISF), RWTH Aachen University, Aachen*

In der Präzisionslandwirtschaft („Precision Farming“) werden immer mehr Methoden zur effizienten und umweltverträglichen Bewirtschaftung von landwirtschaftlichen Flächen entwickelt und eingesetzt. Technische Lösungen zur schnellen Kartierung der Bodenparameter helfen dabei eine effizientere Feldbearbeitung zu ermöglichen. Vorteilhaft für die schnelle Kartierung sind nicht-invasive Methoden, wie zum Beispiel die elektromagnetische Induktion (EMI). Diese Systeme messen die elektrische Leitfähigkeit des Bodens und ermöglichen die Bestimmung verschiedener Bodenparameter (z.B. Bodenschichtung, Wassergehalt, Düngerkonzentration).

Für eine tiefenauflösende Messung, die eine Vielzahl unterschiedlicher Spulenabstände und -ausrichtungen erfordert, ist in der Regel der Einsatz mehrerer kommerzieller EMI-Geräte notwendig. Zur Vereinfachung der Anwendung im Feld wurde ein EMI-System entwickelt, das simultane Messungen mit optimalen Spulenabständen ermöglicht.

Innerhalb der Messdaten-Vorverarbeitung wurde eine Temperaturdriftkorrektur sowie eine modellbasierte Offset-Kalibrierung durchgeführt. Hierzu wurden zwei Ansätze zur Kalibrierung des Offsets getestet.

Im ersten Ansatz wurde das Gerät zur Offset-Kalibrierung über einem Wasserbecken in unterschiedlichen Höhen positioniert, wobei das Wasser als homogene Schicht modelliert wurde, um den Offset zu berechnen. Im zweiten Ansatz wurde ein natürlicher Boden einer Agrarfläche als Untergrund verwendet.

Zur Evaluierung des Ansatzes wurde die Bodenleitfähigkeit mit dem SELMA-RB-System und einem kommerziellen Messsystem auf einem Testfeld in der Nähe von Jülich gemessen. Die vergleichende Darstellung der Leitfähigkeitskarten und der Kalibrierdaten werden präsentiert. Die Ergebnisse zeigen eine Abweichung von wenigen mS/m.

## P-OG-08

### NMR relaxation of peat soils at laboratory and field scale

G. T. Beisembina<sup>1</sup>, T. Splith<sup>2</sup>, S. Costabel<sup>1</sup>, T. Hiller<sup>3</sup>, M. Müller-Petke<sup>2</sup>

<sup>1</sup>Federal Institute for Geosciences and Natural Resources, BGR, Groundwater and Soil Science, Berlin,

<sup>2</sup>LIAG Institute for Applied Geophysics, Geoelectrics and Electromagnetics, Hannover,

<sup>3</sup>Federal Institute for Geosciences and Natural Resources, BGR, Groundwater and Soil Science, Cottbus

We tested a new device for non-invasive soil moisture detection based on the principle of prepolarized surface-nuclear magnetic resonance (PP-SNMR) on a profile covering the transition from mineral to peat soil in the Gnarrenburger Moor in northwest Germany. This prototype has a size of 2.0 by 2.0m and consists of distinct coil systems for prepolarization, stimulation and detection of the proton magnetization of the soil water molecules in the Earth's magnetic field.

To provide ground truth for the in-situ measurements, the laboratory NMR experiments were carried out using undisturbed soil samples from the PP-SNMR measurement positions at depths between 0.0m to 0.66m.

However, the question arises how comparable the relaxation properties of PP-SNMR and laboratory NMR can be, because the latter works at artificial magnetic fields, i.e. at different Larmor frequencies ( $f_L$ ). To identify a possible frequency-dependency of the resulting relaxation time distributions (RTD), we used two NMR devices in the laboratory: a single-sided NMR system (PM25,  $f_L = 13.2$  MHz) and a core scanner (Helios,  $f_L = 0.5$  MHz).

Within their individual confidence intervals, the  $T_2$  RTDs measured in the laboratory are in accordance to each other and also to the RTDs of  $T_2^*$  in the field for relaxation times  $> 0.006$  s, which corresponds to the effective dead time of the PP-SNMR prototype.

As expected, no systematic differences in the water content estimations could be observed between two laboratory methods. However, the signal-to-noise ratio of the core scanner is strongly reduced compared to the single-sided device and leads thus to higher values of uncertainty.

We conclude that, at least for the  $T_2^*$  relaxation, laboratory NMR and PP-SNMR lead to comparable results, i.e. laboratory studies can support PP-SNMR field campaigns, e.g. with calibration data for water retention parameter estimations. However, this observation does not hold for the  $T_1$  relaxation behavior, for which a strong frequency dispersion, at least for weakly decomposed peat soils, is evident.

Our future studies aim on the relationship between NMR relaxation time distribution and the water retention properties of peat soils.

## **P-OG-09**

### **Evaluation of compaction measures on liquefaction susceptible dumps by means of surface-NMR**

**T. Hiller<sup>1</sup>, S. Costabel<sup>2</sup>, G. Erdmann<sup>1</sup>, E. Schönenfeldt<sup>1</sup>**

<sup>1</sup>Bundesanstalt für Geowissenschaften und Rohstoffe, Cottbus,

<sup>2</sup>Bundesanstalt für Geowissenschaften und Rohstoffe, Berlin

In the last 15 years, a sudden spike of liquefaction events after groundwater rebound on inner dumps in the Lusatian mining district resulted in around 30,000 hectares of land closed to public access. Therefore, these restricted areas are unavailable for their designated use. One of the common modern remediation and compaction methods used is the gentle-blast-compaction (GBC), in which minimal explosive charges are placed in defined depth horizons (below the groundwater table) and detonated one after the other from the bottom upwards. The primary objective is to improve the ground stability by locally collapsing the pore structure of the material. This increases the bulk density of the dump material and reduces the air and water-filled proportion of the pore space.

Usually, direct methods like core drillings are used to verify successful compaction. Instead, within the "VerLaUf" project, we want to investigate the suitability of various airborne and ground-based geophysical methods for non-invasive verification of compaction. Here, in this particular study, we evaluate the applicability of surface nuclear magnetic resonance (SNMR). Due to the direct correlation between SNMR signal amplitude and water content (porosity) as well as SNMR relaxation time and pore size, the SNMR method promises not only qualitative but also quantitative statements about the change in the water-filled pore space after GBC. The first field campaign was carried out in fall 2023 before the GBC started. We repeated our SNMR measurements in summer 2024 a few weeks after the GBC. Already in 2023 we determined a reference point approx. 400 m away from the GBC zone to rule out any seasonal variations in the data interpretation. For the reference point, we use identical measurements settings as for the measurements on top of the GBC zone. Unfortunately, not all measurements on the GBC zone showed comparable noise conditions between the 2023 and 2024 campaigns and therefore a direct comparison of the inversion results is difficult. For measurements with comparable noise conditions, a clear reduction of signal amplitude and relaxation time (both by about 17%) is visible for the saturated part of the dump, indicating that the SNMR measurements are suitable to qualitatively detect the compaction of the saturated pore space due to the gentle blast compactions.

## **P-OG-10**

### **Geophysikalische Beiträge zur multidisziplinären Rekonstruktion des Bleichesee in der Egeraue in Nördlingen, Süddeutschland**

**M. Pohle<sup>1</sup>, M. Bauckholt<sup>1</sup>, E. Zvara<sup>2</sup>, S. Pejdanović<sup>3</sup>, I. O. Nießen<sup>4</sup>, L. Werther<sup>5,6</sup>,**

**P. Kühn<sup>3</sup>, C. Zielhofer<sup>2,4</sup>, U. Werban<sup>1</sup>**

<sup>1</sup>Helmholtz-Zentrum für Umweltforschung GmbH - UFZ, Leipzig,

<sup>2</sup>Institut für Geographie, Universität Leipzig, Leipzig,

<sup>3</sup>Bodenkunde und Geomorphologie, Forschungsbereich Geographie, Eberhard Karls Universität Tübingen, Tübingen,

<sup>4</sup>Arbeitsgruppe Historische Anthroposphären, LeipzigLab, Universität Leipzig, Leipzig,

<sup>5</sup>Ur- und Frühgeschichte und Archäologie des Mittelalters, Eberhard Karls Universität Tübingen,

<sup>6</sup>Deutsches Archäologisches Institut, Römisch-Germanische Kommission, Frankfurt

Die Stadt Nördlingen zählt zu den wenigen großflächig erhaltenen mittelalterlichen Städten Deutschlands. Im Mittelalter war Nördlingen ein Zentrum der Gerberei und Färberei, was die

Wasserbauten entlang der Eger prägte und somit erhebliche Auswirkungen auf die stadtnahen Auen hatte. Der SPP 2361 „Auf dem Weg zur Fluvialen Anthroposphäre“ hat seinen Schwerpunkt auf der Erforschung solcher vorindustriellen Auen Mitteleuropas und deren Entwicklung. Innerhalb des Teilprojektes „Lokale Pfade zur Fluvialen Anthroposphäre an Echaz (Rhein) und Eger (Donau)“ steht die multidisziplinäre Rekonstruktion der Landnutzung der Auen und die Rekonstruktion der Auswirkungen des städtischen Handwerks und der Abfallentsorgung auf die Auenverschmutzung im Fokus. Hierzu kommen multidisziplinäre Ansätze zum Einsatz, darunter die Digitalisierung von Altkarten, die Integration digitaler Geländemodelle, geophysikalische Untersuchungen und die Analyse von Sedimentkernen aus der Egeraue.

Wir präsentieren die Ergebnisse geophysikalischer Untersuchungen im Rahmen der umfassenden Auenerkundung am Bleichesee/Nördlingen, bei der wir (1) die elektromagnetische Induktion (EMI) zur flächendeckenden Erfassung und (2) die elektrische Widerstandstomographie (ERT) zur transektweisen Kartierung einsetzen. Wir konnten mit diesem kombinierten Ansatz die Schotterkörper der Eger, die durch eine grobkörnige Verteilung gekennzeichnet sind, effektiv abgrenzen und Regionen mit feinkörnigen Auenablagerungen sowie anthropogene Verfüllungen identifizieren. Auf der Grundlage dieser Erkenntnisse wurden Standorte für Rammkernsondierungen zur detaillierten Sedimentansprache ausgewählt. Zusätzliche konnten Direct push-gestützte Erkundungen vertikal hochauflöste Informationen verschiedener Untergrundparameter (elektrische Leitfähigkeit, Farbspektrum, hydraulische Leitfähigkeit usw.) liefern, wobei wir uns am Standort Nördlingen bei der Untersuchung des Bleichesees auf Farbprofile fokussierten. Diese wurden entlang eines Transektes im Abstand von 25 Zentimetern abgeteuft und liefern so eindrucksvolle Einblicke in die Ablagerungen und Auffüllung des früheren Bleichesees.

Gegenwärtig werden die Ergebnisse der geophysikalischen Messungen und in-situ Beschreibungen mittels Rammkernsondierung sowie die umfangreichen Laboranalysen der Sedimentproben zusammengeführt. Ziel ist die chronostratigraphische Beschreibung der Egeraue und ihrer Belastungsgeschichte.

## **P-OG-11**

### **Mit Georadar auf der Suche nach Sedimentumlagerungen zur Ostseesturmflut vom 20.10.2023**

**M. Scharnweber, A. Knies, E. Erkul, T. Wunderlich, C. Winter**

*Institut für Geowissenschaften CAU, Kiel*

Sturmfluten mit landunter kennt man in Deutschland vor allem von der Nordsee, doch auch in der Ostsee kann es zu folgenschweren Sturmfluten kommen. Am 20. Oktober 2023 hat eine solche Sturmflut die schleswig-holsteinische Ostseeküste getroffen. Dabei handelte es sich um die schwerste Ostseesturmflut seit 1872 mit Pegelständen von über 2m. In Folge dieser Sturmflut wurden Häfen, Boote und Küstenabschnitte zerstört, wodurch ein Sachschaden in Höhe von ca. 200 Millionen Euro entstand. Mithilfe von Georadar-Messungen und küstengeologischen Untersuchungen wurden nach der Sturmflut Sedimentumlagerungen auf der Halbinsel Schleimünde im Nordosten von Schleswig-Holstein untersucht. Mit einer Dualfrequenzantenne wurde auf einem Strandabschnitt zwischen der Ostsee und dem Meeresarm Schlei gemessen, um die Auswirkungen auf den Schichtaufbau bis in eine Tiefe von 2 m zu erkunden. Dabei konnten in den Radargrammen Reflektoren erkannt werden, die in den geologischen Schnitten bestimmten Schichten zugeordnet werden konnten. Eine in den Schnitten sichtbare Grasnarbe korreliert in den Radargrammen mit einem besonders starken Reflektor, welcher als Geländeoberfläche vor der Sturmflut identifiziert werden konnte.

Somit konnte durch die Kombination von Georadar-Messungen und küstengeologischen in-situ Untersuchungen eine Sedimentumlagerung in Form eines Washovers von 20-100 cm Mächtigkeit festgestellt und die Geländeoberfläche vor der Sturmflut rekonstruiert werden.

## **P-OG-12**

### **Revealing hidden polygonal networks in saline alluvial sediments in the Atacama Desert using ground-penetrating radar**

**P. Schwarze<sup>1</sup>, J. Igel<sup>2</sup>, B. Arrué Blanco<sup>2</sup>, C. Sager<sup>3</sup>, A. Airo<sup>3</sup>, J. Feige<sup>3</sup>**

<sup>1</sup>*Universidad de Chile, Departamento de Geofísica, Facultad de Ciencias Físicas y Matemáticas, Santiago, Chile,*

<sup>2</sup>*LIAG - Institut für Angewandte Geophysik, Hannover,*

<sup>3</sup>*Museum für Naturkunde, Leibniz-Institut für Evolutions- und Biodiversitätsforschung, Berlin*

Polygonal networks are prominent near-surface features in saline environments of the hyper-arid Atacama Desert, Chile. These fracture networks in the alluvial sediments consist of salt-poor sand wedges that outline gypsum-rich polygons of approx. 1-5 m in diameter. These structures are often covered by a thin layer of dust and sand. While similar ground patterns in periglacial environments have been investigated with geophysical methods like ground-penetrating radar (GPR), the hyper-arid polygons in the Atacama Desert have not been geophysically characterised so far. They differ from their periglacial analogues by lower water contents, higher soluble contents and a formation based on gypsum dehydration and thermal contraction in salt-cemented soils. We performed 2D and 3D GPR surveys on alluvial surfaces in the Yungay area of the Atacama Desert. Despite the high salinity of the subsurface, our GPR mapping using 400 MHz antennas reaches up to 3 m depth. Below this depth, the GPR performance drops quickly, likely due to a highly conductive layer causing high electromagnetic wave attenuation. The timeslice analysis of a 3D GPR dataset of 10 m x 10 m revealed distinct polygonal structures at shallow depth. Validation was achieved through aerial photographs of a subarea of the grid, taken after the surface cover has been removed. These images confirmed the measured spatial distribution of polygons and their adjacent sand wedges observed in the GPR amplitude pattern. This study demonstrates the capability of GPR to detect and map shallow polygonal structures even when hidden by dust and sand, where traditional drone mapping techniques are ineffective. The study of polygonal networks in the Atacama Desert offers valuable insights for understanding patterned ground on Earth and potentially on Mars.

## **P-OG-13**

### **Vergleich aktiver und passiver seismischer Messungen am Deich des Tümlauer Koogs (Dithmarschen)**

**F. Al Tawashi<sup>1</sup>, D. Köhn<sup>1</sup>, C. Weidle<sup>1</sup>, L. Wiesenbergs<sup>1</sup>, D. Wilken<sup>1</sup>, R. Kirsch<sup>2</sup>, T. Meier<sup>1</sup>**

<sup>1</sup>*Geowissenschaften, Geophysik, Kiel,*

<sup>2</sup>*GEOIMPULS GmbH, Frankfurt*

Die vorliegende Studie untersucht die interne Struktur und den Zustand des Deiches im Tümlauer Koog, Schleswig-Holstein, durch die Kombination aktiver und passiver seismischer Messungen. Mittels Full Waveform Inversion (FWI) wurden Daten einer SH-Wellenmessung entlang eines Profils senkrecht zum Deich viskoelastisch nach der SH-Wellengeschwindigkeit und der Dichte invertiert, wobei die Topographie des Deichs berücksichtigt wurde. Oberflächennahe Schichten weisen in der Regel niedrige Geschwindigkeiten und Dichten (Klei) auf, während darunter sandiges Material höhere Geschwindigkeiten und Dichten auftreten. Die Ergebnisse korrelieren mit der anhand von Sondierungen bestimmten Lithologie.

Zusätzlich wurde über 14 Tage ein passives seismisches Monitoring durchgeführt. Die Spektrogramme zeigen zeitliche Änderungen des seismischen Rauschens im Frequenzbereich von 1 bis 40 Hz. Besonders bemerkenswert waren die zeitlichen Variationen des H/V-Verhältnisses

im Bereich von 2 bis 30 Hz, die als Indikatoren für Veränderungen des Wassergehalts im Deich interpretiert werden. Eine Array-Analyse des seismischen Rauschens ermöglichte die Untersuchung der Ausbreitungsrichtung des Hintergrundrauschens, wobei tiefere Frequenzen aus allen Richtungen und höhere Frequenzen hauptsächlich aus dem Norden stammten. Seismisches Rauschen mit hohen Amplituden kommt vorwiegend aus dem West-Nordwesten und wird daher wahrscheinlich durch die Nordsee angeregt. Mittels Array-Analyse (Beampower und Slowness) sowie anhand der aus ambient noise bestimmten Greenscher Funktionen wurde eine zeitliche Variabilität mit Perioden von 12 und 24 Stunden beobachtet. Diese Ergebnisse belegen das Potenzial passiver seismischer Messungen zur Detektion und zum Monitoring zeitlicher Veränderungen des Deichzustands. Zur Bewertung der Qualität der aus ambient noise berechneten Greenschen Funktionen wurden diese mit Vorwärtsmodellierungen verglichen, die auf den Ergebnissen der aktiven Scherwellenseismik basierten. Die Analyse ergab, dass sowohl P-Wellen als auch Oberflächenwellen in den Greenschen Funktionen identifiziert und für das Monitoring genutzt werden können.

## **P-OG-14**

### **Erkundung von Lagerungsdefekten und Hohlräumen im Bereich von Entwässerungssystemen mittels Georadar**

**M. Lorenzen<sup>1,2</sup>, D. Grundke<sup>2</sup>, M. Bücker<sup>3</sup>**

<sup>1</sup>*Institut für Geophysik und extraterrestrische Physik, TU Braunschweig, Braunschweig,*

<sup>2</sup>*GEO-LOG Ingenieurgesellschaft mbH, Braunschweig,*

<sup>3</sup>*Institut für Geowissenschaften, Christian-Albrechts-Universität zu Kiel, Kiel*

Eine intakte Lagerung und Bettung von Kanälen ist essenziell für den langfristigen Betrieb von Entwässerungssystemen. Zur Untersuchung können neben direkten Untersuchungen des Erdreichs, wie Aufgrabungen oder Probenahmen, auch indirekte geophysikalische Methoden eingesetzt werden. Diese basieren auf den physikalischen Eigenschaften des Bodens, die durch Dichteänderungen im Untergrund beeinflusst werden.

Im Rahmen dieser Untersuchung wurde die Anwendung von Georadar (Ground Penetrating Radar, GPR) zur Detektion von Lagerungsdefekten und Hohlräumen in Entwässerungssystemen untersucht. Ziel war es, praktische Messungen durchzuführen, um die Eignung von Georadar als zerstörungsfreies Verfahren zu bewerten und Daten zur Erkennung von Anomalien physikalischer Parameter (rel. Permittivität, elektrische Leitfähigkeit) im Untergrund bereitzustellen.

Die Messungen fanden, unter Verwendung von Einkanalsystemen mit Antennen (400 MHz, 500 MHz, 1000 MHz), an drei Standorten im Kanalnetz der Stadt Braunschweig statt. Es wurden rechtwinklige Messraster mit Messlinienabständen von 0,1 m bis 1 m vermessen. Die Messlinien verliefen parallel und quer zum Kanalverlauf. Die Auswertemethodik umfasste die Kalibrierung der Ausbreitungsgeschwindigkeit (Anpassung von Diffraktionshyperbeln), Erstellung von Radargrammen und Interpretation von Reflexionen und Diffraktionen. Zudem wurden 3D-Interpolationen und Tiefenschnitte erstellt.

Die Ergebnisse zeigen, dass Lagerungsdefekte und Hohlräume abhängig von den geologischen und hydrogeologischen Bedingungen detektiert werden können. An einem Standort schränkte ein hoher Grundwasserstand die Untersuchung durch starke Signaldämpfungen ein. An einem anderen Ort konnten die Abwasserkanäle trotz hoher Wassergehalte im Untergrund identifiziert werden. Am dritten Standort wurde ein offener und damit direkt nachweisbarer Hohlraum vermessen, der als Referenz für die Hohlraumdetektion mit Georadar dient.

Zusammenfassend erweisen sich Georadarmessungen unter geeigneten Bedingungen als effizientes Werkzeug zur Untersuchung von Entwässerungssystemen. Die Daten liefern wertvolle Referenzen für zukünftige Anwendungen, Regelwerke und Handreichungen, sowie für weiterführende Untersuchungen zu den Zusammenhängen zwischen Bodendichte und den für das Georadar entscheidenden physikalischen Eigenschaften des Bodens.

## **P-OG-15**

### **Erkundung von Bahnstrecken mithilfe eines 3D Georadar-Arraysystems.**

**N. Allroggen, T. Junghans, D. Hofmann**

*DB E&C, Georadar (I.TV-N-U-R), Bremen*

Die Zustandserfassung und Erkundung des Untergrundes von Bahntrassen erfolgt heutzutage immer noch anhand von Bohrungen in definierten Abständen. Ergänzend kommen dabei geophysikalische Messungen, insbesondere Georadarmessungen, zum Einsatz. Durch die schnelle und kontaktlose Datenaufzeichnung erlaubt das Georadarverfahren die Erkundung ganzer Bahnstrecken (mehrere hundert Kilometer) innerhalb eines Tages im Regelbetrieb und ohne Streckensperrungen. Mithilfe von Kalibrierungsbohrungen ist somit eine detaillierte und kontinuierliche Zustandserfassung möglich. Diese Informationen sind unerlässlich für die Instandhaltung und Optimierung der Schieneninfrastruktur, da potenzielle Problemzonen erkannt und Wartungsarbeiten frühzeitig geplant werden können, wodurch kostspielige Reparaturen oder Betriebsunterbrechungen vermieden werden.

Bisher werden bei Georadarbefahrungen vorwiegend einzelne Profile ausgewertet. Durch die Entwicklung schnellfahrender 3D-Georadar-Arraysysteme ist es inzwischen möglich, 3D-Georadarmessungen auf Bahnstrecken durchzuführen. Jedoch ist das Potential solcher 3D-Datensätze bisher kaum untersucht worden und erfordert nicht nur aufgrund der räumlichen Ausdehnung von mehreren Kilometern Länge und einer Breite und Eindringtiefe von wenigen Metern spezielle Auswertungs- und Interpretationsmethoden.

In dieser Studie wollen wir einen solchen 3D-Georadar-datensatz vorstellen, der entlang einer Teststrecke erhoben wurde. Dabei untersuchen wir die Datenqualität und bearbeiten die Daten sowohl als 2D- als auch als 3D-Datensatz. Außerdem untersuchen wir, welche Bearbeitungsschritte die Qualität der Daten erhöhen können und somit die Interpretation erleichtern. Zusammenfassend zeigt unsere Studie, dass die Auswertung von 3D-Georadar-daten ein erhebliches Potenzial für die Zustandsüberwachung und Erkundung von Bahntrassen birgt. Die kontinuierliche und flächendeckende Datenaufnahme ermöglicht es, umfassende Einblicke in den Untergrund zu gewinnen und notwendige Maßnahmen zur Instandhaltung frühzeitig und präzise zu planen. Wir hoffen, dass unsere Forschung einen wichtigen Beitrag zur Weiterentwicklung dieser Technologie leistet und die Grundlage für zukünftige Anwendungen und Studien bildet.

## Geologische Eis-Wärme-Speicher – Reflexionsmessungen mittels Bohrlochgeoradar als Methode zur Abbildung von Gefrier- Tauzyklen in oberflächennahen Aquiferen

A. Burzik<sup>1</sup>, P. Jung<sup>1</sup>, M. Pohle<sup>1</sup>, G. Hornbruch<sup>2</sup>, A. Dahmke<sup>2</sup>, U. Werban<sup>1</sup>

<sup>1</sup>Helmholtz-Zentrum für Umweltforschung - UFZ, Leipzig,

<sup>2</sup>Christian-Albrechts-Universität zu Kiel, Kiel

Eis-Wärme-Speicher (EWS) basieren auf der Nutzung freigesetzter latenter Wärme beim Gefrieren eines Speichermediums. Das gefrorene Medium dient dabei als Kältespeicher für Kühlperioden. Statt der bisher angewendeten kosten- und flächenintensiven Nutzung konventioneller Eis-Wärme-Speichersysteme (z.B. vergrabene Tanks), fokussiert sich das BMBF geförderte Verbundprojekt von CAU Kiel, UFZ Leipzig und IEG Bochum „GEWS“ (Entwicklung und Bau eines tiefenhorizontierten Geologischen Eis-Wärme-Speichersystems als Demonstrationsanlage auf dem Testfeld TestUM / Wittstock) auf die Übertragung des Eisspeicherprinzips auf den geologischen Untergrund und die Nutzung von Grundwasserleitern als Speichermedium. Hierfür wurden 4 x 4 Erdwärmesonden im Abstand von 1m zueinander zur Vereisung eines oberflächennahen quartären Aquifers installiert. Während mehrerer Tau- und Gefrierzyklen wurden energetische Effizienz, Bodendeformation sowie geochemische und mikrobiologische Veränderungen im Grundwasserleiter untersucht und mit numerischen Simulationen sowie Laborversuchen begleitet.

Da sich Permittivität und Widerstand des wassergesättigten Bodens beim Gefrieren stark ändert, eignet sich der Ansatz mittels Bohrloch-Georadar die Grenzfläche von gefrorenem zu ungefrorenem Untergrund abzubilden. Im Reflexionssetup erscheint der Eiskörper somit als Reflektor. Während des Projekts hat sich gezeigt, dass besonders die Reflexionsmessungen Rückschlüsse auf die Änderung der Größe des Vereisungsbereichs ermöglichen. Als Referenz für die Signalveränderung dienten Baselinemessungen im Testfeld, wobei störende Reflexionen von Messstellen und EWS-Sonden auftraten und beachtet werden mussten.

Wir präsentieren die Ergebnisse der Reflexionsmessung aus dem Zeitraum zwischen August 2023 und Juli 2024. Dabei wird sich auf drei Messstellen im Anstrom, drei Messstellen im Abstrom und zwei zentral gelegene Messstellen konzentriert. Es ist erkennbar, dass die Grundwasserströmung einen erheblichen Einfluss auf die Entwicklung des Vereisungsbereichs hat. So ist der Tauprozess im Anstrom aufgrund des natürlich anströmenden wärmeren Grundwassers schneller als der Tauprozess im Abstrom. Mit der abgeschätzten Genauigkeit der Reflexionsmessung von  $\pm 0,1\text{m}$  lässt sich die Gesamtausdehnung des Vereisungsbereichs in südwest-nordost Richtung auf  $\pm 0,2\text{m}$  bestimmen.

## **P-OG-17**

### **Einbau geophysikalischer Sensoren zur Rissdetektion an einem Demonstrationsbauwerk**

**L. I. Pascharat<sup>1</sup>, C. Friedrich<sup>1</sup>, S. Schennen<sup>1</sup>, F. Mielentz<sup>2</sup>, U. Effner<sup>2</sup>, H. Stolpe<sup>2</sup>, M. Behrens<sup>2</sup>, M. Sobiesiak<sup>3</sup>, K. Plenkers<sup>3</sup>, T. Fischer<sup>3</sup>**

<sup>1</sup>Bundesgesellschaft für Endlagerung mbH (BGE), Peine,

<sup>2</sup>Bundesanstalt für Materialforschung und -prüfung (BAM), Berlin,

<sup>3</sup>Gesellschaft für Materialprüfung und Geophysik (GMuG), Bad Nauheim

Im Rahmen eines In-situ-Versuchs wurde ein Demonstrationsbauwerk unter Tage in einem Salzbergwerk errichtet. Hierbei sollen die technische Herstellbarkeit und Handhabbarkeit für ein Streckenabdichtungssegment nachgewiesen sowie die Eigenschaften des Demonstrationsbauwerks untersucht und bewertet werden. Wesentlicher Teil des Untersuchungsprogramms sind stationäre geotechnische und geophysikalische Messungen während der Herstellung des Demonstrationsbauwerkes bis zum weitestgehenden Wiedererreichen der Ausgangstemperatur des Gebirges.

Zur Rissüberwachung während des Betonagezeitraums und im Anschluss wurde ein geophysikalisches Messsystem bestehend aus Mikroakustiksensoren und Ultraschallprüfköpfen installiert. Dabei ist die Aufgabe der Mikroakustik die Aufzeichnung und Lokalisierung der hochfrequenten seismischen Ereignisse. Mit den Ultraschallprüfköpfen werden die seismischen Geschwindigkeiten und deren Änderungen beobachtet und bestimmt.

Die gegebenen Randbedingungen beim Aushärten des Baustoffs (erwartete Temperaturen bis 110 °C und Drücke bis 5 MPa) führten zu technischen Herausforderungen beim Einbau und bei der Durchführung der Messungen.

## **P-OG-18**

### **Beispiele für die Detektion von Feuchtigkeit in Mauerwerk mittels Thermografie**

**Y. E. Esel<sup>1</sup>, N. Isik<sup>2</sup>, S. Jahani<sup>2</sup>, D. Schulte-Kortnack<sup>2</sup>, E. Erkul<sup>2</sup>, D. Köhn<sup>2</sup>, T. Meier<sup>2</sup>**

<sup>1</sup>Deutsche Bundesstiftung Umwelt - DBU, Osnabrück,

<sup>2</sup>Institut für Geowissenschaften – Christian-Albrechts-Universität zu Kiel, Geophysik, Kiel

Die Infrarot-Thermografie (IRT) stellt eine effektive, zerstörungsfreie und berührungslose Methode zur Erkennung und Visualisierung von Strukturen von Mauerwerk, Schadstellen sowie Feuchtigkeit dar. Dabei wird die von den zu untersuchenden Oberflächen abgestrahlte Infrarotstrahlung für die Durchführung von Temperaturmessungen genutzt. Die Erkennung von Feuchtigkeit erfolgt auf Basis von Temperaturunterschieden bzw. geringeren Temperaturänderungen. Im Rahmen der Untersuchungen wurde Ziegelmauerwerk an zwei historischen Kirchen analysiert, nämlich an der St. Nikolai-Kirche in Flensburg (Schleswig-Holstein) und an der St. Jacobi-Kirche in Neuenkirchen (Kreis Dithmarschen, Schleswig-Holstein). Die Nikolai-Kirche ist ein im 14. und 15. Jahrhundert errichteter Backsteinbau. Die St. Jacobikirche wurde ebenfalls im 14. Jahrhundert erbaut, diese wurde allerdings nach Bränden 1704 und 1729 durchgreifend erneuert. Mittels passiver IRT-Messungen wurden die Innenwände beider Objekte sowie an der St. Jacobi-Kirche die Außenwände untersucht. Im Zuge der Untersuchungen wurden kontinuierliche Temperaturmessungen über Zeiträume von zwei bis achtzehn Stunden durchgeführt. Anhand ausgewählter Beispiele erfolgt eine Erläuterung der digitalen Bearbeitung der Daten, der gemessenen zeitlichen Temperaturänderungen (Thermogramme), der mittleren Temperaturunterschiede sowie der zeitlichen Variabilität der Temperatur. Die Ergebnisse der IRT-Messungen werden mit punktuellen in – situ Untersuchungen im Mauerwerk verglichen.

## **P-OG-19**

### **Investigation of Hydrodynamics in Carbonate Rock with Ground Penetrating Radar**

**A. Rieß<sup>1,2</sup>, P. Dietrich<sup>1,2</sup>**

<sup>1</sup>*Helmholtz Zentrum für Umweltforschung - UFZ, Monitoring und Erkundungstechnologien, Leipzig,*

<sup>2</sup>*Eberhard Karls Universität Tübingen, Umwelt- und Ingenieurgeophysik, Tübingen*

Carbonate rock aquifers are an important resource in the face of water scarcity. However, the hydrodynamic processes of the heterogeneous medium are not fully understood. It is necessary to investigate the shallow, weathered zone as the key to drainage, transport and storage. Geophysical techniques are promising, particularly ground penetrating radar (GPR) due to its sensitivity to moisture.

The potential of GPR to investigate hydrogeological structures was experimentally tested in the Lower Muschelkalk of the Rüdersdorf limestone quarry near Berlin. A densely gridded survey field was monitored under three different moisture conditions. Zero offset profiles were measured along the stratigraphic dip with 200 MHz surface GPR and additional perpendicular lines with common midpoint (CMP). The carefully processed radargrams were analysed using CMP semblance analysis, fitting of diffraction hyperbolas and superimposition of picked layers. The resulting EM wave velocities were used as a proxy to calculate water saturation with a petrophysical model for relative comparison.

A classification of moisture conditions based on the precipitation prior to the survey dates was ambiguous. The more generic CMP results were similar to each other and significantly higher than the velocities from the diffraction hyperbolas representing the very local position. The latter showed spatial differences that corresponded to the partly distorted reflections in the otherwise well matching picked layers. This concludes a matrix-dominated hydraulic system with long-term persistent water saturation. Diffraction hyperbolas could form at pronounced fractured-porous zones with increased water storage and hence high dielectric contrast. Preferential flow paths are provided, draining water to bedding planes. Considering the scattered occurrence of hyperbolas, they may indicate precursors of possible sinkholes.

The combination of different analytical methods with focus to EM wave velocities allowed meaningful systemic conclusions to be drawn. In addition, the GPR showed satisfactory data reproducibility throughout the survey dates. Despite the limited penetration depth of 4 metres, these qualities make GPR suitable for integration into hydrological studies in carbonate rocks. The collected dataset offers many opportunities for further analysis approaches.

## **P-OG-20**

### **Comparing Attenuation-Based Methods for Sediment Classification from Sub-Bottom Profiling**

**M. Ibrahimli, A. Schenk**

*Karlsruher Institut für Technologie, Institut für Photogrammetrie und Fernerkundung, Karlsruhe*

Accurately classifying subsurface sediment is crucial for identifying and delineating valuable deposits like sand and gravel in quarry lakes, which are essential raw materials for various industries. Traditional methods for shallow subsurface sampling can be costly and inefficient. As a result, there is a growing need for cost-effective and reliable surveying techniques. Sub-bottom profiling, an echo-sounding technique, offers a promising solution. Recorded normal incidence reflections produce high-resolution seismic images of the subsurface which in turn can be used to obtain the geoacoustic properties of the sediments.

Attenuation-based methods focus on the frequency-dependent loss of energy in viscoelastic media. The grain size of the sediments can be determined through geoacoustic attributes such as the quality factor and relaxation time. The traditional Spectral Ratio (SR) method suffers from interference effects caused by thin reflecting beds. Instantaneous frequency (IF) series calculation is used to account for SR methods limitations but it too suffers from noise pollution. However, enhanced robust signal processing methods have been applied to address these issues.

In this work, we compare different attenuation-based methods by analyzing synthetic data obtained by nonstationary convolution of a particular forward Q filter on a modeled reflectivity series. IF series are calculated using the Hilbert transform method and through the Wigner-Ville Distribution. Moreover, attributes are calculated from the decomposed modes of a synthetic signal obtained by Variational Mode Decomposition.

The results of the different methods are compared, and the advantages over traditional approaches are discussed, highlighting their potential for more accurate and efficient sediment classification.

## **P-OG-21**

### **Transient Electromagnetic Investigation of Sediment Deposits in the Yungay Claypan, Atacama Desert, Chile**

**J. Dielmann<sup>1</sup>, B. Blanco Arrué<sup>2</sup>, B. Tezkan<sup>1</sup>, A. Airo<sup>3</sup>, P. Yogeshwar<sup>1</sup>**

<sup>1</sup>*Institut für Geophysik und Meteorologie, University of Cologne, Köln,*

<sup>2</sup>*LIAG - Institut für Angewandte Geophysik, Hannover,*

<sup>3</sup>*Leibniz-Institut für Evolutions- und Biodiversitätsforschung, Museum für Naturkunde, Berlin*

In the frame of the CRC-1211 and NoSHADE projects, we carried out a transient electromagnetic survey in the Yungay claypan in the Atacama Desert, Chile. The aim was to detect sediment sequences above bedrock and improve the understanding of the region's paleoclimate and paleolandscape.

The survey covered two main profiles with in total 28 soundings. The ABEM WalkTEM system was used in a central loop configuration with a 40 m x 40 m loop size. We used the obtained data with a robust processing scheme to analyze the TEM data and compared the results with those from commercial software.

Standard Occam and Marquardt inversion techniques were used to receive electrical resistivity distribution of the sediment layers and underlying bedrock. The models were stitched together into two main profiles as 2D resistivity depth section and interpreted in a geological context. The model mainly reveals a five-layer subsurface structure.

The detected depth to basement was highly variable, ranging from 50 to 200 meters. We identified two highly conductive layers with a resistivity of 6 Ωm, suggesting multiple flooding events in the claypan, likely linked to two distinct rain or lake phases, during which the claypan was filled with sediments and water. The results also indicate a possible dry period between the two lake phases. Of particular interest is a lower conductive layer that extends southward and forms a distinct gutter. We infer that the water flow direction was likely from west to east.

## **P-OG-22**

### **Landscape reconstruction of the Hebros delta**

**M. Thorwart<sup>1</sup>, W. Rabbel<sup>1</sup>, H. Brückner<sup>2</sup>, A. Dan<sup>3</sup>, C. Karadima<sup>4</sup>, D. Terzopoulou<sup>5</sup>, S. Baris<sup>6</sup>, D. Caka<sup>6</sup>**

<sup>1</sup>*Kiel University, Institute for Geoscience, Kiel,*

<sup>2</sup>*University of Cologne, Köln,*

<sup>3</sup>*CNRS/ENS Paris, Paris, France,*

<sup>4</sup>*Ephorate of Antiquities of Rhodope, Athen, Greece,*

<sup>5</sup>*Ephorate of Antiquities of Evros, Athen, Greece,*

<sup>6</sup>*Kocaeli University, Izmit, Turkey*

The Hebros plain was an important geographical spot in ancient times. In 480 BC, Xerxes assembled his land army and fleet in Doriskos on the north site of the Hebros plain. Ainos is located across the plain and was an trading hub, connecting the Balkan peninsula with the Aegean Sea. The Via Egnatia, which connected Dyrrachium on the Adriatic Sea and Byzantium (modern-day Istanbul), passed nearby. It is believed that the ancient coastline was further inland, forming a bay that has since been silted over by the advancing delta of the Hebros river.

Between 2022 and 2024, three field campaign were conducted using passive seismic measurements to investigate the uppermost geological structure of the Hebros plain and to uncover the ancient landscape. Nine mobile seismic stations were arranged in a mini-array to record the seismic noise for 15 min. The dispersion of the Rayleigh wave is derived from the data and a 1D shear wave velocity model is determined. Maps of the phase velocity and of the shear velocity are compiled. Soil samples were collected additionally in boreholes for age dating.

The most prominent feature is a former sandbar separating a lagoon southeast of Doriskos from the Mediterranean Sea. This is supported by the soil samples. Age dating suggests that the lagoon silted up around 300 BC.

## **P-OG-23**

### **Determination of Allowable Bearing Pressure for Geotechnical Engineering by Combining P- and S-Wave Seismic Refraction Data**

**E. G. Nwaka<sup>1,2</sup>, P. Dietrich<sup>1,2</sup>**

<sup>1</sup>*Helmholtz Centre for Environmental Research – UFZ, Department of Monitoring and Exploration Technologies, Leipzig,*

<sup>2</sup>*Eberhard Karls University of Tübingen, Department of Geosciences, Tübingen*

The allowable bearing pressure (ABP) is a fundamental geotechnical parameter for assessing foundation suitability, supporting construction planning, and mitigating geohazards such as sinkholes. The ABP can be calculated from P-wave and S-wave velocities, which allows for the possibility of getting spatially continuous maps of ABP with seismic surveys.

We illustrate the applicability of this approach with a case study from the Ammer Valley in Tübingen. Our survey was carried out at the margin of a floodplain where complex subsurface structures can be expected. We employed P-wave and S-wave seismic refraction techniques along a 142 m profile with 2 m geophone spacing. For the P-wave survey, an accelerated weight drop generated the seismic signal, while a sledgehammer was used for the S-wave survey on the same profile.

Repeated measurements were carried out to evaluate the accuracy of determining first arrival times. The first-arrival data were analyzed to derive the distribution of P-wave and S-wave velocity in the subsurface. The results of the seismic surveys are then combined to generate an image of the distribution of ABP. Finally, the ABP image will be interpreted in terms of floodplain margin structures. The result of our case study can then be used to evaluate the suitability of the approach for the investigation of larger floodplain margin areas.

## **P-OG-24**

### **Determination of Air Bubble Concentration in Fluids with Ultrasound: An Experimental Approach**

**J. Calderon<sup>1</sup>, M. Dormann<sup>1</sup>, T. Branß<sup>2</sup>, J. Aberle<sup>2</sup>, M. Balcewicz<sup>1</sup>, E. Saenger<sup>1</sup>**

<sup>1</sup>*Hochschule Bochum, Bochum,*

<sup>2</sup>*Technical University of Braunschweig, Braunschweig*

The DFG-funded König-Project is a long-term project focused primarily on the development of a multi-scale wave measurement laboratory to improve flow measurements in an industrial context. Part of this project consists of researching the propagation of ultrasound waves inside a moving fluid, a wide variety of flow scenarios are considered and new methods for ultrasonic measurement of flows can be developed and optimized. As a first step of the investigation, the preliminary results of air bubble concentration and the velocity profile inside a closed rectangular flume are presented in this work.

For this purpose, a modular system is used as an initiative to integrate manufacturer-independent measurement components with open-source software for the acquisition and processing of ultrasound signals. The modular system equipment consists of a multichannel system, which allows the positioning of several transceivers to send and receive ultrasonic waves from different directions along the experimental zone of interest. Classical low-frequency transceivers on the outer walls and submersible are provided, the submersible transceivers can be used to determine the velocity profile near the wall. Bubble concentration will be determined by measuring the reduced transit time caused by the added compressibility of the gas phase.

Characterizing multiphase flows using other techniques can be time-consuming and the accuracy can fall short as the complexity of the fluid grows. The use of ultrasound to characterize fluid flows has many advantages such: as a non-invasive method that doesn't alter the fluid path, real-time data acquisition, high-temporal resolution, it is cost-effective and can be used on opaque fluids. Therefore this technique is gaining more attention in several industrial applications, including oil and gas, hydrogen, and geothermal energy generation.

The results of this preliminary study will be validated with the output of a numerical simulation, in which the boundary conditions and the flow characteristics will be similar to the experimental setup. This first study is expected to serve as a preliminary step in the research program, in which several work packages are proposed. The outcome of this investigation includes determining the production volume in different oil and gas industries or geothermal power plants.

## **P-OG-25**

### **Determination of Air Bubble Concentration in Fluids with Ultrasound: A numerical approach**

**M. Dormann<sup>1,2</sup>, J. Calderon<sup>1,2</sup>, S. Humpert<sup>1</sup>, M. Balcewicz<sup>1</sup>, E. H. Saenger<sup>1,2,3</sup>**

<sup>1</sup>*Bochum University of Applied Sciences, Bochum,*

<sup>2</sup>*Ruhr University Bochum, Bochum,*

<sup>3</sup>*Fraunhofer IEG, Bochum*

The DFG-funded König-Project aims to deepen the understanding of the interaction between ultrasound waves and fluid flow by investigating particle movement or flow velocity. Both controlled laboratory experiments and real-world experiments are performed and compared with numerical results of digital twins.

The effective velocity of the propagation of elastic waves in a fractured solid medium is affected by the concentration of scatterers within. In industry applications, like the surveillance of pipelines, the concentration of gas bubbles within the transported fluids is of interest, we investigate the effect of the concentration of bubbles in a liquid on the propagation of ultrasonic waves. The study was performed experimentally and numerically for an ultrasound transmission measurement where a random uniform distribution of air bubbles was used in the numerical computation.

This work focuses on the numerical study and uses a rotated staggered finite-difference grid for the simulation of the elastic wave propagation. Results show a relation between the effective wave speed and the bubble concentration. Based on a series of tests, we determine the limits in which the method can be used. Future research will then expand the research to moving fluids, advancing the understanding of moving fluids in pipelines.

## **P-OG-26**

### **Rover-gestützte Geomagnetik**

**B. Jacobsen<sup>1</sup>, J. Börner<sup>1</sup>, P. Treichel<sup>2</sup>, T. Planitzer<sup>3</sup>, S. Min<sup>3</sup>, R. Pena<sup>3</sup>, K. Spitzer<sup>1</sup>**

<sup>1</sup>*TU Bergakademie Freiberg, Freiberg,*

<sup>2</sup>*Sächsisches Landesgymnasium St. Afra zu Meißen, Meißen, 3Neurospace GmbH, Berlin*

Rover-gestützte Geophysik kann eine Lücke in der oberflächennahen, hochauflösten Erkundung, die zwischen der klassischen, bodengebundenen Geophysik und der drohnen-gestützten Geophysik besteht, schließen. Sie ermöglicht z.B. die Exploration in gefährlichen Umgebungen, ohne dass der Gefahrenbereich betreten werden muss. Anwendungsfelder ergeben sich unter anderem in Bergwerken, Bereichen giftiger Gasaustritte durch vulkanische Aktivität, munitionsbelasteten Flächen, sowie im extraterrestrischen Maßstab.

Im Zuge der hier vorgestellten Arbeiten wurde am Beispiel der Geomagnetik die Machbarkeit und die Anwendung rover-gestützter geophysikalischer Erkundung untersucht. Dazu wurde in Zusammenarbeit mit der Neurospace GmbH der ferngesteuerte Rover MARVIN (Magnetometer equipped Remote controlled Vehicle for subsurface Investigation) konstruiert. Dieser baut auf der HiveR Roverplattform von Neurospace auf und ist u. a. mit Fluxgate-Magnetometern, GNSS-Positionierung und einer Stereokamera zur 3D-Erfassung der Umgebung ausgerüstet. Im Rahmen von Testmessungen auf der Insel Vulcano (Italien) wurde die Vergleichbarkeit zu herkömmlicher bodengebundener Geophysik hergestellt. Es konnte gezeigt werden, dass der entwickelte Rover die Messungen eines zum Vergleich eingesetzten Kern-Präzessions-Magnetometers akkurat reproduzieren kann. Dabei wurde

das Potential der rover-gestützten Geophysik, eine signifikant höhere Datendichte zu erreichen und kleinere Anomalien räumlich aufzulösen, verdeutlicht. Im Rahmen des Beitrages wird das Messsystem mit seiner Datenerfassung und -integration vorgestellt. Es werden Ergebnisse der Testmessungen gezeigt sowie Potentiale und Herausforderungen der Methodik diskutiert.

## PV – Potentialverfahren

### Poster

#### P-PV-01

### Crossing the scales and disciplines – petrological and geophysical investigations of hydrogen source rocks in the Münchberg Massif, NE Bavaria

M. Bagge<sup>1</sup>, P. Klitzke<sup>1</sup>, M. Hasch<sup>1</sup>, N. Koglin<sup>1</sup>, A. Ruppel<sup>1</sup>, J.-F. Goldmann<sup>1</sup>, A. Löwer<sup>2</sup>

<sup>1</sup>Federal Institute for Geosciences and Natural Resources (BGR), Hannover,

<sup>2</sup>iMAR Navigation GmbH, St. Ingbert

The investigation of hydrogen source rocks and potential hydrogen systems receives increasing attention in the context of the energy transition. Serpentinisation - the hydrothermal alteration of ultrabasic rocks into serpentinites - is identified as one fundamental process for natural hydrogen generation. The greater Münchberg Massif area offers a unique opportunity to investigate hydrogen source rocks. The Münchberg Massif is a metamorphic nappe complex with inverted metamorphic gradient within the Saxothuringian Zone of the Variscan orogen. Serpentinites are part of the Prasinit-Phyllit-Serie, which is the lowermost nappe and crops out in the southern and eastern part of the massif. The main body of this nappe is assumed to occur in about 3 km depth of the massif. The western part of the massif borders the Franconian Lineament, and further serpentinite bodies may occur west of the Franconian Linement beneath the Mesozoic sediments of the Franconian Basin.

In our study, we investigate the serpentinites of the Münchberg Massif using petrological and potential field data. For the petrological analysis (polarization microscope, X-ray diffraction, raman spectroscopy, major and trace element analysis), we collected 17 geological serpentinite samples at two locations, about 20 km apart. Furthermore, we measured magnetic susceptibility at the exposed serpentinites in the field. The recently acquired airborne geophysical data provides complementary information to the field investigation and includes magnetic and gravity data (strapdown gravimeter) acquired by helicopter at 1 km line spacing over the greater Münchberg Massif area. Preliminary results indicate a correlation between positive magnetic anomalies identified in airborne surveys and the mapped serpentinite bodies. The petrological results reveal different degrees of serpentinisation for the sampling locations. It might be possible that a residual potential for serpentinization and thus hydrogen generation still exists locally at depth.

## **Geoelectrical Monitoring of Soil Moisture Dynamics in Plant Ecosystems**

**J. Hoppenbrock<sup>1,2</sup>, M. Beyer<sup>3</sup>, M. Gerchow<sup>1,3</sup>, A. Iraheta<sup>3</sup>, M. W. Strohbach<sup>1,3</sup>, M. Bücker<sup>4</sup>**

<sup>1</sup>*Julius Kühn-Institut, Institute for Plant Protection in Horticulture and Urban Green, Braunschweig,*

<sup>2</sup>*TU Braunschweig, Institute of Geophysics and Extraterrestrial Physics, Braunschweig,*

<sup>3</sup>*TU Braunschweig, Institute of Geoecology, Braunschweig,*

<sup>4</sup>*Kiel University, Institute of Geosciences, Kiel*

Hydrogeophysical monitoring may aid the care and maintenance of plants, especially under stressful conditions like droughts or limited space for the tree's root system. Understanding soil properties and water flow paths in the soil can be an important contribution to managing plant health. Soil moisture, in particular, is a crucial factor that influences plant vitality and the overall ecosystem performance.

We conducted various Electrical Resistivity Tomography (ERT) measurements to better understand the hydrogeological properties of the substrate around plants and to identify water flow paths. Our study involves two experiments on different time scales: monitoring the water uptake by trees over several weeks and conducting infiltration monitoring experiments within a single day to gather insights into water distribution and flow paths in the subsurface. The ERT monitoring profiles were typically between 25 and 50 meters long with an electrode spacing between 0.5 and 1 m. In addition to the ERT data, Time-Domain Reflectometry (TDR) soil moisture sensor data are available for some of the profiles. For the data inversion process, we explored various time-lapse techniques using the pyGIMLi framework, evaluating their effectiveness for our specific objectives.

The time-lapse inversion shows promising results in both applications. For the monitoring of tree water uptake, increased resistivities were detected directly beneath the trees. In the infiltration experiments conducted over shorter timescales of several hours, the data revealed a fast propagation of the water front in the subsurface. By connecting these observations with the infiltration rate, we can determine the velocity of water propagation. Our results provide valuable insights into water movement, enhancing our understanding of the dynamics of water flow in the subsurface.

#### O-SM-01

#### Wie Wellenforminversion die seismische Abbildungsmöglichkeiten erweitert: Projekt Chatseis

T. Burschil<sup>1</sup>, D. Köhn<sup>2</sup>, M. Körbe<sup>3</sup>, J. Großmann<sup>4</sup>, G. Gabriel<sup>3,5</sup>, G. Firla<sup>6</sup>,  
C. Schmalfuß<sup>6</sup>, M. Fiebig<sup>6</sup>

<sup>1</sup>Bundesanstalt für Geowissenschaften und Rohstoffe, B3.2, Hannover,

<sup>2</sup>Christian-Albrechts-Universität zu Kiel, Kiel,

<sup>3</sup>LIAG-Institut für Angewandte Geophysik, Hannover,

<sup>4</sup>Bayerisches Landesamt für Umwelt, Hof,

<sup>5</sup>Leibniz Universität Hannover, Hannover,

<sup>6</sup>Universität für Bodenkultur Wien (BOKU), Wien, Austria

Das ICDP-Projekts DOVE rekonstruiert anhand von Bohrungen in glazial-übertieften Sedimentbecken überregional die Landschaftsentwicklung und Klimageschichte im Alpenraum (Anselmetti et al. 2022). Mit seismischen Methoden lassen sich dafür 1-D Bohrungsinformationen in den Raum projizieren und das Prozessverständnis erweitern. Zur Verbesserung der seismischen Abbildung wird im Projekt Chatseis Wellenforminversion (FWI) mit Reflexionsseismik kombiniert. Für diese methodische Entwicklung wurden Daten an zwei DOVE-Lokationen mit Vibrationsquellen und Sprengungen erhoben (Burschil 2024).

Hochauflösende Reflexionseismik bildet die Beckenstruktur bei Schäftlarn (ICDP site 5068\_3), 30 km südlich von München, ab. Horizontale Reflektoren unterhalb von 280 ms interpretieren wir als flachliegende Sedimente des Molassebeckens im bayerischen Alpenvorland. Geneigte Reflektoren in geringeren Tiefen deuten auf eine eiszeitliche Beckenverfüllung hin. S-Wellenprofile bestätigen das dieses Bild. Seismische Geschwindigkeiten aus Ersteinsatztomographie (FATT) und FWI der Sprengdaten passen gut zu den Reflektoren. Neben der geologischen Interpretation zur Klärung der thematischen Fragestellungen in DOVE sind nächste Schritte das Erweitern der FWI auf Vibroseisdaten und das Einbinden von Reflektoren als Guide für die FWI. Zudem wird das reflexionseismische Processing an die Geschwindigkeiten der FWI angepasst.

An der zweiten Lokation Bad Aussee im Salzkammergut (ICDP site 5068\_5), Österreich, bilden die Vibroseis Daten Reflexionen bis in 750 ms TWT ab, welche auf die eiszeitliche Beckenbasis hindeuten. Die beobachtete TWT lässt sich gut mit einem Bohrkern in Einklang bringen, welcher bis in 880 m Lockersedimente erbohrt hat. Entlang des Profils steigt die Reflexion bis knapp an die Oberfläche, was unsere Interpretation bekräftigt. Reflektoren oberhalb deuten auf eine interne Untergliederung der Beckenfüllung. Ein S-Wellenprofil an gleicher Lokation zeigt ebenfalls ansteigende Reflektoren. Da in Bad Aussee keine Sprengungen realisiert wurden, sind nächste Schritte das Erzeugen passender Startmodelle für die FWI aus FATT und S-Wellenprocessing.

Anselmetti et al. 2022: <https://doi.org/10.5194/sd-31-51-2022>

Burschil 2024: <https://doi.org/10.25928/pet1-6838>; <https://doi.org/10.25928/xpxw-y503>

Gefördert durch die Deutsche Forschungsgemeinschaft (DFG) – 497340281. Besonderer Dank gilt den Projektpartnern für die Durchführung der Sprengungen (B. Kröner, C. Veress) und der Gemeinde Schäftlarn.

## **O-SM-02**

### **Integration of borehole and 2D seismic processing velocities for velocity modeling in Schleswig-Holstein**

**D. Schindler**

*Landesamt für Umwelt des Landes Schleswig-Holstein, Geologischer Dienst Schleswig-Holstein,  
Flintbek*

Developing a large-scale velocity model of the deeper subsurface of Schleswig-Holstein requires a sufficiently high coverage of velocity data. Since check shot data measured at boreholes are available only sparsely across the area, it becomes necessary to incorporate additional sources of information into the development of a model. 2D seismic surveys in particular are much more widely distributed across Schleswig-Holstein than well data and hence cover the modeling region to a much larger extent.

In this presentation, I illustrate the application of an integrated approach that combines both sources of data for the development of a subsurface velocity model. In particular, I perform seismic processing at selected locations using 2D seismic data close to wells in order to determine a suitable velocity model. Since the accuracy of seismic processing velocities varies with depth, I derive confidence intervals for processing velocities that can later be used as a proxy for velocity uncertainties. Using two selected examples of seismic lines, I identify intervals in which the borehole data is outside the processing velocity confidence boundaries. This might be explained by low velocity zones and dipping reflectors.

## **O-SM-03**

### **Seismic site characterization for the Low-Seismic-Lab (Lausitz area)**

**O. Günaydin, F. Hloušek, M. Muhlanga, H. Näser, S. Buske**

*TU Freiberg, Institute of Geophysics and Geoinformatics, Freiberg*

The Low Seismic Lab (LSL) is planned to be built by the German Center for Astrophysics (DZA) in the Lausitz (Lusatia) area, and the same location is also proposed as one of the candidate sites to host the Einstein Telescope. Since one of the purposes of the LSL is to provide an environment of zero seismic noise, the geological setting in that area dominated by the Lusatian granodiorite massive seems favorable for that intention, however, the structural details of this unit and the overlying geological units including potential faulting have to be explored in detail.

For that reason, we conducted two active seismic surveys in that region close to Cunnewitz / Ralbitz-Rosenthal using P- and S-wave sources (Elvis VII): a preliminary single 276 m long 2D line with P- and S-wave sources and two main 2D lines perpendicular to each other with only P-wave source and profile lengths of 2 km and 1.6 km, respectively. All lines have been processed in time- and depth domains using post-stack and pre-stack migration approaches, including the construction of a detailed shallow P- and S-wave velocity model by first-arrival traveltime tomography. The results show a clear image of the shallow subsurface down to depths of approximately 500m with the top of the granodiorite formation at depths of approximately 50 m as the major structural feature

## **O-SM-04**

### **Bearbeitung und Analyse der 3D-Seismik Daten im Bereich der Asse-Salzstruktur (Niedersachsen)**

**N. Kühne<sup>1</sup>, L. Bräunig<sup>1</sup>, F. Hlousek<sup>1</sup>, S. Buske<sup>1</sup>, H. Ding<sup>2</sup>, M. Scholze<sup>2</sup>**

<sup>1</sup>*TU Bergakademie Freiberg, Institut für Geophysik und Geoinformatik, Freiberg,*

<sup>2</sup>*Bundesgesellschaft für Endlagerung, Peine*

Im Jahr 2020 wurde über der Salzstruktur „Asse“ in Niedersachsen eine umfangreiche 3D-Seismikmessung durchgeführt. Die konventionelle Auswertung dieser Daten lieferte ein klares Abbild der reflektierenden sedimentären Horizonte sowie des Salzstocks selbst.

Im Rahmen des Projekts **DOSIS** (Entwicklung eines optimierten, kombinierten und hochauflösenden Abbildungsverfahrens für die Standorterkundung radioaktiver Endlager) werden fortschrittliche seismische Bearbeitungs- und Auswertemethoden entwickelt und kombiniert, die über konventionelle Verfahren hinausgehen. Hauptziel ist dabei die Verwendung eines detaillierten, durch Wellenforminversion abgeleiteten, Geschwindigkeits- und Dämpfungsmodells für eine anisotrope anelastische Fresnel-Volumen-Migration und damit eine hochauflöste und quantitativ auswertbare Abbildung des Untergrundes. Wir haben den 3D-Seismik-Datensatz im Rahmen des Projektes für die folgenden Arbeiten verwendet:

Ersteinsatztomographie zur Ableitung eines detaillierten isotropen 3D P-Wellengeschwindigkeitsmodells. Das resultierende Modell zeigt hochauflöste Strukturen, die eine sehr gute Übereinstimmung mit der bekannten Geologie aufweisen, und wurde für die Anpassung und Erweiterung des oberflächennahen Teils im 3D-Migrationsgeschwindigkeitsmodell verwendet.

Fresnel-Volumen-Migration unter Verwendung isotroper und anisotroper Geschwindigkeitsmodelle, inkl. des o.g. abgeleiteten erweiterten 3D-Migrationsgeschwindigkeitsmodells.

Analyse der Aufzeichnungen der 3D-Seismik-Quellanregungen an Empfängern, die unterteg im Salzstock platziert waren. Dieser zusätzliche Datensatz wurde zum einen zur Verifizierung des abgeleiteten 3D-Geschwindigkeitsmodells verwendet, zum anderen wurde daraus auch ein reflexionsseismisches Abbild erstellt, das im Vergleich zum konventionellen 3D-Seismik-Ergebnis ein zum Teil detaillierteres Abbild der Reflektoren unterhalb des Salzstocks liefert.

## **SM – Seismik**

### **Poster**

## **P-SM-01**

### **Anisotropic anelastic Fresnel-Volume-Migration of the Asse 3D seismic data set**

**N. Kühne<sup>1</sup>, F. Hlousek<sup>1</sup>, S. Buske<sup>1</sup>, L. Bräunig<sup>1</sup>, V. Becker<sup>2</sup>, M. Scholze<sup>2</sup>**

<sup>1</sup>*TU Bergakademie Freiberg, Institute of Geophysics and Geoinformatics, Freiberg,*

<sup>2</sup>*Bundesgesellschaft für Endlagerung, Peine*

In 2020, a comprehensive 3D reflection seismic survey was conducted over the Asse salt structure in Lower Saxony, to support the planning of the retrieval of radioactive waste from the salt mine. While the data has already been processed using conventional seismic imaging

techniques, we present the results from applying the Fresnel-Volume-Migration (FVM) approach that we extended for considering anisotropy and anelastic attenuation. These enhancements aim to provide a more detailed and accurate characterization of the Asse region's complex geology, which is crucial for the safe planning and execution of the waste retrieval process.

A wavefront construction (WFC) technique was employed to calculate the required Green's functions for 3D anisotropic (TTI) velocity models. The WFC method was further extended to also calculate compensation traveltimes ( $t^*$ ) for spatially varying Q-models. These  $t^*$ -fields were then incorporated into the migration process to account for amplitude decay, phase shifts and dispersion due to anelastic attenuation, ultimately leading to a more accurate representation of subsurface reflectivity.

The method was applied to both synthetic 2D data as well as 3D subsets of the Asse seismic data set. Migration with anelastic compensation effectively corrected amplitude losses and phase distortions in the synthetic data. Furthermore, applying the anisotropic FVM to the 3D Asse data set significantly improved image quality. Additionally, the migration was performed in Common Offset Gather (COG) domain to facilitate muting of the corresponding Common Image Gathers (CIGs) and thereby significantly enhancing the quality of the resulting images.

Our study highlights the critical importance of integrating both anisotropy and anelastic attenuation into 3D seismic imaging to obtain reliable, high-resolution subsurface images. Accurate positioning and characterization of reflectors are essential for performing further quantitative seismic processing, e.g. AVO (Amplitude Versus Offset) analysis, which, in turn, facilitates more precise geological interpretations. The seismic imaging advancements developed here also offer promising applications for other applications, e.g. for mineral exploration, geothermal reservoir characterization, as well as within the radioactive waste disposal site selection process.

## P-SM-02

### A 3D high-resolution velocity model of the Asse salt structure (Lower Saxony)

L. Bräunig<sup>1</sup>, N. Kühne<sup>1</sup>, F. Hloušek<sup>1</sup>, S. Buske<sup>1</sup>, V. Becker<sup>2</sup>, M. Scholze<sup>2</sup>

<sup>1</sup>TU Bergakademie Freiberg, Institut für Geophysik und Geoinformatik, Freiberg,

<sup>2</sup>Bundesgesellschaft für Endlagerung, Peine

The project DOSIS („Development of an optimised combined high-resolution seismic imaging system for the investigation of nuclear waste disposal sites“) aims to facilitate finding answers for important geophysical and geological questions in the exploration of repository sites in Germany in the future, using methods like full-waveform inversion for velocity model building and focusing prestack depth migration techniques (e.g. anisotropic anelastic Fresnel-volume migration) for structural imaging. Precise mapping of structures in depth requires a well-resolved velocity model, which is crucial for prestack depth imaging. The principal aim of the 3D seismic survey acquired in 2020 was to increase the understanding of structural formations around the Asse salt mine.

We used the 3D surface seismic dataset for the derivation of a highly resolved P-wave velocity model for the shallow part of the study area (< 1 km) by first-arrival traveltime tomography. The dataset comprises more than 1.5 billion traces acquired by Vibroseis and explosive sources over an area of approximately 7.5 km x 5 km. Main parts of the velocity model building workflow comprise an effective first break picking for all traces and intense testing

of inversion parameters within the first arrival traveltime tomography. The results revealed a 3D velocity model of the upper 1 km with well-resolved structural details that will not only serve as input for the further application of prestack depth imaging and full waveform inversion but also directly contribute to the interpretation of the geological setting. We present the velocity model building workflow, embedding of the results in the geological interpretation, evaluation of the velocities using borehole data as well as a verification of the model using data from in-mine seismic stations that recorded the wavefield during the 3D surface seismic survey.

## **P-SM-03**

### **Reflection seismic imaging at the Asse salt structure from in-mine seismic recordings of a 3D surface seismic survey**

**F. Hlousek<sup>1</sup>, N. Kühne<sup>1</sup>, L. Bräunig<sup>1</sup>, S. Buske<sup>1</sup>, M. Scholze<sup>2</sup>**

<sup>1</sup>*TU Bergakademie Freiberg, Institut für Geophysik und Geoinformatik, Freiberg,*

<sup>2</sup>*Bundesgesellschaft für Endlagerung, Peine*

In 2020, a comprehensive 3D reflection seismic survey was conducted over the Asse salt structure in Lower Saxony, to support the retrieval of radioactive waste from the salt mine. The more than 40.000 shots (Vibroseis and explosives) of this survey were recorded not only by a large surface geophone array but also by 24 vertical-component geophones located within the Asse salt mine.

We used these in-mine data for reflection seismic imaging. To achieve this, we applied Fresnel-Volume-Migration to the 24 common receiver gathers. The assumption of the reciprocity principle allowed us to estimate the emergent angles at the surface, which are essential for Fresnel Volume Migration. The result shows a detailed image of the reflectors below the salt structure, which is in parts superior with improved structural details compared to the images derived from the surface seismic recordings.

## **P-SM-04**

### **Seismic Exploration for the Emerging Lunar Industry**

**O. Cornelius, D. Solis, P. Koch, J. de Freitas**

*IMENSUS UG (haftungsbeschränkt), Stuttgart*

Space agencies are preparing to return humans back to the Moon and establish a permanent presence there. Along with the growing interest in scientific exploration, a new economic sector is emerging. The success of infrastructure projects and In-Situ Resource Utilization (ISRU) missions (the extraction and use of lunar resources, such as regolith or water ice) depends on thorough geoscientific exploration: Infrastructure such as landing pads must be anchored, lava tubes for radiation shielding must be studied as potential future habitats, and exploration and extraction of resources must be planned and executed.

IMENSUS, a young company based in Stuttgart, is at the forefront of space resource exploration. Supported by the ESA Business Incubation Program Baden-Württemberg, the Validation Fund of the University of Kiel (DFG-Funding) and the European Space Resources Innovation Centre (ESRIC), our multidisciplinary team, combining expertise in aerospace engineering and geophysics, serves as the first link in the ISRU process chain. We aim to be a service provider specializing in subsurface exploration within the mission area, facilitating economically efficient and risk-minimized planning for ISRU and infrastructure missions.

To this purpose, we are developing an autonomous seismic survey system with a wide range of configurations and applications. The rover will deploy wireless, space-qualified geophones

(Lunaphone) in a desired array and re-deploy them in a new configuration after surveying. The development of these Lunaphones is currently one of the priorities of our work. A small seismic vibrator is being considered as a source due to its high repeatability and adjustable signal. In addition to the challenges of engineering and technical implementation, it is important to prepare for the data content of such an endeavor. To investigate the achievable resolution of the near subsurface and technical parameters such as source frequency content, we generate synthetic seismic data using the SALVUS software. We generate different seismic subsurface models corresponding to different mission scenarios. The velocity and density values are based on Apollo era seismic experiments. By varying the layer thickness, it is possible to determine the limits of resolution. To simulate the scattering behavior of the regolith, random media are introduced into the homogeneous layered base model. Inversion and analysis of the synthetic seismic data are the final steps.

## **P-SM-05**

### **Velocity modeling in Schleswig-Holstein as part of the TUNB Velo 2.0 project**

**D. Schindler, A. Omlin, F. Hese, C. Liebermann**

*Landesamt für Umwelt des Landes Schleswig-Holstein, Geologischer Dienst Schleswig-Holstein,  
Flintbek*

The Geological Survey of Schleswig-Holstein is project partner in the joint project TUNB Velo 2.0. This R&D project aims to develop large-scale velocity models for the Northwestern German Basin based on all velocity data available.

Previous models rely on borehole velocity data (mainly check shot data) only. However, such measurements are sparsely available throughout the entire modeling region, thus emphasizing the need for additional data types. Velocities obtained during seismic processing, particularly stacking velocities, are originally provided by the oil and gas industry alongside with the corresponding seismic sections. These seismic velocity data are much more widely distributed across Schleswig-Holstein and Hamburg than the borehole data and therefore cover the modeling region to a much larger extent. Furthermore, partly available raw data allow us to conduct our own seismic reprocessing including a velocity analysis.

In our study, we discuss the integration of processing velocities into the regional velocity models by performing our own seismic velocity analyses at specific locations. We thereby derive confidence intervals for velocities. Near check shot measurements, we evaluate the relationship between check shot and processing velocities with regard to a future calibration of both data types.

## **P-SM-06**

### **Enhanced S-Wave Seismic Imaging for Near-Surface Applications**

**S. H. Wadas**

*LIAG-Institut für Angewandte Geophysik, Forschungsabteilung 1 - Geophysikalische Erkundung,  
Hannover*

S-wave reflection seismic imaging has become an important tool for near-surface geophysical investigations, because it offers superior resolution, and greater sensitivity to lithological and geotechnical properties, compared to P-wave methods. This makes it particularly valuable to resolve fine structures in the subsurface, which are crucial for applied investigations in fields such as neotectonics and subrosion/karst, where accurate delineation of structural and stratigraphic features is essential. However, near-surface S-wave data presents numerous

challenges, including complex S-wave propagation, strong velocity contrasts, scattering, and noise contamination. Additionally, unconsolidated sediments, intricate layering, and deformation features exacerbate these challenges. Advanced processing techniques are crucial to overcome these obstacles, but when dealing with reflection seismic S-wave data, very often a simple, general processing sequence, e.g. involving classical NMO-correction, CMP stacking and post-stack FD time migration is applied, as described in, e.g., Krawczyk et al. (2012)<sup>1</sup>, Pugin et al. (2013)<sup>2</sup> and Wadas et al. (2016)<sup>3</sup>. In the case of good data quality and a simple geology these workflows might yield sufficient results, but in the case of poor data quality in combination with a complex geological setting, more sophisticated processing sequences, such as DMO-correction, specialized filters, CRS analysis, and pre-stack time/depth migration, are required.

This work shows reflection seismic S-wave data from different locations in Germany that deal with different complex geological issues, such as neotectonics and subrosion/karst. All the data were acquired utilizing LIAG's electrodynamic micro-vibrator ELVIS as seismic source (source spacing 2m or 4m; sweep frequency from 20 Hz up to 160/200 Hz) and a land-streamer equipped with horizontal geophones (receiver spacing 1m) in a roll-along configuration. Data quality was highly variable due to, e.g., the influence of environmental noise, surface waves, scattering, and attenuation. A comparison between results derived from classical processing sequences and more sophisticated processing of the shear-wave data show how advanced imaging techniques can help to improve S-wave imaging for near-surface applications, and thus the structural and physical characterization of the underground.

<sup>1</sup> doi:10.1016/j.jappgeo.2011.02.003

<sup>2</sup> doi:10.3997/1365-2397.2013005

<sup>3</sup> doi:10.5194/se-7-1491-2016

## P-SM-07

### Erkundung eines potenziellen Wärmespeichers im Untergrund durch Scherwellenreflexionsseismik

**P. Leineweber<sup>1</sup>, R. Kirsch<sup>2</sup>, C. Janout<sup>3</sup>, L. Wicka<sup>4</sup>, R. Mecking<sup>5</sup>, G. Druivenga<sup>1</sup>**

<sup>1</sup>Geosym GmbH, Hannover,

<sup>2</sup>GeoImpuls, Kiel,

<sup>3</sup>KWKon GmbH, Hürup,

<sup>4</sup>Boden Op, Hürup,

<sup>5</sup>-, Wedemark

Eine Energiegenossenschaft im Raum Flensburg (SH) plant für die Versorgung ihres Wärmenetzes einen Untergrundspeicher für Solarthermie. In Solarkollektoren gewonnene Wärme soll mit ca. 50 Erdwärmesonden während des Sommers im Untergrund gespeichert und während der Heizperiode rückgewonnen werden. Der Speicherbereich soll eine Fläche von ca. 50 x 50 m einnehmen.

Die Wärmespeicherung im Untergrund muss in einer grundwassernichtleitenden Schicht (Ton, Geschiebemergel, dichtes Festgestein) erfolgen, um eine thermische Beeinflussung des Grundwassers und Wärmeverluste durch den Grundwasserabstrom zu vermeiden. In der Nähe des geplanten Speicherbereichs wurde eine Geschiebemergellage bis in ca. 70 m Tiefe erbohrt.

Zur Übertragung dieser Punktinformation auf die Speicherfläche und zur Erkundung des Tiefenverlaufs des Speicherhorizontes wurden scherwellenreflexionsseismische Messungen durchgeführt. Die Länge der vier Profile belief sich auf ca. 630 m. Zwei Profile wurden auf As-

phalt mit einem Landstreamer gemessen, für zwei weitere wurden die Geophone in den Boden gesteckt. Als Quelle kam eine ElViS VII Scherwellenquelle zum Einsatz. Die oberflächennahe Schichtung kann in der Seismik bis in eine Tiefe von ca. 100 m aufgelöst werden. Der in der Bohrung vorkommende Geschiebemergel ist in der Seismik identifizierbar. Auf einigen Profilen wird eine linsenförmige Struktur dieser Geschiebemergelschicht erkennbar. Als nächster Arbeitsschritt wird eine Erkundungsbohrung auf der Speicherfläche abgeteuft, mit geophysikalischer Vermessung zur petrophysikalischen Charakterisierung des Speicherhorizontes. Diese Bohrung wird anschließend als Erdwärmesonde ausgebaut und an ihr ein TRT (thermal response test) zur Ableitung der Wärmeleitfähigkeit durchgeführt.

## SO – Seismologie

### Vorträge

#### O-SO-01

#### **Earthquake Location Imaging (ELI) for single-well Distributed Acoustic Sensing using Wavefield Classification**

**A. Komeazi, G. Rümpker**

*Goethe Universität Frankfurt, Frankfurt am Main*

In this study, we explored new approaches to the earthquake location problem using simulation of Distributed Acoustic Sensing (DAS) technology deployed in a single vertical borehole. While traditional methods rely on extensive networks of seismometers distributed over different horizontal locations to determine precise earthquake hypocenters, our approach investigates the feasibility of using DAS seismogram images recorded at 700 virtual receivers along a 3.5 km cable to derive the location of an earthquake event.

We evaluated several methodologies, including cross-correlation-based matching with a database of simulated waveforms and machine learning techniques such as convolutional neural networks (CNNs) and autoencoders. The cross-correlation approach yielded encouraging results for simple velocity models but encountered challenges with more complex, realistic models. To address these limitations, CNNs were employed to classify earthquake locations within a grid. Additionally, an autoencoder model was tested to increase the resolution of the derived location images.

The findings demonstrate the potential of combining DAS technology with machine learning for earthquake location imaging, particularly in scenarios with limited seismic instrumentation. These methods show promise for enhancing the efficiency and accuracy of earthquake monitoring, specifically in regions with lateral variated velocity models.

## **O-SO-02**

### **Using dark fiber-optic cables to support geothermal exploration using passive seismic methods**

**J. Pätzl<sup>1</sup>, A. Yates<sup>1</sup>, C. Caudron<sup>1,2</sup>, J. Govoorts<sup>1,3,4</sup>**

<sup>1</sup>*Université libre de Bruxelles, Brussels, Belgium,*

<sup>2</sup>*WEL Research Institute, Wavre, Belgium,*

<sup>3</sup>*Royal Observatory of Belgium, Seismology and Gravimetry, Brussels, Belgium,*

<sup>4</sup>*Université de Mons, Mons, Belgium*

Distributed Acoustic Sensing (DAS) has seen a rise in popularity for geophysical site characterization and imaging in recent years. Its ability to densely sample the seismic wavefield over distances of several kilometers, along with the possibility of using existing telecommunication infrastructure, makes it particularly appealing for near-surface applications.

To date, most studies have utilized dark fibers in urban contexts for site characterization. Here, we present results from the analysis of DAS data recorded on a dark fiber in a rural region in northern Iceland. The interrogated fiber-optic cable traverses multiple shallow geothermal systems, providing an opportunity to investigate subsurface properties essential for geothermal exploration.

We first examine the characteristics of the seismic noise wavefield on different segments of the fiber-optic cable. Using noise interferometry, we infer local surface wave dispersion characteristics and identify both reflected and trapped surface waves linked to nearby fault zones.

Complementary analysis of the strain response to a near-regional M5.0 earthquake reveals strain amplification in the geothermal production areas and shows a correlation with the degree of subsurface fracturing.

With this study, we aim to demonstrate the potential of using DAS on existing fiber-optic infrastructure to guide and assist geothermal exploration and development through fault detection and subsurface characterization.

## **O-SO-03**

### **QEST - An inversion code to separately estimate the frequency dependence and the depth dependence of intrinsic attenuation and scattering attenuation of seismic shear waves**

**M. van Laaten, U. Wegler**

*Friedrich-Schiller-Universität Jena, Jena*

In local earthquake seismology depth-dependent elastic models of P- and S-wave velocities are indispensable, e. g. to locate earthquakes. If not only travel times but also amplitudes of seismic waves are important, elastic Earth models are insufficient and visco-elastic models are required to include intrinsic absorption of seismic waves. This applies e. g. to the estimation of moment magnitudes and to physics-based ground motion modeling in seismic hazard analysis. The estimation of seismic attenuation parameters of the Earth is significantly more difficult than the estimation of velocities for two reasons: (1) Scattering attenuation as well as intrinsic absorption contribute to the attenuation of seismic waves and it is essential to separate these two effects. (2) Seismic attenuation parameters are inherently frequency dependent, whereas frequency dependence of seismic P- and S-wave velocities can be neglected in almost all cases. Due to the lack of information, attenuation is often completely

neglected in seismic wave simulation, standard values for seismic Q are used, or frequency dependence and depth dependence are ignored. To solve this issue, we develop a computer code,,QEST - Q estimation'. The code is based on a forward modelling using radiative transfer theory in depth-dependent velocity and attenuation models and a global inversion scheme based on a genetic algorithm. Besides frequency- and depth-dependent intrinsic as well as scattering attenuation parameters, earthquake source spectra and frequency dependent receiver site amplifications are a result of the inversion with QEST. We applied the technique to seismograms of earthquakes in the Upper Rhein Graben and in the Leipzig-Regensburg fault zone as examples of regions with thick sedimentary layers and without thick sedimentary layers, respectively. Results show a clear depth and frequency dependence of both, scattering attenuation as well as intrinsic absorption, within the thick sediments of the graben. The region without thick sediments, on the contrary, shows clear frequency dependence of attenuation parameters but less depth dependence.

## O-SO-04

### Investigation of seismicity in the Eifel region, using data from the Eifel Large-N Network

P. Laumann<sup>1</sup>, H. Zhang<sup>1</sup>, M. P. Isken<sup>1</sup>, G. Petersen<sup>1</sup>, P. Büyükkapınar<sup>1</sup>, T. Dahm<sup>1</sup>, B. Schmidt<sup>2</sup>

<sup>1</sup>GFZ Potsdam, Section 2.1, Potsdam,

<sup>2</sup>Geological Survey of Rhineland-Palatinate, State Seismological Service, Mainz

The Laacher See volcano, with a VEI 6 Plinian eruption just 13,000 years ago, is the second youngest silicic-carbonatic magma system in the world. Although the volcano is currently classified as dormant, phenomena such as CO<sub>2</sub> degassing, ground uplift, subsidence, and seismic activity persist as indicators of potential magmatic processes occurring at depth. A comprehensive analysis of this seismic activity can provide valuable insights into both the magmatic and tectonic dynamics of the region. Such knowledge could, for instance, be employed to enhance the planning and implementation of geothermal energy projects in the locality.

To improve the understanding of the magmatic system under, a seismic network comprising over 350 seismic stations was deployed in the East Eifel region, from September 2022 to August 2023. Furthermore, a 60 km long dark fiber DAS cable was utilized for data collection over a three-month period.

Given the substantial amount of data collected by the Large-N network, it is recommended to use rapid machine learning techniques for the identification and localization of seismic events. For this purpose, a stacking and migration approach combined with neural network phase characterization was employed. Based on the results, a catalog of 1715 microseismic earthquakes with magnitudes (ML 0.5-3.3), we identified multiple spatio-temporal clusters of seismicity. We perform probabilistic moment tensor inversions for the largest events with the aim to compare the obtained fault planes with the hypocenter distributions to identify active faults.

Besides events in the upper crust, the study area is known for deep low frequency (DLF) events (depth range approx. 1 -19 km). In cases of anomalous waveforms or frequency spectra, the phase characterization method applied for the upper crust events fails because such events were not included in the training datasets. To address this limitations, we explore alternative techniques to effectively detect and localize DLF events. The aim of our study is to establish a more comprehensive catalog of local seismicity and to gain insights into the underlying seismic sources and their relation to the volcanic system.

## **O-SO-05**

### **The upper crustal structure of the Eifel volcanic region, southwest Germany from local earthquake tomography using Large-N seismic network data**

**H. Zhang, C. Haberland, T. Dahm, M. P. Isken, P. Laumann, P. Büyükkapınar**

*Helmholtz Centre Potsdam GFZ German Research Centre For Geosciences, Potsdam*

From September 2022 to August 2023, a temporary large-N seismic network consisting of more than 450 stations was deployed around the Eifel region of southwest Germany, a world-class intraplate volcanic field in central Europe. The local earthquake data set from such a dense seismological network provides an unprecedented opportunity to image, for the first time, precise subsurface structures of the Vp and the Vp/Vs ratios in this region. Based on the recorded local earthquakes, we first derived a minimum 1-D Vp velocity model and average Vp/Vs ratios. 3-D tomographic Vp and Vp/Vs models of the upper crust were then calculated using a filtered catalogue of more than 700 high-quality local earthquakes with 62,696 P-wave and 52,345 S-wave arrival times picked by machine-learning detection approach. To obtain more robust and reliable models, we ran 126 inversions with different grids to avoid artifacts from single model parametrization and to increase the resolution. The final results were obtained by averaging the models from all inversions. In each inversion we used a flexible but regular grid with a node spacing of 2 km around the Laacher See volcano (LSV), and assessed the resolution by synthetic tests and analysis of the resolution matrix and ray density.

Our minimum 1-D Vp model and the average Vp/Vs ratio of 1.61 for the upper crust, likely caused by crustal lithology at a former terrain boundary, are in agreement with previous studies, but are constrained by much more data. The LSV region experiences massive degassing of mantle-derived CO<sub>2</sub>, which may further reduce Vp/Vs ratios. We have interpreted the final 3-D Vp and Vp/Vs structures with associated seismicity and other geophysical data. Our results show a high Vp/Vs, conduit-like anomaly with below average Vp velocities beneath the LSV. This anomaly dips from the LSV to the southeast, reaching a depth of ~10 km, and may indicate a fluid bearing or partially melting region. The spatial correlation between this observed anomaly and the deep low-frequency event channel from previous observations suggests that magmatic fluids from deeper sources may still be migrating beneath the LSV and are associated with the anomalous region. Other shallower anomalies are found around neighbouring volcanoes such as Rieden and Korretsberg in the East Eifel volcanic field. In addition, the long SW-NE trending Siegen thrust, characterized by relatively high Vp velocities in the upper crust, dips with 50°–60° towards SE.

## **O-SO-06**

### **What crustal magmatic reservoirs lie beneath the East Eifel volcanic fields? Clues from the Eifel Large-N passive seismic experiment**

**T. Dahm<sup>1,2</sup>, H. Zhang<sup>1</sup>, P. Laumann<sup>1</sup>, P. Büyükkapınar<sup>1</sup>, M. Isken<sup>1</sup>, S. Heimann<sup>2</sup>**

<sup>1</sup>*Helmholtzzentrum für Geowissenschaften GFZ, Potsdam,*

<sup>2</sup>*Universität Potsdam, Institut für Geowissenschaften, Potsdam*

The Quaternary volcanoes of the east Eifel volcanic field (EEVF) experienced their last explosive eruption at Laacher See 13,000 years ago and are classified as volcanically active. Recent evidence for active magmatism beneath the volcanic fields, such as massive degassing of mantle-generated CO<sub>2</sub>, is provided by the occurrence of deep, low-frequency earthquakes and the detection of large-scale uplift and radial extension of the region at a rate of up to 0.7 mm / year.

The large-scale uplift can be explained by upwelling and partial melting of rocks in the upper mantle. In addition, the uplift can be explained by sill-like intrusions at the crust-mantle boundary and in the upper mantle (Silveri et al., 2024, GRL). Distributed sill reservoirs in the lower crust would also explain the depth distribution of xenoliths in the East and West Eifel volcanic products.

Between September 2022 and August 2023, we were able to carry out a large-scale passive experiment with more than 495 stations in the Eifel to study the magmatic systems. Initial analyses have allowed the precise localisation of more than 760 micro-earthquakes and the reconstruction of a 3D velocity model for the uppermost 12 km beneath the EEVF. However, deeper magmatic reservoirs cannot be resolved by local earthquake tomography.

The seismogram sections of individual earthquake data show evidence of reflections from the lower crust, which may be related to magmatic reservoirs. We propose a systematic study of subcrustal reflections from the Large-N data using travel-time analysis, comparison with synthetic seismograms and simple modelling of the energy flux of the reflections.

## **O-SO-07**

### **Automatic ML Catalogs in Action: Mapping Iceland's Volcanic Activity in High Detail**

**M. Isken<sup>1</sup>, T. Fischer<sup>2</sup>, T. Dahm<sup>1</sup>, P. Hrubcová<sup>3</sup>, J. Vlček<sup>2</sup>, J. Doubravová<sup>3</sup>, J. Burjánek<sup>3</sup>, E. Á. Guðnason<sup>4</sup>, T. Agustsdóttir<sup>4</sup>**

<sup>1</sup>*GFZ Potsdam, Potsdam,*

<sup>2</sup>*Charles University, Prague, Czech Republic, Faculty of Science, Prague, Czech Republic,*

<sup>3</sup>*Academy of Sciences, Institute of Geophysics, Prague, Czech Republic,*

<sup>4</sup>*Iceland GeoSurvey, ISOR, Reykjavík, Iceland*

We present high-resolution automatic seismic catalogues imaging the volcanic activity in Reykjanes, Iceland. We apply the data-driven qseek framework to automatically detect and locate seismicity within a large continuous seismic data set delivered by a dense seismic network on the Reykjanes Peninsula. We focus on (1) the intense seismicity during the rapid intrusion of a 15 km-long dike in November 2023 and (2) the pre-eruptive seismicity of the fissure eruption of 18 December 2023 near Sundhnúkur and of 19 March 2021 near Fagradalsfjall.

These automatic detailed catalogues are based on a combination of machine learning and waveform attribute stacking and do not need phase associations. They are robust and provide high-quality relative locations if station correction terms are automatically considered. The approach is, therefore, attractive for analysing volcanic swarms and unrest in quasi-real-time. It further offers insights into the dynamic processes driving volcanic activity. We interpret the seismicity and compare the ML catalogue performance delivered by qseek against established methods and reference catalogues.

## **O-SO-08**

### **Linking seismicity, dyke and graben formation: a case study from the Reykjanes Peninsula**

**T. J. Fischer<sup>1</sup>, J. Vlček<sup>1</sup>, P. Hrubcová<sup>2</sup>, A. Lomax<sup>3</sup>**

<sup>1</sup>*Charles University, Faculty of Science, Applied geophysics, Praha, Czech Republic,*

<sup>2</sup>*Geophysical Institute, Academy of Science, Praha, Czech Republic,*

<sup>3</sup>*ALomax Scientific, Mouans-Sartoux, France*

The current volcanic unrest on the Reykjanes peninsula began in March 2021, when a fissure eruption occurred in the area of Fagradalsfjall, and was followed by two further eruptions from the same volcanic dyke in the following years. All these eruptions were preceded by intense seismic swarms and were accompanied by surface deformation indicating extension and vertical movement. In autumn 2023 the seismic activity moved westwards - to the Grindavík/Svartsengi area, where an intensive seismic swarm activated the Reykjanes oblique rift zone. On 10 November the seismicity highlighted a narrow NE trending zone of about 15 km in length, which was accompanied by rapid subsidence resulting in the formation of a graben 9 km long and up to 4 km wide. The subsequent seismic swarm gradually diminished until 18 December, when the first Sundhnúkur eruption of the ongoing series began.

We analyse the space-time distribution of the precise hypocentre locations of the 10 November seismic swarm and find a bilaterally propagating tensile rupture of dyke-like character. Comparison with surface displacements measured by the GPS network shows that dyke growth derived from seismic migration is closely correlated with graben-related surface displacements. The type of earthquake focal mechanisms varies along the dyke and correlates with graben occurrence. We also propose a model linking the volcanic and tectonic drivers of the Reykjanes Peninsula extension.

## **O-SO-09**

### **Sustainable preservation of analogue seismic data in Germany – Digitization test and reference earthquake source parameters.**

**G. Kulikova<sup>1</sup>, F. Krueger<sup>2</sup>, C. Hadzioannou<sup>3</sup>**

<sup>1</sup>*UP Transfer GmbH at the University of Potsdam, Potsdam,*

<sup>2</sup>*University of Potsdam, Institute of Geosciences, Potsdam,*

<sup>3</sup>*University of Hamburg, Institute of Geophysics, Hamburg*

At last year's DGG conference, we have presented the initial results of our feasibility study, which aims to assess the potential for digitizing all analogue seismic data in Germany. This study is funded by the Federal Institute for Geosciences and Natural Resources (BGR) and is being conducted by a small working group of researchers from the University of Potsdam and the University of Hamburg.

We have completed the preliminary inventory of the contents of the analogue seismic data archives in Germany. Information from 12 German institutions, which stored analogue seismic records, was collected and compiled into a single database. This database, along with a report detailing the contents of all analogue seismic data archives in Germany, has been published, providing comprehensive information about their holdings.

Here, we present the results of our test run, conducted to estimate the workload involved in the continuous scanning and digitization of seismic records. Paper seismograms from three seismic stations were collected over three distinct time periods, each for one month.

Corresponding metadata information was also gathered. These records were scanned using various scanning techniques and parameters, utilizing different equipment. The data was then vectorised using two different tools, and the results were compared.

Additionally, we analysed the test event—the Albstadt earthquake of November 16, 1911—to evaluate the methods for determining earthquake source parameters, such as the epicentre location, magnitude, and focal mechanism, using digitized analogue data.

Each step of the digitization process will be thoroughly documented, accompanied by detailed recommendations for data collection, digitization, and subsequent processing of the digitized data. These recommendations will be compiled into a manual, which will serve as the foundation for developing a long-term strategy for the preservation and digitization of all analog seismic records and their associated metadata in Germany.

## **O-SO-10**

### **The Collm Archive - Preserving the legacy of several generations of Observatory members for future generations.**

**L. Sonnabend<sup>1</sup>, P. Buchholz<sup>2</sup>, G. Vogt<sup>3</sup>, S. Wendt<sup>2</sup>, T. Duteloff<sup>3</sup>**

<sup>1</sup>*Sächsisches Landesamt für Umwelt Landwirtschaft und Geologie, Abteilung Geologie / Referat  
102 Geologische Kartierung und Geophysik, Freiberg,*

<sup>2</sup>*Universität Leipzig, Leipzig,*

<sup>3</sup>*Sächsisches Landesamt für Umwelt Landwirtschaft und Geologie, Abteilung Geologie / Referat  
101 Geologisches Archiv, Freiberg*

In 1902, the University of Leipzig installed a Wiechert seismograph. This made it one of the first institutions to join the new and growing worldwide network of seismological observatories. It has been in continuous operation ever since, with the oldest seismograms being from 1911. In 1935, the newly modernised Wiechert seismograph was moved to the newly built Collm Geophysical Observatory, where it remains and still works today. Although digital seismological recording now dominates, analogue recording on photographic paper was the primary medium until the end of the 20th century. The tireless work of many generations of seismologists and technicians has resulted in an archive of over 100,000 paper seismograms at Collm Observatory. As this historically important site is sadly on the verge of closing its doors forever, the LfULG is preserving this analogue archive. All seismograms have been moved from Collm to Freiberg and were professionally restored to prevent the otherwise inevitable self-destruction (acid decomposition).

All the seismograms from the Wiechert and many other modern instruments from the Collm Observatory are now available in the geological archive of the LfULG.

We hope to preserve this irreplaceable treasure for many generations to come.

The talk will give an overview of what we did in detail, how long it took and what lessons learned.

## **O-SO-11**

### **Development of a unified earthquake catalog for the Vogtland/West Bohemia swarm region for the investigation of the geometry of the crustal brittle-ductile boundary**

**A. Olivar-Castaño<sup>1</sup>, M. Ohrnberger<sup>1</sup>, P. Büyükkapınar<sup>2</sup>, T. Dahm<sup>2</sup>, J. Doubravová<sup>3</sup>,  
T. Fischer<sup>4</sup>, J. Wasserman<sup>5</sup>, U. Wegler<sup>6</sup>, S. Wendt<sup>7</sup>**

<sup>1</sup>*Universität Potsdam/Institut für Geowissenschaften, Potsdam,*

<sup>2</sup>*GFZ Deutsches GeoForschungsZentrum, Potsdam,*

<sup>3</sup>*Czech Academy of Sciences/Institute of Geophysics, Prague, Czech Republic,*

<sup>4</sup>*Charles University, Prague, Czech Republic,*

<sup>5</sup>*Ludwig-Maximilian Universität München, Department für Geo- und Umweltwissenschaften,  
München,*

<sup>6</sup>*Friedrich-Schiller Universität Jena/Institut für Geowissenschaften, Jena,*

<sup>7</sup>*Universität Leipzig/Institut für Erdsystemwissenschaft und Fernerkundung, Leipzig*

The Vogtland/West Bohemia region is one of Europe's most geodynamically active areas, characterized by massive CO<sub>2</sub> degassing and persistent mid-crustal earthquake swarms. A widespread hypothesis links these phenomena to deep-seated magmatic activity.

Since 1984, most swarm activity in the Vogtland region has concentrated in the area around the Czech village of Nový Kostel, near the German states of Saxony, Bavaria, and Thuringia. The depth distribution of earthquakes in the Nový Kostel area ranges from 6 to 12 km in its central part, with the lower boundary appearing to deepen with increasing distance from the center. It has been proposed that the lateral variation in the lowermost depth of the observed earthquakes could possibly depict a regional-scale updoming of the brittle-ductile boundary linked to the hypothesized deep magmatic activity in the region. However, these observations are based on hypocentral locations produced by different institutions in Germany and the Czech Republic, each using its own seismic network, location procedure, and velocity model. As a result, the locations and their associated errors are not easily comparable, which could bias the apparent trends in the distribution of the deepest earthquakes.

In this work, we aim to specify in greater detail the geometry of the brittle-ductile boundary in the Vogtland swarm region. We begin by creating a unified earthquake catalog based on nearly 16 years of P- and S-wave traveltimes observations from four different seismic networks: the Czech WEBNET and the German SaxonNET, BayernNetz, and Thüringer Seismologisches Netz. We then invert the unified phase traveltimes dataset using an iterative damped least-squares tomographic algorithm (SIMULPS2023) to develop an updated P-wave velocity model of the crust in the region and new, joint earthquake locations.

## **O-SO-12**

### **Rapid detection of small signal-to-noise ratio seismic events using fast time-reverse imaging**

**C. Finger**

*Fraunhofer IEG, Bochum*

Detection of seismic events with very small signal-to-noise ratios in continuous time series is crucial for completing existing catalogues. The lower the magnitude of completeness, the better for monitoring subsurface reservoirs or estimating seismic hazard. Wave-propagation

based tools such as time-reverse imaging (TRI) excel at locating these tiny events but require large computational resources. Thus, they are not feasible to apply on continuous time series. Employing a detector prior to the application of TRI would reduce the number of analyzed time windows but limits the sensitivity of TRI to the detection thresholds of the used detector. Since most available detectors require a minimum signal-to-noise ratio of more than one, the benefits of TRI would be deteriorated.

In this study, we propose to use low-resolution time-reversed wavefield simulations on small overlapping time windows to rapidly analyse long continuous time series. Using the maximum of the total energy density as imaging condition, the continuous time series can, thus, be scanned for times of high wavefield convergence. Essentially, this can be used as a rapid detector sensitive to similar signal-to-noise ratio limitations as TRI. Time windows with high convergence of the time-reversed wavefield can then be analysed with higher model resolution to obtain hypocenter locations and moment tensors.

We demonstrate this approach using synthetic waveforms generated with varying complex source mechanisms first and then apply the workflow to a continuous day of recording the passive seismic wavefield with the ZB network in the area surrounding Eschweiler-Weisweiler in North-Rhine Westphalia. Results indicate that in addition to larger seismic events consistent with regional seismic monitoring, smaller events could be identified. Thus, the existing catalogs can be complemented with hypocenters and moment tensors. This could enable more in-depth fault mapping from natural seismicity or more detailed seismic hazard assessments.

## O-SO-13

### Microseismic activity in the Eastern Alps: Seismic sequences, rupture mechanisms, and active faults

G. Petersen<sup>1</sup>, L. Hofman<sup>2</sup>, J. Kummerow<sup>2</sup>, S. Cesca<sup>1</sup>

<sup>1</sup>GFZ German Research Centre for Geosciences, Potsdam,

<sup>2</sup>Freie Universität, Berlin

The large-N installations of the Swath-D (2017-2019) and AlpArray (2016-2021) seismic networks provide unmatched opportunities to study the microseismicity in the Eastern Alps in unprecedented detail. For the first time in the study area, the homogeneous station spacing allows a consistent analysis of seismicity across the entire area. The southern and eastern Alps are an interesting target because they include the deformation front of Adria-Europe convergence with historically large events (e.g., M 6.0 Friuli 1976) and areas where seismicity seems more or less absent despite geologically mapped large fault systems and past deformation fronts.

We show how a combined workflow, including spatio-temporal clustering, cross-correlation-based clustering, relative relocations, and MT inversions of microseismicity ( $M_w > 1$ ), sheds light on the seismicity of the study area. We observe strong zonations of seismic activity rates, seismic sequence characteristics, and rupture mechanisms, coinciding with dominant tectonic deformation styles and subsurface properties such as Qp attenuation. In addition, we identify and characterize multiple likely unknown fault systems that experience local stresses deviating from the regionally dominant Adria-Europe convergence. We show that our findings agree well with the occurrence of large historical earthquakes while simultaneously shedding light on much smaller seismogenic features.

## **O-SO-14**

### **Using 3D dynamic rupture simulations to probe the effects of source-station geometry and fault-zone architecture on spectral corner frequency**

**M. Roßbach<sup>1</sup>, N. Schliwa<sup>2</sup>, R. M. Harrington<sup>1</sup>, A.-A. Gabriel<sup>3</sup>, E. S. Cochran<sup>4</sup>**

<sup>1</sup>*Ruhr-Universität Bochum, Institut für Geologie, Mineralogie und Geophysik, Bochum,*

<sup>2</sup>*Ludwig-Maximilians-Universität München, München,*

<sup>3</sup>*University of California, San Diego, San Diego, United States of America,*

<sup>4</sup>*United States Geological Survey, Pasadena, United States of America*

The static stress released in an earthquake relates the average slip on a fault to the rupture area. It is commonly estimated from the spectral corner frequency and exhibits roughly constant values of 1-10 MPa, but may vary from 0.1 to 100 MPa. The cube dependence on corner frequency implies that small uncertainties in corner-frequency estimates propagate to large uncertainties in stress-drop values. As a result, many open questions remain regarding whether the range in observed values results from physical differences between earthquakes or observational constraints. In this study, we analyze synthetic waveforms generated from 3D dynamic-rupture simulations of the M6.4 foreshock of the 2019 Ridgecrest earthquake with the aim of investigating the effect of source-station distance, back azimuth, and the presence of a fault zone on the earthquake spectral corner frequency and radiated seismic energy.

We use synthetic waveforms generated from dynamic-rupture scenarios that consider 3D fault geometry and velocity structure, viscoelastic attenuation, and off-fault plasticity. The simulations resolve frequencies up to 1-2 Hz that are generated both with and without a prescribed shallow fault zone represented by a reduction of elastic moduli around the fault planes. Synthetic waveforms are generated at nodes co-located with seismic stations at distances less than 1° from the epicenter. We use multi-taper spectral estimation of synthetic-source spectra to determine the corner frequency using a least-squares fit to a Boatwright spectral model. We examine the relative influence of several factors (back-azimuth, distance, fault zone, and varying attenuation assumptions) under the implicit assumption that other observational constraints do not influence corner-frequency estimates. We also compare synthetic and observed spectra to examine whether trends in both corner-frequency and radiated energy estimates from data mirror the synthetics. Finally, we present stress drop values estimated from both synthetic and real displacement spectra together with direct calculations resulting from the modeled on-fault stress changes.

## **O-SO-15**

### **Microstructural evidence of episodic deformation at hypocentral depth recorded by fault rocks**

**L. M. Beiers<sup>1,2</sup>, C. A. Trepmann<sup>2</sup>, F. Dellefant<sup>2,3</sup>**

<sup>1</sup>*Hochschule Bochum, Reservoir Geophysics, Bochum,*

<sup>2</sup>*Ludwig-Maximilians-Universität München, Department für Geo- und Umweltwissenschaften, München,*

<sup>3</sup>*Ludwig-Maximilians-Universität München, Department für Kulturwissenschaften und Altertumskunde, München*

Deformation processes at the base of the seismogenic zone of the continental crust, i.e. at greenschist facies conditions, are episodic and characterized by rapid loading to high stresses followed by stress relaxation. The response of crustal rocks to transient stresses is governed

by grain-scale processes, which influence large-scale tectonic processes, e.g., translation of crustal blocks on km-scale along fault zones. The episodic deformation during the seismic cycle is still poorly understood, as seismological data and the inversion of the postseismic surface deformation does not provide information on grain-scale resolution. Moreover, the entire range of the relevant temporal and spatial scales cannot be captured by deformation experiments.

However, the stress and strain conditions during episodic deformation that only transiently prevail can be constrained by characteristic microfabrics within exhumed fault rocks. The preserved (micro-)structural indicators, investigated by polarized light (including universal stage) and scanning electron microscopy (EDX, BSE, EBSD), can be combined with experiments to serve as paleopiezometers. Fast stress-loading rates to transient high peak stresses ( $\sigma_d > 400$  MPa) are evident by mechanical twins within pseudotachylite-bearing rocks from the Silvretta thrust fault, Austria. Fast stress relaxation is recorded by the growth of strain-free new grains aligned along cleavage cracks generated coeval with seismic rupturing. The coseismically high stresses and fast unloading rates are related with stress redistribution, controlled by the distance to the propagating fault tip, as manifested by the systematic variations of deformation mechanisms at the same greenschist facies conditions. Pseudotachylites formed associated with high-stress crystal plasticity close to the rupture front, whereas mylonitic quartz microstructures reflect accelerated creep at lower stresses (~100 MPa) at larger distance. The specific stress and strain-rate conditions are decisive in determining the rheological behavior, as well as their implications on the strength of various crustal rocks during the different stages of seismic faulting, as opposed to a change in pressure-temperature conditions. Exhumed fault rocks deformed at greenschist facies conditions, i.e., they originate at hypocentral depth, can serve as direct evidence of the deformation history through the seismic cycle, not directly accessible for in-situ measurements.

## O-SO-16

### An Image and Slab Model of the Northern Chilean Subduction Zone Forearc from P and PP Receiver Functions

W. Bloch<sup>1,2</sup>, B. Schurr<sup>2</sup>, X. Yuan<sup>3</sup>, F. Tilmann<sup>3</sup>, C. Faccenna<sup>2</sup>

<sup>1</sup>NORSAR, Applied Seismology, Kjeller, Norway,

<sup>2</sup>GFZ Deutsches GeoForschungs Zentrum, Dynamik der Lithosphäre, Potsdam,

<sup>3</sup>GFZ Deutsches GeoForschungs Zentrum, Seismologie, Potsdam

The Northern Chilean forearc between 18 and 24°S is a well-instrumented natural laboratory to study subduction zone processes. We here complement the suite of available structural information with receiver function common conversion point images and inverse modeling results. Our data are based on P- as well as PP-receiver functions from the Chilean National and IPOC networks and additional seismic experiments conducted over the past ~30 years, ensuring a good back-azimuthal coverage of the long time series.

Our images reveal internal structures of the overriding plate as well as of the subducting slab that often correlate with seismicity patterns. We are able to image the oceanic Moho as a continuous, east dipping converter. A contorted, likewise east-dipping low-velocity zone above the Moho testifies to the presence of internal structures within the subducting oceanic crust that correlate with seismicity, produced by tectonic-metamorphic process. An illusive low velocity zone below the oceanic Moho present in some profiles likely indicates hydration of the incoming oceanic mantle. The conversion signal may carry important information about the bulk water budget of the slab.

In the overriding plate we can identify the continental Moho as well as the mantle wedge corner. In some profiles, we find a low velocity structure that connects the slab to the upper crust. This structure was previously interpreted as a magma conduit that feeds the volcanic arc. High-velocity structures beneath the Coastal Cordillera may relate to Jurassic Batholiths that leave a discernible imprint in the gravity field.

## **O-SO-17**

### **AdriaArray – a passive seismic experiment to explore geodynamic drivers of plate deformation and geohazards in the Central Mediterranean**

**T. Meier<sup>1</sup>, P. Kolinsky<sup>2</sup>**

<sup>1</sup>CAU Kiel, Institut für Geowissenschaften, Kiel,

<sup>2</sup>Czech Academy of Sciences, Prague, Czech Republic

The densely populated area around the Adriatic Sea is prone to geohazards including earthquakes, tsunamis, landslides, floods and volcanic activity as the Adriatic Plate is consumed in a tectonically active belt spanning from Sicily, over the Apennines to the Alps, Dinarides, and Hellenides, generating earthquakes up to magnitude 7. To identify drivers of associated plate deformation, the plate boundaries, slabs, properties of active faults and of the stress field have to be determined. AdriaArray, a dense plate-scale regional seismic network deployed in the central Mediterranean, provides data for imaging of the crust and upper mantle structure and for the analysis of seismic activity. The network consists of 1068 permanent and 444 temporary broad-band stations from 24 mobile pools. 96 % of the planned temporary stations have already been installed. A homogeneous coverage by broad-band stations in an area from the Massif Central in the west to the Carpathians in the east, from the Alps in the north to Sicily and the Kefalonia Fault Zone in the south, is achieved. The backbone network (2022 – 2025) is complemented by locally densified and LargeN networks, e.g. in the western Carpathians (Poland, Slovakia, Hungary), along the Dubrovnik fault (Croatia), in the Vrancea region (Romania), and in Albania. Data recorded by temporary stations is transmitted in real-time to 9 nodes of the European Integrated Data Archive (EIDA). Regular availability and quality checks ensure high data usability. AdriaArray, the largest passive seismic experiment in Europe so far, is based on cooperation between local network operators, mobile pool providers, field teams, ORFEUS (Observatories and Research Facilities for European Seismology) and EPOS (European Plate Observing System), encompassing 64 institutions from 30 countries. They form the AdriaArray Seismology Group, founded in 2022. Collaborative Research Groups are being established to coordinate the data analysis. We present maps of the AdriaArray Seismic Network, station properties, coverage, contributing institutions, data quality checks and collaborative research topics. In Germany, AdriaArray data will be analysed in the framework of the DFG Priority Program DEFORM that will start in 2025.

## **O-SO-18**

### **Seismic Analysis and Remote Sensing Precursors of the February 13, 2024 Çöpler Gold Mine Landslide in Erzincan, Eastern Turkey**

**P. Büyükkapınar<sup>1</sup>, A. Carrillo-Ponce<sup>1</sup>, H. Tanyas<sup>2</sup>, M. B. Munir<sup>2</sup>, E. Karasozan<sup>3</sup>, D. Ertuncay<sup>4</sup>**

<sup>1</sup>*GFZ, Potsdam,*

<sup>2</sup>*University of Twente, Enschede, Netherlands,*

<sup>3</sup>*University of Alaska Fairbanks, Alaska, United States of America,*

<sup>4</sup>*The Seismological Research Center - OGS, Udine, Italy*

On February 13, 2024, at 11:28 UTC, a catastrophic landslide ( $\sim 6$  million m<sup>3</sup>) struck the Çöpler gold mine in Erzincan, Eastern Turkey. This rapid, flow-type landslide ( $\sim 12$  m/s), which occurred in heap-leached material, resulted in the tragic loss of nine miners. Beyond the immediate aftermath of this event, we investigated the source characteristics and failure mechanisms of the landslide using seismic techniques coupled with analysis of spaceborne optical and radar imagery.

Seismic stations operated by regional networks (AFAD and KOERI) recorded the landslide up to 300 km away. Displacement waveforms showed two peaks between 0.08-0.15 Hz, separated by 48 seconds. To characterize the source mechanism of the landslide, we applied a simplified single-force model using a Bayesian bootstrap-based probabilistic inversion scheme with uncertainty estimates. The results indicate that the landslide propagated in two directions: (1) northeast toward the old mine and (2) eastward. The two forces were estimated to be  $F_1 = (4.4 \pm 1.9) \times 10^9$  N and  $F_2 = (1.4 \pm 0.2) \times 10^{10}$  N, with a total moment release equivalent to Mw 3.7. These results are in good agreement with field investigations and surface deformations detected by the Interferometric Synthetic Aperture Radar (InSAR) technique.

The InSAR analysis provided additional insights beyond the immediate impacts. It showed that the failed slopes had been moving slowly for at least four years, with average velocities of up to 60 mm/year (VLOS). Significant deformation was also observed on the cyanide leach pond, with a VLOS of 85 mm/year. Although the pond has not yet failed, these findings underscore the urgent need for monitoring and preventative measures to mitigate potential future failures at the site.

## **O-SO-19**

### **Elephant activity patterns in a zoo setting: a pilot study using co-located seismic and infrasound measurements**

**F. Limberger<sup>1</sup>, G. Rümpker<sup>1</sup>, T. Spengler<sup>2</sup>, M. Becker<sup>2</sup>**

<sup>1</sup>*Goethe-University Frankfurt, Institute of Geosciences, Frankfurt,*

<sup>2</sup>*Opel-Zoo, Education and Research, Kronberg im Taunus*

In this pilot study, we evaluate the feasibility of recording elephant rumbles at the Opel-Zoo near Frankfurt am Main using co-located seismic and infrasound sensors. In August 2024, we detected over 1350 rumbles, observing significant temporal variability. Rumble activity shows a diurnal correlation with visitor numbers, remaining low around zoo opening in the morning and increasing during midday and afternoon. These tone-like signals have fundamental frequencies of 10–25 Hz, with harmonics above 25 Hz, lasting 1–8 seconds. Many rumbles occur in sequences, suggesting elephant interaction. Most rumbles are accompanied by ground motion due to body motions, such as locomotion or trampling of the elephants not detectable with sound sensors. This highlights the value of combined seismic and infrasound data. While seismic noise is higher during zoo opening hours, infrasound provides clearer signals during daytime, with both sensors equally effective during zoo closing hours.

We also find indication for rare seismic-only rumbles with untypically long durations (up to 20s) and there is systematic increased activity during atmospheric pressure drops preceding precipitation, however, further verification from long-term data is needed. Although some questions remain unanswered, the rumble catalogue developed in this study highlights the need for deeper investigation into elephant behavior and communication within a zoo environment, an anthropogenic setting that remains underexplored compared to natural habitats or wildlife parks. Future plans include incorporating additional measurements using seismic data, sound recordings, and video footage to deepen the behavioural understanding, which is helpful for improving elephant welfare strategies zoos.

## SO – Seismologie

### Poster

#### P-SO-01

#### A dataservice for precomputed seismic noise cross-correlations functions

J. Lehr, C. Sens-Schönfelder, A. Heinloo, J. Quinteros

*Geoforschungszentrum, Potsdam*

Analysis of ambient seismic noise using interferometric techniques has become a common tool in seismology. Typical applications include the use of seismic noise correlation wavefields for

imaging of the subsurface and observing velocity changes over time, e.g. to monitor a volcano or hydrological conditions.

All techniques rely on timeseries of noise cross-correlation functions (CCFs) between pairs of stations and/or channels which require computationally expensive processing steps that are most often preceded by downloading huge amounts of raw data.

Even though there is not (yet) a single accepted processing scheme, most researchers apply a selection of fairly standard procedures and aim for similar outcomes. Hence, many researchers are currently repeating very similar computations over and over again.

We believe that these computational costs and data traffic can be drastically reduced by processing the data and computing the CCFs directly at the data center and providing them as a data product to the community. We also believe that the open availability of community datasets of ambient noise correlation functions will facilitate new research in the field of seismic interferometry as it removes the computational burden of the initial processing.

We are currently developing such a data service to be hosted at the GEOFON data center. We envision that researchers can request the computation of CCF data sets for stations and time periods of their interest using a combination of the standard processing methods of their choice. The typical use-case is the computation of a CCF dataset for a temporary networks initiated by the PI of the experiment. The resulting dataset of CCFs will then be available to the community via a webservice. The processing steps and necessary parameters can be selected and tested beforehand using a small subset of stations.

Although in a very early stage, we are interested in feedback, ideas and suggestions from and exchange with potential users. By providing pre-computed CCFs, we hope, to not only save network and computational resources but also enable researchers from different fields, e.g. environmental research, to benefit from seismological research and data.

## **P-SO-02**

### **On the quantification of ambient seismic noise amplitudes**

**C. Sens-Schönfelder**

*Deutsches GeoForschungsZentrum Potsdam, Potsdam*

Quantification of the strength of a recorded seismic signal is required in different applications. While this is fairly straight forward for signals from impulsive sources, temporally extended signals have been studies using very different quantities. While probabilistic power spectral density plots inform about the probability distribution of the spectral components, they do not inform about their temporal evolution. Real time seismic amplitudes, mean squared amplitudes, squared mean absolute amplitudes, spectral amplitudes and median amplitudes have been used to measure volcanic, environmental and anthropogenic noise.

Using the statistical distribution of signal envelopes I discuss pros and cons of the different approaches depending on involved timescales of the target signal and disturbances from other sources. The goal is to develop an objective and comparable method to quantify the energy of the ambient seismic field on time scales of minutes, days or weeks in the various frequency bands to improve the investigation of environmental, anthropogenic, volcanic and tectonic sources.

## **P-SO-03**

### **Seismic noise field investigations at the EMR gravitational wave telescope candidate site**

**D. Becker, C. Hammer, C. Hadzioannou**

*Universität Hamburg, Institut für Geophysik, Hamburg*

The ambient seismic noise field interferes with the detection capabilities of the planned next generation gravitational wave detector (so-called Einstein telescope) in two ways: a) by the ground displacement at the underground detector site due to passing seismic waves and b) the change in gravity acceleration at the detector site due to temporal density changes in the surrounding by the same passing seismic waves (so called Newtonian noise). While the first challenge can in principle be addressed by decoupling the actual measurement units from the solid underground and active feedback loops, the disturbances due to Newtonian noise can not be compensated.

In any case, a good understanding of the ambient seismic noise field at the detector site with respect to the composition of the wavefield, its sources and its temporal variability is needed to optimize the installation and operation of the gravitational wave detector and the subsequent interpretation of the obtained results. In this study, we present first results from the investigation of the seismic noise field recorded by several temporary deployments of short period sensors in the so-called EMR region (Euregio Meuse-Rhine) between Maastricht, Liège and Aachen which is a candidate site for the Einstein telescope. Apart from spectral analysis to determine the spatio-temporal amplitude changes at the recording sites, we also apply array analysis and Matched Field Processing (MFP) to pinpoint source locations of the seismic wavefield outside and within the study region.

## P-SO-04

### Monitoring temporal seismic velocity changes in the western Bohemian Massif area using cross-correlation of ambient noise

S. Mandal<sup>1</sup>, T. Fischer<sup>1</sup>, B. Růžek<sup>2</sup>

<sup>1</sup>Charles University, Institute of Hydrogeology, Engineering Geology and Applied Geophysics,, Prague, Czech Republic,

<sup>2</sup>Institute of Geophysics of the Czech Academy of Science, Prague, Czech Republic

Various types of loadings, such as variations of temperature and precipitation, on crustal rocks can induce responses leading to triggering of seismicity, changes in seismic velocities and crustal strain. Monitoring these responses can be useful for tracking the evolving stress, which often leads to seismicity, faulting, and subsurface fluid behaviour. For a long time, this monitoring has been done using earthquakes or human-made explosions. However, a major problem is that it is rare to observe repeated earthquakes with similar source positions and mechanisms, and there is no control over their occurrence. Human-made explosions are quite expensive to use on a regular basis. Over the last decade, the passive imaging method became very popular among researchers because the apparent source position corresponding to one receiver does not change with time and the noise data are continuously available.

In this study, we present our results on relative seismic wave speed changes ( $dv/v$ ) in the Western Bohemian Massif area; and Saxothuringian unit, based on the analyses of several years of seismic noise records from the stations of the regional seismic network. We test the applicability of 'stretching' and 'doublet' methods to the target area intending to verify the potential of the methods in estimating the seismic velocity change. We observe a peak-to-peak amplitude of the seasonal ( $dv/v$ ) change of ~0.5 per cent in the 0.1-0.5 hz frequency band. These  $dv/v$  variations are compared with the annual rainfall pattern and annual temperature variations to clarify the cause(s) of the observed velocity changes.

## P-SO-05

### Rayleigh-wave Ambient Noise Analysis for the OHANA Experiment in the Northeast Pacific

G. Laske<sup>1</sup>, G. Atkisson<sup>1</sup>, J. A. Collins<sup>2</sup>, D. K. Blackman<sup>3</sup>

<sup>1</sup>Scripps Institution of Oceanography, Institute of Geophysics and Planetary Physics - 0225, La Jolla, United States of America,

<sup>2</sup>Woods Hole Oceanographic Institution, Woods Hole, United States of America,

<sup>3</sup>University of California Santa Cruz, Santa Cruz, United States of America

The 2022-2023 OHANA OBS deployment in the northeast Pacific ocean provides a rich dataset for comprehensive seismic studies to explore the crust, lithosphere and asthenosphere in a 600~km wide region west of the Moonless Mountains. The study area covers mainly 40-to-50 Myr old Pacific lithosphere. A fundamental question to be addressed is whether this particular area has the signature of a typical oceanic lithosphere that has a normal plate cooling history. Alternatively, we seek evidence for a previously proposed reheating process, e.g. resulting from small-scale shallow-mantle convection.

Continuous 4-component data (broadband ground motion and pressure) were recovered at 24 sites. In a top-down approach, we start with the assembly and analysis of ambient-noise cross-correlation functions (CCFs) of the vertical components, between 5 and 35 s. The CCFs contain prominent waveforms from overtones that can help improve resolution as a function of depth.

We present the analysis of path-averaged dispersion curves for the fundamental mode. Forward modeling and the inversion of the average dispersion across the OHANA network both indicate normal oceanic crust over a fairly typical mature oceanic lithosphere though shear velocities in the upper lithosphere are a few percent lower than is expected for a 50-Myr old lithosphere. Velocities in the mid-to-lower lithosphere may be 2-3% higher than expected but resolution degrades with increasing depth. We juxtapose this analysis to an earthquake-based analysis that reaches deeper into the lower lithosphere.

## P-SO-06

### Full-waveform modeling and ML-based tomography of volcanic edifices

R. Medappil Pinatt<sup>1,2</sup>, G. Rümpker<sup>1</sup>, A. Komeazi<sup>1</sup>, F. Limberger<sup>1</sup>

<sup>1</sup>Goethe-University Frankfurt, Institute of Geosciences, Frankfurt,

<sup>2</sup>Indian Institute of Science Education and Research(IISER), Pune, India

Seismic tomography is an essential method for exploring the structure of volcanic features beneath the surface, such as conduits and magma chambers. These insights are crucial for a more profound understanding of volcanic processes. However, the complex and heterogeneous nature of the subsurface, along with the limited availability of data, presents substantial challenges in accurately mapping the internal structure of volcanoes, often leading to interpretive uncertainties.

In this study, we propose a novel ML-based tomography method using artificial neural networks (ANNs) to investigate the internal structure of volcanoes. Initial tests using 2D travel-time simulations for simplified cases showed that the ANN approach outperforms traditional linear inversion techniques, especially when seismic data is sparse. Building on these results, we aim to extend the method to more complex and realistic scenarios. In the first step, we demonstrate the efficiency of the proposed method also in three dimensions. Furthermore, we simulate seismic wavefields using full-waveform modeling, generate corresponding seismograms, and use these as inputs for the neural network. To train the network, we create thousands of randomized velocity models and their associated synthetic seismograms, using supervised learning to map each seismogram to its respective velocity model. Once the network is trained, we aim to obtain the velocity structure from previously unseen seismograms. This approach could help identify velocity anomalies linked to magmatic processes and improve our understanding of subsurface dynamics in volcanic regions. We believe this method represents a step forward in developing more effective tools for studying volcanic systems.

## P-SO-07

### Seismic signals associated with plume events and inner crater collapses during the 2021 Geldingadalir eruption

A. Joachim<sup>1</sup>, S. Heimann<sup>1</sup>, E. P. S. Eibl<sup>1</sup>, L. Rees<sup>1</sup>, M. Dwars<sup>1</sup>, É. Á. Gudnason<sup>2</sup>, T. Ágústsdóttir<sup>2</sup>, G. P. Hersir<sup>3</sup>, T. Winder<sup>4</sup>, N. Rawlinson<sup>5</sup>, T. Fischer<sup>6</sup>, J. Doubravová<sup>7</sup>, J. Burjánek<sup>7</sup>, O. D. Lamb<sup>8</sup>

<sup>1</sup>University of Potsdam, Institute for Geosciences, Potsdam,

<sup>2</sup>ISOR, Iceland GeoSurvey, Kópavogur, Iceland,

<sup>3</sup>Independent Researcher, Reykjavík, Iceland,

<sup>4</sup>University of Iceland, Reykjavík, Iceland,

<sup>5</sup>University of Cambridge, Department of Earth Sciences, Cambridge, United Kingdom,

<sup>6</sup>Charles University, Faculty of Science, Prag, Czech Republic,

<sup>7</sup>Czech Academy of Sciences, Institute of Geosciences, Prag, Czech Republic,

<sup>8</sup>Te Pū Ao GNS Science, Wairakei Research Centre, Taupō, New Zealand

In March 2021, a 6-month long eruption began in the Geldingadalir valley on the Reykjanes Peninsula in Iceland. This eruption generated volcanic tremor that was recorded by networks of seismometers and acoustic sensors. In early May, the tremor transitioned from continuous to episodic tremor, with minutes-long durations and reposes. Between mid-June and early July continuous tremor resumed, but subsequently, for the first time during this eruption, the lava pond in the active crater completely drained and the continuous tremor ceased. Shortly after the draining, a large dark plume and several smaller plumes emerged, accompanied by transient seismic signals and six distinct acoustic signals that peaked before the seismic peaks. Following these events, minute-long tremor episodes transitioned into hour-long episodes. Here, we investigate the connection between these plume events and this tremor transition. We study the seismic events in detail, using seismometers within a 6 km radius of the crater, and we use different source models: moment tensor and single force models. We also calculated a decreasing Volcanic Acoustic-Seismic Ratio (VASR) over time from the seismic and acoustic signals, which we will discuss during our presentation. Additionally, we analyse possible causes of the plumes, using video data from local webcams to identify possible sources and discuss a possible link between them and the signals.

## P-SO-08

### Investigating Magmatic Processes in the Reykjanes Peninsula Through Seismic Velocity Monitoring: Vp/Vs Ratio and Shear Wave Velocity Variations During Volcanic Eruptions

A. Masihi, T. Fischer

Charles University, Faculty of Science, Prague, Czech Republic

The Reykjanes Peninsula in southwestern Iceland has experienced intense volcanic activity in recent years, marked by eruptions at Fagradalsfjall (2021, 2022, 2023) and Sundhnúkur (since December 2023 and ongoing). These eruptions, combined with continuous data from the 15-station REYKJANET seismic network, provide a unique natural laboratory for studying volcanic processes and their precursors. Monitoring seismic velocity variations during these events offers valuable insights into magmatic migration, fluid transport, and stress redistribution beneath volcanic structures.

In previous research, we analyzed in-situ Vp/Vs ratio variations from 2017 to 2023 swarms at Fagradalsfjall using the Double-Difference Wadati method. This approach revealed rheological changes linked to magmatic intrusions, showing that abrupt shifts in Vp/Vs ratios can act

as eruption precursors. In this study, we extend our analysis to include seismic activity related to the Sundhnúkur eruptions sequence. We also apply coda wave interferometry (CWI) to estimate shear wave velocity ( $V_s$ ) changes within seismic clusters preceding these eruptions. The method leverages intersource interferometry by correlating scattered coda waves from closely spaced earthquakes. Constructive interference in cross-correlation functions within the stationary phase zone reveals interevent travel times. This approach was successfully applied in the 2018 West Bohemia swarm before. Coda waveforms are filtered between 10-40 Hz, and travel-time differences are extracted within defined coda windows. To enhance scattered wave contributions, interevent distances below 1 km are prioritized. Data normalization and phase-weighted stacking are applied to improve signal coherence, with the impact of noise reduced and measurement reliability enhanced.

The method's sensitivity allows for higher spatial resolution compared to standard seismic tomography. Additionally, results can be validated against previous analyses using the Double-Difference Wadati method, where we successfully tracked  $V_p/V_s$  ratio changes during the same swarm. Our approach enhances understanding of magmatic processes by offering a precise, data-driven means of monitoring subsurface velocity variations, applicable to future swarms and eruptions in the region.

## P-SO-09

### Seismicity of the High-Altitude Volcano Ojos del Salado

L. Murray-Bergquist<sup>1,2</sup>, M. Thorwart<sup>3</sup>, A. Garcia Pina<sup>4</sup>, C. Ulloa<sup>4</sup>, J. van Ginkel<sup>5</sup>, R. Wessels<sup>6</sup>, L. van Huisstede<sup>1</sup>, S. Rebolè Canals<sup>4</sup>, A. Beniest<sup>1</sup>

<sup>1</sup>*Vrije Universiteit Amsterdam, Amsterdam, Netherlands,*

<sup>2</sup>*GEOMAR Helmholtz Center for Ocean Research Kiel, Kiel,*

<sup>3</sup>*Kiel University, Institute for Geoscience, Kiel,*

<sup>4</sup>*Universidad de Atacama, Copiapo, Chile,*

<sup>5</sup>*Swiss Seismological Service (SED), ETH Zurich, Zurich, Switzerland,*

<sup>6</sup>*Utrecht University, Utrecht, Netherlands*

Ojos del Salado Volcano, the highest altitude volcano in the world, is a complex stratovolcano with a largely buried caldera. Although the major eruptions occurred in the Pleistocene and into the Holocene, steam was observed rising from near the caldera as recently as 1993, and the summit remains seismically active. Ojos del Salado lies at the southern end of the Central Andean Volcanic Zone (CAVZ). To the north is a long line of active volcanism, while to the south is a flat slab segment of the Nazca plate resulting in a gap in volcanism. Around 25 km NNE of Ojos del Salado lies a hypersaline lake, the Laguna Verde. Several springs feed heated water into the southern shore of the Laguna, but the heat source is unknown, and it is unclear how Laguna Verde relates to the Ojos del Salado and the surrounding smaller volcanoes in the CAVZ. This position at the end of a volcanic chain near a change in the dip of the subducting plate, and near a geothermally feed lake, makes Ojos del Salado an interesting study location.

This study aims to apply seismic methods to determine the activity levels of the Ojos del Salado and the nearby smaller volcanoes, as well as whether these are seismically linked to the Laguna Verde. To this end, a network of 29 geophones were deployed around the Ojos del Salado and up to the Laguna Verde for the month of February, 2024. The geophones were grouped into six sub-arrays so that array techniques such as beamforming could be used to better locate events slightly outside the network. The complete network recorded for 19 days.

We present here the current seismic catalogue from this investigation. Within the recording time we found 63 Volcano-Tectonic (VT) events, with local magnitudes above 0. The largest event had a local magnitude ML 2.8. These events were mainly clustered on the western flank of Ojos del Salado, with a smaller, less-dense cluster to the north. Twelve events were large enough to calculate fault plane solutions, most of these were just south of the summit and show normal faulting suggesting north-south extension. However, one event north of the summit shows potential thrust faulting suggesting east-west compression. We compare the catalogue results with what is known of the local geology and regional stress field, to learn more about this unique, and clearly seismically active, volcano.

## **P-SO-10**

### **The cascade of events triggering a teleseismic week-long monochromatic signal**

**A. Carrillo-Ponce<sup>1,2</sup>, S. Heimann<sup>2</sup>, G. Petersen<sup>1</sup>, T. R. Walter<sup>1,2</sup>, S. Cesca<sup>1</sup>, T. Dahm<sup>1</sup>**

<sup>1</sup>*GFZ German Research Centre for Geosciences, Potsdam,*

<sup>2</sup>*Universität Potsdam, Potsdam*

A cascade of events took place in a remote area of East Greenland on 16 September 2023. Using seismological data on regional and global scales we can reconstruct the series of events, which is also validated with high-resolution satellite images. The seismic signals generated in the Dickson fjord are dominated by two distinct frequency ranges: a long-period (LP) signal (0.02-0.06 Hz) immediately followed by a very-long period (VLP) monochromatic signal (0.0109 Hz). The latter signal was strongly recorded even at 5000 km distance and lasted over a week. To characterize the processes we perform single force (SF) inversions to both signals and obtain that the LP oscillation is well reproduced by a downward SF with orientations consistent to the rockslide observed in satellite imagery. The VLP signal, on the other hand, is characterized by a horizontal force that is perpendicular to the fjord, which is consistent with water seiching back and forth in the fjord. To understand the long duration of the VLP oscillation, we analyse the stacks of three teleseismic arrays signals, where the best fit of the amplitude decay is explained with a damped oscillator model. A simple analytical model is also considered to explain the force direction and frequency of water seiching in a narrow fjord.

Carrillo-Ponce et al. (2024); The 16 September 2023 Greenland Megatsunami: Analysis and Modeling of the Source and a Week-Long, Monochromatic Seismic Signal. *The Seismic Record*; 4 (3): 172–183. doi: <https://doi.org/10.1785/0320240013>

## **P-SO-11**

### **Deciphering plausible driving mechanisms of swarms in the western Peloponnese (Greece) using earthquake clustering and statistical properties**

**S. Ahmadnia, D. Essing, R. M. Harrington, G. M. Bocchini**

*Ruhr-Universität Bochum, Institut für Geologie, Mineralogie und Geophysik, Bochum*

The Peloponnese lies in the north-western Hellenic Subduction System (Greece) where the oceanic Nubian plate is currently subducting beneath the continental Aegean microplate at ~35 mm/yr. The fast plate convergence rates result in intense seismicity along the entire western coast of Peloponnese and offshore to the west. While large-scale deformation along the plate interface is well studied, small-scale variations in the spatiotemporal distribution of earthquakes in the upper Aegean microplate remain poorly resolved. In this study, we investi-

gate the deformation mechanisms associated with an earthquake swarm located at shallow depth, with specific aim of determining the plausibility of fluid migration as a driving mechanism. Specifically, we examine the seismicity around Kaiafas Lake, near the town of Zacharo, where a cluster of roughly 90 earthquakes occurred in May 2024 at ~5km depth over a period of several weeks. Notably, the swarm at Kaiafas Lake began approximately one month after an offshore M5.9 earthquake occurred on March 29, 2024 at a depth of 30-40 km, about 50 km west from Lake Kaiafa. We will present our analysis of seismic activity from February 2011 through 2024 taken from the National Observatory of Athens earthquake catalog to provide the context of longer-term seismicity in the region and interpret potential earthquake interactions via dynamic triggering. We will also present first results of additional cluster analysis that statistically quantify the cataloged seismicity, including the magnitude-frequency relation  $b$ -value and its temporal variation, as well as possible migration patterns. Based on the statistical analysis and migration patterns, we will present first interpretations of the physical mechanisms driving swarms within the study area around Kaiafa Lake and place it in context of the regional tectonic setting in the western Peloponnese.

## P-SO-12

### **Modeling historical earthquakes to quantify the Coulomb Failure Stress changes leading up to the 2023 Kahramanmaraş, Türkiye earthquake sequence**

**C. Fockenberg, A. Verdecchia, G.-M. Bocchini, R. M. Harrington**

*Institut für Geologie, Mineralogie und Geophysik, Bochum*

On 6 February 2023 at 01:17:34 UTC, two M7+ earthquakes ruptured the Eastern Anatolian Fault Zone (EAFZ) in southeastern Türkiye and northern Syria. The largest of the two earthquakes, a M7.8, extended from Bay of İskenderun in the SW to Çelikhan in the NE and ruptured multiple segments of the EAFZ over a distance of 310 km. The 2023 earthquake doublet followed a series of 13 historical earthquakes documented in the EAFZ with magnitudes  $\geq 7.0$  since 1114 CE that have dictated the stress evolution of the region leading up to the recent events. In this work, we perform Coulomb Failure Stress modeling of the historical earthquakes in order to test whether they promoted or inhibited the failure of the first M7.8 earthquake of the 2023 sequence.

Our analysis uses historic magnitude estimates and standard scaling relations to produce 3D fault slip-distribution models that are used as input for the Coulomb Failure Stress models. We consider two scenarios with a 3D fault geometry: one considering the stress evolution governed by changes from the successive rupture of historical earthquakes (coseismic stress), and the second considering both the stress changes produced by historical earthquakes and the tectonic loading (interseismic stress). Our results show that in both models, 12 out of the 13 historical earthquakes occur in areas with positive Coulomb stress changes on the order of at least  $\geq +0.1$  bar. However, for the 2023 M7.8 earthquake, the model with tectonic loading shows increased Coulomb stress perturbations of 50 bars that promote failure on the segment where the M7.8 nucleated. In contrast, the model that excludes tectonic loading produces stress changes of -20 bar (inhibiting failure), suggesting that tectonic loading is the dominant contributing factor to the nucleation of the 2023 M7.8 event. In addition to stress changes induced by loading and earthquake interactions, we present evidence that the fault geometry exhibits control on Coulomb stress accumulation in regions of geometric complexity. In particular, fault complexity may have facilitated rupture propagation across multiple fault segments during the 2023 sequence.

## P-SO-13

### A repeating earthquake catalog for Northern Chile

J. Folesky<sup>1</sup>, J. Kummeow<sup>1</sup>, L. J. Hofman<sup>2</sup>

<sup>1</sup>*Freie Universität Berlin, Geophysik, Berlin,*

<sup>2</sup>*Freie Universität Berlin, Berlin*

Repeating earthquakes are nearly identical seismic events that occur reiteratively on the same patch of a fault with very consistent focal mechanisms, and can therefore be identified by their high similarity in waveform. Their magnitude-dependent recurrence intervals can be used to

estimate local fault slip and infer the spatial and temporal pattern of aseismic creep zones at depth. They can be used to describe fault slip behavior or to resolve detailed fault structures. Subtle changes in their waveforms can also reveal variations in rupture processes or temporal changes in local seismic velocity structures.

Here we construct the first long-term repeating earthquake catalog for northern Chile. Using the waveforms of about 180,000 earthquakes from a recent regional seismicity catalog as templates, we perform GPU-based template matching to search for repeating earthquakes in the continuous multi-annual seismological data of the regional permanent IOPC station network for the period 2006 to 2023. The resulting catalog of repeating earthquakes contains ~11,000 events grouped into ~3,200 families. We observe a remarkable variability in size and behavior of the families, ranging from long-lasting regular sequences to short-lived burst-type repeaters.

In addition, two megathrust earthquakes in 2007 and 2014 have a strong influence on the spatio-temporal distribution of repeaters in the vicinity of the coseismic slip zones: series in the immediate vicinity show a strong after-slip-driven decay behavior, which systematically decreases in strength for more distant repeaters.

Using the repeater catalog, we are able to provide a time-dependent slip map for large areas of the slip interface between the subducting Nazca slab and the overriding South American plate.

The final reported catalog consists mainly of interface repeaters, but also includes many crustal upper plate repeaters, as well as deep intraslab repeaters. It will facilitate future detailed analysis of rupture processes, source structure, and of the spatio-temporal evolution of slow slip at depth. It additionally allows for comparative studies with repeater catalogs from other subduction zones, such as Japan.

## P-SO-14

### Out of the box or own model for ML phase picking at local (GRSN) and teleseismic distances (IMS)?

A. Steinberg, K. Stammler, C. Ramos, G. Hartmann, P. Gaebler, T. Plenefisch, B. Goebel

*Bundesanstalt für Geowissenschaften und Rohstoffe (BGR), Erdbebendienst des Bundes,  
Kernwaffenteststopp, Hannover*

We present our work on training and the application of machine learning algorithms (ML) for the automated phase picking of body waves on data from the German Regional Seismic Network (GRSN).

Phase picking is a necessary step before event localization and characterization. Deep learning based models have been proven to perform well at this task. PhaseNet and EQTransformer are two prominent state-of-the-art phase picking algorithms that have been retrained on several different datasets.

We train new phase pickers based on the PhaseNet architecture and a database of 20 years listed in the earthquake catalog of BGR. The models are trained and evaluated with manual phase picks of BGR analysts. We compare the performance of the newly trained models by also applying other pre-trained PhaseNet and EQTransformer based phase pickers on unseen data.

We determine if already pre-trained models can be used satisfactory out of the box for phase picking of waveforms of the German Regional Seismic network.

To assess the capabilities for automatic teleseismic phase selection we further train a PhaseNet model on primary and auxiliary stations from the International Monitoring System (IMS) of the CTBTO. For training we use good quality picks from manual event analysis of the CTBTO events between 2013 until 2023. We apply the IMS model both on unseen IMS data from 2024 and to the data of the German Regional Seismic Network to determine generalization.

## P-SO-15

### Heterogene seismische Anisotropie in der Erdkruste und Auswirkungen auf XKS-Splittinganalysen

M. Kaus, J. P. Kruse, A. Kaviani, G. Rümpker

Goethe-Universität Frankfurt, Institut für Geowissenschaften, Frankfurt am Main

Seismische Anisotropie im Erdinneren liefert wertvolle Einblicke in geodynamische Prozesse und die Deformationsgeschichte des Erdmantels. Zur Charakterisierung der Anisotropie wird häufig die Messung des Scherwellen-Splittings herangezogen. Der Einfluss der kleinräumigen und stark heterogenen Anisotropie der Erdkruste auf XKS-Splittinganalysen ist jedoch bislang nicht vollständig geklärt. Oft wird angenommen, dass die Anisotropie der Kruste im Vergleich zum Erdmantel nur einen geringen Beitrag zum XKS-Splitting leistet und daher vernachlässigt werden kann. Demgegenüber weisen Laborstudien an Gesteinsproben häufig stark ausgeprägte anisotrope Eigenschaften nach.

In dieser Studie wird die Hypothese untersucht, dass auch eine stark ausgeprägte Anisotropie der Kruste aufgrund ihrer Heterogenität von langwelligen teleseismischen XKS-Phasen nicht aufgelöst werden kann. Hierfür wurden numerische Finite-Differenzen-Modellierungen des seismischen Wellenfeldes durchgeführt. Die Kruste wurde als Schicht mit lateralen Abfolgen anisotroper Zonen modelliert, deren schnelle Achsen in jeder Zone unterschiedlich orientiert sind. Die charakteristische Korrelationslänge der anisotropen Zonen variierte dabei zwischen 1 und 100 km. Der darunterliegende Erdmantel wurde als anisotrope Schicht mit einheitlicher schneller Achse und einer Delaytime von 1,0 s angenommen.

Die Ergebnisse zeigen, dass es bei Korrelationslängen zwischen 5 und 20 km einen Übergangsbereich gibt, in dem die Kruste signifikante Auswirkungen auf die Splittinganalysen hat. Für kleinere Korrelationslängen erscheint die Kruste nahezu isotrop, selbst wenn die effektive Delaytime der anisotropen Zonen 0,5 s beträgt. Erst bei Korrelationslängen im Übergangsbereich oder darüber beeinflusst die Anisotropie der Kruste die Splittinganalysen deutlich.

Die Ergebnisse dieser Studie unterstreichen, dass es sinnvoll ist, bei XKS-Splittinganalysen die komplexen Wechselwirkungen zwischen Krusten- und Mantelanisotropien stärker zu berücksichtigen, um geodynamische Prozesse im Erdinneren besser zu verstehen.

## The SIEGFRIED passive seismological network

M. Dietl<sup>1</sup>, M. P. Roth<sup>2</sup>, S. Carrasco<sup>2</sup>, S. Neugebauer<sup>1</sup>, N. Fazlibašić<sup>1</sup>, C. Finger<sup>1</sup>

<sup>1</sup>Fraunhofer IEG, Bochum,

<sup>2</sup>Ruhr-Universität Bochum, Bochum

Geothermal energy is a renewable, weather-independent energy source, but carries socio-economic risks such as induced seismicity. The application of innovative methods offers the opportunity to base geothermal projects not only on static geological subsurface models, but also to incorporate stress predictions.

The SIEGFRIED project aims to make the seismic risk of deep geothermal projects in the Lower Rhine Embayment assessable in a spatially differentiated manner. Based on the combination of seismological, geological and geomechanical data sets and modeling, we will create earthquake hazard maps and thus offer the possibility of evaluating potential geothermal sites for their suitability in terms of earthquake hazard.

As a first step towards those goals, we installed the YV seismic station network consisting of eight broadband stations within a 15 km radius around the town of Eschweiler-Weisweiler to supplement existing data sets of the region. Seven stations are transmitting data in real time and the eighth station is in the base of a dam without telecommunication reception. One of the stations is installed in a 100 m deep borehole close to the town center of Eschweiler-Weisweiler and has been installed to reduce the impact of the very high urban noise level in the center of the network on the seismic network performance. Six out of the eight stations are sampling at 100 Hz. The borehole and dam stations are sampling at 500 Hz.

We present the network's instrumentation and geometry and give an insight into the data quality by determining probabilistic power spectral densities (PPSD) of the ambient vibrations. These PPSDs show the seismic power for different frequencies and are used for assessing the noise levels of individual seismological stations. This enables us to investigate the suitability of the station locations for longer-term monitoring purposes in the area. We also inspect waveforms for the visibility of local earthquakes, which also contributes to the assessment of data quality.

Based on the results and combined with data of other stations previously operating in the area, we show that the noise level correlates strongly with the local geology, especially with varying sediment thicknesses. In addition, we compare the noise level of the borehole station with neighboring surface stations to quantify the benefits of the borehole station and evaluate its advantage for the network.

## **P-SO-17**

### **Seismologische Überwachung im Freistaat Sachsen: Migration des Sachsen-Netzes SXNET von der Universität Leipzig an die TU Bergakademie Freiberg**

**C. Alexandrakis-Zieger<sup>1</sup>, F. Hänel<sup>1</sup>, F. Käßner<sup>1</sup>, S. Funke<sup>2</sup>, R. Voigt<sup>2</sup>, M. Korn<sup>2</sup>, L. Sonnabend<sup>3</sup>, S. Buske<sup>1</sup>**

<sup>1</sup>*TU Bergakademie Freiberg, Institute of Geophysics and Geoinformatics, Freiberg,*

<sup>2</sup>*Universität Leipzig, Institut für Geophysik und Geologie, Leipzig,*

<sup>3</sup>*Sächsisches Landesamt für Umwelt, Landwirtschaft und Geologie, Geologische Kartierung und Geophysik, Freiberg*

Die seismologische Überwachung im Freistaat Sachsen wurde im Laufe des Jahres 2024 von der Universität Leipzig an das Institut für Geophysik und Geoinformatik der TU Bergakademie Freiberg (TUBAF) verlegt. Der Umzug des Projektes soll planmäßig bis Ende Februar 2025 abgeschlossen sein. Er wurde notwendig, weil es an der Universität Leipzig seit 2021 keine seismisch orientierte Arbeitsgruppe mehr gibt.

In diesem Poster stellen wir die neue Konfiguration und den aktuellen Stand der Migration inkl. Instrumentierung, Hard- und Software sowie die personelle Situation am neuen Standort TUBAF vor.

## **P-SO-18**

### **Seismische Ereignisse in der südwestlichen Ostsee – Harmonisierung des deutschen und dänischen Ereigniskatalogs**

**J. Horrmann, C. Weidel, T. Meier**

*Christian-Albrechts-Universität zu Kiel, Kiel*

Das norddeutsche Becken und die angrenzenden Küstenmeere sind insgesamt seismisch schwach aktiv. Verfügbare Erdbebenkataloge aus Deutschland (Leydecker 2011, fortgeschrieben durch BGR) und Dänemark (vom dänischen geologischen Dienst, GEUS) enthalten eine große Anzahl an Explosionsereignissen, allerdings treten gerade in der deutschen Ostsee im Bereich der Kadetrinne und in der Region um Bornholm (DK) auch wiederkehrend tektonische Ereignisse auf. Ein Vergleich des deutschen mit dem dänischen Ereigniskatalog für die südwestliche Ostsee zeigt in vielen Fällen Inkonsistenzen sowohl in den Lokalisierungen als auch in der Bewertung des Quelltyps.

Um natürliche Seismizität in der Region besser bewerten zu können, ist eine Harmonisierung der Ereigniskataloge erstrebenswert. Für Ereignisse seit 1992 liegen digitale Wellenformen vor, welche für alle Ereignisse zusammengetragen und anhand von Seismogrammsektionen, Wellenformvergleichen und Spektrogrammen neu bewertet wurden. Die Reevaluation von Ereignissen welche in beiden Katalogen gelistet sind, zeigt zum einen, dass einige der als „tektonisch“ markierten Ereignisse eher als Explosionsereignis zu bewerten sind. Zum anderen ist die Lokation einzelner Ereignisse nicht eindeutig rekonstruierbar. Eine Betrachtung älterer Ereignisse würde eine sehr aufwändige Auswertung analoger Seismogramme erfordern. Aufgrund des Ausbaus der seismologischen Infrastruktur in Mecklenburg-Vorpommern seit 2019 sind die Unsicherheiten sowohl in der Lokalisierung als auch der Quellbewertung in den letzten Jahren deutlich gesunken.

## P-SO-19

### Illuminating Subsurface Dynamics During Injection and Production Restart in Deep Geothermal Wells Using Fiber-Optic Distributed Dynamic Strain Sensing

J. Hart<sup>1,2</sup>, C. Wollin<sup>1</sup>, A. Andy<sup>3</sup>, T. Ledig<sup>4</sup>, T. Reinsch<sup>5,6</sup>, C. Krawczyk<sup>1,2</sup>

<sup>1</sup>GFZ Helmholtz-Zentrum für Geoforschung, Potsdam,

<sup>2</sup>Technische Universität Berlin, Berlin,

<sup>3</sup>Technische Universität München, München,

<sup>4</sup>Stadtwerke München, München,

<sup>5</sup>Fraunhofer IEG, Bochum,

<sup>6</sup>Ruhr Universität Bochum, Bochum

This work presents the first results from Distributed Dynamic Strain Sensing (DDSS or DAS) measurements within a deep geothermal well doublet. This technology's unrivaled high spatio-temporal resolution enables us to monitor seismic activity, strain, and temperature changes along the sensing cable.

We measured a 3.7 km and an approximately 4.0 km long fiber optic cable in a production and injection borehole, respectively, both installed post borehole completion and reach into the reservoir. Distributed sensing was accomplished with a commercial DDSS acquisition system sampling the boreholes at a 1 m spatial period and 2000 Hz.

This work focuses on the DDSS recordings from the initial production and injection phase and shows a broad spectrum of subsurface dynamics. Low- and high-frequency strain dynamics were quantified by applying a cascading decimation routine and calculating a proxy for the vibrational energy with the root mean square (RMS). The results reveal various processes related to the reservoir properties and well integrity.

We present the initial results of our monitoring campaign in the framework of the GFK-Monitor project. These results demonstrate the vast potential of DDSS to detect complex geophysical phenomena in geothermal environments. Our research can advance downhole monitoring technologies to better understand subsurface processes and optimize geothermal energy production.

## P-SO-20

### Fiber-optics-based observational platforms for investigating the urban subsurface: the InDySE Project

V. Rodríguez Tribaldos<sup>1</sup>, L. Pinzón Rincón<sup>1</sup>, C. Krawczyk<sup>1,2</sup>, P. Martínez-Garzón<sup>3</sup>,

M. Bohnhoff<sup>3,4</sup>

<sup>1</sup>GFZ Helmholtz Centre for Geosciences, Geophysical Imaging, Potsdam,

<sup>2</sup>Technical University Berlin, Institute for Applied Geosciences, Berlin,

<sup>3</sup>GFZ Helmholtz Centre for Geosciences, Geomechanics and Scientific Drilling, Potsdam,

<sup>4</sup>Free University Berlin, Department of Earth Sciences, Berlin

Urban sustainable development and improved resilience to geohazards requires an exhaustive understanding of the geological structure, physical properties and dynamics of the shallow subsurface underneath urbanized areas at the sub-kilometer scale. Yet, our current understanding of the urban subsurface is limited by our ability to image its structure and temporal variations at high resolution using classical geophysical approaches. Recently, the application of conventional ambient noise interferometry analysis to dynamic strain data recorded using Distributed Acoustic Sensing (DAS) deployed on unused telecommunication fiber-optic cables (dark fibers) has emerged as an attractive alternative for cost-efficient, regional scale (10's of km) seismic imaging and monitoring at high resolution. Still, its application to urban areas remains vastly underutilized. One of the most significant hurdles is the

lack of efficient data exploration and processing tools to address and harness the unique challenges of DAS-based urban seismic noise data, which include the complexity of the noise field, unconventional array geometries and non-uniform coupling conditions, and massive data volumes.

The InDySE project (Interrogating the Dynamic Shallow Earth) aims at addressing these challenges to develop and validate the next generation of subsurface imaging and monitoring platforms in urban areas based on the combination of existing fiber-optic networks and infrastructure noise. Our pilot study site is the metropolitan area of Istanbul (Turkey), where understanding the shallow subsurface at high resolution is critical for evaluating exposure to a variety of geohazards. Since May 2024, DAS data have been continuously acquired along a 17 km-long dark fiber traversing part of the densely populated district of Kartal, crossing almost perpendicularly the underinvestigated Kartal Fault. Both ambient seismic noise and local and regional earthquakes have been captured by the array and will be analyzed to illuminate the Kartal and other potential hidden faults, to obtain high-resolution maps of geological materials that can be translated into maps of local site response to large earthquakes, and to track seismic velocity changes linked to hydrological dynamics related to ground movements such as landsliding and subsidence. Ultimately, InDySE aims at developing efficient approaches for using dark fiber in urban subsurface investigations with implications in geohazard assessment.

## VU – Vulkanologie Vorträge

### O-VU-01

#### Observation of electric phenomena associated with eruptions of Strokkur Geyser, Iceland

J. Börner<sup>1</sup>, M. Hort<sup>1</sup>, D. Peppel<sup>2</sup>, M. Scheunert<sup>1</sup>, C. Schneider<sup>2</sup>, K. Spitzer<sup>1</sup>

<sup>1</sup>TU Bergakademie Freiberg, Institut für Geophysik und Geoinformatik, Freiberg,

<sup>2</sup>Universität Hamburg, Institut für Geophysik, Hamburg

Strokkur Geyser, located in the geothermal area of Haukadalur, Iceland, is one of the World's most active geysers. It erupts every 5 to 10 minutes, shooting a column of hot water and steam up to 35 meters into the air. The entire eruption cycle of Strokkur is, however, not fully understood yet. While the general mechanism—water heating, pressure buildup, and sudden release—provides a framework, many aspects, like the exact dynamics of bubble formation, the role of dissolved gases, and the interactions between water chemistry, temperature and pressure as well as rock structures remain unclear.

To contribute to the investigation of Strokkur's geothermal activity and hydrothermal dynamics we wanted to take a closer look at the electric environment and carried out a multi-EM time-lapse monitoring field survey including the DC resistivity, induced polarization and time-domain electromagnetic methods. Repetition periods were as short as 2 s yielding high temporal resolution of the eruption cycle. Exploiting all available information about the observation site, the experimental layouts for all methods were designed in advance using our electromagnetic finite element simulation and inversion library FEMALY and adjusted in the field. In addition to the electromagnetic methods, a seismic monitoring station, an infrasound recorder, and a tilt meter were operated to supplement the monitoring approach. Finally, video footage was taken to provide unique time stamps for the eruption events

including intermittent oscillations of the conduit's water level presumably associated with collapsing gas bubbles at depth.

We will present a first glimpse on the recorded data. At this point, we can tell that the response of each method shows clear evidence of the eruption process. All electromagnetic methods display consistent temporal variations of the electric resistivity probably situated in the near-surface range around Strokkur's conduit and pond. Even the small signals associated with the fluctuating water level of the pond are mapped onto the different electromagnetic responses which speaks for the overall high sensitivity of all EM methods. Nevertheless, a full explanation of the cause of these changes remains unclear.

Future work will include a full 3D inversion of the TEM data using FEMALY to derive a spatial setting of the electric conductivity on a larger scale, as well as a thorough interpretation of the observed phenomena in the light of existing theories.

## **O-VU-02**

### **TEM at breathtaking heights: Imaging the shallow fumarolic system of Lastarria volcano, Chile**

**T. Vondenhoff<sup>1</sup>, B. Blanco-Arrué<sup>2</sup>, J. Roas-Domingo<sup>1</sup>, B. Tezkan<sup>1</sup>, D. Diaz<sup>3</sup>, P. Yogeshwar<sup>1</sup>**

<sup>1</sup>*Institute für Geophysik und Meteorologie, Universität zu Köln, Köln,*

<sup>2</sup>*LIAG Institute for Applied Geophysics, Hannover,*

<sup>3</sup>*Department of Geophysics, University of Chile, Santiago, Chile*

Volcanic activity poses significant risks to human life and infrastructure while offering valuable insights into geological processes. Volcanoes can serve as natural laboratories for studying subsurface processes on a larger scale.

This study presents the findings of transient electromagnetic (TEM) measurements conducted on the Lastarria volcano in Chile, aimed at investigating the shallow subsurface dynamics that drive volcanic activity. The focus is on understanding electrical conductivity variations around a field of fumarolic vents emitting hot sulfuric gases. By combining state-of-the-art inversion techniques, extensive sensitivity studies, and electromagnetic induction (EMI) mapping, we aim to better understand the processes occurring within the shallow subsurface (~250 m) and their implications for the broader volcanic system.

Here, we present 1D inversion results derived using conventional Marquardt-Levenberg and Occam inversion techniques, where 1D models are compiled into quasi-2D sections. Model parameter importance and equivalent modeling are applied to assess the model uncertainties. Additionally, we showcase 3D inversion results obtained using the recently developed Julia Package (3DTEMinv) for time-domain 3D inversion and modeling.

Our results reveal a robust and consistent subsurface structure characterized by two key features. First, a double conductive layer is observed between 30 m and 60 m depth beneath the volcanic edifice. This feature exhibits remarkable spatial continuity and highly agrees with surface manifestations and the EMI data. Second feature identified is a deep seated conductor (>200 m). Both structures were validated through sensitivity modeling. Although the precise resistivity and spatial extent of the deep conductor remains uncertain, its presence is vital for a good fit, suggesting complex interactions within the deeper volcanic system.

Overall, the 1D and 3D results exhibit strong agreement and correlate well with surface manifestations and EMI mapping data. These findings enhance our understanding of magmatic-hydrothermal processes at the Lastarria volcano.

## **O-VU-03**

### **Onshore seismic monitoring of submarine Kavachi volcano reveals vigorous eruptive activity**

**G. Rümpker<sup>1,2</sup>, C. Roga<sup>3</sup>, A. Kaviani<sup>1</sup>, F. Limberger<sup>1</sup>, L. Bitzan<sup>1</sup>, P. Laumann<sup>1</sup>, C. Tatapu<sup>3</sup>, J. Gwali<sup>3</sup>, T. Manker<sup>1</sup>, C. Vehe<sup>3</sup>**

<sup>1</sup>*Goethe-Universität Frankfurt, Frankfurt,*

<sup>2</sup>*Frankfurt Institute for Advanced Studies, Frankfurt,*

<sup>3</sup>*Ministry of Mines, Energy and Rural Electrification, Geological Survey Division, Honiara, Solomon Islands*

Submarine volcanoes pose considerable challenges in monitoring their activity. Kavachi, situated in the Western Province of the Solomon Islands, is a highly active submarine volcano that presents potential risks to nearby communities, as well as to air and marine traffic in the region. In this study, we employ onshore seismic stations to observe Kavachi's eruptive activity by analyzing volcano-seismic signals. Based on recordings from seismic array stations situated on Nggatokae Island, approximately 27 km and 36 km away from the volcanic edifice, we detected and quantified the eruptive activity of Kavachi between February and November 2023.

We first employed a dual-station approach, with stations separated by 9 km, to identify and quantify characteristic seismo-volcanic signals. This method leverages station-specific band-limited amplitude ratios, inspired by techniques originally developed in bioacoustics for detecting whale sounds in seismograms. Using this approach, we documented significant variability in volcanic activity, ranging from quiescent periods with no detected events to intense phases exceeding 2,500 seismic events per day, associated with episodic volcanic tremors and short-duration explosive signals.

Additionally, array analysis was conducted using data from four closely spaced seismic stations (average spacing of 190 m) on the southern coast of Nggatokae. Cross-correlation techniques were applied to determine the back-azimuth and apparent velocity of volcanic events. Results indicated a consistent mean back-azimuth of 222.6°, closely aligning with the theoretical value of 225° for Kavachi.

Interpretation of these signals was further supported by waveform modeling to provide insights into the source mechanisms and path effects. The findings demonstrate that onshore seismic arrays can effectively monitor submarine volcanic eruptions. This methodology not only offers insights into the eruptive activity of Kavachi volcano but presents potential applications for monitoring other submarine volcanoes globally.

## **O-VU-04**

### **The nature of volcanic tremor at Oldoinyo Lengai volcano, Tanzania**

**M. C. Reiss<sup>1</sup>, D. Roman<sup>2</sup>, C. Caudron<sup>3</sup>, P. Hering<sup>4</sup>**

<sup>1</sup>*Gutenberg Universität Mainz, Institut für Geowissenschaften, Mainz,*

<sup>2</sup>*Carnegie Science, Washington, United States of America,*

<sup>3</sup>*Université Libre de Bruxelles, G-Time, Brüssel, Belgium,*

<sup>4</sup>*Igem, Bingen*

Volcanoes produce eruptions – some of which have catastrophic results for our society, environment, climate and economy. Though seismology has been on the forefront of monitoring volcanoes and imaging magmatic systems at depth, one seismic signal remains particularly

elusive: volcanic tremor. Difficult to locate due a lack of clear onsets, lasting between minutes to years, and varying from volcano to volcano in duration, frequency content, recurrence interval and relationship to other observables such as gas emission, deformation and eruptive activity, these observations have led to a myriad of source models. Using data from a short-term seismic deployment on Earth's only currently active carbonatite volcano Oldoinyo Lengai, Tanzania, we exploit coherent seismic signals in the frequency domain to locate volcanic tremor. Here we show that narrow-band tremor occurs dominantly in an aseismic mush zone in the upper 6 km of the volcano bsl as well as down to depths of 20 km. We relate this to carbonatite melt ascent across the crust. We further show how narrow-band tremor is interceded by quasi-harmonic tremor which we interpret as the interplay of deeper magmatic injections below and the resonance of a sill-like structure at shallow depth. We use these observations to overturn decade-long debates on the proposed shallow nature of tremor and propose that tremor holds the key to understanding yet unresolved problems regarding the dynamics of magmatic plumbing systems.

## VU – Vulkanologie Poster

### P-VU-01

#### Three-Dimensional Inversion of Magnetotelluric Data from Mt. Ruapehu, New Zealand

P. Semper<sup>1</sup>, T. Bertrand<sup>2</sup>, G. Caldwell<sup>2</sup>, W. Heise<sup>2</sup>, M. Scheunert<sup>1</sup>, K. Spitzer<sup>1</sup>

<sup>1</sup>TU Bergakademie Freiberg, Institut für Geophysik und Geoinformatik, Freiberg,

<sup>2</sup>GNS Science, Lower Hutt, New Zealand

The andesite–dacite stratovolcano Mt. Ruapehu formed ~230 ka ago at the southern termination of the Taupo Volcanic Zone (TVZ), a rifted arc and a centre of active rhyolitic volcanism. In the last century, Mt. Ruapehu has been frequently active with the last large phreatomagmatic eruption in 1995/96 and a steam driven eruption in 2007.

To image the magmatic system beneath Mt. Ruapehu, 40 magnetotelluric (MT) measurements were acquired in the area between 2007 and 2009. Previous 2-D and 3-D modelling of these data show the underlying electrical resistivity structure. However, due to the relatively sparse site distribution and the use of a finite difference 3-D inversion code that does not include topography, the resolution of existing models is coarse. To improve these resistivity models, in 2023, 28 new MT measurements were acquired at Mt. Ruapehu to fill gaps in the existing data, and achieve a uniform coverage of measurements around the volcano.

Here, we present preliminary results of the 3-D inverse modelling of the complete set of MT data acquired at Mt. Ruapehu using FEMALY: A Finite Element MAtlab LibrarY for Electromagnetics. Impedances were inverted for 18 periods between 3 ms and 341 s with particular emphasis on an appropriate representation of the rugged topography. In a first attempt, we adapted the level of detailedness of the topography using an inverse distance weighting scheme, which resolves the main topographic features.

We will also compare our initial inversion findings from Mt. Ruapehu with the latest detailed models from the adjacent Mt. Tongariro.



## Index of authors

(bold = first author)

■ Abe, S.	P-S2-02, <b>P-S2-08</b>	Bischoff, M.	O-OG-12, P-S2-01
Aberle, J.	P-OG-24	Bitzan, L.	O-VU-03
Abu Jaish, Y.	O-OG-02, O-OG-03	Blackman, D. K.	P-SO-05
Ágústsdóttir, T.	O-SO-07, P-SO-07	Blanco-Arrué, B.	O-VU-02, <b>P-OG-04</b> , P-OG-21
Ahmadnia, S.	<b>P-SO-11</b>	Bloch, W.	<b>O-S2-03, O-SO-16</b>
Ahrensmeier, L.	O-S4-01	Bocchini, G. M.	O-GD-03, P-SO-11, P-SO-12
Airo, A.	P-OG-12, P-OG-21	Bohlen, T.	P-MI-01, P-MI-02, P-MI-03
Al Tawashi, F.	<b>P-OG-13</b>	Bohnhoff, M.	P-SO-20
Alaei, N.	<b>O-OG-08</b>	Boitz, N.	<b>O-KI-04, O-S2-02</b>
Alexandrakis-Zieger, C.	<b>P-SO-17</b>	Bookhagen, B.	O-AG-03
Allroggen, N.	<b>P-OG-15</b>	Börner, J. H.	<b>O-S4-PV, O-VU-01,</b>
Amarawardana, D.	<b>O-S4-06</b>	Börner, R.-U.	P-S4-02, P-OG-26
Amelung, F.	O-AG-03	Böse, C.	P-GT-02, <b>P-MI-05</b>
Andersson, H.	O-MI-07	Bostock, M.	O-S2-05
Andy, A.	P-SO-19	Bou-Rabee, F.	O-S2-03
Anthony, E.	<b>P-MI-03</b>	Boxberg, M. S.	O-OG-04
Antonov, Y.	O-MI-07	Brandl, P. A.	P-MI-04
Arrué Blanco, B.	P-OG-12	Branß, T.	P-MG-04
Atkisson, G.	P-SO-05	Bräunig, L.	P-OG-24
Ávila-García, J.	O-GD-02	Breede, K.	O-SM-04, P-SM-01, <b>P-SM-02</b> ,
		Breitzke, M.	P-SM-03
■ Babeyko, A.	O-GO/OS-02, O-GO/OS-03	Brogi, C.	<b>O-S4-04, P-S4-08</b>
Bagge, M.	<b>P-PV-01</b>	Brömer, B.	<b>P-MG-01, P-MG-01</b>
Balcewicz, M.	P-BL-01, P-BL-04, P-OG-24, P-OG-25	Brückner, H.	P-OG-07
Balza Morales, A.	<b>O-MI-03</b>	Buchholz, P.	O-S4-03
Baris, S.	P-MG-03, P-OG-22	Büchner, J.	P-OG-22
Bartzke, G.	P-MI-08	Bücker, M.	O-SO-10
Bauckholt, M.	P-OG-10		O-S1-03
Bauer, F.	O-OG-10, P-OG-06		O-OG-07, O-S4-03, <b>O-S4-04</b> ,
Bayat, M.	<b>P-AG-01</b>		P-OG-01, P-OG-14, P-PV-02,
Becken, M.	O-AG-02		P-S4-08
Becker, D.	<b>P-SO-03</b>	Buness, H.	O-OG-08
Becker, M.	O-SO-19	Burberg, S.	<b>O-OG-04</b>
Becker, V.	P-SM-01, P-SM-02	Burger, I.	<b>P-OG-05</b> , P-S4-04
Bedford, J.	O-S3-01, <b>O-S3-02, O-S3-02</b> , P-S3-01	Burjánek, J.	O-SO-07, P-SO-07
Behrens, D.	<b>P-MI-08</b>	Burschil, T.	<b>O-SM-01</b>
Behrens, M.	P-OG-17	Burzik, A.	<b>P-OG-16</b>
Beiwers, L. M.	<b>O-SO-15</b>	Buske, S.	O-KI-03, O-SM-03, O-SM-04,
Beisembina, G. T.	O-OG-06, <b>P-OG-08</b>	Busse, A.	P-GO-02, P-SM-01, P-SM-02,
Beniest, A.	P-SO-09	Büyükkapınar, P.	P-SM-03, P-SO-17
Bense, F.	O-MI-06		P-GO-01
Bergers, R.	P-GO-01		O-SO-04, O-SO-05, O-SO-06,
Bernard, J.	P-OG-07		O-SO-11, <b>O-SO-18</b>
Berrios Amador, E.	<b>P-GT-02</b>		
Bertrand, T.	P-VU-01		
Beyer, M.	P-OG-01, P-PV-02		

■ Caka, D.	P-OG-22	■ Ebbing, J.	P-GT-01
Calderon, J.	<b>P-OG-24</b> , P-OG-25	Eckardt, T.	O-OG-08
Caldwell, G.	P-VU-01	Edem, S.	P-BL-07
Carrasco, S.	<b>P-S2-04</b> , P-SO-16	Effner, U.	P-OG-17
Carrillo-Ponce, A.	O-SO-18, <b>P-SO-10</b>	Eibl, E. P. S.	P-SO-07
Carter, C.	P-GT-01	Eisen, O.	P-GT-01
Caudron, C.	O-SO-02, O-VU-04	El Fatih, G.	<b>P-MI-04</b>
Cesca, S.	O-SO-13, P-SO-10	Erdmann, G.	P-OG-09
Chatziliadou, M.	<b>P-BL-03</b>	Erkul, E.	O-OG-01, <b>P-MG-03</b> , P-OG-11,
Chen, J.	P-MI-02		P-OG-18
Chen, X.	P-S2-04	Ertuncay, D.	O-SO-18
Chi, Y.	O-S1-03	Esel, Y. E.	<b>P-OG-18</b>
Cochran, E. S.	O-SO-14	Essing, D.	<b>O-GD-03</b> , P-SO-11
Cökerim, K.	<b>O-S3-01</b>		
Collins, J. A.	P-SO-05	■ Faccenna, C.	O-SO-16
Corbi, F.	P-S3-01	Fahl, A.	O-KD-01
Cornelius, O.	<b>P-SM-04</b>	Fazlibašić, N.	P-SO-16
Costabel, S.	O-OG-06, P-OG-08, P-OG-09	Fechner, T.	O-KI-04
Cotton, F.	O-GO/OS-03	Feige, J.	P-OG-12
Crosetto, S.	O-S3-03	Feldmann, F.	O-OG-07
Crutchley, G.	O-GD-01	Fernandes, W.	O-MI-07
		Fertig, J.	<b>O-GO/OS-01</b>
■ Dahlin, T.	O-OG-02, O-OG-03	Fichtner, A.	<b>O-S1-PV</b>
Dahm, T.	O-S3-05, O-SO-04, O-SO-05, <b>O-SO-06</b> , O-SO-07, O-SO-11, P-SO-10	Fiebig, M.	O-SM-01
Dahmke, A.	P-OG-16	Finger, C.	<b>O-SO-12</b> , P-S2-04, P-SO-16
Dan, A.	P-OG-22	Firla, G.	O-SM-01
Danaei, S.	P-BL-07, <b>P-BL-08</b>	Fischer, K. D.	P-S2-03
de Freitas, J.	P-SM-04	Fischer, S. L.	<b>O-OG-01</b> , P-MG-03
Deckert, H.	P-S2-02, P-S2-08	Fischer, T.	P-OG-17
Dellefant, F.	O-SO-15	Fischer, T. J.	O-SO-07, <b>O-SO-08</b> , O-SO-11, P-S2-06, P-S2-07, P-SO-04, P-SO-07, P-SO-08
Deng, Z.	<b>O-S3-05</b>	Fockenberg, C.	<b>P-SO-12</b>
Diaz, D.	O-VU-02	Folesky, J.	<b>P-SO-13</b>
Dick, M.	<b>P-OG-07</b>	Forderer, A.	O-MI-03
Dick, P.	O-S2-05	Förster, T.	<b>O-S2-05</b>
Dielmann, J.	<b>P-GO-01</b> , <b>P-OG-21</b>	Franke, S.	P-GT-01
Dietl, M.	P-S2-04, <b>P-SO-16</b>	Freienstein, J.	P-GT-01
Dietrich, P.	P-OG-19, P-OG-23	Friederich, W.	P-S2-03
Dillah, M.	P-S1-03, <b>P-S1-04</b>	Friedrich, C.	P-OG-17
Ding, H.	O-SM-04	Frietsch, M.	P-S2-05
Dogar, S.	P-OG-07	Fröhlich, Y.	P-S1-03, P-S1-04
Donner, S.	O-OG-12	Funiciello, F.	P-S3-01
Dormann, M.	P-OG-24, <b>P-OG-25</b>	Funke, S.	P-SO-17
Dorn, F.	<b>P-S1-03</b> , P-S1-04		
Doubravová, J.	O-SO-07, O-SO-11, P-SO-07	■ Gabriel, A.-A.	O-GO/OS-03, O-SO-14
Drolet, D.	O-S2-03	Gabriel, G.	O-OG-08, O-SM-01
Druivenga, G.	P-SM-07	Gaebler, P.	P-SO-14
Duane, M.	O-OG-04	Garcia Pina, A.	P-SO-09
Duteloff, T.	O-SO-10	Garland, S.	P-S4-02
Dwars, M.	P-SO-07	Gasimov, E.	P-MG-03
Dyatlov, G.	O-MI-07	Gehrig, J.	<b>P-GT-01</b>
		Geisler, O.	<b>O-KD-03</b>

Gerchow, M.	P-OG-01, P-PV-02	Heise, W.	P-VU-01
Gerhards, C.	P-GT-02	Hellwig, O.	<b>P-GO-02</b>
GIAME Seismic Working Group, A.	O-GD-02	Helm, V.	P-GT-01
Giese, R.	O-S2-05	Hering, P.	O-VU-04, <b>P-S2-02</b> , P-S2-08
Gilder, S. A.	O-S1-01	Hersir, G. P.	P-SO-07
Gödickmeier, P.	O-KD-01	Hese, F.	P-SM-05
Goebel, B.	O-OG-12, P-SO-14	Heuel, J.	<b>P-S2-05</b>
Goertz-Allmann, B.	<b>O-S2-PV</b>	Heyde, I.	<b>P-MG-04</b>
Goldmann, J.-F.	P-PV-01	Hilbich, C.	P-MI-06
Gomba, G.	O-S3-03	Hiller, T.	P-OG-08, <b>P-OG-09</b>
Govoorts, J.	O-SO-02	Hloušek, F.	O-KI-03, O-SM-03, O-SM-04, P-SM-01, P-SM-02, <b>P-SM-03</b>
Grayver, A.	P-GO-01	Hobiger, M.	<b>O-OG-12</b>
Gremmler, S.	P-KD-01, P-KD-02	Hoffmann, J.	O-OG-01, P-MG-03
Grobla, L.	O-S4-07	Hofman, L. J.	P-SO-13, O-SO-13
Großmann, J.	O-SM-01	Hofmann, D.	P-OG-15
Gross, F.	P-MG-03	Hoppenbrock, J.	O-OG-07, P-OG-01, <b>P-PV-02</b>
Grundke, D.	P-OG-14	Hördt, A.	O-S4-05, P-GT-03, P-OG-05, P-S4-03, P-S4-04
Guðnason, É. Á.	P-SO-07	Hornbruch, G.	P-OG-16
Guillemoteau, J.	<b>P-KD-03, P-OG-02</b>	Hormann, J.	<b>P-SO-18</b>
Günaydin, O.	<b>O-SM-03</b>	Hort, M.	O-VU-01
Günther, T.	O-AG-02, O-MI-08, O-OG-05, O-OG-08, P-AG-01	Hoven, D.	<b>O-OG-09</b>
Guðnason, E. Á.	O-SO-07	Hrubcová, P.	O-SO-07, O-SO-08
Gwali, J.	O-VU-03	Huhn-Frehers, K.	P-MI-08
<span style="background-color: #cccccc;">■</span> Haberland, C.	O-SO-05, P-S3-03	Huisman, J. A.	P-OG-07
Hadzioannou, C.	O-GO/OS-03, O-SO-09, P-SO-03	Humpert, S.	P-OG-25
Häfner, R.	O-KI-02, O-OG-11	Hüttner, G.	P-GT-01
Hägg, K.	O-OG-02, O-OG-03	<span style="background-color: #cccccc;">■</span> Ibraheem, I. M.	O-OG-04
Hahn, S.	O-S1-03	Ibrahimli, M.	<b>P-OG-20</b>
Haji, A.	O-S4-03	Iden, S.	P-OG-01
Halisch, M.	P-S4-01	Igel, H.	O-GO/OS-03
Hammer, C.	P-SO-03	Igel, J.	P-OG-12
Hänel, F.	P-SO-17	Iraheta, A.	P-PV-02
Hannemann, K.	P-MG-05	Isik, N.	P-OG-18
Hansen, U.	O-S1-04, O-S1-05, P-S1-05	Isken, M. P.	O-SO-04, O-SO-05, O-SO-06, <b>O-SO-07</b>
Haroon, A.	P-MG-03	<span style="background-color: #cccccc;">■</span> Jacobsen, B.	<b>P-OG-26</b>
Harrington, R. M.	O-GD-03, O-SO-14, P-S2-04, P-SO-11, P-SO-12	Jahani, S.	P-OG-18
Hart, J.	<b>P-SO-19</b>	Janout, C.	P-SM-07
Hartmann, A.	<b>O-MI-07</b>	Jaron, A.	<b>O-MI-08</b>
Hartmann, G.	P-S2-01, P-SO-14	Jimenez Martinez, V.	P-MI-09
Hasch, M.	P-PV-01	Joachim, A.	<b>P-SO-07</b>
Hase, J.	P-S4-05, <b>P-S4-07</b>	Jonsson, P.	O-OG-02, O-OG-03
Hauck, C.	P-MI-06	Joswig, M.	<b>O-KI-01, O-KI-02, O-OG-11</b>
Hawemann, F.	P-BL-06	Julius, S.	P-OG-04
He, C.	<b>P-MI-02</b>	Jung, P.	P-OG-16
He, K.	<b>O-MI-05</b>	Junghans, T.	P-OG-15
Hedblom, P.	O-OG-02, O-OG-03		
Heimann, S.	O-SO-06, P-SO-07, P-SO-10		
Heinloo, A.	P-SO-01		

Kakar, N.	<b>O-AG-03</b>	Laske, G.	<b>P-SO-05</b>
Kaldy, E.	<b>P-S2-06</b>	Latypova, E.	<b>O-S3-01, P-S3-01</b>
Kaplanvural, I.	O-OG-01, P-MG-03	Laumann, P.	<b>O-SO-04</b> , O-SO-05, O-SO-06,
Karadima, C.	P-OG-22		O-VU-03
Karaszen, E.	O-SO-18	Lauterjung, J.	O-GO/OS-02
Karim, F.	<b>P-BL-07</b>	Lazecky, M.	O-AG-03
Karimi, K.	<b>O-OG-14, P-S2-07</b>	Ledig, T.	P-SO-19
Kasburg, V.	<b>O-S2-01</b>	Lehr, J.	<b>P-SO-01</b>
Käßner, F.	P-SO-17	Leineweber, P.	<b>P-SM-07</b>
Kaus, M.	<b>P-SO-15</b>	Lhuillier, F.	<b>O-S1-03</b>
Kaviani, A.	O-VU-03, P-SO-15	Li, Y.	P-OG-03
Keiser, F.	O-S4-04, <b>P-S4-03</b>	Liebermann, C.	P-SM-05
Keller, M.	O-KD-02	Limberger, F.	<b>O-SO-19</b> , O-VU-03, P-SO-06
Kemna, A.	O-MI-08, P-S4-05, P-S4-07	Linck, R.	P-KD-02
Kerkmann, N.	<b>P-BL-02</b>	Linke, M.	O-MI-07
Keßler, S. S.	<b>P-MI-01</b>	Lomax, A.	O-SO-08
Kirsch, R.	P-OG-13, P-SM-07	Lorek, A.	P-S4-02
Klahold, J.	P-MI-06	Lorenzen, M.	<b>P-OG-14</b>
Kletetschka, G.	O-OG-14	Löwer, A.	P-PV-01
Klitzke, P.	P-PV-01	Lügges, A.	O-MI-02
Klitzsch, N.	<b>O-S4-01</b>		
Klotzsche, A.	O-OG-09, O-OG-10, P-OG-06	<b>P-S1-05</b>	
Knies, A.	P-OG-11	Mackens, S.	O-KI-04
Koch, P.	P-SM-04	Mahgoub, A. N.	O-S1-02
Ködel, U.	O-KI-04	Majchczack, B. S.	O-KI-05
Koglin, N.	P-PV-01	Manarcescu, A. C.	O-S1-03
Köhn, D.	O-SM-01, P-OG-13, P-OG-18	Mandal, S.	<b>P-SO-04</b>
Kolinsky, P.	O-SO-17	Manker, T.	O-VU-03
Komeazi, A.	<b>O-SO-01</b> , P-SO-06	Männel, B.	P-S3-03
Kopp, H.	O-GD-01	Mansfeld, A. M.	<b>P-S4-05</b>
Körbe, M.	O-SM-01	Mansouri, H.	<b>P-BL-06</b>
Korn, M.	P-SO-17	Martin, T.	O-OG-02, O-OG-03
Korte, M.	<b>O-S1-02</b>	Martínez-Garzón, P.	P-SO-20
Kouamo Keutchafo, N.-A.	P-BL-02, <b>P-BL-04</b>	Masihi, A.	<b>P-SO-08</b>
Krawczyk, C.	P-S3-03, P-SO-19, P-SO-20	Mastella, G.	P-S3-01
Kreith, D.	<b>O-S4-03</b> , O-S4-04, P-S4-08	Maurer, H.	O-MI-04
Kroll, S.	P-KD-01	Maurer, V.	P-S2-05
Krueger, F.	O-SO-09	Mecking, R.	P-SM-07
Kruschwitz, S.	O-S4-07	Medappil Pinatt, R.	<b>P-SO-06</b>
Kruse, J. P.	P-SO-15	Medinger, N.	P-S2-02
Kühn, P.	P-OG-10	Meier, T.	<b>O-SO-17</b> , P-OG-13, P-OG-18,
Kühne, N.	<b>O-SM-04, P-SM-01</b> ,		P-SO-18
	P-SM-02, P-SM-03	Meire, V.	O-OG-14
Kukowski, N.	O-MI-01, O-S2-01, P-MI-07	Mellage, A.	O-S4-06, P-S4-01
Kulikova, G.	<b>O-SO-09</b>	Menzel, N.	<b>P-OS-01</b>
Kummerow, J.	O-SO-13, P-SO-13	Mester, A.	P-OG-07
Kunicki, A.	P-OG-04	Metzger, S.	O-AG-03, O-S3-03, P-S3-02
Kuntze, A.	<b>O-S3-04</b>	Micallef, A.	P-MG-03
Küperkoch, L.	P-S2-02	Mielentz, F.	P-OG-17
		Min, S.	P-OG-26
Lamb, O. D.	P-SO-07	Ming, L.	P-OG-03
Lärm, L.	O-OG-10, <b>P-OG-06</b>	Mizera, J.	O-OG-14

Mörbe, W.	P-OG-03	Plenefisch, T.	O-OG-12, <b>P-S2-01</b> , P-SO-14
Motagh, M.	O-AG-03	Plenkers, K.	O-S2-05, P-OG-17
Muhlanga, M.	O-SM-03	Plourde, A.	O-S2-03
Muhuri, A.	O-AG-01	Pohle, M.	<b>P-OG-10</b> , P-OG-16
Müller, B.	P-S2-03	Prayag, A.	<b>O-OG-02</b> , <b>O-OG-03</b>
Müller, J.	O-S2-01	Putri, M. N.	O-S1-03
Müller, N.	<b>O-OG-07</b>		
Müller-Petke, M.	O-OG-05, O-OG-06, P-OG-04, P-OG-08	■ Quinteros, J.	O-GO/OS-03, P-SO-01
Mumand, F.	<b>P-MI-09</b>	■ Rabbel, W.	O-KI-05, O-OG-01, P-MG-03, P-OG-22
Munir, M. B.	O-SO-18	Radic, T.	<b>P-S4-06</b>
Munsch, S.	<b>O-S4-07</b>	Rahmani, A.	<b>P-S4-01</b>
Murray-Bergquist, L.	<b>P-SO-09</b>	Raj, V.	O-KI-03
■ Napp, M.	O-OG-12	Ramatschi, M.	O-S3-05
Näser, H.	O-SM-03	Ramm, M.	P-OG-07
Nasrat, N. A.	O-AG-03	Ramos, C.	P-SO-14
Natour, G.	P-OG-07	Rawlinson, N.	P-SO-07
Nazari, S.	<b>O-AG-02</b> , P-AG-01	Rebolè Canals, S.	P-SO-09
Neugebauer, S.	P-SO-16	Rees, L.	P-SO-07
Niederhuber, T.	P-S2-03	Reinsch, T.	P-SO-19
Niemz, P.	<b>O-S2-06</b>	Reiss, M. C.	<b>O-VU-04</b>
Nießen, I. O.	P-OG-10	Ren, Y.	P-MG-05
Nwaka, E. G.	<b>P-OG-23</b>	Renner, J.	P-BL-07, P-BL-08, P-MI-09
■ Ohrnberger, M.	O-SO-11	Rheinbach, O.	P-KI-02
Olivar-Castaño, A.	<b>O-SO-11</b>	Riedel, M.	O-GD-01
Omlin, A.	P-SM-05	Rieß, A.	<b>P-OG-19</b>
Oye, V.	O-S2-03	Rietbrock, A.	P-S2-05
■ Pahlings, J.	<b>P-S1-02</b>	Rische, M.	<b>P-S2-03</b>
Pankow, K.	O-S2-06	Ritter, J. R. R.	P-S1-03, P-S1-04
Pascharat, L. I.	<b>P-OG-17</b>	Ritter, O.	P-S3-03
Pätzl, J.	<b>O-SO-02</b>	Roas-Domingo, J.	O-VU-02
Paul, C.	<b>P-KI-01</b>	Rochlitz, R.	O-AG-02
Paulwitz, B.	<b>O-KI-03</b>	Rödder, J.	P-OG-06
Pechník, R.	O-OG-08	Rodríguez Tribaldos, V.	<b>P-SO-20</b>
Peikert, U.	O-MI-07	Roga, C.	O-VU-03
Pejdanović, S.	P-OG-10	Roman, D.	O-VU-04
Pekşen, E.	O-OG-01, P-MG-03	Ronczka, M.	P-AG-01
Pena, R.	P-OG-26	Rondón, F.	O-GD-02
Peppel, D.	O-VU-01	Roßbach, M.	<b>O-SO-14</b>
Perez-Gamboa, P.	<b>P-OG-03</b>	Rosenthal, A.	<b>O-S1-06</b>
Petersen, G.	O-S2-06, O-SO-04, <b>O-SO-13</b> , P-SO-10	Rossi, M.	O-OG-02, O-OG-03
Pilgermann, E.	<b>P-GT-03</b>	Roth, M. P.	O-GD-03, P-S2-04, P-SO-16
Pinzón Rincón, L.	P-SO-20	Rudloff, A.	<b>O-GO/OS-02</b>
Pischke, A.	P-S4-04	Rumpe, B.	O-MI-02
Planitzer, T.	P-OG-26	Rümpker, G.	O-SO-01, O-SO-19, <b>O-VU-03</b> , P- SO-06, P-SO-15
Platzer, S.-M.	<b>O-S1-01</b>	Ruppel, A.	P-PV-01
		Rutledge, J.	O-S2-06
		Růžek, B.	P-SO-04

■ Saenger, E. H.	P-BL-01, P-BL-02, P-BL-04, P-OG-24, P-OG-25	Sitte, H. W.	<b>O-S1-04</b>
Sager, C.	P-OG-12	Skibbe, N.	<b>O-OG-05</b>
Sander, L.	P-MG-03	Slater, L.	O-S4-02
Schäfer, W.	<b>O-GD-01</b>	Smeaton, C. M.	O-S4-06
Scharnweber, M.	<b>P-OG-11</b>	Sobiesiak, M.	P-OG-17
Schenk, A.	P-OG-20	Söding, H.	<b>O-MI-04</b>
Schennen, S.	P-OG-17	Solis, D.	P-SM-04
Scherer, B.	P-OG-07	Sonnabend, L.	<b>O-SO-10, P-SO-17</b>
Scheunert, M.	O-VU-01, P-VU-01	Spengler, T.	O-SO-19
Schiebel, S.	<b>O-OG-10</b>	Spitzer, K.	O-VU-01, P-KI-02, P-OG-26, P-VU-01
Schiffller, M.	O-AG-02	Splitth, T.	<b>O-OG-06, P-OG-08</b>
Schimschal, C.	<b>O-MI-06</b>	Stammler, K.	P-SO-14
Schindler, D.	<b>O-SM-02, P-SM-05</b>	Stein, C.	O-S1-04, <b>O-S1-05</b>
Schirra, L.	<b>P-OG-01</b>	Stein, O.	<b>O-AG-01</b>
Schliwa, N.	O-SO-14	Steinberg, A.	<b>P-SO-14</b>
Schlömer, A.	<b>P-S3-02</b>	Stele, A.	P-KD-02
Schmalfuß, C.	O-SM-01	Stellmach, S.	P-S1-06
Schmidt, B.	O-SO-04	Steuer, A.	O-AG-02
Schmidt, V.	P-KI-01	Stiller, B.	O-OG-08
Schmidt, W.	O-S4-07	Stolpe, H.	P-OG-17
Schmitz, M.	O-GD-02, <b>O-OG-13</b>	Stork, A.	O-KI-04
Schmoldt, J.-P.	<b>O-KD-01, O-KD-01, P-KD-01,</b> P-KD-02, P-KD-03	Strohbach, M. W.	P-PV-02
Schneider, C.	O-VU-01	Strollo, A.	O-GO/OS-02, O-GO/OS-03
Schneider von Deimling, J.	P-MG-03	Strunga, V.	O-OG-14
Schnepf, A.	O-OG-10, P-OG-06	Sudhaus, H.	O-AG-01, O-S3-04
Scholze, M.	O-SM-04, P-SM-01, P-SM-02, P-SM-03	Sugand, M.	<b>O-S4-05</b>
Schöne, T.	O-AG-03	Szrek, J.	<b>O-S3-03</b>
Schönfeldt, E.	P-OG-09	Szwillus, W.	P-GT-01, <b>P-S1-01</b>
Schulte-Kortnack, D.	P-OG-18	■ Tanyas, H.	O-SO-18
Schulz, A.	<b>O-MI-01, P-MI-07</b>	Tatapu, C.	O-VU-03
Schulz, R.	P-OG-05, <b>P-S4-04</b>	Tegtow, W.	O-S2-02
Schurr, B.	O-SO-16	Terzopoulou, D.	P-OG-22
Schwalenberg, K.	<b>P-MG-02</b>	Tezkan, B.	O-OG-04, O-VU-02, P-MG-03, P-OG-03, P-OG-21
Schwarze, P.	<b>P-OG-12</b>	Thiede, A.	O-AG-02
Segschneider, M.	O-KI-05	Tholen, S.	P-BL-06
Seidel, M.	<b>O-KD-02</b>	Thomas, C.	P-MG-05, P-S1-02
Seiter, K.	P-OG-04	Thorwart, M.	<b>P-OG-22, P-SO-09</b>
Semper, P.	<b>P-VU-01</b>	Tilgner, A.	O-S1-06
Sen, E.	P-MG-03	Tilmann, F.	O-GO/OS-02, <b>O-GO/OS-03</b> , O-SO-16
Sener, A.	P-MG-03	Toy, V.	P-BL-06
Sens-Schönfelder, C.	P-SO-01, <b>P-SO-02</b>	Treichel, P.	P-OG-26
Serje Gutierrez, A.	<b>P-BL-01</b>	Trepmann, C. A.	O-SO-15
Serpelloni, E.	<b>O-S3-PV</b>	Tronicke, J.	P-OG-02
Shakas, A.	P-BL-03		
Shapiro, S.	O-S2-02		
Shata, O.	<b>P-KD-02</b>		
Shinu, S.	O-S1-02		
Sieger, M.	P-BL-02, P-BL-04		

Uhlemann, S.	P-OS-01	Yates, A.	O-SO-02
Uhlmann, S.	<b>O-S2-04</b>	Yegres Herrera, L. A.	<b>O-GD-02</b>
Ulloa, C.	P-SO-09	Yogeshwar, P.	O-AG-02, O-MI-08, O-OG-04, O-VU-02, P-MG-03, P-OG-03, P-OG-21
Urlaub, M.	P-MG-05		
van der Kruk, J.	O-OG-09, P-OG-06	Yolcubal, I.	P-MG-03
van Ginkel, J.	P-SO-09	Yuan, X.	O-SO-16
van Huisstede, L.	P-SO-09		
van Laaten, M.	O-S2-01, <b>O-SO-03</b>		
Vanderborght, J.	P-OG-06	Zeckra, M.	P-S2-04
Vehe, C.	O-VU-03	Zehner, M.	O-S2-01
Verdecchia, A.	P-SO-12	Zhang, H.	O-SO-04, <b>O-SO-05</b> , O-SO-06
Vereecken, H.	O-OG-09, O-OG-10, P-OG-06	Zhang, Z.	O-S4-04, <b>P-BL-05</b> , P-S4-08
Virgil, C.	P-GT-03	Zielhofer, C.	P-OG-10
Vlček, J.	O-SO-07, O-SO-08	Ziesch, J.	O-MI-06
Vogt, G.	O-SO-10	Zimmer, H.	<b>P-MG-05</b>
Voigt, R.	P-SO-17	Zimmermann, E.	P-OG-07
von Harten, J.	<b>O-MI-02</b>	Zimmermann, G.	O-S2-05
Vondenhoff, T.	<b>O-VU-02</b>	Zimmermann, L.	<b>P-S4-02</b>
Wadas, S. H.	<b>P-SM-06</b>	Zitoun, R.	P-MG-04
Wagner, F. M.	O-MI-03, O-MI-04, O-MI-08, P-MI-04, <b>P-MI-06</b> , P-OS-01	Zschoke, K. H.	P-GT-02
Waizy, H.	O-AG-03	Zvara, E.	P-OG-10
Walter, M.	O-OG-11		
Walter, T. R.	P-SO-10		
Walther, C.	O-AG-02		
Wassermann, J.	O-SO-11, P-S3-02		
Wawerzinek, B.	<b>P-S3-03</b>		
Weber, C.	O-S1-04, <b>P-S1-06</b>		
Wegler, U.	O-SO-03, O-SO-11, P-S2-01		
Weidel, C.	P-SO-18, P-OG-13		
Weihermüller, L.	P-OG-06		
Weit, S.	<b>P-KI-02</b>		
Weller, A.	<b>O-S4-02</b> , O-S4-04, P-BL-05, P-S4-08		
Wellmann, F.	O-MI-02, O-MI-03		
Wendt, S.	O-SO-10, O-SO-11		
Wennmacher, A.	P-GO-01		
Wentzki, J.	O-S4-03		
Werban, U.	P-OG-10, P-OG-16		
Werther, L.	P-OG-10		
Wessels, R.	P-SO-09		
Westermann, S.	P-OG-05, P-S4-04		
Whidden, K.	O-S2-06		
Wicka, L.	P-SM-07		
Wiesenbergs, L.	P-OG-13		
Wilken, D.	O-KI-05, P-OG-13		
Winder, T.	P-SO-07		
Winter, C.	P-OG-11		
Wollin, C.	P-SO-19		
Wunderlich, T.	O-KD-01, <b>O-KI-05</b> , P-KD-03, P-OG-11		
Wüstner, P.	P-OG-07		